ISSN 2413-5577

№ 4 Октябрь – Декабрь 2023

Экологическая безопасность прибрежной и шельфовой зон моря

Ecological Safety of Coastal and Shelf Zones of Sea

No. 4 October – December 2023

ecological-safety.ru

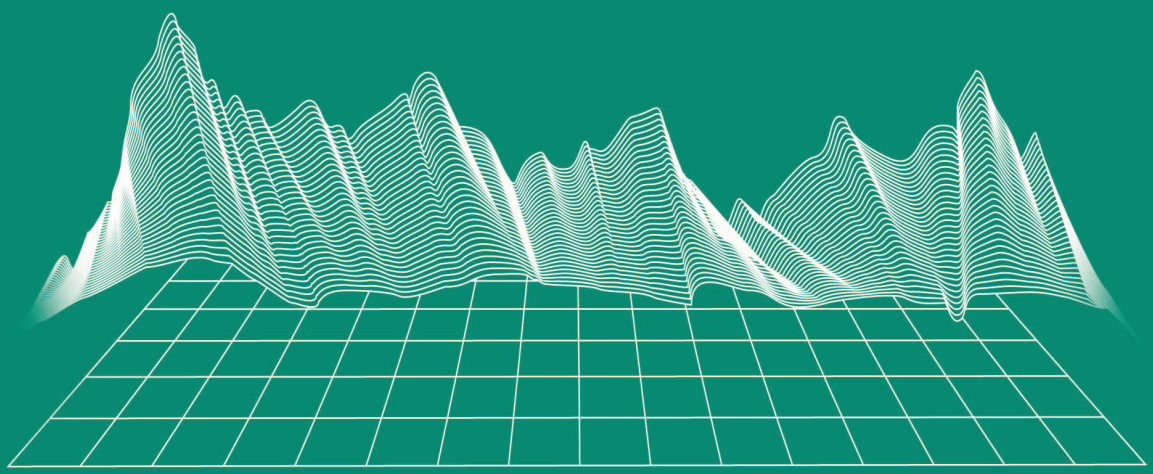

ISSN 2413-5577
No. 4, 2023
October – December

Publication frequency:
Quarterly
16+

ECOLOGICAL SAFETY OF COASTAL AND SHELF ZONES OF SEA

Scientific and theoretical peer reviewed journal

FOUNDER AND PUBLISHER:
Federal State Budget Scientific Institution
Federal Research Centre
"Marine Hydrophysical Institute of RAS"

The Journal publishes original research results, review articles (at the editorial board's request) and brief reports.

The Journal aims at publication of results of original scientific research concerning the state and interaction of geospheres (atmosphere, lithosphere, hydrosphere, and biosphere) within coastal and shelf areas of seas and oceans, methods and means of study thereof, ecological state of these areas under anthropogenic load as well as environmental protection issues.

The Journal's editorial board sees its mission as scientific, educational and regulatory work to preserve the ecological balance and restore the resource potential of coastal and shelf areas believing that despite the geographical limitations of the areas under study, the processes taking place within them have a significant impact on the waters of the seas and oceans and economic activity.

The Journal publishes original research materials, results of research performed by national and foreign scientific institutions in the coastal and shelf zones of seas and oceans, review articles (at the editorial board's request) and brief reports on the following major topics:
- Scientific basis for complex use of shelf natural resources
- Marine environment state and variability
- Coastal area state and variability; coast protection structures
- Monitoring and estimates of possible effects of anthropogenic activities
- Development and implementation of new marine environment control and monitoring technologies

The outcome of the research is information on the status, variability and possible effects of anthropogenic activities in the coastal and shelf marine areas, as well as the means to perform calculations and to provide information for making decisions on the implementation of activities in the coastal zone.

e-mail: ecology-safety@mhi-ras.ru

website: http://ecological-safety.ru

Founder, Publisher and Editorial Office address:
2, Kapitanskaya St.,
Sevastopol, 299011, Russia

Phone, fax: + 7 (8692) 54-57-16

РЕДАКЦИОННАЯ КОЛЛЕГИЯ

CONTENTS

№ 4. 2023 October – December, 2023

СОДЕРЖАНИЕ

№ 4. 2023 Октябрь – Декабрь, 2023

Original article

Spatial and Temporal Variability of Hydrophysical Parameters of the Northern Black Sea Waters from 2021 Measurements

A. N. Morozov *, E. V. Mankovskaya

Marine Hydrophysical Institute of RAS, Sevastopol, Russia
* *e-mail: anmorozov@mhi-ras.ru*

Abstract
The paper uses the results of measurements of salinity, temperature and current velocity profiles in three expeditions of the R/V *Professor Vodyanitsky* (22 April – 08 May, 29 June – 10 July, 03–19 September 2021) in the central sector of the northern Black Sea (31°–37° E, 43°–45° N) to study features of the spatial distribution of hydrophysical parameters in various seasons of 2021 and to compare them with the data of previous expedition studies in 2016–2019. The horizontal distributions of currents in the spring, summer and autumn expeditions of 2021 were analysed. The averaged profiles of current velocity, density, temperature, buoyancy frequency, and kinetic energy were considered. The vertical structure of water temperature reflects the persistent warming trend of the cold intermediate layer core derived earlier from the 2016–2019 data. Based on all 2016–2021 measurements, the vertical profiles of kinetic energy show decreasing values in the upper sea layer in summer and increasing values in spring, autumn and winter seasons of the year. The profiles can be approximated by linear relationships that cross zero at a density of 16.75 kg/m^3. The seasonal variability of the average kinetic energy is traceable to the depth of occurrence of this particular isopycnic.

Keywords: Black Sea, current velocity, density, temperature, buoyancy frequency, kinetic energy, cold intermediate layer

Acknowledgements: The work was performed under state assignment of MHI RAS on topics no. FNNN-2021-0003 “Operational oceanology”, no. FNNN-2021-0005 “Coastal research”; the data were obtained during the 116th, 117th and 119th cruises of the R/V *Professor Vodyanitskiy* (the core facility R/V *Professor Vodyanitskiy* of A.O. Kovalevsky Institute of Biology of the Southern Seas of RAS).

For citation: Morozov, A.N. and Mankovskaya, E.V., 2023. Spatial and Temporal Variability of Hydrophysical Parameters of the Northern Black Sea Waters from 2021 Measurements. *Ecological Safety of Coastal and Shelf Zones of Sea*, (4), pp. 6–18.

Пространственно-временная изменчивость гидрофизических параметров вод северной части Черного моря по данным измерений 2021 года

А. Н. Морозов *, Е. В. Маньковская

Морской гидрофизический институт РАН, Севастополь, Россия
** e-mail: anmorozov@mhi-ras.ru*

Аннотация
На основе результатов измерения профилей солености, температуры и скорости течения в трех экспедициях НИС «Профессор Водяницкий» (22 апреля – 08 мая, 29 июня – 10 июля, 03–19 сентября 2021 г.) в центральном секторе северной части Черного моря (31°–37° в. д., 43°–45° с. ш.) исследованы особенности пространственного распределения гидрофизических параметров в различные сезоны 2021 г. и проведено сопоставление с данными предыдущих экспедиционных исследований 2016–2019 гг. Проанализированы горизонтальные распределения течений в весенней, летней и осенней экспедициях 2021 г. Рассмотрены осредненные профили скорости течений, плотности, температуры, частоты плавучести, кинетической энергии. Вертикальная структура температуры воды отражает сохраняющуюся тенденцию к потеплению ядра холодного промежуточного слоя, выявленную ранее по данным 2016–2019 гг. По данным всех измерений 2016–2021 гг., вертикальные профили кинетической энергии показывают уменьшение значений в верхнем слое моря в летний период и возрастание в весенний, осенний и зимний сезоны года. Профили могут быть аппроксимированы линейными зависимостями, которые пересекают нулевое значение при плотности 16.75 кг/м^3. Сезонная изменчивость средней кинетической энергии прослеживается до глубины залегания именно этой изопикны.

Ключевые слова: Черное море, скорость течения, плотность, температура, частота плавучести, кинетическая энергия, холодный промежуточный слой

Благодарности: работа выполнена в рамках государственного задания ФГБУН ФИЦ МГИ по темам № FNNN-2021-0003 «Оперативная океанология», № FNNN-2021-0005 «Прибрежные исследования»; данные получены в 116, 117 и 119-м рейсах НИС «Профессор Водяницкий» (Центр коллективного пользования «НИС Профессор Водяницкий» Федерального государственного бюджетного учреждения науки Федерального исследовательского центра «Институт биологии южных морей имени А.О. Ковалевского РАН»).

Для цитирования: *Морозов А. Н., Маньковская Е. В.* Пространственно-временная изменчивость гидрофизических параметров вод северной части Черного моря по данным измерений 2021 года // Экологическая безопасность прибрежной и шельфовой зон моря. 2023. № 4. С. 6–18. EDN QEZCBF.

Introduction

Since 2016, Marine Hydrophysical Institute has been conducting annual expeditionary research in the central sector of the northern Black Sea onboard the R/V *Professor Vodyanitsky*. CTD probes (conductivity, temperature, depth) and measurements of current velocity profiles with the use of a Lowered Acoustic Doppler Current Profiler (LADCP) are traditionally carried out at hydrological stations during expeditions [1, 2]. The joint analysis of the CTD and LADCP data makes it possible to obtain averaged characteristics of the thermohaline structure

and dynamics of the waters, as well as to assess their spatial and temporal variability [3–7].

The study on the peculiarities of the Black Sea waters dynamics remains an urgent task nowadays. LADCP probes make it possible to conduct more detailed and advanced research of current variability patterns over a wide range of spatial and temporal scales. The empirical parameters of the horizontal and vertical structure of the current velocity field obtained in this case may be used to test the results of water dynamics numerical modelling, interpret remote sensing data and evaluate various exchange processes.

The vertical thermohaline structure of the Black Sea waters is also the subject of constant monitoring and studying. In recent decades, significant changes have been observed, for instance, in the form of a trend towards decreasing salinity of the surface layer and increasing salinity of the pycnocline [8] or a tendency to the cold intermediate layer (CIL) core warming [9–13]. At the present stage, according to the field data, waters with temperatures below 8 °C (the typical boundary of the CIL) are becoming less common in the Black Sea. The Argo floats data also show that the volume of cold water in the CIL decreased, the lower boundary of the layer rose and the layer itself can disappear altogether [14]. Climatic changes in air temperature (in particular, its increase) during the winter season, which is directly related to the winter convective-turbulent cooling of the upper layer sea waters and the renewal of the CIL waters, represent one of the reasons concerning the abovementioned.

Results of the CTD and LADCP probes obtained during three 2021 Black Sea expeditions are reported and discussed in this paper. The averaged profiles of current velocity, density, temperature, buoyancy frequency and kinetic energy are considered. The purpose of the work is to investigate the features of the spatial distribution of hydrophysical parameters in different seasons of 2021 and compare them with the data of previous expedition studies in 2016–2019.

Data, tools and methods

The data of the 2021 expeditions onboard the R/V *Professor Vodyanitsky* in the central sector of the northern Black Sea (31°–37° E, 43°–45° N) were used:

1) 22 April – 08 May (expedition 116);
2) 29 June – 10 July (expedition 117);
3) 03–19 September (expedition 119).

The CTD probes were performed with the help of the IDRONAUT OCEAN SEVEN 320PlusM sounding complex. The results were interpolated onto a 1 m spacing grid. According to the description of devices, the temperature and salinity measurements have their initial accuracy of 10^{-3} °C and 10^{-3} PSU.

The current velocity profile measurements were carried out with the use of the LADCP based on the Workhorse Monitor WHM300 manufactured by RDI (operating frequency – 300 kHz, nominal range – 120 m, resolution capability – 4 m). The device operation parameters were set as follows: the LADCP option was enabled in broad-band mode, which implied high resolution/low range, time discreteness of 1 s, depth discreteness of 4 m. During the measurements, the R/V was

drifting with the speed determined by the marine navigation system (GPS) and taken into account when processing primary data.

On deep water (over 200 m), the measurements were carried out at horizons of 160–180 m. The measurement sequence included holding the device near the sea surface at a depth of ~3 m for 5 minutes, its further plunging at a speed of 0.5 m/s to the depth of sounding, its holding at this horizon for 5 min and subsequent lifting to the surface at a speed of 0.5 m/s. The measured current velocity profiles started from a 10-meter depth. The current velocity measurement error is ~3 cm/s for a single impulse.

In the coastal areas (sea depth up to 100 m), the measurements were carried out via holding the device near the R/V board for 5 min, the influence of the R/V hull on the magnetic compass was compensated on the basis of the *Bottom Track* and GPS data comparison.

The LADCP data processing was performed with the help of the LDEO Software, version IX.12. The program is adapted to the measurement conditions of the Black Sea, it makes it possible to calculate the vertical profiles of the current velocity at the deep-water stations in a layer extending from ~30 m to the depth of sounding. At the shallow-water stations (sea depth up to ~90 m), the current velocity profile is calculated from the data of the ADCP measurement near the R/V board with the use of specialised software taking into account the influence of the R/V hull on the device compass readings [15].

To obtain the averaged profiles of hydrophysical parameters, isopycnic averaging over the set of stations for each expedition was applied in the further data processing. This is for the necessity to compensate for the dome-shaped isopycnic surfaces caused by the cyclonic nature of the large-scale circulation in the Black Sea waters [16].

Results of measurements and their discussion

The field data were obtained in different seasons: spring, summer and autumn of 2021. Fig. 1 shows the current velocity vectors averaged in the 10–30 m layer. The hydrological stations were located quite evenly (except for the summer surveys) in the area of the Rim Current and outside it, closer to the centre of the sea. The cyclonic nature of the large-scale circulation in the Black Sea waters was well expressed in all distributions, and the westerly current direction prevailed. The velocity and intensity of the Rim Current were very high in spring, then they decreased in summer and increased again in autumn. In each of the expeditions, an increase of the current velocity was noted in the area of the depth dump by the southern tip of the Crimean Peninsula (Cape Kikineiz), as the Rim Current intensifies there. It should be noted that the main stream in all distributions was not pressed against the continental slope of the Crimean Peninsula, but was shifted to the southwest.

In the spring expedition, the horizontal distribution of currents revealed an anticyclonic mesoscale eddy (the Crimean anticyclone) with the typical scale of ~40 km in the eastern part of the polygon. The measurements at the hydrological stations falling within the eddy zone were carried out on 05.05.2021.

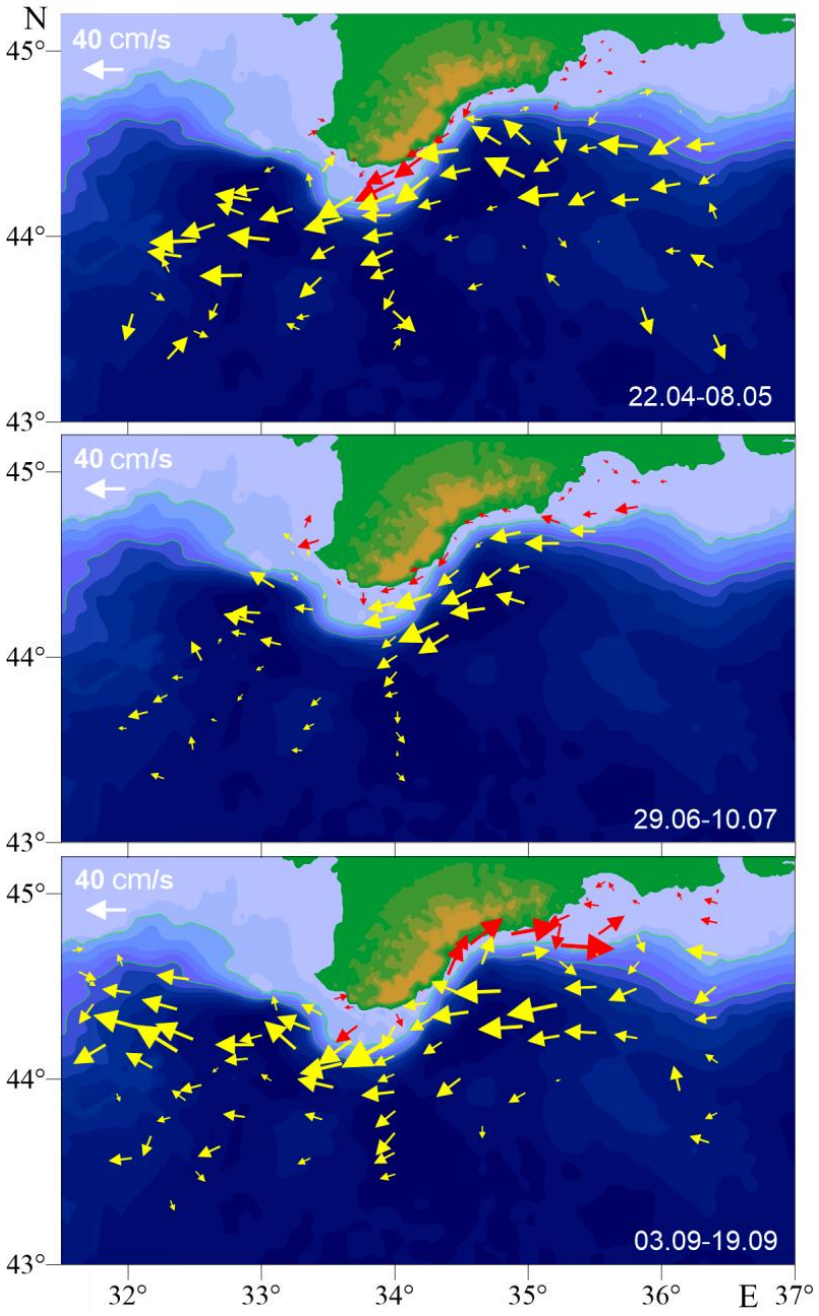

F i g. 1. Current velocity vectors averaged in the 10–30 m layer (red arrows are shallow-water stations (< 100 m), yellow arrows are deep-water stations (> 100 m); the arrow point denotes the station location)

It was also confirmed by the remote sensing data of sea surface temperature on 05.05.2021 (Fig. 2), in which the eddy anticyclonic formation was observed.

In the autumn expedition, a powerful alongshore current at velocities of up to 40 cm/s was observed at the Southern coast of Crimea in the nearshore shelf zone. The current was moving in the direction opposite to the intense Rim Current (30–40 cm/s). At the same time, this current maintained its direction throughout the whole water column at the stations with maximum current velocity values. According to the authors of [17–20], the alongshore flow directed to the east and northeast (against the Rim Current) accounts for 10–12% in the bimodal distribution of the nearshore current direction repeatability by the Southern coast of Crimea. The main reason for the appearance of the so-called countercurrents is considered to be the formation of coastal anticyclonic eddies during the interaction of the Rim Current with the coast [20–24] as well as the impact of regional wind conditions [25]. The recent paper [26] systematised the results of the field studies on the regional nearshore water circulation peculiarities previously obtained in various areas of the Black Sea. The features, conditions and duration of the nearshore current direction bimodality structure by the Southern coast of Crimea were also considered.

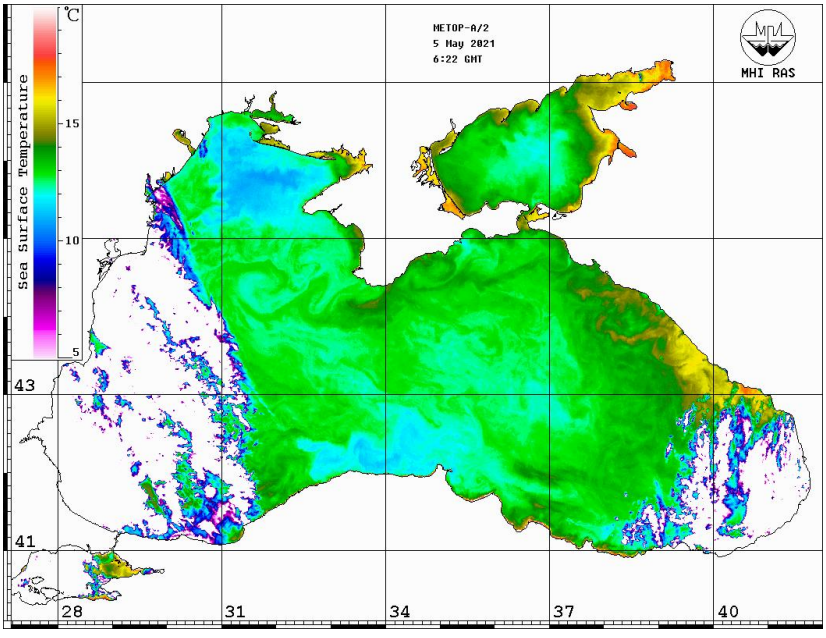

F i g. 2. Sea surface temperature on 5 May 2021 from METOP-A/2 data

Fig. 3 shows the vertical structure of the isopycnically averaged water temperature against the average profile of density and buoyancy frequency for three expeditions. Below the upper homogeneous surface layer, a regional minimum of the buoyancy frequency was observed at a potential density of ~14.5 kg/m^3 with a maximum of ~15.0 kg/m^3. The minimum temperature values were observed at a potential density of 14.7–14.8 kg/m^3: 8.68 °C in May, 8.65 °C in July, 8.71 °C in September. Earlier, we determined that the CIL, according to the contact measuring in the same sea area, tends to warm [5], and a criterion for the CIL boundary was proposed in the form of a temperature of 8.6 °C. However, according to the discussed data of the 2021 expeditions, it is not suitable. Only the 8.8 °C boundary can be considered.

The root mean square (RMS) profile of the current velocity modulus in all seasons shows its decrease with depth (Fig. 4, *a*). At the same time, in the 30–100 m depth range, the values of the current velocity modulus in spring and autumn were higher than in summer when large-scale sea circulation weakens and a seasonal thermocline is formed. Up to a density value of 14.5 kg/m^3 corresponding to the minimum buoyancy frequency, the current velocity varied slightly. In the 40–100 m depths layer (14.5–16.0 kg/m^3 density range), there was a sharp (almost twofold) decrease in the current velocity modulus caused by the transition of a part of kinetic energy into potential one, determined by the isopycnic surfaces deviation from the horizontal position.

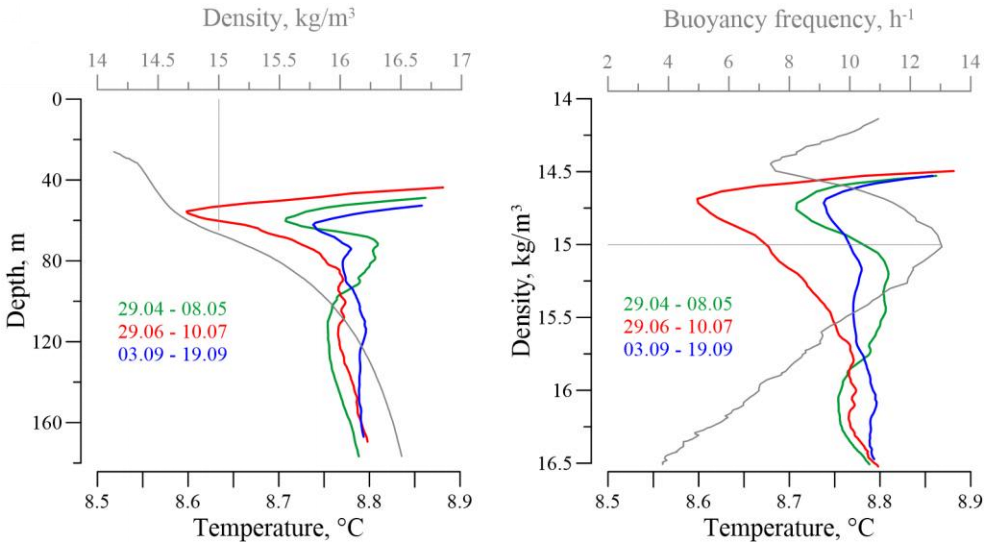

F i g. 3. Temperature vertical profiles isopicnically averaged over the set of 2021 expedition stations, together with the density distribution (*a*) and buoyancy frequency (*b*). The temperature scale is limited above by the value of 8.9 °C

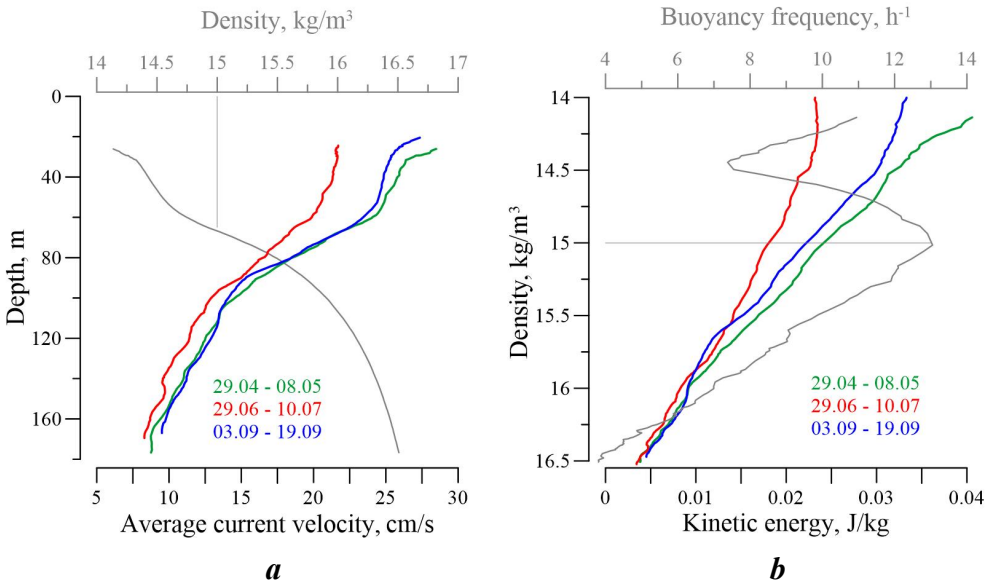

F i g. 4. Vertical profiles of current velocity and density (*a*), kinetic energy and buoyancy frequency (*b*), isopycnically averaged over the set of 2021 expedition stations

As for the tasks of comparing the results of water dynamics numerical modelling with the current velocity profiles field measurements, the vertical distribution of kinetic energy averaged over a certain set of stations is more suitable. Fig. 4, *b* shows kinetic energy profiles for all three expeditions considered in the present paper, isopycnically averaged over a set of stations (see Fig. 1). A decrease in the upper layer kinetic energy in summer and its increase in spring and, especially, in autumn were well traced. The profiles can be approximated by linear relationships crossing the zero value at a density of 16.75 kg/m^3. Similar results were obtained according to the data of the 2016–2019 expeditionary research (Fig. 5, *b*). According to Fig. 5, the values of kinetic energy in the upper layer of the sea (at a density of 14 kg/m^3) in summer did not exceed 0.02 J/kg. The same was observed according to the data of the 2021 summer expedition.

Fig. 5, *a* shows the isopycnically averaged temperature profiles obtained from the measurements carried out in 2016–2019 [6]. The renewal of the CIL waters in its classic form (< 8 °C) took place only in 2017. It was due to the relatively cold winter of 2016–2017. Since that time, there has been a tendency to the CIL core warming, which still persists, according to the measurements carried out in 2020–2021 (Fig. 6). The graphs in Fig. 6 show the air temperature in Kerch together with the average temperature of the CIL core from the beginning of 2016 to the end of 2021. It can be seen that winter air temperatures did not correspond to the values of 2017 and did not fall below them.

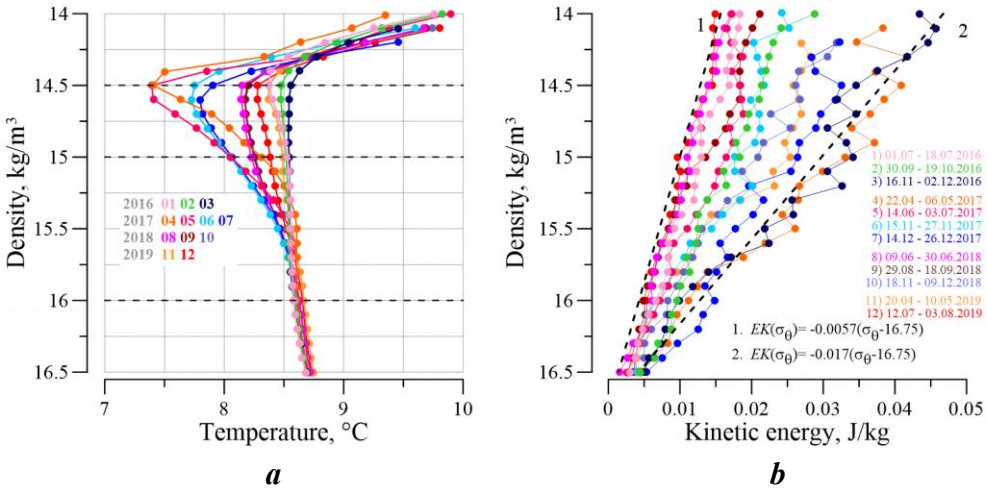

F i g. 5. Vertical profiles of temperature (*a*) and kinetic energy (*b*), isopycnically averaged over the set of stations, for 12 expeditions of 2016–2019

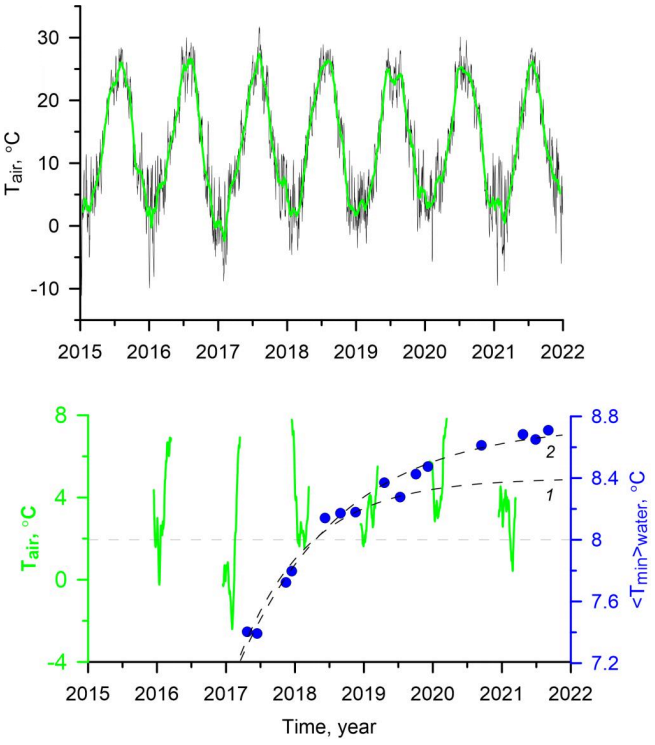

F i g. 6. Mean daily (grey line) and mean monthly (green line) air temperature in Kerch (*a*), mean values of the minimum water temperature in the profiles at the stations for the 2017–2021 expeditions and mean monthly winter air temperature in Kerch (*b*). Lines *1* and *2* are approximating functions

Accordingly, the decrease in the temperature of the CIL waters and their renewal were not observed. Dashed line *1* shows the earlier proposed relationship [5], according to which the temperature of the CIL increases after its renewal in 2017. The approximating function has the following form: $\langle T_{min} \rangle(t) = 7 + 1.4\ (1 - \exp(-(t - 2017)))$, where t – time period, year. Taking into account the new data of expeditionary measurements, the updated relationship is as follows (dashed line *2*): $\langle T_{min} \rangle(t) = 7 + 1.75\ (1 - \exp(-(t - 2017)/1.5))$.

Conclusions

According to the CTD and LADCP probes in three 2021 expeditions, spatial distributions of hydrophysical parameters were obtained in the northern Black Sea. The current velocity horizontal distribution in all seasons was dominated by westerly directions with the clearly expressed Rim Current, which was not pressed against the continental slope of the Crimean Peninsula, but was shifted to the deep sea. The Rim Current velocity reached 50 cm/s in spring, then decreased in summer and increased again in autumn. The average values of the current velocity at a depth of 40 m were 26 cm/s in spring, 21 cm/s in summer and 27 cm/s in autumn. The maximum current velocities were observed in each of the expeditions in the area of the depth dump by the southern tip of the Crimean Peninsula (Cape Kikineiz).

In the spring expedition, the horizontal distribution of currents revealed an anticyclonic mesoscale eddy (the Crimean anticyclone) with the typical scale of ~40 km in the eastern part of the polygon. In the autumn expedition, a powerful alongshore current at a velocity of up to 40 cm/s was observed by the Southern coast of Crimea in the nearshore shelf zone. It was moving in the direction opposite the intense Rim Current (30–40 cm/s) and maintained its direction throughout the whole water column.

As a result of the CTD and LADCP data joint analysis, averaged vertical profiles of current velocity, density, temperature, buoyancy frequency and kinetic energy were obtained. The vertical structure of the water temperature reflects the continuing warming tendency of the CIL core. The minimum temperature values were 8.68 °C in May, 8.65 °C in July, 8.71 °C in September, i. e. waters with temperatures below 8 °C (the typical CIL boundary) were not observed. The CIL temperature increases after its renewal in 2017 in accordance with the following time relationship: $\langle T_{min} \rangle(t) = 7 + 1.75\ (1 - \exp(-(t - 2017)/1.5))$.

The RMS profile of the current velocity modulus in all seasons shows its decrease with depth. At the same time, up to a density value of 14.5 kg/m^3, the current velocity varied slightly. In the 40–100 m depths layer (14.5–16.0 kg/m^3 density range), there was an almost twofold decrease in the current velocity modulus, which was caused by the transition of a part of kinetic energy into potential one.

A decrease in kinetic energy of the upper layer in summer and its increase in spring and, especially, in autumn were well traced in the vertical profiles. These profiles can be approximated by linear relationships that cross the zero value at a density of 16.75 kg/m^3. Similar results were obtained according to the data

of the 2016–2019 expeditionary research. The values of kinetic energy in the upper layer of the sea (at a density of 14 kg/m^3) in summer did not exceed 0.02 J/kg, according to all the measurements carried out in 2016–2021.

References

1. Firing, E. and Gordon, R., 1990. Deep Ocean Acoustic Doppler Current Profiling. In: IEEE, 1990. *Proceedings of the IEEE Fourth Working Conference on Current Measurement*. Clinton, MD, USA: IEEE, pp. 192–201. doi:10.1109/CURM.1990.110905
2. Visbeck, M., 2002. Deep Velocity Profiling Using Lowered Acoustic Doppler Current Profilers: Bottom Track and Inverse Solutions. *Journal of Atmospheric and Oceanic Technology*, 19(5), pp. 794–807. doi:10.1175/1520-0426(2002)019<0794:DVPULA>2.0.CO;2
3. Morozov, A.N., Lemeshko, E.M., Shutov, S.A., Zima, V.V. and Deryushkin, D.V., 2017. Structure of the Black Sea Currents Based on the Results of the LADCP Observations in 2004–2014. *Physical Oceanography*, (1), pp. 25–40. doi:10.22449/1573-160X-2017-1-25-40
4. Morozov, A.N. and Mankovskaya, E.V., 2019. Seasonal Variability of Currents Structure in the Black Sea Northern Part from Field Measurements in 2016. *Fundamentalnaya i Prikladnaya Gidrofizika,* 12(1), pp. 15–20. doi:10.7868/S2073667319010027
5. Morozov, A.N. and Mankovskaya, E.V., 2020. Cold Intermediate Layer of the Black Sea according to the Data of the Expedition Field Research in 2016–2019. *Ecological Safety of Coastal and Shelf Zones of Sea*, (2), pp. 5–16. doi:10.22449/2413-5577-2020-2-5-16 (in Russian).
6. Morozov, A.N. and Mankovskaya, E.V., 2021. Modern Studies of Water Dynamics in the North-Western Part of Black Sea from LADCP Measurements. In: MSU, 2021. *InterCarto. InterGIS. GI Support of Sustainable Development of Territories: Proceedings of the International Conference*. Moscow: MSU, Faculty of Geography. Vol. 27, part 3, pp. 5–15. doi:10.35595/2414-9179-2021-3-27-5-15 (in Russian).
7. Morozov, A.N. and Mankovskaya, E.V., 2021. Spatial Characteristics of the Black Sea Cold Intermediate Layer in Summer, 2017. *Physical Oceanography*, 28(4), pp. 404–413. doi:10.22449/1573-160X-2021-4-404-413
8. Polonsky, A.B., Shokurova, I.G. and Belokopytov, V.N., 2013. Decadal Variability of Temperature and Salinity in the Black Sea. *Morskoy Gidrofizicheskiy Zhurnal*, (6), pp. 27–41 (in Russian).
9. Belokopytov, V.N., 2010. Interannual Variations of the Renewal of Waters of the Cold Intermediate Layer in the Black Sea for the Last Decades. *Physical Oceanography*, 20(5), pp. 347–355. https://doi.org/10.1007/s11110-011-9090-x
10. Piotukh, V.B., Zatsepin, A.G., Kazmin, A.S. and Yakubenko, V.G., 2011. Impact of the Winter Cooling on the Variability of the Thermohaline Characteristics of the Active Layer in the Black Sea. *Oceanology*, 51(2), 221. https://doi.org/10.1134/S0001437011020123
11. Capet, A., Troupin, C., Carstensen, J., Grégoire, M. and Beckers, J.-M., 2014. Untangling Spatial and Temporal Trends in the Variability of the Black Sea Cold Intermediate Layer and Mixed Layer Deepth Using the DIVA Detrending Procedure. *Ocean Dynamics*, 64(3), pp. 315–324. doi:10.1007/s10236-013-0683-4
12. Novikova, A.M. and Polonsky, A.B., 2018. Inter-Decadal Variability of the Black Sea Surface and Cold Intermediate Layer Temperature. In: INTS, 2018. *Monitoring Systems of Environment*. Sevastopol: INTS. Iss. 34, pp. 110–115 (in Russian).

13. Miladinova, S., Stips, A., Garcia-Gorriz, E. and Macias Moy, D., 2017. Black Sea Thermohaline Properties: Long-Term Trends and Variations. *Journal of Geophysical Research: Oceans*, 122(7), pp. 5624–5644. doi:10.1002/2016JC012644
14. Stanev, E.V., Peneva, E. and Chtirkova, B., 2019. Climate Change and Regional Ocean Water Mass Disappearance: Case of the Black Sea. *Journal of Geophysical Research: Oceans*, 124(7), pp. 4803–4819. doi:10.1029/2019JC015076
15. Morozov, A.N. and Lemeshko, E.M., 2006. Methodical Aspects of the Application of Acoustic Doppler Current Profilers in the Black Sea. *Physical Oceanography*, 16(4), pp. 216–233. doi:10.1007/s11110-006-0027-8
16. Suvorov, A.M. and Shokurova, I.G., 2004. Annual and Interdecadal Variability of the Available Potential Energy in the Black Sea. *Physical Oceanography*, 14(2), pp. 84–95. doi:10.1023/B:POCE.0000037872.25674.ac
17. Boguslavsky, S.G., Koveshnikov, L.A., Kaminsky, S.T. and Markov, A.A., 1992. Features of the Currents at a Bold Coast. *Soviet Journal of Physical Oceanography*, 3(5), pp. 357–365. https://doi.org/10.1007/BF02198066
18. Belokopytov, V.N., Sarkisov, A.A. and Shchurov, S.V., 2003. Currents near the Part of the Crimean Coast from the Sarych Cape to Katcivelli. In: MHI, 2003. *Ekologicheskaya Bezopasnost' Pribrezhnoy i Shel'fovoy Zon i Kompleksnoe Ispol'zovanie Resursov Shel'fa* [Ecological Safety of Coastal and Shelf Zones and Comprehensive Use of Shelf Resources]. Sevastopol: MHI. Iss. 8, pp. 64–68 (in Russian).
19. Krivosheya, V.G., Moskalenko, L.V. and Titov, V.B., 2004. On the Current Regime over the Shelf near the North Caucasian Coast of the Black Sea. *Oceanology*, 44(3), pp. 331–336.
20. Ovchinnikov, I.M. and Titov, V.B., 1990. Anti-Cyclonic Vorticity of Currents in the Offshore Zone of the Black Sea. *Doklady Akademii Nauk SSSR*, 314(5), pp. 1236–1239 (in Russian).
21. Titov, V.B., 1992. About the Role of Eddies in Current Regime Formation on the Black Sea Shelf and Ecology Coastal Zone. *Oceanology*, 32(1), pp. 39–48 (in Russian).
22. Zatsepin, A.G., Elkin, D.N., Korzh, A.O., Kuklev, S.B., Podymov, O.I., Ostrovskii, A.G. and Soloviev, D.M., 2016. On Influence of Current Variability in the Deep Black Sea upon Water Dynamics of Narrow North Caucasian Continental Shelf. *Physical Oceanography*, (3), pp. 14–22. doi:10.22449/1573-160X-2016-3-14-22
23. Serebryany, A.N. and Lavrova, O.Yu., 2008. [Anticyclonic Eddy on the Shelf of the North-Eastern Black Sea: Joint Analysis of Space Images and Acoustic Sounding Data of the Sea Water Column]. *Sovremennye Problemy Distantsionnogo Zondirovaniya Zemli iz Kosmosa*, 5(2), pp. 206–215 (in Russian).
24. Titov, V.B., Krivosheya, V.G. and Moskalenko, L.V., 2002. Currents Regime in Russian sector of the Black Sea. In: A. G. Zatsepin and M. V. Flint, eds., 2002. *Multidisciplinary Investigations of the Northeast Part of the Black Sea*. Moscow: Nauka, pp. 48–54 (in Russian).
25. Ivanov, V.A. and Belokopytov, V.N., 2013. *Oceanography of Black Sea*. Sevastopol: ECOSI-Gidrofizika, 210 p.
26. Kuznetsov, A.S. and Ivashchenko, I.K., 2023. Features of Forming the Alongcoastal Circulation of the Coastal Ecotone Waters nearby the Southern Coast of Crimea. *Physical Oceanography*, 30(2), pp. 171–185. doi:10.29039/1573-160X-2023-2-171-185

Submitted 16.06.2023; accepted after review 3.07.2023;
revised 11.10.2023; published 20.12.2023

About the authors:

Alexey N. Morozov, Senior Research Associate, Marine Hydrophysical Institute of RAS (2 Kapitanskaya St., Sevastopol, 299011, Russian Federation), PhD (Tech.), **ORCID ID: 0000-0001-9022-3379, Scopus Author ID: 7202104940, ResearcherID: ABB-4365-2020**, *anmorozov@mhi-ras.ru*

Ekaterina V. Mankovskaya, Senior Research Associate, Marine Hydrophysical Institute of RAS (2 Kapitanskaya St., Sevastopol, 299011, Russian Federation), PhD (Tech.), **ORCID ID: 0000-0002-4086-1687, Scopus Author ID: 57192647961, ResearcherID: AAB-5303-2019**, *emankovskaya@mhi-ras.ru*

Contribution of the authors:

Alexey N. Morozov – problem statement, processing, analysis and description of the study results, article text editing

Ekaterina V. Mankovskaya – measurement data processing, collection of information to study, discussion of the results, preparation of the article text and graphic materials

All the authors have read and approved the final manuscript.

Original article

Material Accumulation in the Modern Accumulative Body of the Anapa Barrier Beach (Caucasian Coast of the Black Sea): Paleolithodynamic Prerequisites

V. V. Krylenko *, M. V. Krylenko, D. V. Krylenko

Shirshov Institute of Oceanology RAS, Moscow, Russia
* *e-mail: krylenko.slava@gmail.com*

Abstract
The Anapa Barrier Beach is a large Holocene coastal accumulative form formed by sediments of terrigenous and marine origin in the north-western Caucasian coast of the Black Sea. In recent decades, the barrier beach shoreline has been retreating. The main reason for the retreat is the natural processes that caused the shortage and redistribution of sediments in the lithodynamic system of the barrier beach. With the sea level rising, the coast retreat may accelerate, and in the future, it may lead to degradation of the entire geosystem of the Anapa Barrier Beach. The paper aims to analyze and generalize information about the origin of the sediment material composing the accumulative body and the mechanisms of its redistribution in time and space, which is necessary for assessing the stability of the modern accumulative body. Based on a comprehensive analysis, which includes a number of paleogeographic, geomorphological, cartographic, granulometric, and mineralogical studies, several options for accumulating a large supply of sand were considered. It is shown that the development of the accumulative body of the Anapa Barrier Beach was determined by changes in the shore configuration, fluctuations in the sea level, as well as the direction and length of alongshore sediment flows. The Phanagorian regression interrupted the previous course of development of the accumulative geosystem of the Anapa Barrier Beach. The geosystem acquired its modern form during the Nymphean transgression. The accumulative body of the modern barrier beach was formed from the abrasion material of the indigenous shores of the Taman Peninsula and alluvium of the Kuban River. The alluvium came directly to the seashore during the Phanagorian regression.

Keywords: Black Sea, Caucasian coast, Anapa Barrier Beach, lithodynamic processes, sea-level fluctuations, accumulation, sediment flow, shoreline

Acknowledgments: The work was carried out under state assignment on topic FMWE-2021-0013.

For citation: Krylenko, V.V., Krylenko, M.V. and Krylenko, D.V., 2023. Material Accumulation in the Modern Accumulative Body of the Anapa Barrier Beach (Caucasian Coast of the Black Sea): Paleolithodynamic Prerequisites. *Ecological Safety of Coastal and Shelf Zones of Sea*, (4), pp. 19–33.

Палеолитодинамические предпосылки накопления материала современного аккумулятивного тела Анапской пересыпи (Кавказское побережье Черного моря)

В. В. Крыленко*, М. В. Крыленко, Д. В. Крыленко

Институт океанологии им. П.П. Ширшова РАН, Москва, Россия
** e-mail: krylenko.slava@gmail.com*

Аннотация
Анапская пересыпь – крупная голоценовая прибрежно-морская аккумулятивная форма, сформированная наносами терригенного и морского происхождения на северо-западе Кавказского побережья Черного моря. В последние десятилетия наблюдается отступание берега пересыпи. Основной причиной отступания являются природные процессы, обусловившие дефицит и перераспределение наносов в литодинамической системе пересыпи. На фоне повышения уровня моря отступание берега может ускориться, а в дальнейшем – привести к деградации всей геосистемы Анапской пересыпи. Целью работы является анализ и обобщение информации о происхождении слагающего аккумулятивное тело пересыпи материала и механизмах его перераспределения во времени и пространстве, что необходимо для оценок устойчивости современного аккумулятивного тела. На основе комплексного анализа, включающего ряд палеогеографических, геоморфологических, картографических, гранулометрических и минералогических исследований, проанализировано несколько вариантов накопления большого запаса песка. Показано, что развитие аккумулятивного тела Анапской пересыпи определялось изменениями конфигурации берега, колебаниями уровня моря, направлением и протяженностью вдольбереговых потоков наносов. Фанагорийская регрессия прервала предшествующий ход развития аккумулятивной геосистемы Анапской пересыпи, а современный вид геосистема приобрела в ходе нимфейской трансгрессии. Аккумулятивное тело современной пересыпи было сформировано из аллювия реки Кубани, поступавшего непосредственно на морской берег во время фанагорийской регрессии, и материала абразии коренных берегов Таманского полуострова.

Ключевые слова: Черное море, Кавказское побережье, Черноморское побережье Кавказа, Анапская пересыпь, литодинамические процессы, колебания уровня моря, аккумуляция, поток наносов, береговая линия

Благодарности: работа выполнена в рамках государственного задания ИО РАН, тема FMWE-2021-0013.

Для цитирования: *Крыленко В. В., Крыленко М. В., Крыленко Д. В.* Палеолитодинамические предпосылки накопления материала современного аккумулятивного тела Анапской пересыпи (Кавказское побережье Черного моря) // Экологическая безопасность прибрежной и шельфовой зон моря. 2023. № 4. С. 19–33. EDN QBVRWW.

Introduction

The Anapa Barrier Beach is a large Holocene coastal accumulative form formed by sediments of terrigenous and marine origin. It is located on the sea edge of the lowland alluvial plain of the north-eastern Black Sea region, in the junction zone of tectonic elements of the north-western (Caucasian) and sublatitudinal (Kerch–Taman) extension. The accumulative body of the 47-kilometer Anapa Barrier Beach (Fig. 1) is composed of quartz sand with an admixture of shell detritus and pebbles. Its width is maximum in the south-eastern part (almost 1.5 km) and decreases gradually to 150–200 m to the northwest. Transverse and longitudinal sediment flows are observed within the lithodynamic system of the Anapa Barrier Beach. The alongshore sediment flow is characterized by a bimodal regime with a predominance of transport to the south-east [1–4].

In recent decades, there has been a retreat of the barrier beach shoreline. In some areas, the retreat made about 80 m in 50 years [5]. The main reason for the retreat is the natural processes that caused the shortage and redistribution of sediments in the lithodynamic system of the barrier beach. With the sea level rising, the coast retreat may accelerate, and in the future, it may lead to degradation of the entire geosystem of the Anapa Barrier Beach [1].

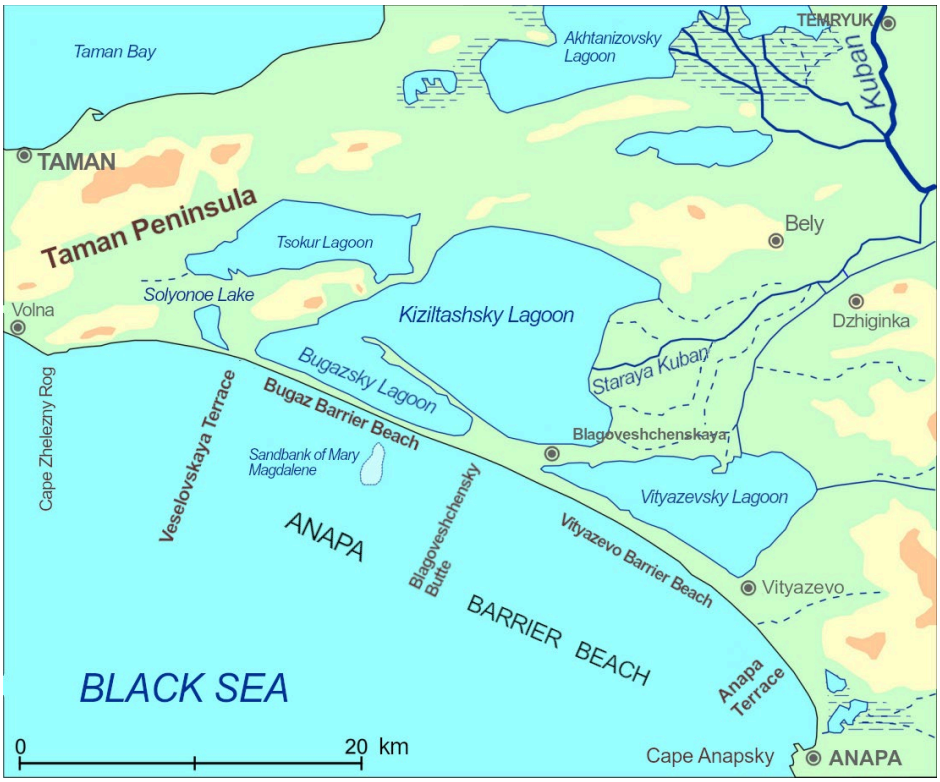

F i g. 1. Map of the Anapa Barrier Beach

To determine the limits of stability of the barrier beach accumulative body, it is necessary to obtain information about the origin of the material composing it and the reserves of such material. The paper aims to analyze and generalize information about the origin of the sediment material composing the accumulative body and the mechanisms of its redistribution in time and space, which is necessary for assessing the stability of the modern accumulative body. To analyze the origin of the accumulative forms of the Anapa Barrier Beach, it is necessary to consider the following important issues – what is the genesis of the material composing them, when and how it entered the lithodynamic system.

Materials and methods of research

Materials from geological surveys, field studies, remote sensing, archival and literary sources were used in the research. In the 1970s, a longitudinal drilling profile consisting of two dozens of wells with a depth of up to 200 m was made along the entire length of the Anapa Barrier Beach. At the same time, a transverse profile was drilled through the Staraya Kuban River valley along the Dzhiginka–Bely line [6]. In the early 2000s, a complex of studies was carried out (mollusk fauna, carbon dating, mineral and granulometric composition) based on the data from a network of wells with the depth up to 10 m (44 wells along 10 profiles). In 1998, archaeological and paleogeographical research was carried out on the Taman Peninsula, the purpose of which was to study the variation of the Black Sea level in the last 3–4 thousand years [7]. In 2005, Ya. A. Izmailov reconstructed the formation history of the Anapa Barrier Beach in detail, based on the analysis of a complex of geological and geomorphological data [6]. Since 2010, employees of the Southern Branch of the Institute of Oceanology of RAS and of the Faculty of Geography of Moscow State University have studied the processes of formation of land and underwater relief, landscape and morphological structure, spatial features of sediment distribution and hydrological regime on the Anapa Barrier Beach [1, 8–12].

Results and discussion

Stages and factors of formation of the Anapa Barrier Beach before the Phanagorian regression

Possible scenarios concerning the origin of the Anapa Barrier Beach have been studied by many researchers [6, 7, 13–16]. The formation of the accumulative body of the future Anapa Barrier Beach began with the end of the last ice age from the alluvium of the proto-Kuban, accumulated during the period of its direct flow into the Black Sea. As the sea level rose, part of the material moved along with the shoreline movement in the form of a bar, which is typical during the development of such accumulative forms [17]. It is possible that the material available at that time was sufficient to form accumulative forms that completely or partially blocked the baymouths.

After the Black Sea reached a level close to the modern one (5–5.5 kya) [18], the entire delta region of the Kuban River was flooded. The alluvium sedimentation

began after the formation of bays deeply cut into the land [1)]. In that period, the configuration of the indigenous shore was determined by the presence of several capes or islands, among which spits, barrier beaches or tombolos were formed. The rate and vectors of growth of accumulative forms were different. In different periods of time, their development could occur independently or concertedly.

From that moment, the formation of the Anapa Barrier Beach took place due to the material formed in the process of the indigenous shore abrasion and shells coming from the underwater slope. As studies of the sediment thickness of various profiles of the Anapa Barrier Beach show, the proportion of shells (shell detritus) is up to 5% in the total volume of sediments, and this value is almost independent of their age [1]. It is more difficult to determine the proportion of sediments resulting from abrasion. Since the abrasion shores to the north-west of the Anapa Barrier Beach have retreated over the past 5 thousand years to a distance of about 2 km, and some of their profiles have been completely washed away, the composition of their rocks is unknown. In the modern cliff, the content of beach-forming material is no more than 10%, the predominant part of which is represented by well-graded fine and medium sands of alluvial origin of the Pliocene age [2)]. After wave processing, these sands cannot be distinguished from the Kuban alluvium, so it is not possible to determine the share of abrasion material in the total volume of the Anapa Barrier Beach. The presence of abrasion material is indicated by the insignificant number of pebbles from ferruginized limestones, the source of which is considered to be rocky crags located on the underwater slope or at the base of Cape Zhelezny Rog. These pebbles are found in small quantities along the entire length of the barrier beach, including its rear part. The number and size of the pebbles decreases in the direction from the north-west to the south-east. In general, the lithodynamics of the modern Anapa Barrier Beach is determined by sands, while the influence of shells, and especially pebbles, is of a subordinate nature.

Rapid growth of the southern part of the future Anapa Barrier Beach occurred due to the predominance of sediment movement from the north-west to the south-east. The Anapa Cape, composed of rocks, retained incoming sediment, and the resulting accumulative forms remained stable and moved towards the sea. The rear part of the barrier beach is exactly the area where the most ancient surface accumulative sediments were discovered [6].

In the central part of the barrier beach, south of the Blagoveshchensky butte, several generations of beach and dune ridges are observed. The oldest and most distant from the sea ridges are located at an angle to the modern shoreline [10, 11, 19]. Probably, these ridges appeared when the configuration of the sea edge of the Blagoveshchensky butte was different, and the orientation of the spit that formed to the south-east of it differed from the orientation of the modern shoreline of the barrier beach.

[1)] Zenkovich, V.P., 1958. [*Morphology and Dynamics of the Black Sea Coasts Within the USSR Boundaries. Vol. 3, Part 3. Regional. Section 2. The Central Part (Southern Crimea, Kerch and Taman Peninsulas)*]. Moscow: Izd-vo Akademii Nauk, 187 p. (in Russian).

[2)] Azhgirey, G.D., ed., 1976. [*Geology of the Greater Caucasus*]. Moscow: Nedra, 262 p. (in Russian).

In the northern part of the Anapa Barrier Beach (within the Bugaz Barrier Beach), ancient generations of accumulative forms were not preserved, which was a consequence of the rapid destruction of the indigenous shores composed of unconsolidated rocks by the sea, and constant retreat of accumulative forms deep into the lagoon. Nevertheless, the existence of such accumulative forms is indicated indirectly by the fact that, according to [20–22], 3.5 kya, it was the Bugaz Barrier Beach, along which one of the most important land transport routes between the Taman Peninsula and the Anapa Region passed.

It is difficult to state when the complete destruction of the capes in the central part of the future Anapa Barrier Beach occurred, but this event led to significant changes in the lithodynamic regime. According to the work [6], the connection of the northern and southern parts (Bugaz and Vityazevo Barrier Beaches) with the formation of a uniform lithodynamic system took place no earlier than 2.5 kya. This connection is close in timing to the beginning of the Phanagorian regression (perhaps caused by it). Subsequently, the northern part of the formed abrasion-accumulative shore arc, more than 50 km long, shifted over time as accumulative forms retreated deeper into the bays [23], and the southern part moved out to the sea due to the growth of new generations of beach ridges.

In addition to spatial changes caused by accumulative or abrasion processes, the development of the accumulative body was complicated by fluctuations in the sea level. From the point of view of assessing the stability of the accumulative body of the modern Anapa Barrier Beach, the final stage of its formation is interesting, the beginning of which was stipulated by the Phanagorian regression and the subsequent Nymphean transgression.

Development of the Anapa Barrier Beach during the Phanagorian regression

The Dzhemetinsky stage (5.2–2.5 kya) [6] ended with a regression known in the Black Sea region as Phanagorian. Most modern researchers [24–27] estimate the decrease in sea level during the Phanagorian regression at 5.0–5.5 m relative to the previous and modern level.

In the work [22, p. 75], the authors wonder why no ancient authors “tell us about the presence of the vast Kiziltashsky (Paleo-Kuban) Lagoon.” According to the work [6], on the profile in the northern part of the Bugaz Barrier Beach (near the Bugaz spout) between the late Dzhemetinsky (dated 2660–2520 years ago) and Nymphean sediments (dated 1110 years ago), a layer of fine sands of the alluvial type with a base elevation of minus 6.6 m was observed, i.e. the level of the river bottom was significantly lower than the modern sea level. According to the profile in the central part of the Bugaz Barrier Beach between the Upper Dzhemetinsky (dated 2750 years ago) and Nymphean (dated 1940 years ago) sediments, a layer of the eolian sands with an absolute mark of the base minus 1.55 m was traced (at the same time, extrapolation shows high probability of tracing the marks of the base of the eolian sands to minus 2.5 m [6]). Taking into account the fact that the modern eolian sediments are located 1.5 m above the sea level, the sea level near the Bugaz Barrier Beach during that period was lower than the modern one by at least 3.5 m. At this sea level, the level of the lagoons connected to it hydraulically should have decreased by the same amount.

Taking into account the hydrological characteristics (the depths in most of the area of modern lagoons not exceeding 1 m) [28], the estimated value of the level drop and geological data, it can be argued that during the Phanagorian regression period (i.e., in ancient times), no extensive bays or lagoons existed in the place of the modern Kiziltashsky Lagoon.

The flow of the Kuban River into the sea was carried out through the water area of the lagoons, which dried out as the sea level decreased, along erosive channels carved out in previous sediments. The geological profile (Fig. 2) [29] shows two pronounced erosional channels filled with alluvial sands. The composition of the sediments indicates that current velocities were high enough to transport large volumes of driven sediments, in this case the sand. The bottom of the channels is located at minus 5 m. With no lagoons, the basis of erosion for the Kuban River during this period was the Black Sea level. Therefore, the Kuban River solid runoff flowed directly into the Black Sea during the period under consideration. In the above-mentioned paper [22, p. 75], the authors provide a figurative description of Hipponactus from Ephesus, ancient Greek poet (second half of the 6th century BC), presumably referring specifically to the Kuban mouth.

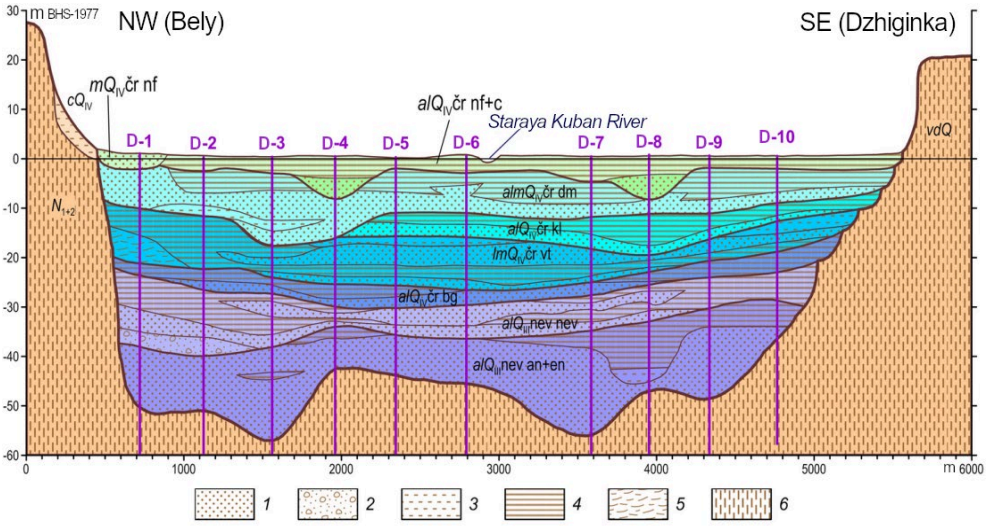

F i g. 2. Dzhiginsky geological profile across the Staraya Kuban River (adapted from [29, p. 82]). Lithological composition: 1 – sand; 2 – sand with pebbles; 3 – siltstone; 4 – clays; 5 – silts; 6 – loess. Genesis: a – river; l – lagoon; m – marine; v – eolian; d – slope; c – landslide. Age: N1+2 – Neogene; Q – Quaternary; an+en – Antsky-Yenikalsky; nev – Novoevksinsky horizon; nev nev – Novoevksinsky layer; QIVčr – Black Seahorizon; bg – Bugazsky; vt – Vityazevsky; kl – Kalamitsky; dm – Dzhemetinsky; nf – Nymphean, modern; D-5 – well numbers

Downcutting of a river channel into underlying sediments as a result of sea level decrease was observed during the Caspian Sea level drop in 1931–1945. At the mouth of the Kura River, the sea level drop did not affect the entire length of the longitudinal profile immediately, but spread from the mouth upstream gradually. In general, the decrease in the Caspian Sea level accompanied by the active downcutting of rivers on its western coast, contributed to a significant increase in the areas of mouth formations [3)]. This process was actively influenced by alongshore sediment flows and shell bars covering mouth parts.

As indicated in the work [30], with alongshore sediment flows, active downcutting of channels into the underlying sediments is not necessarily accompanied by a significant movement of the mouth parts towards the sea. Entering river sediments are actively involved in alongshore transport contributing to the development of accumulative form within the entire lithodynamic system. Probably, the Anapa Barrier Beach developed in a similar way during the Phanagorian regression.

Development of the Anapa Barrier Beach during the Nymphean transgression

During the Nymphean transgression, a vast water area with actively occurring hydro- and lithodynamic processes was formed again within the dried lagoons, as indicated by the presence of beach accumulative ridges and small lagoons at the foot of the indigenous slope. Dating of shell material from relict accumulative forms [15] makes it possible to attribute their formation to the middle of the 2nd millennium AD [20]. Similar, though more ancient, accumulative forms in the line between the village of Dzhiginka and the khutor of Bely can be traced in the form of two shell sand spits (approximate age 2.8–3.5 kya) directed towards each other from the western and eastern sides of the valley at level 2.5–4.5 m below modern sea level [20].

In the work [21, p. 339], it is suggested that during transgressive periods, "erosion and flooding of the Bugaz Barrier Beach took place with the transformation of the lagoon into a marine shallow open bay, the shores of which were exposed to the influence of the open sea waves." This assumption is confirmed by the formation of abrasion ledges on the indigenous sides of valleys and accumulative forms on the western shore of the Kiziltashsky Lagoon. In the work [20, p. 488], it is stated that "In the second half of the first millennium AD, a rise in sea level by 2–3 m caused the flooding of the ancient barrier beach that separated the paleo-Bugaz lagoon, and the short-term transformation of the lower reaches of the ancient Kuban (modern Kiziltashsky) Lagoon into an open sea bay." The authors of the work [20] argue that recovery of the barrier beach and formation of a lagoon with limited connection to the sea, which was subsequently filled with lagoonal-alluvial sediments, occurred only as the transgression slowed down.

[3)] Leontev, O.K., 1963. [*Brief Course of Marine Geology. A Textbook*]. Moscow: MGU, 461 p. (in Russian).

It should be noted that the authors of the works [20, 21] do not take into account the rates and mechanisms of formation of surface sandy capping forms under transgression conditions. The Nymphaean transgression was not catastrophic (as indicated by the lack of literary information). The Nymphean rise in sea level did not lead to the destruction of the Anapa Barrier Beach or its parts, but its accumulative body shifted towards the land. Under conditions of a gradual rise in level, sandy barrier beaches on shallow coasts exhibit the ability to shift along with the horizontal elevation of the shoreline towards the land [31, 32], maintaining their integrity and even morphological structure.

Thus, we believe that the Nymphean rise in sea level resulted not in the destruction of the Bugaz Barrier Beach, but rather in the displacement of its body towards the lagoon. At the same time, the lagoon basin was filled with water, and the size and configuration of the resulting water area determined the activation of abrasion-accumulation processes on its shores inevitably. Bilateral water exchange through the Bugaz spout determined the presence of shells of marine conch mollusks in the accumulative sediments on the lagoon shores (nowadays, shells are still found there). Lagoon level fluctuations influenced by floods or storm surges, contributed to the active abrasion of the lagoon shores. In some areas, abrasion is observed even now, after the river flow cutoff and in the actual absence of free water exchange with the sea.

Composition, age and mechanism of redistribution of the Anapa Barrier Beach modern sediments

In the southern and central parts of the Anapa Barrier Beach, the relief and sediment composition are distinguished by an ancient generation of coastal-marine sediments in the lagoonal part and a modern generation stretching along the seashore in a continuous bar up to 200 m wide. The structure and dynamics of this bar display features of both a full-profile beach and a dune ridge. The lower layers of sediments are represented predominantly by quartz sand with a significant (up to 30%) admixture of shells. In contrast to the sediments of more ancient parts of the barrier beach, the material of the new generation contains relatively few pebbles of ferruginized limestones. In the upper part of the sediments of the shoreline bar, well-graded quartz sands with a low (up to 3%) shell content occur and migrate actively.

In his work [1)], V. P. Zenkovich asks: “What is the origin of the pure (quartz) sands that form the outer bar of the southern and central part of the barrier beach? ... The formation of a clean sand bar more than 200 m wide in the eastern part of the barrier beach shows that there was a period when these masses of sand came from the bottom to the shore, but now such process is not observed.” By now, based on the materials of numerous studies, it is possible to propose several opinions concerning the origin of the material that became the basis for the modern generation of sediments in the central and southern parts of the Anapa Barrier Beach.

Opinion 1. The Phanagorian regression (a drop in sea level by 5 m in the period 2.5–1.7 kya) led to the resumption of alluvium entry from the Kuban River directly into the Black Sea coastal area. The alongshore transport

of this material to the south-east contributed to the extension of the coast and increase in the width of the beaches. The mineral and mechanical composition of the sediments (well-graded alluvial sands) favoured the growth of eolian formations that overlaid earlier sediments with a noticeable admixture of pebbles and shells.

Opinion 2. During the period of Phanagorian regression, sediments arriving from the north (sands mixed with pebbles and shells) were traversed and accumulated between a sandbank or island at the site of the modern Sandbank of Mary Magdalene (depth of 1–5 m). After the level rose, the alongshore transport of accumulated sediments to the southeast was resumed. Opinion 2 is easily combined with opinion 1 and even enhances it, but it does not inherently explain the simultaneous appearance of a large amount of well-graded sand in the southern part of the barrier beach.

Opinion 3. During the period of Phanagorian regression, sediment accumulation occurred in the form of a beach ridge near the shoreline, which was located more seaward and lower at that time. During the Nymphean transgression, that ridge was displaced towards the land and joined the previous generations of beach ridges. Opinion 3 is easily combined with opinion 1, but it does not inherently explain the origin of the sand.

Analysis of paleontological and archaeological finds makes it possible to clarify the time frame for the beginning of the arrival of large masses of sand. The Blagoveshchensky butte composed of Neogene clay loams is located in the central part of the Anapa Barrier Beach. The accumulative body of the barrier beach is attached to an ancient abrasion ledge and grows into a marine accumulative terrace. The Blagoveshchensky butte is characterized by a vast (about 20 ha) area in its north-western part, where the dunes are located on the surface of the indigenous shore, that is, they are raised relative to the level of the accumulative terrace to a height of 15–20 m [1]. The appearance of dunes on the surface of the Blagoveshchensky butte makes it possible to clarify the dating of the beginning of the movement of large masses of sand.

In the work [33], the ancient settlement of Blagoveshchensky-4, which existed from the 6th century BC to the 2nd–3rd century AD, is noted to the north of the dune massif. The settlement is oriented along an ancient road to the Bugaz Barrier Beach (Fig. 3). The abundance of pottery and no remains of capital structures make it possible to suggest that the settlement of Blagoveshchensky-4 was a logistics center where transshipment from sea vessels to land or river transport could be carried out. In accordance with the works [20, 21], one of the most important land transport routes passed there. In the work [33], unfortunately, no dune massif is mentioned. Meanwhile, a large number of fragments of ancient pottery were discovered on the surface of the indigenous clay loams under the dunes blown by wind [1]. Estimated datings made by A.M. Novichikhin and N.I. Sudarev, show that the earliest finds date back to the 6th century BC, and the latest ones – to the 2nd–3rd centuries AD. The given datings coincide with the datings of finds from the settlement of Blagoveshchensky-4 [33] and indicate that the eolian accumulative formations did not exist on the surface of the Blagoveshchensky butte at least until the beginning of the 3rd century AD.

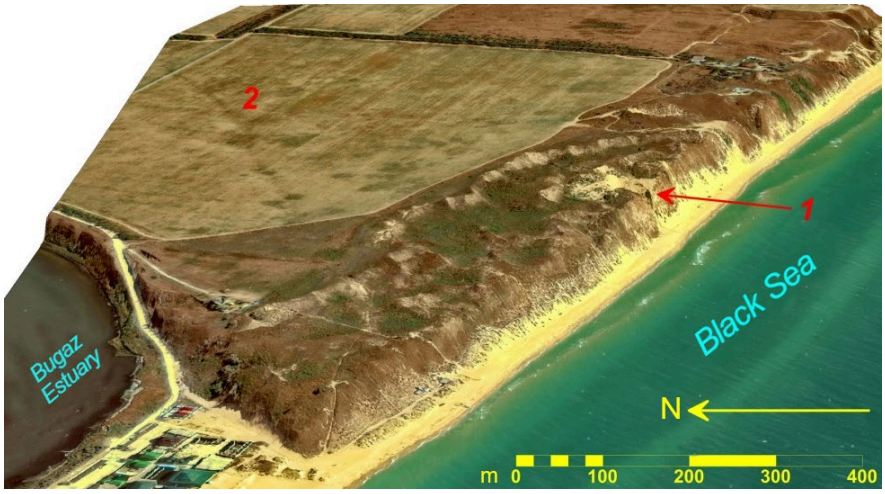

F i g. 3. Dune field on the NW tip of the Blagoveshchensky butte: *1* – dune; *2* – localization of the main finds of the ancient settlement of Blagoveshchensky-4 along an ancient road

After the comparison of paleogeographic reconstructions of the Black Sea level variation [6, 34] and archaeological data, it becomes possible to conclude that the formation of dunes on the butte surface occurred no earlier than the beginning of the Early Nymphean transgression around 1.7 kya. Perhaps, it was the consequences of this transgression that contributed to the cessation of economic activity in the indicated area of the Blagoveshchensky butte. The water level decrease in the lagoons cut off the Blagoveshchensky butte from a number of land transport routes [20], and the arriving sand prevented the use of this area.

Conclusion

The development of the accumulative body of the Anapa Barrier Beach was determined by changes in the shore configuration, fluctuations in the sea level, as well as the direction and length of alongshore sediment flows. More ancient generations formed during the Dzhemetinsky period, distant from the sea, and modern generations stretching along the coastal area, are clearly distinguished in the barrier beach structure. The coastal areas of the Anapa Terrace, the Vityazevo Barrier Beach, and the southern part of the Blagoveshchenskaya Terrace are of Nymphean age. The Nymphean generation of beach ridges, the formation period of which covers the last 1.5 thousand years, adjoins the ancient generation of beach ridges on the seaward side. Under the modern generation, a layer of sediments that chronologically occupies an intermediate position between the Nymphean and Dzhemetinsky generations, was revealed in the process of drilling. These sediments are represented by the silts of the lagoon type with the chronological range of accumulation 2.7–1.6 kya confirmed by a series of shell material carbon dating, which characterizes the period of sea level position 3.5–5.5 m below the modern one.

Thus, we have the sufficient grounds to assert that the Phanagorian regression interrupted the previous course of development of the accumulative geosystem of the Anapa Barrier Beach. The geosystem acquired its modern form during the Nymphean transgression. The accumulative body of the modern barrier beach was formed from the abrasion material of the indigenous shores of the Taman Peninsula and alluvium of the Kuban River. The alluvium came directly to the seashore during the Phanagorian regression. In general, it is possible to assume the following course of events:

– during the Phanagorian regression, the shoreline moves towards the sea and becomes stable;

– the Kuban River solid runoff (well-graded quartz sand) flows into the coastal zone of the sea again, being involved in alongshore transport;

– during the period of regression, the alluvium, which enters the coastal area and becomes redistributed along it, forms a beach ridge;

– a shallow lagoon is formed between the growing new and old beach ridges (it prevents the development of the eolian forms towards the shore);

– vegetation, including trees, appears along the shores of the lagoon;

– the Nymphean transgression mobilizes the formed beach ridge, which moves towards the shore, thus blocking the lagoon gradually;

– as the lagoon disappears, material from the new beach ridge is drawn into the eolian transport, accumulating along the rows of woody vegetation and forming ridges of stable dunes;

– when the sea level becomes stable, the intensity of sediment (primarily eolian) migration decreases gradually until the anthropogenic impact brings the system out of balance again.

References

1. Kosyan, R.D., Krylenko, V.V. and Krylenko, M.V., 2021. *Geosystem of the Anapa Bay-Bar*. Moscow: Nauchny Mir, 262 p. (in Russian).
2. Kosyan, R.D., Kosyan, A.R., Krylenko, V.V. and Fedorova, E.A., 2020. Distribution and Composition of Anapa Bay-Bar Sediments. *Oceanology*, 60(2), pp. 267–278. doi:10.1134/S0001437020020058
3. Divinsky, B. and Kosyan, R., 2018. Parameters of Wind Seas and Swell in the Black Sea Based on Numerical Modeling. *Oceanologia*, 60, pp. 277–287. doi:10.1016/j.oceano.2017.11.006
4. Kosyan, R., Divinsky, B. and Fedorova, E., 2018. Sandy Sediment Transport along Anapa Bay Bar (the Black Sea, Russia). In: K. Themistocleous, G. Papadavid, S. Michaelidas, V. Ambrosia and D. G. Hadjimitsis, 2018. *Proceedings of SPIE. Sixth International Conference on Remote Sensing and Geoinformation of the Environment (RSCy2018), 2018, Paphos, Cyprus*. Paphos. Vol. 10773. 107731A. doi:10.1117/12.2322835
5. Krylenko, V.V., 2015. Seashore Dynamics of the Anapa Bay-Bar. *Oceanology*, 55(5), pp. 742–749. https://doi.org/10.1134/S00014370150500709
6. Izmailov, Ya.A., 2005. [*Evolutionary Geography of Coasts of the Sea of Azov and Black Sea. Book 1. Anapa Bay-Bar*]. Sochi: Lazarevskaya poligrafiya, 175 p. (in Russian).
7. Kaplin, P.A., Porotov, A.V., Yanina, T.A., Gorlov, Yu.V. and Fouache, E., 2001. [Age and Formation Conditions in Bugazskaya Bay-Bar]. *Vestnik Moskovskogo Universiteta. Seria 5, Geografia*, (2), pp. 87–95 (in Russian).

8. Boyko, E., Krylenko, V. and Krylenko, M., 2015. LIDAR and Airphoto Technology in the Study of the Black Sea Accumulative Coasts. In: D. G. Hadjimitsis, K. Themistocleous, S. Michaelides and G. Papadavid, eds., 2015. *Proceedings of SPIE. Third International Conference on Remote Sensing and Geoinformation of the Environment, 2015, Paphos, Cyprus*. Paphos. Vol. 9535, 95351Q. https://doi.org/10.1117/12.2192577
9. Kravtsova, V.I., Krylenko, V.V., Drugov, M.N. and Boyko E.S., 2017. Investigation of Relief Dynamics at the North-Western Part of Anapa Bay Bar by Aerial Laser Scanning. *Geoinformatika*, (4), pp. 48-62 (in Russian).
10. Kravtsova, V.I., Tutubalina, O.V., Krylenko, V.V., Krylenko, M.V. and Chalova, E.R., 2015. Mapping the Anapa Bay-Bar Geosystems on the Basis of Satellite Remote Sens-ing and Ground Data. In: D. G. Hadjimitsis, K. Themistocleous, S. Michaelides and G. Papadavid, eds., 2015. *Proceedings of SPIE. Third International Conference on Remote Sensing and Geoinformation of the Environment, 2015, Paphos, Cyprus*. Paphos. Vol. 9535, 95351X. doi:10.1117/12.2193682
11. Kravtsova, V.I. and Chalova, E.R., 2018. Mapping of the Landscape-Morphological Structure of the Eastern Bugaz Part of Anapa Bay Bar by Digital Air-Survey Materials. *Izvestia Vuzov "Geodesy and Aerophotosurveying"*, 62(3), pp. 303–313. doi:10.30533/0536-101X-2018-62-3-303-313 (in Russian).
12. Krylenko, V.V., Goryachkin, Yu.N., Kosyan, R.D., Krylenko, M.V. and Kharitonova, L.V., 2021. Similarities and Differences of Small Bay-Bars of the North-Eastern Part of the Black Sea. *Ecological Safety of Coastal and Shelf Zones of Sea*, (1), pp. 63–83. doi:10.22449/2413-5577-2021-1-63-83 (in Russian).
13. Flerov, A.F., 1931. [Sandy Landscapes of the Azov and Black Sea Coasts, their Origin and Evolution]. *Izvestiya Gosudarstvennogo Geograficheskogo obshchestva*, 63(1), pp. 21–42 (in Russian).
14. Nevessky, E.N., 1957. [History of the Development of the Anapa-Beach]. In: IO RAS, 1957. *Trudy Instituta Okeanologii = Transactions of the Institute of Oceanology*. Moscow: Izd-vo AN SSSR. Vol. 21, pp. 165–174 (in Russian).
15. Izmailov, Y.A., Arslanov, K.A., Tertychnaya, T.V. and Chernov, S.B., 1989. [Reconstruction and Dating of Holocene Coastlines in Kuban-Delta Area (East Azov-Black Sea Region)]. *Vestnik LGU. Series 7: Geology, geography*, 3(21), pp. 61–69. (in Russian).
16. Izmaylov, Y.A. and Krylenko, V.V., 2016. *The Anapa Sand-Spit (Black Sea Coast): Geological Composition, Paleogeography and New Data on the Modern Dynamics. Routes of Evolutionary Geography*: *Proceedings of the Scientific Conference in Memory of Professor A.A. Velichko (Moscow, November 23–25, 2016).* Moscow: Institute of Geography RAS, pp. 118–123. (in Russian).
17. Leont'yev, I.O., 2014. *Morphodynamic Processes in the Coastal Zone of the Sea*. Saarbrücken: LAP LAMBERT Academic Publishing. 2014. 251 p. (in Russian).
18. Balabanov, I.P., 2009. *Paleogeographical Prerequisites of Formation of the Modern Environments and the Long-term Forecast of the Holocene Terraces Development on the Black Sea Coast of the Caucasus*. Moscow; Vladivostok: Dal'nauka, 350 p. (in Russian).
19. Krylenko, D.V., Krylenko, V.V. and Krylenko, M.V., 2022. Field Studies of the Structure of Sedimentary Strata of the Northern Part of the Vityazevskaya Bay-Bar. *Bulletin of Science and Practice*, 8(11), pp. 119–127. doi:10.33619/2414-2948/84/16 (in Russian).
20. Sudarev, N.I., Porotov, A.V. and Garbuzov, G.P., 2018. The Way from Sindica to Sindica: the Importance of Anapa Sandspit in the History of the Region. In: V. N. Zin'ko and E. A. Zin'ko, eds., 2018. *XIX Bosporan Readings. Cimmerian Bosporus and the World of Barbarians in Antiquity and the Middle Ages. Traditions and Innovations*, Kerch: IP Litvinenko E.A., pp. 485–493 (in Russian).

21. Porotov, A.V., Sudarev, N.I. and Garbuzov, G.P., 2021. Some Results of Studying the Paleogeographic Development of the Kuban Delta in Ancient Times. In: V. N. Zin'ko and E. A. Zin'ko, eds., 2021. *XXII Bosporan Readings. Cimmerian Bosporus and the World of Barbarians in Antiquity and the Middle Ages. New Discoveries, New Projects.* Kerch: IP Kifnidi G.I., pp. 335–344 (in Russian).
22. Sudarev, N.I., Porotov, A.V. and Garbuzov, G.P., 2022. On the Question of Ancient Roads and Crossings of the Southern Part of the Taman Peninsula. *Bosporos Studies*,(44), pp. 62–85 (in Russian).
23. Zenkovich, V.P., 1958. [*Coast of the Black and Azov Seas*]. Moscow: Geografgiz, 374 p. (in Russian).
24. Gorlov, Yu.V., Porotov, A.V., Yanina, T.A., Fouache, E. and Müller, C., 2002. The Historico-Geographical Situation on the Taman Peninsula in the Period of Greek Colonization. *Journal of Historical, Philological and Cultural Studies,* 12, pp. 248–257 (in Russian).
25. Porotov, A.V., Gorlov, Yu.V., Yanina, T.A. and Fouache, E., 2004. The Evolution of the Black Sea's Coastal Zone of Taman' Peninsular in the Late Holocene. *Geomorfologiya*, (4), pp. 63–77 (in Russian).
26. Gorlov, Yu.V., 2008. Geographical Situation on Taman Peninsula in Second Half of Holocene. *Journal of Historical, Philological and Cultural Studies*, (21), pp. 415–437 (in Russian).
27. Bolikhovskaya, N.S., Porotov, A.V., Kaitamba, M.D. and Faustov, S.S., 2014. Reconstruction of the Changes of Sedimentation Environments, Vegetation and Climate Within the Black Sea Part of the Kuban River Delta Area for the Last 7000 Years. V*estnik Moskovskogo Universiteta. Seria 5, Geografia*, (1), pp. 64–74 (in Russian).
28. Mikhailov, V.N., Magritsky, D.V. and Ivanov, A.A., eds., 2010. [*Hydrology of the Delta and Mouth Coastal Area of the Kuban*]. Moscow: GEOS, 728 p. (in Russian).
29. Izmailov, Ya.A. and Arslanov, Kh.A., 2006. Formation of the Anapa Sand-Spit and Late Holocene Fluctuation of the Black Sea Level. In: IGCP, 2006. *IGCP 521 Second Plenary Meet-ing and Field Trip "Black Sea-Mediterranean Corridor During the Last 30 ka: Sea Level Change and Human Adaptation"*. Odessa: Astroprint, pp. 81–82 (in Russian).
30. Fedorova, S.I., Chebanova, E.F., Artyukhin, Yu.V., Artyukina, O.I. and Kutz, A.G., 2010. [Reactions of Longitudinal Profiles and River Mouths of the Azov and Black Sea Basins to Variability of Natural Factors and Anthropogenic Impact]. In: MSU, 2010. *Erozionnye i Ruslovye Protsessy*. Moscow: MGU. Iss. 5, pp. 387–406 (in Russian).
31. Vykhovanetz, G.V., 2003. [*Aeolian Process Within Sea Coast*]. Odessa: Izd-vo Astroprint, 360 p. (in Russian).
32. Badyukova, E.N., Zhindarev, L.A., Lukyanova, S.A. and Solovieva, G.D., 2017. Large Accumulative Forms of Relief on the Southeastern Coast of the Baltic Sea. *Oceanology*, 57(4), pp. 580–588. https://doi.org/10.1134/S0001437017040026
33. Gorlov, Yu.V., Porotov, A.V. and Trebeleva, G.V., 2005. [*Archeological Site of Blagoveshchensky Butte*]. In: IA RAS, 2005. *Drevnosti Bospora*. Moscow. Iss. 8, pp. 143–158 (in Russian).
34. Porotov, A.V., 2013. Changes of the Black Sea Level During the Holocene According to Geo-Archeological Indicators. *Vestnik Moskovskogo Universiteta. Seria 5, Geografia*, (1), pp. 76–82 (in Russian).

Submitted 29.05.2023.; accepted after review 15.06.2023;
revised 11.10.2023; published 20.12.2023

About the authors:

Viacheslav V. Krylenko, Senior Research Associate, Shirshov Institute of Oceanology of the Russian Academy of Sciences, Southern Branch (36 Nakhimovsky Prospekt, Moscow, 117997, Russian Federation), Ph.D. (Geogr.), **ORCID ID: 0000-0001-8898-8479**, *krylenko.slava@gmail.com*

Marina V. Krylenko, Senior Research Associate, Shirshov Institute of Oceanology of the Russian Academy of Sciences, Southern Branch (36 Nakhimovsky Prospekt, Moscow, 117997, Russian Federation), Ph.D. (Geogr.), **ORCID ID: 0000-0003-4407-0548**, *krylenko@mail.ru*

Daria V. Krylenko, Engineer, Shirshov Institute of Oceanology of the Russian Academy of Sciences, Southern Branch (36 Nakhimovsky Prospekt, Moscow, 117997, Russian Federation), **ORCID ID: 0000-0002-2541-5902**, *dasha20000222@gmail.com*

Contribution of the authors:

Viacheslav V. Krylenko – concept development, data processing and analysis, article text preparation, cartographic and illustrative material

Marina V. Krylenko – problem statement, data processing and analysis, article text preparation

Daria V. Krylenko – literature review on the research problem, article text preparation

All the authors have read and approved the final manuscript.

Original article

Granulometric Composition of Sediments in the Coastal Zone of Koktebel Bay (Crimea)

K. I. Gurov

Marine Hydrophysical Institute of RAS, Sevastopol, Russia
e-mail: gurovki@gmail.com

Abstract
The paper aims to study the local features and factors of sediment fractional composition formation in the coastal zone of Koktebel Bay. The paper uses *in situ* data and the results of granulometric composition analysis of sediment samples from the swash and beach zones of Koktebel Bay to reveal that the beach sediments on the shoreline in the swash zone were represented by coarse gravel with the inclusion of medium and fine gravel. The material in the western and central parts of the coastal zone of the bay was moderately and poorly graded, while in the eastern part it was well graded. The granulometric composition of the beach material differed for the central and rear sections. The sediments in the central parts of the beaches were mainly represented by coarse gravel (27%) and coarse sand (26%) with inclusions of fine gravel (18%) and medium sand (14%). The material of gravel-sand beaches in the eastern part and the gravel beaches in the western part were well graded, while the beach material in the central study part was poorly graded. In the rear section of the beaches, the material was poorly graded and consisted mainly of coarse gravel, the portion of which decreases from the western part to the eastern one. In the samples from the rear part of the beaches, an increased proportion of silty material (1–13%) was noted. The features of the fractional composition of beach sediments are determined by the interception and retention of gravel material by numerous structures located directly in the shoreline, as well as by the supply of clay-sandy material as a result of wave abrasion of natural cliffs and its accumulation in the central section of the beaches as their width increases.

Keywords: Koktebel, coastal zone, sediments, beach, granulometric composition, anthropogenic impact

Acknowledgements: The work was carried out under state assignment on topic no. FNNN-2021-0005 “Coastal research”.

For citation: Gurov, K.I., 2023. Granulometric Composition of Sediments in the Coastal Zone of Koktebel Bay (Crimea). *Ecological Safety of Coastal and Shelf Zones of Sea*, (4), pp. 34–45.

Гранулометрический состав наносов береговой зоны бухты Коктебель (Крым)

К. И. Гуров

Морской гидрофизический институт РАН, Севастополь, Россия
e-mail: gurovki@gmail.ru

Аннотация
Цель работы – исследовать локальные особенности и факторы формирования фракционного состава наносов в береговой зоне бухты Коктебель. На основании данных натурных наблюдений и результатов исследования гранулометрического состава проб наносов из приурезовой полосы и пляжевой зоны бухты Коктебель установлено, что наносы пляжей на урезе в зоне заплеска представлены крупным гравием с включением среднего и мелкого гравия. Материал, отобранный в западной и центральной частях приурезовой полосы бухты, средне и плохо сортирован, а в восточной части – хорошо сортирован. По гранулометрическому составу материал пляжей в центральной и тыловой зонах различается. Наносы в центральной зоне пляжей представлены преимущественно фракциями крупного гравия (27 %) и крупного песка (26 %) с включениями мелкого гравия (18 %) и среднего песка (14 %). Материал гравийно-песчаных пляжей в восточной части исследуемой зоны и гравийных пляжей в западной ее части хорошо сортирован, а в центральной – материал пляжей плохо сортирован. В тыловой зоне пляжей материал плохо сортирован и состоит преимущественно из крупного гравия, доля которого от западной части к восточной уменьшается. В пробах наносов, отобранных в тыловой зоне пляжей, отмечается повышенная доля илистого материала (1–13 %). Особенности фракционного состава наносов пляжей определяются перехватом и удерживанием гравийного материала многочисленными сооружениями, расположенными непосредственно в приурезовой полосе, а также поступлением глинисто-песчаного материала в результате волновой абразии природных клифов и его накоплением в центральной зоне пляжей с увеличением их ширины.

Ключевые слова: Коктебель, береговая зона, наносы, пляж, гранулометрический состав, антропогенное воздействие

Благодарности: работа выполнена в рамках государственного задания ФГБУН ФИЦ МГИ по теме № FNNN-2021-0005 «Прибрежные исследования».

Для цитирования: *Гуров К. И.* Гранулометрический состав наносов береговой зоны бухты Коктебель (Крым) // Экологическая безопасность прибрежной и шельфовой зон моря. 2023. № 4. С. 34–45. EDN PYURTV.

Introduction

The coastal regions of Crimea are under active anthropogenic impact. Over the past 30 years, the intensification of anthropogenic activity in the coastal zone has caused disruption of the natural course of hydro- and geodynamic processes. As a result, the regulation of natural watercourses (a source of material for beach sediments), sand mining and active construction in the coastal zone led to the destruction of coastal infrastructure facilities.

The granulometric composition of sediments and the peculiarities of their distribution in the coastal zone are key parameters used in mathematical modelling of the morphodynamics of sand beaches [1].

The relevance of the study of coastal zone sediments on the Southeastern coast of Crimea in the zone of Koktebel Bay is primarily stipulated by the lack of current data on their granulometric composition (fraction content, average particle diameter, sorting coefficient), as well as a significant acceleration of development of the recreational potential of this region as a result of the implementation of the construction projects of the embankment and coastal protection structures.

The purpose of the paper is to investigate local features and factors of formation of the fractional composition of sediments in the coastal zone of Koktebel Bay. Previously, similar works were carried out by the author in relation to sections of the coastal zone of Kalamita Bay in general [2] and the Lake Sakskoye bay-bar in particular [3]. The obtained *in situ* data fill the gap of information about the structure and factors of bottom sediment formation in the area under study and can be used in the future when planning coastal protection measures aimed at the rational use of coastal zone resources.

Characteristics of study area

Koktebel Bay is a water area in the southeastern Crimea located from Cape Planerny in the west to Cape Chameleon in the east (Fig. 1). The length of the coastline of the bay is about 4000 m, the maximum depth is 15–20 m [4–6].

The shore of the bay is abrasion-landslide and abrasion-erosive. It is represented mainly by the cliff of homogeneous composition with a height of 3–30 m with narrow pebble-boulder beaches [4–6]. The cliffs are composed of Quaternary gravelly loams, Middle and Upper Jurassic clays [6]. The average rate of abrasion of the Koktebel Bay shores [1)] is 0.2–0.5 m/year. The width of the beaches is 5–10 m in the western, 30–40 m in the central and 3–10 m in the eastern parts of the bay.

After the regulation of shallow watercourses, which are a source of sediment material, the movement of clay-sand material into the study area decreased [4, 5]. Currently, the beach-forming material comes as a result of the destruction of cliffs in the western and eastern parts of the bay coastal zone. In the western part, most of the cliffs are actively built up. There is a cascade of coastal protection structures in the form of concrete groynes with a length of 65 m and a number of mooring walls up to 35 m long, located directly on the shoreline. These concrete structures disrupted the sediment transport system, which led to a complete reduction of beaches in this area. The most significant reason for the degradation of the natural complexes of the Koktebel Bay coastal zone was the construction of the embankment in the late 1960s and unauthorized private construction on adjacent sites in the 1990s, carried out without any necessary assessments of lithodynamic processes for this area [4].

[1)] Shnyukov, E.F., ed., 1982. [*Geology of the Shelf of the Ukrainian Soviet Socialistic Republlic. Environment. History and Study Methods*]. Kiev: Naukova Dumka, 180 p. (in Russian).

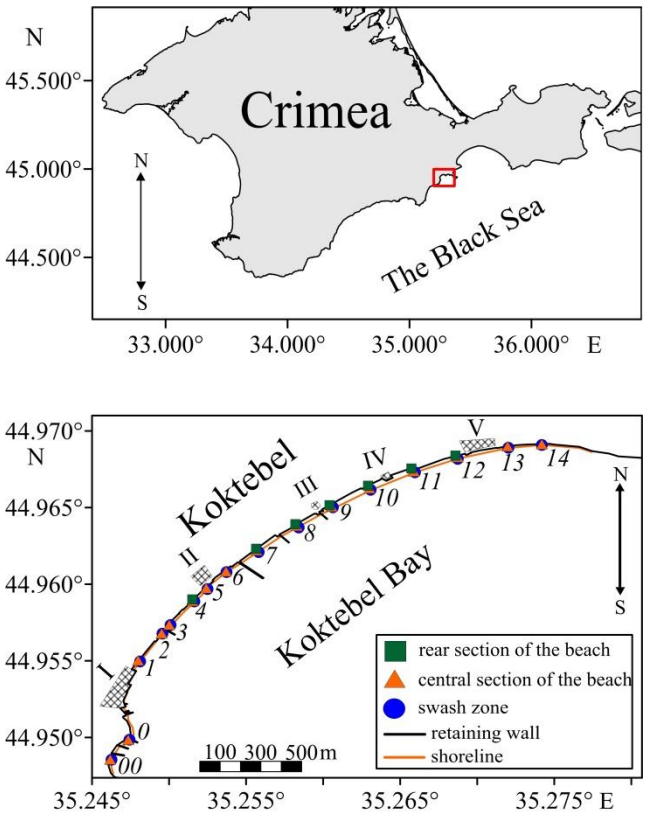

F i g. 1. Location of the study area (the red rectangular) (*a*); a map of soil sampling from the beach surface and the shoreline in the swash zone on the Koktebel Bay coast, 2021 (the Arabic numerals denote station numbers; the Roman numerals denote the following objects: I – Beliy Grifon Hotel Resort, II – M. A. Voloshin Memorial House, III – Koktebel Dolphinarium, IV – Junge Hill, V – boat sheds *Zhemchuzhina Koktebelya*) (*b*)

Materials and methods

Sediment samples from the Koktebel Bay coastal zone in areas near the shoreline (in the swash zone), as well as in the central and rear sections of the beaches, were taken in November 2021. The granulometric composition of bottom sediments was determined by the mass content of particles of various sizes, expressed as a percentage relative to the mass of the dry soil sample taken for analysis

(GOST 12536-2014). The screening of the sediment samples was carried out using a set of sieves with 10; 7; 5; 2.5; 2; 1; 0.5; 0.25; 0.1; 0.05 mm holes. Sampling spots on the surface of beaches and near the water shoreline were selected in such a way that it was possible to assess how coastal protection structures affect the granulometric composition of the material moving along the shore.

Cumulative curves were used to visualize the data of granulometric analysis of sediment samples, as well as to calculate some characteristic coefficients.

Cumulative curves are especially valuable for calculating various granulometric coefficients, in particular those proposed by P. Trask [7] and W. Krumbein [8] of the average (median) particle diameter (M_d), grading coefficient (S_o) and asymmetry coefficient (S_k).

The average (median) diameter (M_d), i.e. the second quartile, or the grain size relative to which half of the grains is larger and the other half is smaller, is determined directly from the cumulative curve: from the point of the curve with an ordinate of 50%, the perpendicular is lowered onto the abscissa axis, thus determining the desired size. The average diameter is an important characteristic of the granulometric composition of the sample, since it determines its granulometric type, although often roughly [2)].

The grading coefficient is determined with the following formula:

$$S_o = \sqrt{\frac{Q_3}{Q_1}},$$

where Q_3 and Q_1 – values of the third and first quartiles, i.e. the particle sizes corresponding to the ordinates of 25 and 75%, respectively, when the values of the size and proportion of the largest fractions are set from the beginning of the coordinate axes.

In well graded sands and siltstones $S_o < 1.5$; in medium graded ones $S_o = 1.5–2$ and in poorly graded ones $S_o > 2$.

The asymmetry coefficient (S_k) is calculated in accordance with the following formula:

$$S_k = \frac{Q_1 \ Q_3}{M_d^2}.$$

With $S_k > 1$, fine fraction prevails in the sediment; with $S_k < 1$, large fraction prevails.

Results and discussion

The features of the spatial distribution of granulometric fractions in the Koktebel Bay coastal zone are shown in Fig. 2.

It has been established that, according to the granulometric composition, sediments in the Koktebel Bay coastal zone are quite diverse. It is noted that on the shoreline the coarse-grained pebble-gravel material prevails.

[2)] Parmuzina, L.V., 2011. [*Granulometric Analysis of Sandy-Aleuritic Rocks: Guidelines for Performance of Laboratory Work under discipline Lithology of Natural Gas and Oil Reservoir for Students with Major in Oil and Gas Geology*]. Ukhta: UGTU, 23 p. (in Russian).

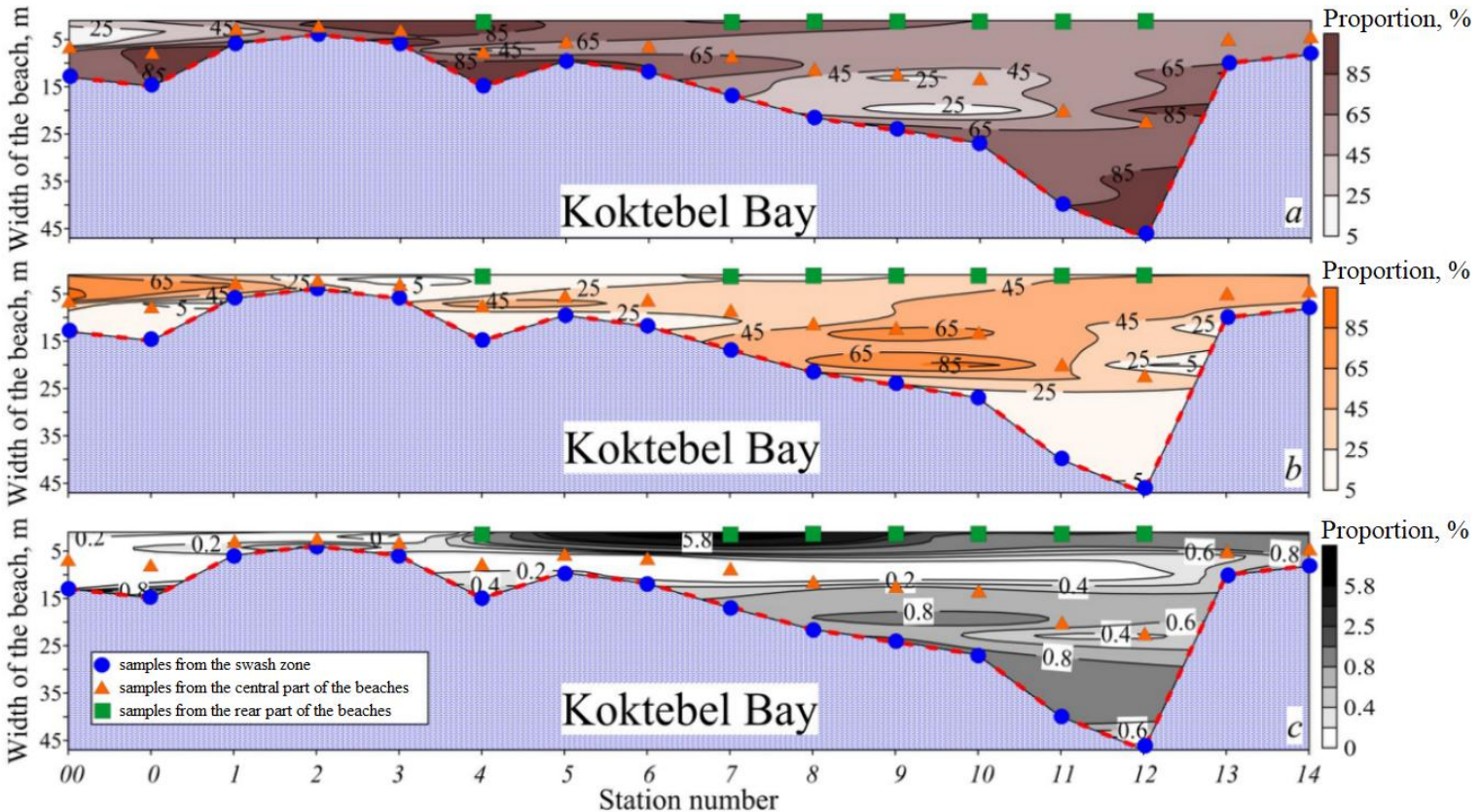

F i g. 2. Spatial distribution of the gravel (*a*), sand (*b*), and silt (*c*) fractions in the sediments of the Koktebel Bay shoreline. The dashed curve denotes the shoreline

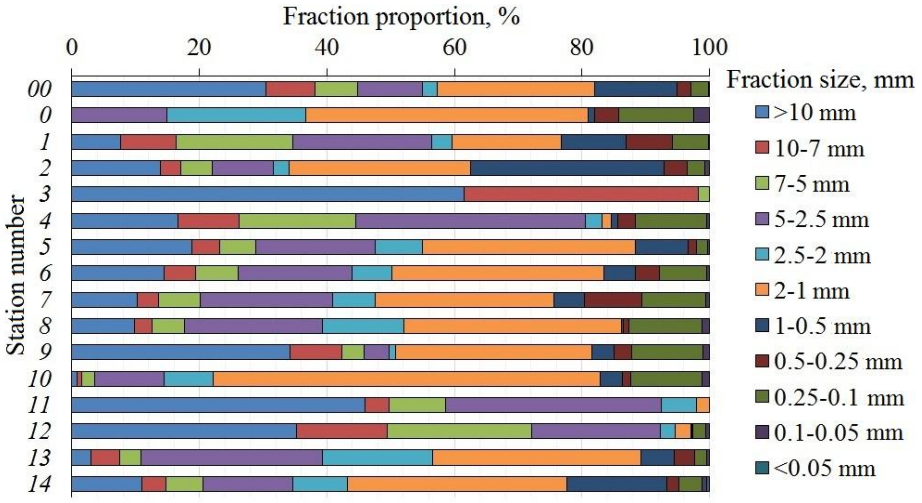

F i g. 3. Spatial distribution of the bottom sediment fractions at the shoreline in the swash zone of Koktebel Bay coast

Its share averages 84% and increases within the study area from west to east. The proportion of sand material in the coastal zone is insignificant (on average 15%) and is represented by coarse and fine-grained fractions. The proportion of fine-grained fraction does not exceed 1%. An analysis of the features of the spatial distribution of sediment material by size in the coastal zone made it possible to single out several characteristic areas (Fig. 3).

The first area (stations *00–2*) is characterized by dense anthropogenic development including a cascade of coastal protection structures (groynes), as well as dwelling houses and recreational facilities located close to the shoreline. It resulted in a limitation of the flow of sediment coming from the shore abrasion in the western part of the bay and a decrease in the proportion of gravel material in this area. The groyne in the area between stations *2* and *3* seems to prevent the sediment flow from east to west. For this area, the maximum proportion of the sand fraction in the coastal zone sediments is noted (on average 24%), which is reflected in the increased values of S_k (Fig. 4).

The second area (stations *3–11*) is characterized by the material that is heterogeneous in its granulometric composition, which is reflected in the values of the grading coefficient: in the area between stations *4* and *9*, it is 1.9 on average (Fig. 4). On the stretch of coastline between stations *3* and *7*, a decrease in both the proportion of gravel material and its size is observed. This is stipulated by the filling of beaches in this area, as well as the location of hydraulic structures intercepting sediment material moving along the shoreline. In addition, an increase in the width of the beaches from west to east leads to the movement of sand material into the coastal zone. Thus, the amount of coarse-grained material

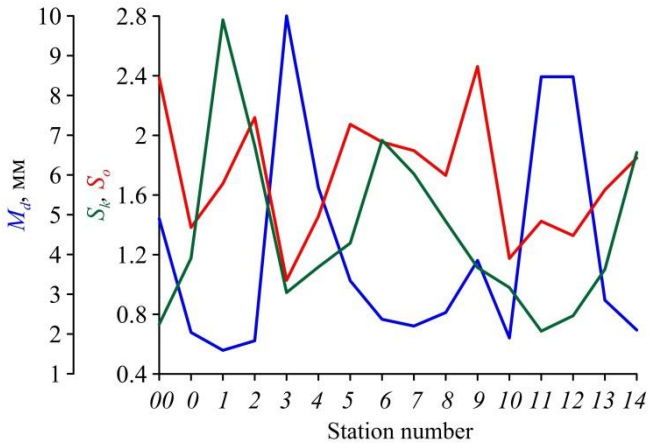

F i g. 4. Spatial distribution of granulometric coefficients for the samples taken at the shoreline in the swash zone

moving from west to east decreases, and the proportion of sand material coming from the beach to the shoreline increases.

As for the third area (stations *12–14*), an increase in the content of sand (from 2 to 21%) and silty (0.4 to 1.2%) material is observed, on the one hand, and a decrease in the proportion of gravel material (from 97 to 78%), on the other. In this area, the increase in the proportion of sand and silty fractions is determined by the structure of cliffs formed by clay-sand material. Since the cliffs in the eastern part of the Koktebel Bay coastal zone are not developed, the clay-sand material entering the coastal zone as a result of wave abrasion is the main source of terrigenous matter for beach sediments. This is also reflected in the S_k coefficient increase (Fig. 4).

The samples taken on the shoreline were characterized by varying degrees of grading. The material in the first and second areas is medium and poorly graded, and in the third one it is well graded (Fig. 4). Rather weak, though obvious, correlation dependence of the grading coefficient on the size of the material was obtained. The correlation of S_o with the gravel fraction was −0.5, and with the sand fraction it was 0.5. Another dependence, more explicit one, was obtained when comparing the values of M_d and the proportion of sand and gravel material. It was found that the correlation of M_d with the gravel fraction was 0.8, and with the sand fraction it was −0.8.

Since the width of the beaches of the Koktebel Bay coastal zone varies significantly, the granulometric composition of sediments in the central and rear sections of the beaches is quite diverse.

It was found that sediments in the central section of beaches were mainly represented by fractions of coarse gravel (27%) and coarse sand (26%) with inclusions of fine gravel (18%) and medium sand (14%). The proportion of coarse-grained

gravel is maximum in the sediments of beaches in the western part of the study area, which is explained by its accumulation in the groyne spacing. From west to east, the proportion of coarse and medium-grained gravel decreases, while the proportion of fine-grained gravel increases. The proportion of coarse (1–0.5 mm) and medium (0.5–0.25 mm) sand fractions, on the contrary, increases from the western part of the area to the eastern one. The features of the spatial distribution of gravel and sand material in the central section of beaches are determined by the morphometric parameters of the beaches themselves (width, angle of inclination), the nature of development in the coastal zone, as well as the type of cliff rocks in the areas not affected anthropogenically.

The heterogeneity of the spatial distribution of granulometric composition fractions in beach sediments made it possible to identify several characteristic areas (Fig. 5).

The first area (stations *00–4*) is characterized by the greatest heterogeneity of the beach material, alternating zones of accumulation of gravel and sand fractions. First of all, this is stipulated by the minimum width of the beaches and the maximum level of anthropogenic impact on the section of the coastal zone in this area. Zones of accumulation of gravel material (stations *0*, *2*, *3*) are located between coastal protection structures (groynes) and in areas with a minimum width of the beach (up to 5 m), near the buildings located close to the shoreline. The maximum concentration of sand material at station *00* is explained by its moving as a result of the natural cliff abrasion. Spatial heterogeneity of the material affected the M_d values, which vary in a wide range from 0.7 for medium and coarse-grained sand sediments to 10 for coarse-grained gravel sediments. The maximum values of the M_d parameter at stations *2*, *3* are explained by the minimum width of the beaches and the movement of coarse-grained gravel material from the coastal zone.

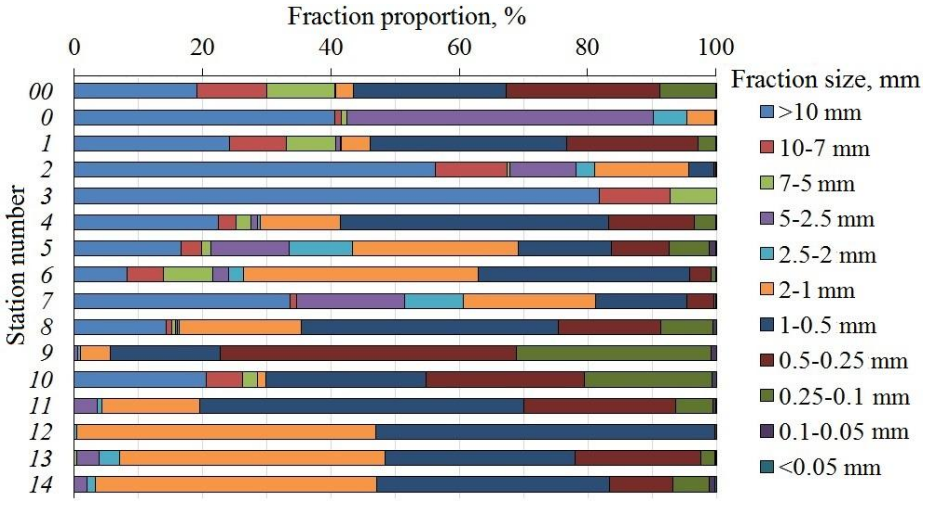

F i g. 5. Spatial distribution of bottom sediment fractions in the central section of the beaches

In the second area (stations *5–10*), a decrease in the proportion of gravel material from west to east (from 77 to 2%) is observed with an increase in the proportion of sand material (from 22 to 97%). Increased proportion of coarse-grained fraction (62–78%) at the beginning of this area (stations *5–7*) is explained by the fact that there are two piers with extensions located close to the shoreline, and the width of the beaches does not exceed 15 m. In the second half of this area (stations *9–10*), an increase in the width of the beaches (up to 40 m) and the absence of structures near the shoreline seem to result in the absence of the sand material in the longshore sediment flow in the central section of the beaches and to its accumulation. The maximum proportion of fine-grained sand fraction (27%) and the minimum value of M_d equal to 0.6 for the entire coastal zone under study are noted in this area.

The third area (stations *11–14*) is characterized by a gradual decrease in the width of the beaches from 43 to 5 m. As a result, the amount of sand material decreases, and the amount of gravel one increases. A slight increase in the proportion of silty material is explained by its moving from the cliffs composed of clay-sand sediments in the rear section of the beach.

In general, the material in the central section of beaches is medium graded (1.8). The material of gravel-sand beaches in the eastern part of this section and gravel beaches in its western part is well graded, and in the central part the material of beaches is poorly graded (Fig. 6). At stations *5*, *8*, *11*, the bicomponent structure of sediments formed as coarse-grained gravel, as well as coarse and medium-grained sand, leads to the fact that at these stations the sediment material is not graded as much as possible (S_o is 2.7, 3.2 and 3.3, respectively). The average median diameter was 2.6, which is significantly higher than the values obtained in [9].

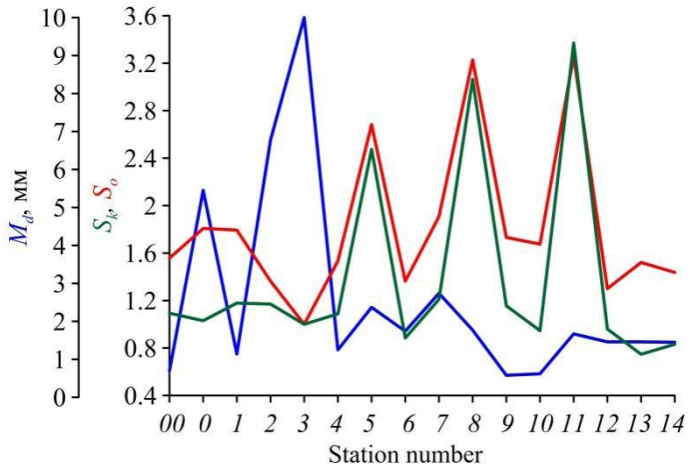

F i g. 6. Spatial distribution of granulometric coefficients for the samples taken in the central section of the beaches

Additionally selected material in the rear section of the beaches at stations *4*, *7–12* showed that the sediments are composed mainly of coarse gravel (on average 60%). The ratio of gravel and sand material at these stations is diametrically different from the composition of sediments in the central section of beaches. In some areas, sediments are sprinkled with a 5–12 cm layer consisting of small pebbles and coarse gravel, followed by mixed gravel-sand sediments with the inclusion of detritus and plant residues. Apparently, this is stipulated by the supply of coarse-grained gravel material into the rear section of the beach during severe storms and its accumulation there. The increased proportion of silty material (up to 13%) in the sediments of the beaches rear section due to the absence of natural cliffs and total development of the coastal zone may be explained by the moving of these sediments with stormwater runoff from nearby sites.

Conclusions

Significant anthropogenic impact on the Koktebel Bay coastal zone (coastline concreting, construction of dams, piers, dwelling, recreational and technical buildings located close to the shoreline) resulted in the disruption of natural processes of sediment material supply and its transport. As a result, the granulometric composition of sediments in the coastal zone (in the swash zone) and in the central and rear sections of beaches differs significantly.

Sediments on the shoreline are represented by gravel material of various sizes. The proportion of sand material in the sediments of the coastal zone averaged 15%, and the proportion of silty ones is less than 1%. The degree of grading of the material is average with minimum values in the eastern part of the coastal zone and with maximum values in its central part. The features of the fractional composition of sediments on the shoreline are determined by two factors: 1) interception and retention of coarse and medium-grained material by numerous structures located directly in the coastal zone; and 2) increase of the beach width and movement of sand material.

According to the granulometric composition, the material of the beaches in the central and rear sections differs. The central section of the beaches is characterized by sediments consisting of coarse and fine-grained gravel with the inclusion of coarse and medium-grained sand. The median diameter of beach sediments decreases from the western part of the coastal zone to the eastern one, and the degree of grading increases from the periphery to the central part of the coastal zone. Sediments in the rear section of the beaches are poorly graded and formed by coarse gravel with inclusions of silty material, which comes with stormwater runoff from nearby sites and accumulates with no material dynamics.

REFERENCES

1. Gurov, K.I. and Fomin, V.V., 2021. Influence of Storm Conditions on Changes in the Granulometric Composition of Bottom Sediments in the Coastal Zone of the Western Crimea. *Ecological Safety of Coastal and Shelf Zones of Sea*, (2), pp. 30–46. doi:10.22449/2413-5577-2021-2-30-46 (in Russian).
2. Gurov, K.I., 2018. Results of Sediment Granulometric Composition Monitoring in Coastal Zone of the Kalamitsky Bay. *Ecological Safety of Coastal and Shelf Zones of Sea*, (3), pp. 56–63. doi:10.22449/2413-5577-2018-3-56-63
3. Gurov, K.I., 2020. Results of Coastal Zone Dynamics and Beach Sediment Granulometric Composition Monitoring in the Central Part of the Kalamitsky Gulf. *Ecological Safety of Coastal and Shelf Zones of Sea*, (1), pp. 36–46. doi:10.22449/2413-5577-2020-1-36-46 (in Russian).
4. Goryachkin, Yu.N., ed., 2015. *The Current State of the Coastal Zone of Crimea.* Sevastopol: ECOSI-Gidrofizika, 252 p. (in Russian).
5. Goryachkin, Yu.N. and Dolotov, V.V., 2019. *Sea Coasts of Crimea*. Sevastopol: Colorit, 256 p. (in Russian).
6. Vronskiy, A.A., Krivobokov, E.M., Kostenko, N.S., Baranov, I.A., Beskaravaynyy, M.M., Budashkin, Yu.I., Vladimirov, E.I., Klyukin, A.A., P'yanykh, S.V. [et al.], 1997. [*Health Resort Koktebel*]. Kiev: Naukova Dumka, 134 p. (in Russian).
7. Trask, P.D., 1932. *Origin and Environment of Source Sediments of Petroleum.* Houston, USA: Gulf Publishing Co., 323 p.
8. Krumbein, W.C., 1936. Application of Logarithmic Moments to Size-Frequency Distribution of Sediments. *Journal of Sedimentary Research*, 6(1), pp. 35–47. https://doi.org/10.1306/D4268F59-2B26-11D7-8648000102C1865D
9. Bratus, O.S., 1965. [Granulometric Composition of Arenaceous Beach-Deposits of Crimea]. *Doklady Akademii Nauk SSSR*, 163(2), pp. 431–434 (in Russian).

Submitter 26.05.2023; accpeted after review 20.06.2023;
revised 11.10.2023; published 20.12.2023

About the author:

Konstantin I. Gurov, Junior Research Associate, Marine Hydrophysical Institute of RAS (2 Kapitanskaya Str., Sevastopol, 299011, Russian Federation), **ORCID ID: 0000-0003-3460-9650, ResearcherID: L-7895-2017**, *gurovki@gmail.com*

The author has read and approved the final manuscript.

Original article

A Software Tool for Operative Data Preparation for Assessing the Structure of Longshore Sediment Flows in the Coastal Zone of the Sea

V. V. Dolotov *, V. F. Udovik

Marine Hydrophysical Institute of RAS, Sevastopol, Russia
* *e-mail: dolotov_v_v@mhi-ras.ru*

Abstract
The paper describes the geoinformation software developed for automated formation of an array of input parameters necessary to assess the direction and relative intensity of alongshore sediment flows using the wind energy method. This method establishes a direct relationship between the energy of wind action on the water surface and the intensity of sediment movement. The method can be applied to calculations for shallow and relatively straight coastal sections with sand and gravel deposits. As input parameters, the software uses information about both the wind direction and speed, as well as the length of the wave acceleration along the sectors of different directions and the average depth along the acceleration rays. These parameters are individual for each segment of the approximation of the study coast section. The possibility of using wind data as the only parameter characterizing the driving force provides an advantage when using the method to conduct preliminary and reconnaissance assessments of the structure and main parameters of sediment movement in the areas that are poorly studied or not covered with disturbance data. The basics of the method were developed in the absence of computer technology. Therefore, the considerable complexity of preparing regional data limited the possibility to detail the coastline when approximating it by a piecewise linear function. The same limitation was imposed on the number of sectors in the wind direction when calculating the energy interpreted as a sediment movement force. The development and availability of modern geoinformation technologies in terms of creating new digital models of the bottom relief or using existing ones predetermined that the authors develop a modified version of the calculation scheme of the wind energy method and a specialized software tool to automate the preparation stage of a set of regional input parameters. The software allows to significantly accelerate preparation of digital data arrays to clarify the structure of sediment flows for extended sections of the coastal zone of Western Crimea.

Keywords: longshore sediment flows, wind energy method, wind-wave regime, GIS, lithodynamics processes, coastal zone, automation of calculations

Acknowledgments: The work was performed under state assignment of MHI RAS on topics no. 0827-2020-0004 “Coastal research”.

For citation: Dolotov, V.V. and Udovik, V.F., 2023. A Software Tool for Operative Data Preparation for Assessing the Structure of Long-Shore Sediment Flows in the Coastal Zone of the Sea. *Ecological Safety of Coastal and Shelf Zones of Sea*, (4), pp. 46–55.

Программный инструмент оперативной подготовки данных для оценки структуры вдольбереговых потоков наносов в прибрежной зоне моря

В. В. Долотов *, В. Ф. Удовик

Морской гидрофизический институт РАН, Севастополь, Россия
* *e-mail: dolotov_v_v@mhi-ras.ru*

Аннотация
Описываются результаты разработки геоинформационного программного инструмента, предназначенного для автоматизированного формирования массива входных параметров, необходимых для оценки направления и относительной интенсивности вдольбереговых потоков наносов с использованием ветроэнергетического метода. Указанный метод устанавливает непосредственную связь между энергией ветрового воздействия на водную поверхность и интенсивностью перемещения наносов. Его применение корректно в случае выполнения расчетов для отмелых и относительно прямолинейных участков береговой зоны с песчано-гравийными наносами, при этом в качестве входных параметров используется информация о направлении и скорости ветра, а также длина разгона волнения по секторам различного направления и средняя глубина по лучам разгона. Указанные параметры являются индивидуальными для каждого отрезка аппроксимации исследуемого участка побережья. Возможность использования данных о ветре как о единственном параметре, характеризующем вынуждающую силу, предоставляет преимущество при использовании метода для проведения предварительных и рекогносцировочных оценок структуры и основных параметров движения наносов в малоизученных и не обеспеченных данными о волнении районах. Основы метода разрабатывались в условиях отсутствия вычислительной техники, поэтому значительная трудоемкость подготовки региональных данных накладывала ограничения на возможности детализации береговой линии при ее аппроксимации кусочно-линейной функцией. То же ограничение накладывалось и на количество секторов по направлению ветра при подсчете энергии, интерпретируемой в качестве наносодвижущей силы. Развитие и доступность современных геоинформационных технологий в части создания новых либо использования уже существующих цифровых моделей рельефа дна послужили предпосылкой к разработке авторами модифицированного варианта расчетной схемы ветроэнергетического метода и специализированного программного инструмента для автоматизации этапа подготовки набора региональных входных параметров. Практическое его применение позволило значительно ускорить процесс подготовки цифровых массивов данных для уточнения структуры потоков наносов для протяженных участков береговой зоны Западного Крыма.

Ключевые слова: вдольбереговые потоки наносов, ветроэнергетический метод, ветро-волновой режим, ГИС, литодинамические процессы, береговая зона моря, прибрежная зона, автоматизация расчетов

Благодарности: работа выполнена в рамках государственного задания ФГБУН ФИЦ МГИ по теме № 0827-2020-0004 «Прибрежные исследования».

Для цитирования: *Долотов В. В., Удовик В. Ф.* Программный инструмент оперативной подготовки данных для оценки структуры вдольбереговых потоков наносов в прибрежной зоне моря // Экологическая безопасность прибрежной и шельфовой зон моря. 2023. № 4. С. 46–55. EDN PTTPUK.

Introduction

The study of lithodynamic processes in the coastal zone of the sea is one of the most important and relevant areas in the development of scientific research in the coastal zone of the seas, which is reflected in a variety of both classical [1), 2)] [1, 2] and modern [3)] [3–5] publications. This is stipulated by the urgent need to use the results of such research when studying the state of sea coasts and forecasting trends in their development, manifested both in natural conditions and under various scenarios of anthropogenic impact. Such results are especially important when implementing projects of large-scale technogenic transformation of the coastal zone, aimed at preserving coastal areas in use and infrastructure facilities located on them. The projects for the development of new promising regions of the Russian Federation, which primarily include hard-to-reach areas on the Arctic and Far East coast, can serve as one more example.

In such cases, the main direction of engineering surveys is to identify and clarify the qualitative and quantitative characteristics of the coastal topography transformation in the work area at various spatial and temporal scales under the influence of natural and anthropogenic factors. At the same time, at the initial stages of planning and feasibility studies of projects, it is often necessary to obtain information about the main cause-and-effect relationships between the wind-wave regime and the longshore movement of sediments within the boundaries of a separate coastal section in a short time.

In the absence of the required amount of field observation data, it is now possible to use methods based on simplified empirical and semi-empirical relationships so that to obtain the required preliminary information with a minimum set of input parameters promptly and to solve such problems [3), 4)]. Most of such methods were developed before the implementation of computer technology. However, they are still relevant today. Thus, the research is conducted, primarily aimed at calibrating coefficients while maintaining the basic calculation formulas [6].

[1)] Zenkovich, V.P., 1962. [*Fundamentals of Theory of Marine Coasts Development*]. Moscow: Nauka, 710 p. (in Russian).

[2)] Longinov, V.V., 1963. [*Dynamics of the Coastal Area of Tideless Seas*]. Moscow: Izd-vo Akademii Nauk, 379 p. (in Russian).

[3)] CERC, 1984. *Shore Protection Manual*. Vicksburg: Coastal Engineering Research Center. Vol. II. 652 p.

[4)] Production and Research Institute for Engineering Survey for Construction, 1975. [*Manual on Methods for Investigations and Calculations of Sediment Transport and Coastal Dynamics in Engineering Surveys*]. Moscow: Gidrometeoizdat, 239 p.

The development and availability of digital technologies, especially in terms of creating new digital models of the bottom relief or using existing ones, predetermined that the authors develop a modified version of the calculation scheme of the known wind energy method (WEM). Subsequently, it resulted in a specialized software tool to automate the preparation stage of a set of regional input parameters.

The paper is aimed at the development of software algorithms and a simple tool for spatial calculations of coefficients determined by the influence of external conditions on the characteristics of sediment flows.

Materials and methods of research

Hydrometeorological methods should be highlighted among the calculation methods for the operational assessment of the direction and intensity of sediment flows, which determine the main trends in the topography transformation of the coastal zone relief [9]. Based on the results of a large number of studies and field observations, they are successfully used in order to solve practical issues related to the implementation of coast protection, construction of hydraulic structures, maintenance of port water areas and approach channels. As a rule, such geomorphological characteristics of the study area as bottom topography, coastline detail and particle size distribution of offshore sediments, influence the choice of a specific calculation scheme.

In shallow and relatively straight coastal sections with sand and gravel deposits, the WEM, which was proposed in the 1930s [5), 6)] and was subsequently developed and improved [7), 8)], is recommended for usage [7–9]. This method establishes a direct connection between the energy of wind action on the water surface and the intensity of sediment movement. The calculation scheme is based on the summation of energy transferred to the aquatic environment under winds of different directions relative to the coastline orientation. In this case, the entire range of wind directions is divided into separate sectors, for each of which the general expression for the transmitted energy is written in the following form:

$$e = p \cdot W^n \cdot D^m, \quad (1)$$

where p – wind frequency within a sector (in relative units or percentage); W – average wind speed; D – length of wind acceleration over the water surface;

---

5) Munch-Petersen, I., 1933. [Sediments Transport Along Shores of Tideless Seas. Conference Report]. In: LGGI, 1933. P*roceedings of the 4th Hydrological Conference of Baltic Countries.* Leningrad: LGGI, 17 p. (in Russian).

6) Glushkov, V.G., 1934. [Role of Wind Influence, Migration Vector, Sediment Transport Vector and Drag Vector]. In: LGGI, 1934. *Za Ratsionalizatsiyu Gidrologii*. Leningrad: LGGI, pp. 13–27 (in Russian).

7) Knaps, R.Ya., 1962. [Hydrometeorological Method for Characterising the Movement Regime of Sand Sediments]. In: Mintransstroy, 1962. [*Technical Guidelines for the Design of Offshore Shore Protection Structures on Sandy Shores. VSN 80-62*]. Moscow: Orgtransstroy (in Russian).

8) Shishov, N.D., 1956. [Method for Calculating Capacity and Flow of Sand Sediments in Seas and Large Lakes]. In: SoyuzmorNIIproekt, 1956. *Trudy SoyuzmorNIIproekta*. Moscow: Morskoy Transport, iss. 3, pp. 45–56 (in Russian).

n and m – exponents that can vary in different conditions. In the standard version, it is recommended to use sectors within the boundaries of geographic points (through 45°) or half-points (through 22.5°) and to enter the point sector completeness coefficient to calculate e values. The acceleration length is determined by the limit value calculated according to the relation $D_{lim} = 0.8W^2$.

It is possible to apply several variants of calculation formulas built on the basis of expression (1), the most common of which are those given in [7, 9]. In this case, exponent n is set as equal to two or three by different authors, and exponent m is usually equal to 1/3. The energy dimension e is given by all authors in conventional units.

Without going into the details of the method, which are discussed in a number of works, such as [10, 11], it is possible to organise the information described above as follows.

The currently used WEM is quite simple, and the main obstacle to its operational use is the large volume of pre-prepared data characterized by the homogeneous tabular format. Based on the general approach, the coastline of the study area is approximated by a set of straight segments, from the middle of which a number of rays are drawn towards the sea in directions from the normal to the shore up to 120° in both directions every 5 or 10° until intersecting with the opposite shore or, in some cases, with the border of the map. The adopted step is designed to use data from direct measurements of wind speed, based on the fact that the directional error is 5–10° for most modern instruments. After this, if data on the bathymetry of the adjacent sea region is available, the vertical depth profile along each of the rays is determined. Thus, the spatial resolution of the bathymetry data affects the accuracy of subsequent calculations. Therefore, the total number of tables with data for calculation is $m \cdot n$, where m – number of rays equal to 25 when their interval is 10° and 49 when their interval is 5°; n – number of approximated coastline segments.

This marks off the direct work with the tool. According to the above sources, further steps involve geometric summation of longshore components calculated for all active sectors. Based on the summation results, vectors that characterize the direction and relative intensity of longshore sediment flows at each segment within the boundaries of the coastal section under study, are constructed. Similar results have been repeatedly published in the public domain and are not considered in this paper.

Main results

In order to automate the entire complex of time-consuming work on preparing input data for the WEM, the authors created a specialized software tool based on the use of GIS technologies. The main task of the tool is to calculate the lengths of the wind acceleration rays above the sea surface and the average depths along the bottom profile for each segment of the coastline approximation.

In this case, depth arrays of varying granularity and coastline detail covering the study area are used as initial data. Taking into account the characteristics of the source data, the information structures presented by *Golden Software*, an American company, in the form of contour files (BLN) and regular spatial grid arrays (GRD) were chosen as the main formats. In fact, the GRD is a digital elevation model (DEM) of the bottom surface. A description of the structure of these arrays is on the open Internet and free to download from it [9]. Herewith, all operations with the described tool consist of loading pre-prepared regional arrays and indicating the geographic coordinates of the middle of the coastline approximation segment.

In the version of the tool developed for the Windows operating system, the interface is traditionally made in a windowed version for visualizing the cartographic basis of the data with the placement of management tools in the form of a menu and information board (Fig. 1).

Two stages are necessary to work with the tool. At the first stage, the contour of the coastline is loaded with the automatic loading of the DEM of the same name. The loading process is accompanied by a zoomable coastline visualization, while the depth map is initially hidden so as not to clutter the ray display later. The lower information line displays the characteristics of the grid cell corresponding to the current cursor position on the map, which makes it possible to control such values as latitude, longitude and depth. Additionally, the corresponding menu displays the full version of the depth array in the form of an independent table with the ability to edit it interactively.

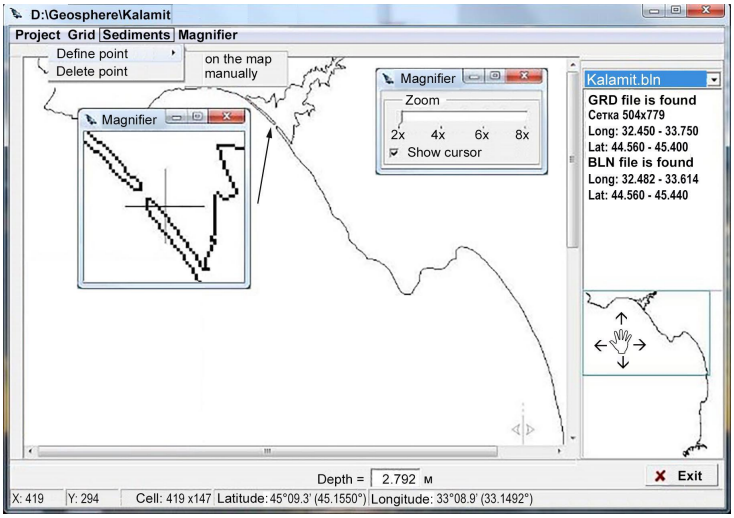

F i g. 1. The user interface of the software tool

[9] Available at: www.goldensoftware.com [Accessed: 30 November 2023].

At the second stage, a design point, which is located near the coastline and represents the middle of the modeled section of the coast, is assumed to be indicated. This information can be entered either digitally in a pop-up window when called by the menu, or indicating its position directly on the map. In this case, for more accurate positioning, it is possible to use the tool to enlarge the area of the map in which the cursor is located (inset in Fig. 1). The implementation of this feature makes it possible to correct the position of a given point promptly in cases where it falls on the coastline or an adjacent strip of land.

Further operation of the tool is based on an algorithm presented on the example of a coastline approximation segments corresponding to the maximum eastern point of the Gulf of Kalamita, the Crimean Peninsula. The results obtained after calculations are subsequently saved for each point automatically based on its coordinates and DEM resolution.

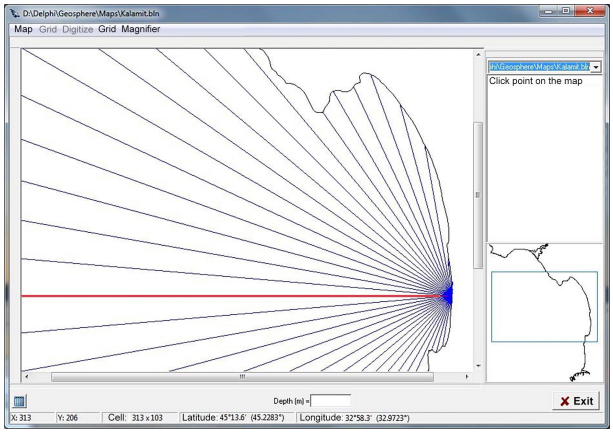

F i g. 2. Visualization of the construction of acceleration beams for one of the shoreline approximation segments in the Gulf of Kalamita

After confirming the correct input data, the program constructs a series of rays automatically, starting from the central one, specified by the value of the normal angle and highlighted in red during the visualization process (Fig. 2).

Reference point #23

№	Long	Lat	D, km	Hcp, m
1	33.61483	44.90917	0.383	0.041
2	33.61483	44.90917	0.383	0.075
3	33.61483	44.90917	0.383	0.484
4	33.61483	44.90917	0.383	0.981
5	33.61149	44.90083	1.206	3.014
6	33.60815	44.89333	2.057	5.751
7	33.58813	44.84583	7.555	7.141
8	33.57144	44.83750	8.836	8.487
9	33.55976	44.84083	8.874	9.818
10	33.28273	44.56083	46.847	56.075

Save as text | Send to Excel | Exit

F i g. 3. The resulting table of the bottom profile along one of the acceleration beams in the Gulf of Kalamita

Together with the construction of rays along the drawn transversal lines, depth profiles corresponding to the loaded DEM grid are determined, from which, in turn, average values are calculated and displayed in the resulting table simultaneously with the coordinates of the end points of the acceleration rays (Fig. 3).

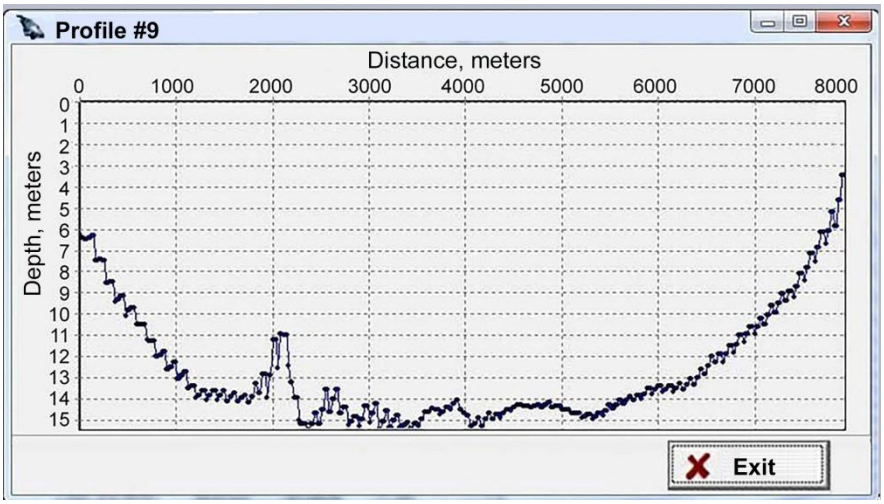

F i g. 4. Example of a graphical representation of the bottom profile along one of the acceleration beams in the Gulf of Kalamita

In addition, the ability to graphically represent the bottom profile in the metric system has been implemented for the purpose of visual control of the bottom profile for each segment (Fig. 4).

This makes it possible to evaluate the blocking effect of critical bottom rises on the transfer of wave energy directly into the sediment movement zone under rugged relief. To calculate distances in this representation, the Haversine method [12] is used, which showed good results in the authors' previous papers.

Conclusions

A software tool for preparing data for a modified WEM calculation algorithm was used to study the structure and parameters of longshore migrations and integral sediment movement in extended sections of the coastal zone of Western Crimea. The results obtained made it possible to clarify the scheme of sediment flows and highlight the features of alongshore redistribution of sediments in different seasons of the year at the present stage of development of the lithodynamic system of this region.

With the use of the WEM, the developed software geoinformation tool makes it possible to prepare a set of data for calculating the direction and relative intensity of longshore sediment flows promptly in an automated mode. In addition, eliminating time-consuming work with cartographic material makes it possible to approximate the coastline in more detail by increasing the number of segments and improve the accuracy of processing data on wind speed in directions significantly as a result of reducing the width of a single sector.

A modified WEM-based version of the calculation scheme makes it possible to obtain estimates of the structure and relative intensity of longshore sediment transport in a wide range of time intervals. In this case, such intervals should be covered by the overall study period determined by the length of the data used concerning wind direction and speed. This makes it possible to study the contribution to sediment dynamics of individual periods of intense wind impact, including at the level of individual storm events, in more detail.

Thus, the implemented procedure for automated preparation of input data for the WEM can be used in calculating wind wave parameters based on the regime characteristics of the wind, when it is necessary to apply such initial values as wave acceleration lengths along open points and changes in depths along acceleration rays.

REFERENCES

1. Bird, E.C.F., 1985. *Coastline Changes: A Global Review*. Chichester; N.Y.: John Wiley & Sons, 232 p.
2. Longinov, V.V., 1964. Some Aspects of Wave Action on A Gently Sloping Sandy Beach. *International Geology Review*, 6(2), pp. 212–227. https://doi.org/10.1080/00206816409474613
3. Dyer, K.R., 1986. *Coastal and Estuarine Sediment Dynamics*. Chichester: Wiley, 358 p.
4. Dean, R.G. and Dalrymple, R.A., 2001. *Coastal Processes with Engineering Applications*. Cambridge: Cambridge University Press, 489 p. https://doi.org/10.1017/CBO9780511754500
5. Kos'yan, R.D., Podymov, I.S. and Pykhov, N.V., Eds., 2003. *Dynamical Processes in the Sea Nearshore Zone*. Moscow: Scientific World, 320 p. doi:10.13140/RG.2.1.4589.7761 (in Russian).
6. Smith, E.R., Wang, P. and Zhang, J., 2003. Evaluation of the CERC Formula Using Large-Scale Model Data. In: R. A. Davis Jr., A. H. Sallenger Jr. and P. Howd, Eds., 2003. *Coastal Sediments 2003: Crossing Disciplinary Boundaries – Proceedings of the International Conference*. Vol. 3. Vicksburg, Mississippi, 2003. CD-ROM.
7. Knaps, R.J., 1968. On Computations of the Power of the Sea Shore Sand Drifts. *Oceanology*, 8(5), pp. 848–857 (in Russian).
8. Shishov, N.D., 1961. The Methods of Constracting a Distribution Curve of the Alongshore Sand Drift Transport Intensity at the Subwater Slope. *Oceanology*, 1(5), pp. 915–919 (in Russian).
9. Pravotorov, I.A., 1961. [On Application of the Hydrometeorological Method to Study Longshore Transport of Marine Sediments]. *Vestnik MGU. Seriya Geograficheskaya*, (2), pp. 28–33 (in Russian).
10. Ivanov, V.A. and Udovik, V.F., 2005. Evaluation of the Balance of Drift Flow Intensity and the General Tendency of Coastal Area Reformation on the North-Eastern Coast of the Tuzla Island in 2004. In: MHI, 2005. *Ekologicheskaya Bezopasnost' Pribrezhnoy i Shel'fovoy Zon i Kompleksnoe Ispol'zovanie Resursov Shel'fa* [Ecological Safety of Coastal and Shelf Zones and Comprehensive Use of Shelf Resources]. Sevastopol: MHI. Iss. 13, pp. 159–178 (in Russian).
11. Goryachkin, Y.N., Udovik, V.F. and Kharitonova, L.V., 2011. Estimations of the Parameters of the Flux of Sediments near the West Coast of the Bakal'skaya Spit under the Conditions of Heavy Storms in 2007. *Physical Oceanography*, 20(5), pp. 356–365. https://doi.org/10.1007/s11110-011-9091-9

12. Hartanto, S., Furqan, Mhd., Siahaan, A.P.U. and Fitriani, W., 2017. Haversine Method in Looking for the Nearest Masjid. *International Journal of Recent Trends in Engineering and Research*, 3(8), pp. 187–195. doi:10.23883/IJRTER.2017.3402.PD61H

Submitted 01.06.2023.; accepted after review 05.09.2023;
revised 11.10.2023; published 20.12.2023

About the authors:

Vyacheslav V. Dolotov, Senior Research Associate, Marine Hydrophysical Institute of RAS (2 Kapitanskaya St., Sevastopol, 299011, Russian Federation), PhD (Chem.), **ORCID ID: 0000-0002-1485-2883**, **ResearcherID: E-5570-2016**, *dolotov_v_v@mhi-ras.ru*

Vladimir F. Udovik, Junior Research Associate, Marine Hydrophysical Institute of RAS (2 Kapitanskaya St., Sevastopol, 299011, Russian Federation), **ORCID ID: 0000-0002-3832-2537, ResearcherID: AAV-7570-2020**, *udovik_uvf@mhi-ras.ru*

Contribution of the authors:

Vyacheslav V. Dolotov – the algorithm and software tool development, preparation of the article text and illustrations

Vladimir F. Udovik – problem statement, data processing and analysis, preparation of the article text

All the authors have read and approved the final manuscript.

Original article

Modelling Salt Water Intrusion into Main Branches of the Don Delta depending on Wind Situation

A. L. Chikin [1] *, A. V. Kleshchenkov [1], L. G. Chikina [2]

[1] *Federal State Budgetary Institution of Science "Federal Research Center Southern Scientific Center of the Russian Academy of Sciences", Rostov-on-Don, Russia*

[2] *Federal State Autonomous Educational Institution of Higher Education "Southern Federal University", Rostov-on-Don, Russia*

* *e-mail: chikin1956@gmail.com*

Abstract

The paper presents a mathematical model that combines a model of salinity distribution in the Sea of Azov and a model of substance transport in branches of the Don delta. In the channel model of the Don delta area, the input data are the water level and salinity in the recipient water body, Taganrog Bay. The hydrodynamic component of the model for the Sea of Azov is described by the shallow water equations, and the movement in branches of the Don delta is described by the Saint-Venant equations. The distribution of salt concentration in the sea and in the Don branches is determined using the convection–diffusion equations written for two-dimensional and one-dimensional cases, respectively. The problem was solved by finite difference methods on uniform grids. In the marine model, the resulting systems of linear algebraic equations were solved using the Aztec package. In the channel model, the LAPACK package was used. Depending on the wind situation over the Sea of Azov, the proposed model allows calculating the current parameters and salinity distribution in the entire Sea of Azov, including Taganrog Bay. These parameters are input data for the channel model, which further determines the velocity of currents, the water surface level, and salinity in the main branches of the Don delta. The paper compares the calculated values of hydrophysical parameters with the observed data obtained during sea expeditions. The comparison showed the adequacy of the model.

Keywords: mouth area, shallow water equations, Saint-Venant equations, transport equation, free surface level, computational experiment

Acknowledgments: The publication has been prepared under state assignment; state registration no. 122011900153-9. The work was performed on the equipment of the Joint Center for Scientific and Technological Equipment of the SSC RAS (research, development, approbation) No. 501994. The calculations were performed on the cluster of the High-Performance Computing Center of Southern Federal University.

For citation: Chikin, A.L., Kleshchenkov, A.V. and Chikina, L.G., 2023. Modelling Salt Water Intrusion into Main Branches of the Don Delta depending on Wind Situation. *Ecological Safety of Coastal and Shelf Zones of Sea*, (4), pp. 56–72.

Моделирование проникновения соленых вод в основные рукава дельты Дона в зависимости от ветровой ситуации

А. Л. Чикин [1]*, А. В. Клещенков [1], Л. Г. Чикина [2]

[1] *Федеральное государственное бюджетное учреждение науки «Федеральный исследовательский центр Южный научный центр Российской академии наук», Ростов-на-Дону, Россия*

[2] *Федеральное государственное автономное образовательное учреждение высшего образования «Южный федеральный университет», Ростов-на-Дону, Россия*

* *e-mail: chikin1956@gmail.com*

Аннотация

Представлена математическая модель, объединяющая в себе модель распределения солености в Азовском море и модель транспорта вещества в рукавах дельты Дона. В русловой модели дельтовой области Дона входными данными являются уровень воды и соленость в принимающем водоеме – Таганрогском заливе. Гидродинамическая составляющая модели для Азовского моря описывается уравнениями мелкой воды, а движение в рукавах дельты Дона – уравнениями Сен-Венана. Распределение концентрации соли в море и в рукавах Дона определяется с помощью уравнений конвекции – диффузии, записанных соответственно для двухмерного и одномерного случая. Задача решается конечно-разностными методами на равномерных сетках. В морской модели полученные системы линейных алгебраических уравнений решаются с помощью пакета *Aztec*. В речной модели используется пакет *LAPACK*. Предлагаемая модель позволяет в зависимости от ветровой ситуации над акваторией Азовского моря рассчитать параметры течения и распределение солености во всем Азовском море, включая Таганрогский залив. Эти параметры являются входными данными для русловой модели с дальнейшим определением скорости течения, уровня водной поверхности и солености в основных рукавах дельты Дона. Приводится сравнение расчетных значений гидрофизических параметров с данными, зафиксированными в ходе морских экспедиций. Сравнение показало достаточную адекватность модели.

Ключевые слова: устьевая область, уравнения мелкой воды, уравнения Сен-Венана, уравнение переноса, уровень свободной поверхности, вычислительный эксперимент

Благодарности: публикация подготовлена в рамках реализации ГЗ ЮНЦ РАН, № госрегистрации проекта 122011900153-9. Работа выполнена на оборудовании ЦКП «Объединенный центр научно-технологического оборудования ЮНЦ РАН (исследование, разработка, апробация)» № 501994. Расчеты выполнены на кластере ЦКП Южного федерального университета «Высокопроизводительные вычисления».

Для цитирования: *Чикин А. Л., Клещенков А. В., Чикина Л. Г.* Моделирование проникновения соленых вод в основные рукава дельты Дона в зависимости от ветровой ситуации // Экологическая безопасность прибрежной и шельфовой зон моря. 2023. № 4. С. 56–72. EDN KFZQNW.

Introduction

The Don mouth area is a key region of the basin of the Sea of Azov, where complex processes of interaction between river and sea waters occur. Here, surge level fluctuations, associated with the flow of sea transformed waters into the branches of the Don delta, are especially pronounced [1, 2].

A serious threat of flooding is posed by extreme downsurges with easterly winds and upsurges with westerly winds. The situation is particularly dangerous when the water surges down before the upsurge. This occurs when the easterly wind suddenly changes its direction to the west. Thus, flooding occurs faster, and it is greater in scale than with a constant westerly wind. A similar picture was observed on 23 March 2013, when the easterly wind (3–11 m/s) changed to southwesterly (15 m/s with gusts of 20–22 m/s). This phenomenon is confirmed by the performed numerical experiments, in which the wind direction changes to the opposite one [3]. Such extreme upsurges are only possible with strong southwesterly winds. In addition, surges can be influenced by seiche fluctuations, which are significant in the Sea of Azov [4], but are not taken into account in the presented model.

Under certain hydrometeorological conditions, salt waters of Taganrog Bay intrude into the Don River delta, where the water intakes of the Rostov agglomeration largest cities, such as Azov and Taganrog, are located. Moreover, a new water pipeline was put into operation in the Donetsk region. During a strong upsurge in June 2014, the sea level rose to 1.7 m, and the salinity at the Don mouth reached 5 PSU [5, 6]. In September 2014, water with increased salinity (5–9 PSU) intruded along the Don to Azov and entered the city water supply system. Subsequently, the similar situation was observed several times, being the most significant in February 2021 [7].

In recent decades, we have observed large-scale climate changes, which led to significant changes in environmental conditions in the Don basin and the Sea of Azov. The Don low water has been continuing for 17 years and is the longest one in the last 100 years. This led to a significant decrease in freshwater flow into Taganrog Bay of the Sea of Azov and an increase in salinity both in the sea and in Taganrog Bay. The average sea water salinity increased to 14 PSU (in the 1970s, such salinity was considered critical for the marine ecosystem), and in Taganrog Bay it reached 10 PSU [8]. Analysis of field data from the oceanological research of the Southern Scientific Center of the Russian Academy of Sciences indicates a continuing increase in salinity. The decrease of the Don flow to historical minimums, as well as the anomalous advection of the Black Sea waters led to the abnormally high salinity observed in Taganrog Bay during 2014–2016 (up to 12 PSU) [2]. It should be noted that the current rate of increase in the average annual sea water salinity exceeds the rate observed in the mid-1970s, during the previous period of the Don low water levels [9]. In this regard, the study of the intrusion of salt sea water into the Don River delta is becoming increasingly relevant.

Currently, many papers are aimed at modeling the intrusion of salt water into river mouths. These studies are mainly related to tidal processes. Thus, the model of salt inflow into the mouth of the San Francisco River is described in [10]. In this case, a numerical solution of advection–diffusion problems in hydrodynamics on an unstructured grid is used [11].

A numerical model for studying seasonal variability of currents and salinity at the Indus River mouth in Pakistan is given in [12]. The model is calibrated using observed water level, current velocity, and salinity data. The modeling results show that salt water intrudes far upstream, approximately 65 km.

The Don mouth is not subject to any tidal processes. The intrusion of salt water into the Don main channels occurs during upsurges, when the water level rises significantly in Taganrog Bay. Therefore, the intrusion of salt water into the Don main branches is directly related to the salinity of water at the mouth of the branches, as well as the movement of water in the channels. Here, the flow of water in the river channel is influenced primarily by the water level in the receiving basin, in this case in Taganrog Bay.

The paper is aimed at computational study of this phenomenon. Use of a mathematical model based on equations for incompressible liquid motion and equations for convection–diffusion (transfer) allows studying saline water intrusion into the Don delta during its flooding.

For these reasons, when modeling the process of intrusion of salt water into the Don main channels, the following steps are necessary to calculate the required parameters.

1. Determination of the water level at the mouths of the branches for a given wind situation over the Sea of Azov and Taganrog Bay.
2. Determination of the salinity of water at the mouths of the branches.
3. Determination of the velocity of water movement and distribution of salinity in the Don main branches.

The first two problems are solved using a two-dimensional model of the hydrodynamics of wind currents in the Sea of Azov, as well as a model of salinity distribution in it [13]. The third problem is solved using one-dimensional models of water movement in channels and substance transport [14].

Materials and methods

Since the beginning of the 2000s, during marine expeditions, the Southern Scientific Center of the Russian Academy of Sciences has been conducting systematic observations of the thermohaline structure of the waters of the Don River coastal estuary and delta. Since the summer of 2014, studies of the dynamics of salinity and water temperature changes, together with measurement of the current direction and velocity, have been regularly carried out using an integrated current meter Aanderaa RSM-9LW (https://www.aanderaa.com/media/pdfs/Seaguard_RCM-TD262b_001.pdf) at a stationary buoy station on the seaside 5 km from the edge of the delta (the first leading mark of the Azov-Don Seaway Canal) and at the mouth of the Don (the khutor of Donskoy, the village of Kagalnik), as well as in the Don delta at the network of ship oceanological stations. In parallel with this, meteorological parameters and water level have been observed at the hydrological station of Donskoy and water level station of Taganrog.

To study the spatial distribution of sea water temperature and salinity in the Sea of Azov and Taganrog Bay, continuous recording of data on the temperature and electrical conductivity of surface water was performed with thermosalinograph SBE21 SEACAT (https://www.seabird.com/sbe-21-seacat-thermosalinograph/product?id=60762467702) during the voyages of the R/V *Deneb*.

The area of calculation is the mouth section of the Lower Don from the stanitsa of Razdorskaya to Taganrog Bay, including its eastern part. This section consists of the main channel of the Don and its main branches, the Old Don, the Bolshaya Kalancha turning into the Mokraya Kalancha and the Bolshaya Kuterma (Fig. 1). White circles indicate points in Taganrog Bay where calculated water level values were taken, black triangles indicate the hydrological stations where observations were made.

The salinity transport in the Sea of Azov is described by a system containing equations for long waves in a homogeneous incompressible fluid in a Coriolis force field and a transport equation under the assumption that the propagated substance is conservative [15]:

$$\begin{gathered}
\frac{\partial u}{\partial t}+u\frac{\partial u}{\partial x}+v\frac{\partial u}{\partial y}-f\cdot v=-g\frac{\partial \zeta}{\partial x}+\frac{\tau_{sx}}{H}-\frac{\tau_{bx}}{H},\\
\frac{\partial v}{\partial t}+u\frac{\partial v}{\partial x}+v\frac{\partial v}{\partial y}+f\cdot u=-g\frac{\partial \zeta}{\partial y}+\frac{\tau_{sy}}{H}-\frac{\tau_{by}}{H},\\
\frac{\partial \zeta}{\partial t}+\frac{\partial (Hu)}{\partial x}+\frac{\partial (Hv)}{\partial y}=0,\\
\frac{\partial c}{\partial t}+\frac{\partial (uc)}{\partial x}+\frac{\partial (vc)}{\partial y}=\varepsilon_{xy}\left(\frac{\partial^2 c}{\partial x^2}+\frac{\partial^2 c}{\partial y^2}\right),
\end{gathered} \tag{1}$$

where $H = h + \zeta$; $h = h(x, y)$ – depth; f – Coriolis parameter; ζ – water level difference; $u = u(x, y, t)$, $v = v(x, y, t)$ – velocities; c – concentration; ε_{xy} – horizontal turbulent diffusion coefficient; τ_{sx}, τ_{sy} – projections on the OX and OY axes of the force of wind friction on the surface of the basin; τ_{bx}, τ_{by} – projections on the OX and OY axes of the force of wind friction on the bottom. These values depend on the velocity of wind $\mathbf{W}_B = \{W_x; W_y\}$ and current $\mathbf{W}_T = \{u; v\}$ and are determined as follows [16]:

$$\tau_s = \gamma\left|\mathbf{W}_B\right|\mathbf{W}_B, \qquad \tau_b = \beta\left|\mathbf{W}_T\right|\mathbf{W}_T,$$

where $\left|\mathbf{W}_B\right| = \sqrt{W_x^2 + W_y^2}$, $\left|\mathbf{W}_T\right| = \sqrt{u^2 + v^2}$; γ – coefficient of t he friction of wind on a free surface, β – coefficient of the friction of liquid on the bottom.

Sliding conditions are set along the solid boundary or the rates of inflow or outflow of water are specified (for example, for river mouths). It is assumed that there is no flow through the free surface and the side boundary.

In accordance with [17], the Don delta is represented as a graph (inset in Fig. 1), consisting of five edges and six vertices. The edges correspond to sections of open channels, i. e. the Don main channel and its branches. Four vertices correspond to end nodes (*1*, *3*, *5*, *6*), and two – to branch nodes (*2*, *4*).

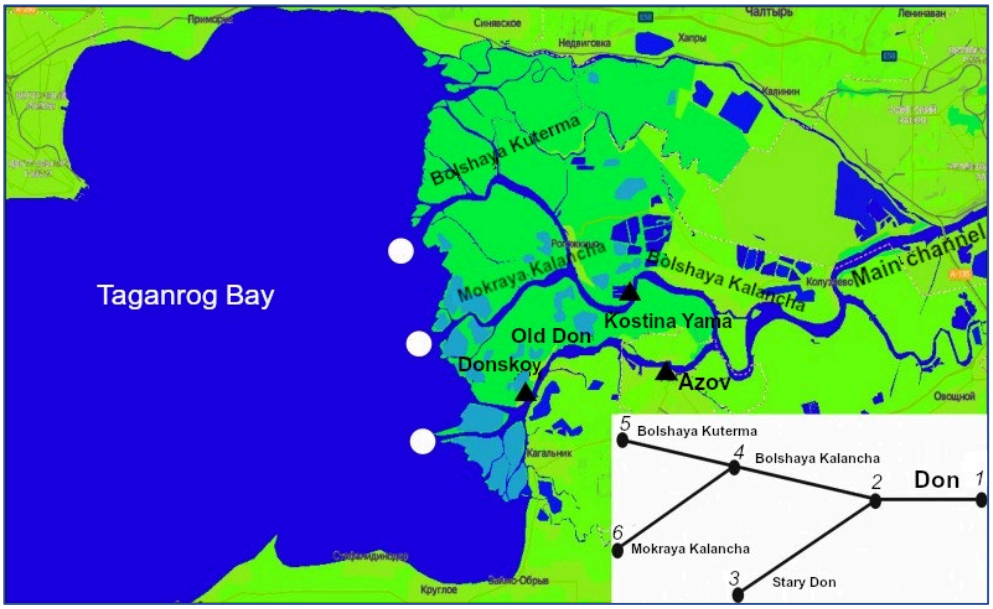

F i g. 1. The area of calculation of the Don River mouth section. The inset shows the diagram of the delta part: *1*, *3*, *5*, *6* – end nodes; *2*, *4* – branch nodes

The intrusion of salt water into the Don branches is described by one-dimensional equations of water movement in an open channel and the conservative substance transport [18]. No zones of sharp changes in the channel cross section, as well as distributed lateral inflow due to its insignificance, are assumed to be in the studied section of the Don channel. In the case when the channel cross section has a parabolic profile, this system can be rewritten in the following form:

$$\frac{\partial Q}{\partial t} + gW\left(\frac{\partial z}{\partial x} + \frac{Q|Q|}{K^2}\right) = 0,$$

$$b\frac{\partial z}{\partial t} + \frac{\partial Q}{\partial x} = 0, \qquad (2)$$

$$\frac{\partial S}{\partial t} + v\frac{\partial S}{\partial x} - \mu\frac{\partial^2 S}{\partial x^2} = 0,$$

where x – coordinate; t – time; Q – water consumption; z – water level; W – cross section area; K – rate of discharge; g – acceleration of gravity; b – channel width; S – concentration; v – velocity of water movement in the channel; μ – turbulent diffusion coefficient. Rate of discharge K is calculated by formula $K = \omega \cdot C\sqrt{R}$, where R – hydraulic radius; C – Chezy's velocity factor found using Manning formula $C = \sqrt[6]{R}/n$, n – bottom roughness.

The first two equations of system (2) (hydrodynamic component) are reduced to the following characteristic equations:

$$\frac{gW}{c_*}\frac{\partial z}{\partial t}+\frac{\partial Q}{\partial t}+gW\frac{\partial z}{\partial x}+c_*\frac{\partial Q}{\partial x}=-gW\frac{Q|Q|}{K^2},$$

$$-\frac{gW}{c_*}\frac{\partial z}{\partial t}+\frac{\partial Q}{\partial t}+gW\frac{\partial z}{\partial x}-c_*\frac{\partial Q}{\partial x}=-gW\frac{Q|Q|}{K^2},$$

where $c_*=\sqrt{gW/b}$.

As boundary conditions, discharge of incoming water $Q_0(0,\ t)$ is set at the initial point (node *1*), and level in the receiving basin $z_k(X_k,\ t)$ is set at the end points (nodes *3*, *5*, *6*). At branching nodes, the boundary conditions are set as follows: the sum of inflows and outflows is equal to zero $\sum_i Q_i=0$ (i – number of branches coming to the branching node), and the water surface levels are equal to each other: $z_i = z$.

The boundary conditions are set at the ends of the branches depending on the sign of the current velocity. If water enters the branch, the following condition is set: $\frac{\partial S}{\partial x}=\frac{v}{\mu}(S-S^*)$, where S^* – salt concentration value at the end of the branch. In the case when water leaves the branch, the following condition is set: $\frac{\partial S}{\partial x}+S\frac{v}{\mu}=0$, which corresponds to the disposal of salt from the branch.

Thus, during strong upsurges at the boundary of the branches coinciding with the mouths in Taganrog Bay, the following condition is set: $\frac{\partial S}{\partial x}=\frac{v}{\mu}(S-S_{zal})$, where S_{zal} – salt concentration value in Taganrog Bay. If the end of the branch contains lumped parameters, in particular concentration, S_{zal} should be replaced with S^* – concentration at the branch point, which is calculated as follows:

$$S^*=\frac{\sum S_iQ_i}{\sum Q_i}.$$

Summing-up is performed only over the branches flowing into the branch point.

The problem is solved by finite-difference methods using implicit schemes. In the "marine" model (1), a grid with steps $\Delta x = 660$ m, $\Delta y = 685$ m is constructed, and in the "channel" model (2), the step is $\Delta x = 1000$ m. Stable counting is observed at time step Δt = 30 s. At each time step, hydrophysical parameters are first calculated for the entire Sea of Azov, then the values of salinity and water level are selected at the points corresponding to the mouths of the Don branches. These points are indicated by circles in Fig. 1. Next, the calculation continues in the Don channel area. Then, a transition to a new temporary layer is performed.

Results of calculation and discussion

Based on the salinity observations, calculations were performed under corresponding wind situations. Coastal weather stations located around the Sea of Azov provided the wind data. For each calculated point, three nearest weather stations were determined, and then, using linear interpolation, zonal and meridional coordinates of the wind velocity were determined in this point.

From 23 September 2014 to 27 September 2014, an extreme upsurge accompanied by salt water intrusion into the Don branches, was observed [6]. At the beginning of the period, an easterly wind of 2–4 m/s took place. From 10 a. m. on 24 September 2014, the wind changed its direction to southwesterly and increased to 20 m/s. This led to a sharp rise in water and increased salinity. The maximum values of water level and salinity in the area of the port of Azov occurred on September 24–25 and amounted to 3.82 m and 5.59 PSU, respectively. Fig. 2 shows changes in water salinity and water level in the water area of the port of Azov. Calculations confirm the fact that changes in salinity are directly proportional to changes in water level. The calculation error is 19.1 % for salinity and 22.8 % for water level.

One of the last relatively strong upsurges with the salt water intrusion into the Don branches was observed on 12–16 February 2021. During this period, water rise was observed twice. From 03:00 p. m. on 12 February 2021, influenced by a westerly wind of 13–16 m/s, the first rise of water took place. Then, as the wind weakened to 4–6 m/s, the level decreased. But starting from 12:00 p. m.

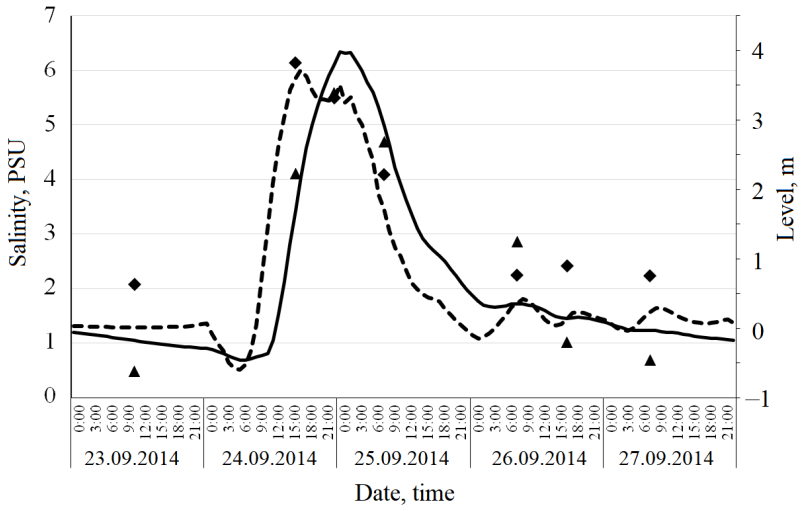

F i g. 2. Water salinity and water level in the water area of the port of Azov from 24 September 2014 to 27 September 2014. The triangles are observed concentration; the solid line is calculated concentration. The diamonds are the observed level; the dashed line is the calculated level

on 13 February 2021, the wind again rose up to 12–16 m/s, which led to a new water rise. Then the wind weakened to 1–2 m/s and took a northwesterly direction.

For a second time, sampling was performed in Rostov-on-Don (city beach) and Azov (port). In such points of Rostov-on-Don as Nakhichevan Duct, khutor of Koluzaevo, khutor of Dugino, khutor of Rogozhkino, sampling was performed only once. Fig. 3 shows changes in salinity in the area of the Rostov beach and the port of Azov, as well as in the current velocity in the area of the port of Azov.

The table shows the time of water sampling, calculated and observed salinity, as well as calculation error.

The change in salinity depends directly on fluctuations in the water level at the mouths of the branches, which is quite natural. It can be seen that the change in salinity in the port of Azov, which is located 15 km from the mouth, occurs with larger amplitudes than in the area of the Rostov beach, located 50 km from the same mouth (Fig. 3). It can also be seen that salinity increases almost immediately after the current velocity becomes negative (reverse current), and decreases when the direct current returns.

From 22 November 2022 to 23 November 2022, measurements of salinity and current velocity were performed at the hydrological station of Donskoy. At the beginning of this period, a southwesterly wind was observed with a force of 4–5 m/s, which then intensified to 12–14 m/s, resulting in an upsurge with the salt water intrusion into the Don delta. A comparison of the results of calculating salinity

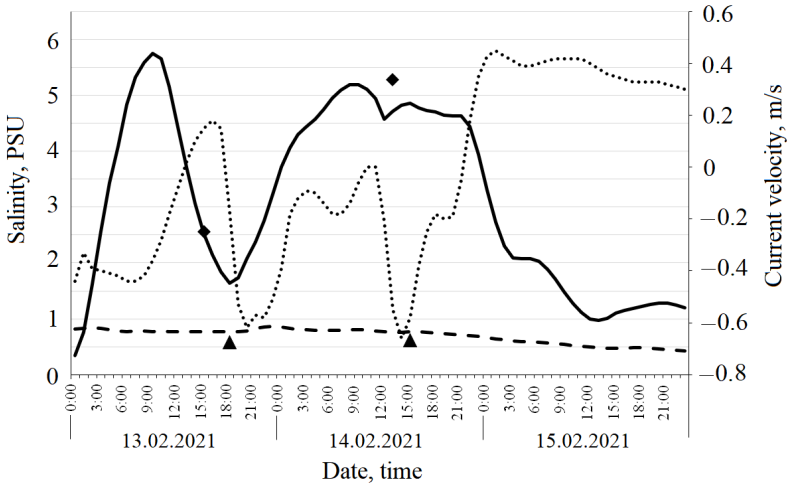

F i g. 3. Salinity and velocity of current in the area of the port of Azov from 13 February 2021 to 15 February 2021. The triangles are the Rostov beach (observed). The dashed line is the Rostov beach (calculated). The diamonds are the port of Azov (observed). The solid line is the port of Azov (calculated). The dotted line is the velocity of current (the port of Azov)

Comparison of calculated salinity values (PSU) with observations

Sampling location	Distance from the mouth, km	Date, time	Salinity		Error, %
			Observed	Calculated	
Rostov-on-Don (Nakhichevan Duct)	52.3	13.02.2021 14:54	0.79	0.756	4.30
Rostov-on-Don (city beach)	49.4	13.02.2021 15:41	0.79	0.768	2.78
Rostov-on-Don (city beach)	49.4	14.02.2021 12:27	0.83	0.760	8.43
khutor of Koluzaevo	34.5	14.02.2021 16:35	0.85	0.694	18.35
khutor of Dugino	22.3	13.02.2021 17:48	3.24	0.768	76.30
khutor of Rogozhkino	11.7	13.02.2021 17:22	3.97	1.023	74.23
city of Azov (port)	15.0	13.02.2021 14:36	2.56	2.534	1.02
city of Azov (port)	15.0	14.02.2021 12:15	5.28	4.72	10.61

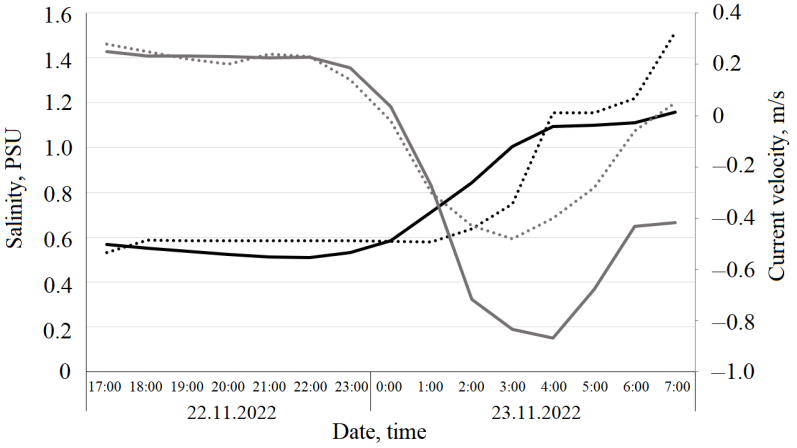

F i g. 4. Salinity and velocity of current at the hydrological station of Donskoy from 22 November 2022 to 23 November 2022. The black lines are salinity; the grey lines are velocity; the solid lines are calculations; the dotted lines are observations

and current velocity with the observed data is shown in Fig. 4. A noticeable increase in salinity begins at the moment when the current changes direction to the opposite, from the sea to the river, and the velocity becomes negative (Fig. 4).

The calculation errors are 27.7 % for water level, 16.8% for salinity, 92.6 % for current velocity. The large current velocity calculation error is explained by the assumption that the bottom profile is parabolic, which does not fully correspond to reality in this hydrological section.

When comparing the observed and calculated values, attention is drawn to the large error in the calculations of salinity in the khutors of Dugino and Rogozhkino located in the Bolshaya Kalancha branch, while at other points located in the Don main channel and in the Old Don branch, this error is acceptable (table).

To clarify the reasons of the above mentioned, additional hydrodynamic calculations were performed in the Don delta region in November 2022 based on the wind situation for a moderate upsurge. At that time, measurements of the velocity and direction of currents and water salinity were performed from the board of the R/V *Deneb* in the Old Don branch (hydrological station of Donskoy, 7.2 km from the mouth) and in the Bolshaya Kalancha branch (down the hydrological station of Dugino, 18 km from the mouth). The change of the water level in the delta during the upsurge was measured by a level gauge at the hydrological station of Donskoy. Fig. 5 shows the observed and calculated values of the water level for the observation period from 17 November 2022 to 21 November 2022.

Fig. 6 shows changes in calculated and observed current velocities and salinity at the hydrological station of Donskoy for the period from 17 November 2022 to 21 November 2022. Moreover, the observations here are presented only from 07:00 p. m. on 17 November 2022 to 07:00 a. m. on 18 November 2022, and then the values obtained from the calculation based on the wind situation for the specified period, are given.

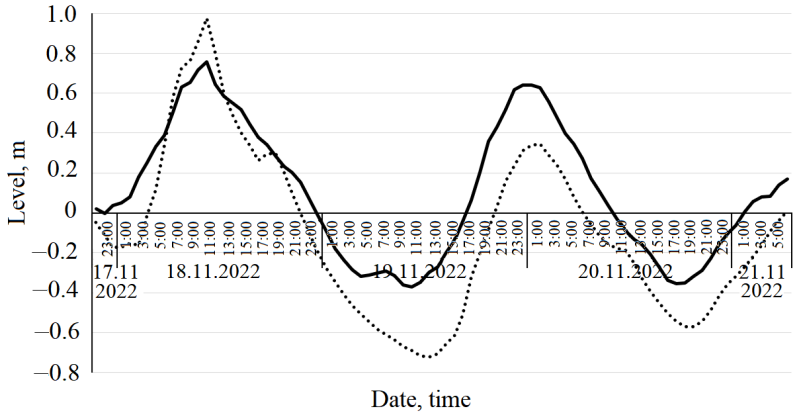

F i g. 5. Change in the water level at the hydrological station of Donskoy from 17 November 2022 to 21 November 2022. The dotted line is observations. The solid line is calculations

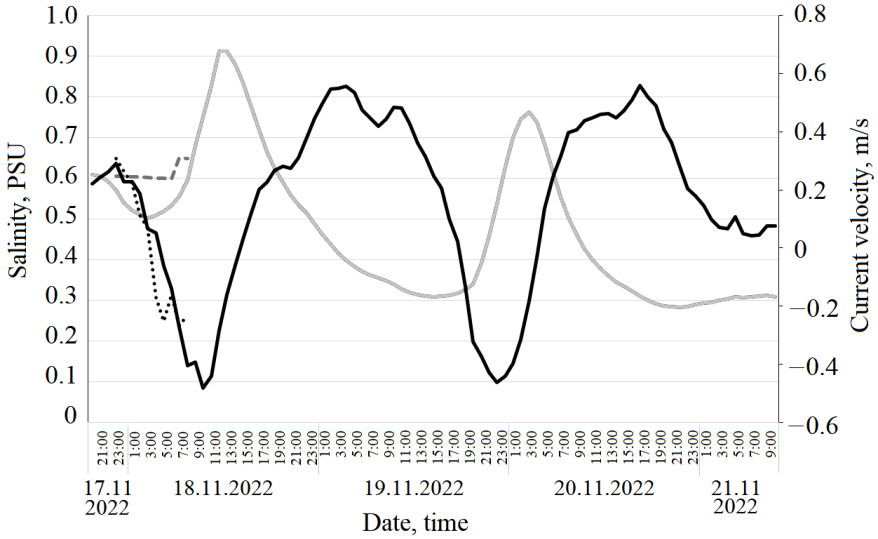

F i g. 6. Calculated and observed values of the current velocity and salinity at the hydrological station of Donskoy from 17 November 2022 to 21 November 2022. The dashed line is observed salinity; the solid grey line is calculated salinity. The dotted line is observed velocity; the solid black line is calculated velocity

Thus, a clear connection between the direction of the current and the change in salinity is observed: at a negative velocity, when there is a reverse current directed from the sea to the river, salinity increases, and at a positive velocity, salinity decreases. This connection is confirmed by observations (Fig. 6).

From 10:00 p. m. on 17 November 2022, the current velocity decreased, remaining positive until approximately 02:30 a. m. At that time, the salinity values were close to 0.60 PSU. Then, a reverse current began to develop, and at 05:00 a. m. on 18 November 2022, a sharp increase in salinity occurred. The time difference between the beginning of the reverse current and the jump in salinity is explained by the fact that Donskoy is located 6.5 km from Taganrog Bay, and it takes time for salt water to reach the observation point. It can be seen (Fig. 7) that during the reverse current, starting from 05:00 a. m. on 18 November 2022, the salinity increases sharply. This figure is an enlarged copy of the initial part of the graph presented in Fig. 6.

Fig. 8 shows change in calculated and observed values of current velocity during the observation period from 10:00 p. m. on 17 November 2022 to 07:00 a. m. on 18 November 2022. The dynamics of the calculated and observed values agree well with each other. However, there is a discrepancy between observation data and modeling results at the night period, when the observed level values are oscillatory. This can be due to an error in the wind field interpolation or the occurrence of proper oscillations.

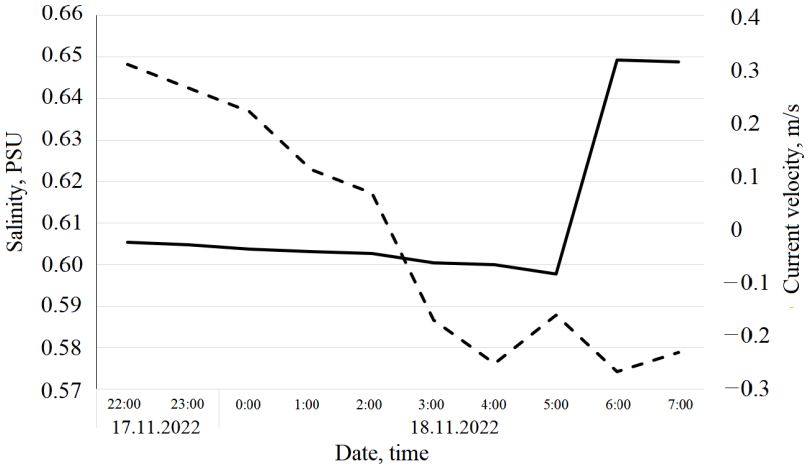

F i g. 7. The dependence of salinity at the hydrological station of Donskoy on the current velocity from 17 November 2022 to 18 November 2022 (observed values). The solid line is observed salinity. The dashed line is observed velocity

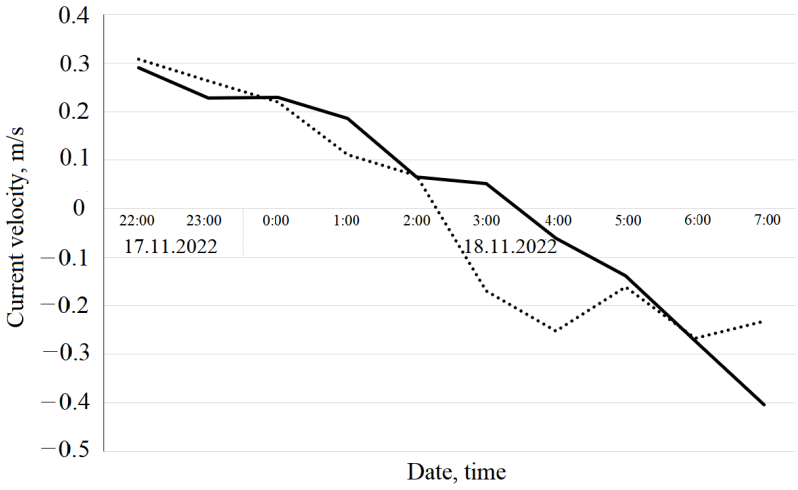

F i g. 8. Calculated and observed values of the current velocity at the hydrological station of Donskoy from 10 p. m. on 17 November 2022 to 7 a. m. on 18 November 2022. The dotted line is observed velocity. The solid line is calculated velocity

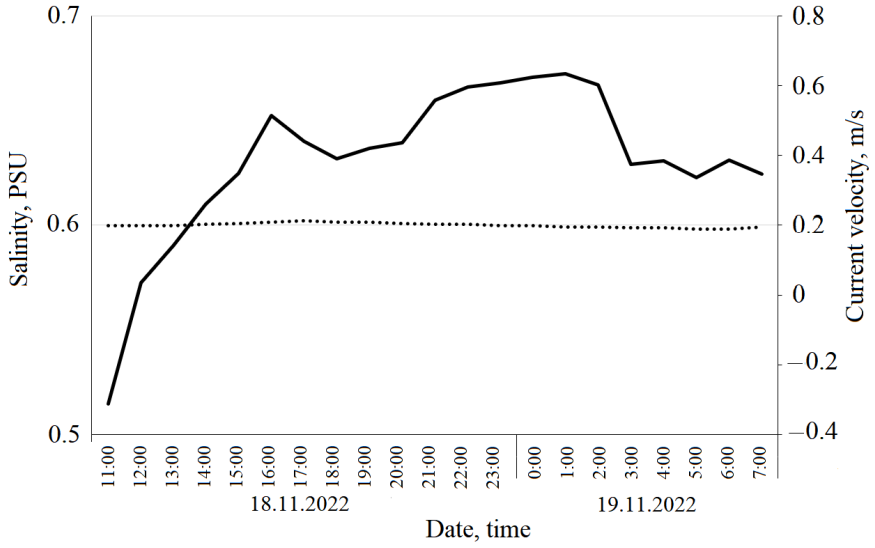

F i g. 9. The dependence of salinity on the velocity of current in the area of Kostina Yama from 18 November 2022 to 19 November 2022 (observed values). The dotted line is observed salinity. The solid line is observed velocity

At the observation point in the area of Kostina Yama, the relationship between the current direction and the change in salinity is not as clear as in Donskoy. In fact, in this section of the Bolshaya Kalancha channel, changes in the current velocity and direction during upsurge conditions are instrumentally recorded and coincide satisfactorily with the calculated values, but almost no change in salinity is observed (Fig. 9).

This is explained by the fact that observation points Donskoy and Kostina Yama are located at different distances from the mouth of the corresponding branches of the delta. In addition, the distribution of flow along the branches is also uneven, as the Old Don accounts for 40% of the Don flow, and the Bolshaya Kalancha – 60%. And finally, the longitudinal profile of the Old Don channel is more uniform, as the Azov-Don Seaway Canal passes through this branch, and dredging works are regularly performed resulting in favorable conditions for the salt water intrusion. At the same time, the profile of the Bolshaya Kalancha channel is characterized by shallower average depths and alternating river reaches and rifts, which complicates salt water the intrusion into this branch.

Conclusions

Correct setting of the initial salinity field in Taganrog Bay is a challenging part of the problem under consideration. Further distribution of salinity values at the mouth coastal area and then in the Don branches, depends on it, which significantly affects the calculation results. Based on the data obtained during spring, summer, and autumn surveys, salinity values were calculated along the route of the R/V *Deneb* from the Don mouth in Taganrog Bay to the Kerch Strait. Using the obtained data, the Sea of Azov and Taganrog Bay were divided into the areas where salinity was considered constant. In the absence of such data, it is possible to use corresponding salinity maps for a certain time of year. This will make it possible to obtain the initial distribution of water salinity with some approximation. However, this approach cannot ensure an acceptable initial distribution of salinity during the time period when the calculation is performed, especially for a future forecast.

This model makes it possible to determine the current velocity, water surface level, and salt concentration in the Don delta main branches depending on the wind situation in the Sea of Azov and Taganrog Bay.

The comparison of the calculated water level values with the values obtained at observation stations shows identical dynamics of their change, which indicates the adequacy of the presented model. The proposed methodology can be applied to other water areas in the joint calculation of currents in mouth channels and wind currents in a receiving basin.

REFERENCES

1. Mishin, D.V. and Polonskiy, V.F., 2013. Research of Non-Stationary Water Streams in Nontidal Mouth of Don River. In: Polonskiy, V.F., ed., 2013. *SOI Proceedings*. Moscow, iss. 214, p. 166–179 (in Russian).
2. Matishov, G.G., Grigorenko, K.S. and Moskovets, A.Yu., 2017. The Salinization Mechanisms in the Taganrog Bay under the Conditions of the Don River Extremely Low Runoff. *Nauka Yuga Rossii = Science in the South of Russia*, 13(1), pp. 35–43. doi:10.23885/2500-0640-2017-13-1-35-43 (in Russian).
3. Matishov, G.G., Berdnikov, S.V., Sheverdyaev, I.V. and Chikin, A.L., 2014. The Extreme Flood in the Don River Delta, March 23–24, 2013, and Determining Factors. *Doklady Earth Sciences*, 455(1), 360–363. https://doi.org/10.1134/S1028334X14030295 (in Russian).
4. Matishov, G.G., Matishov, D.G. and Inzhebeikin, Yu.I., 2008. The Effect of Seichelike Oscillations on Extremal Azov Sea Levels and Currents. *Vestnik SSC RAS*, 4(2), pp. 46–61 (in Russian).
5. Fomin, V.V. and Diansky, N.A., 2018. Simulation of Extreme Surges in the Taganrog Bay with Atmosphere and Ocean Circulation Models. *Russian Meteorology and Hydrology*, 43(12), pp. 843–851. https://doi.org/10.3103/S1068373918120051
6. Matishov, G.G., 2015. Extreme Saline Water Advection into the Don River Delta and Ice Advections into Kerch Strait. *Doklady Earth Science*, 465(1), pp. 1154–1158. https://doi.org/10.1134/S1028334X15110057
7. Kleshchenkov, A.V. and Moskovets, A.Yu., 2021. Salt Water Intrusions into the Don River Delta: Development Patterns and Consequences. *Nauka Yuga Rossii = Science in the South of Russia*, 17(3), pp. 30–37. doi:10.7868/S25000640210304 (in Russian).
8. Dashkevich, L.V., Kulygin, V.V. and Berdnikov, S.V., 2017. Many-Year Variations of the Average Salinity of the Sea of Azov. *Water Resources*, 44(5), pp. 749–757. https://doi.org/10.1134/S0097807817040042
9. Berdnikov, S.V., Dashkevich, L.V. and Kulygin, V.V., 2019. Climatic Conditions and Hydrological Regime of the Sea of Azov in the XX – Early XXI Centuries. *Aquatic Bioresources and Environment*, 2(2), pp. 7–19. doi:10.47921/2619-1024_2019_2_2_7
10. Andrews, S.W., Gross, E. S. and Hutton, P.H., 2017. Modeling Salt Intrusion in the San Francisco Estuary prior to Anthropogenic Influence. *Continental Shelf Research*, 146, pp. 58–81. doi:10.1016/j.csr.2017.07.010
11. Casulli, V. and Zanolli, P., 2005. High Resolution Methods for Multidimensional Advection–Diffusion Problems in Free-Surface Hydrodynamics. *Ocean Modelling*, 10(1–2), pp. 137–151. doi:10.1016/j.ocemod.2004.06.007
12. Wang, J., Li, L., He, Z., Kalhoro, N.A. and Xu, D., 2019. Numerical Modelling Study of Seawater Intrusion in Indus River Estuary, Pakistan. *Ocean Engineering*, 184, pp. 74–84. doi:10.1016/j.oceaneng.2019.05.029
13. Chikin, A.L., Kleshchenkov, A.V. and Chikina, L.G., 2019. Simulating Salinity Variations in the Gulf of Taganrog at Storm Surges. *Water Resources*, 46(6), pp. 919–925. doi:10.1134/S0097807819060046
14. Chikin, A.L., Kleshchenkov, A.V. and Chikina, L.G., 2019. Numerical Study of the Water Flow Effect on the Water Level in the Don Mouth. *Physical Oceanography*, 26(4), pp. 316–325. doi:10.22449/1573-160X-2019-4-316-325
15. Fillipov, Yu.G., 2014. Calculations of a Degree in the Eastern Part of the Taganrog Bay. In: Sychev, Yu.F., ed., 2014. *Proceedings of N.N. Zubov State Oceanographic Institute*. Moscow. Iss. 215, pp. 136–143 (in Russian).

16. Filippov, Yu.G., 1970. [On a Method for Calculations of Marine Currents]. In: SOI, 1970. *Proceedings of N.N. Zubov State Oceanographic Institute*. Moscow: Moskovskoe Otdelenie Gidrometeoizdata. Iss. 103, p. 87 (in Russian).
17. Voevodin, A.F., Nikiforovskaya, V.S. and Ovcharova, A.S., 1983. [Numerical Methods for Solving the Problem of Unsteady Water Flow at River Mouths]. In: AARI, 1983. *Trudy Arkticheskogo i Antarkticheskogo Nauchno-Issledovatelskogo Instituta*. Leningrad: Gidrometeoizdat. Iss. 378, pp. 23–34 (in Russian).
18. Savenije, H.H.G., 2012. *Salinity and Tides in Alluvial Estuaries*. Elsevier, 2012, 194 p. doi:10.1016/B978-0-444-52107-1.X5000-X

Submitted 15.06.2023.; accepted after review 02.10.2023;
revised 11.10.2023; published 20.12.2023

About the authors:

Aleksey L. Chikin, Chief Research Associate, the Southern Scientific Centre of the Russian Academy of Sciences (41 Chekhova Ave., Rostov-on-Don, 344006, Russian Federation), Dr.Sci. (Phys.-Math.), Senior Research Associate, **SPIN-code: 3845-9760, ORCID ID: 0000-0002-4065-010X, Scopus Author ID: 8240627300**

Aleksey V. Kleshchenkov, Leading Research Associate, the Southern Scientific Centre of the Russian Academy of Sciences (41 Chekhova Ave., Rostov-on-Don, 344006, Russian Federation), Ph.D. (Geogr.), **ResearcherID: E-6619-2014, ORCID ID: 0000-0002-7976-6951, Scopus Author ID: 57016697100**

Lyubov G. Chikina, Professor, Southern Federal University (105 Bolshaya Sadovaya St., Rostov-on-Don, 344006, Russian Federation), Dr.Sci. (Phys.-Math.), Associate Professor, **SPIN-code: 4295-3950**

Contribution of the authors:

Aleksey L. Chikin – study initiation, development of the numerical model; preparation of the initial version of the text; review of the literature on the study problem; text revision; construction of tables, graphs, diagrams

Aleksey V. Kleshchenkov – statement of the goals and objectives of the study, abstract writing, analysis and summary of the study results, drawing conclusions, review of the literature on the study problem, data collection and systematization, construction of tables, graphs, diagrams, computer work

Lyubov G. Chikina – selection and justification of numerical methods for solving equations, correction of the numerical model and calculations, computer implementation of algorithms

All the authors have read and approved the final manuscript.

Original article

Metabolic Response of Cultivated Bivalve Mollusks to Acidification in the Black Sea

O. Yu. Vialova

A.O. Kovalevsky Institute of Biology of the Southern Seas of RAS (IBSS), Sevastopol, Russia

e-mail: vyalova07@gmail.com

Abstract

The Black Sea, which is potentially the largest sink of CO_2 among the seas of the Atlantic Ocean, has been experiencing a decrease in pH over the last decades. Information on the acidification of the Black Sea and its impact on the marine biosystem is scarce. Based on literature and our own experimental data, we analyse the effect of low seawater pH values on the energy metabolism of the main commercial bivalve molluscs – the mussel *Mytilus galloprovincialis* and the oyster *Magallana gigas*. These species showed the ability to adapt energy metabolism levels over a wide pH range, from 7.0 to 8.1. When the pH was lowered by 0.1 unit, the oxygen consumption of mussels decreased on average by 10–20% in the pH range 7.5–8.2. At pH 7.2–7.5, the respiration rate of *M. galloprovincialis* did not change and remained at 9.15–9.38 µg O_2/(g dry tissue·h) and then dropped to 6.8 µg O_2/(g dry tissue·h) at pH 7.0. In *M. gigas*, the oxygen consumption rate decreased uniformly: on average by 10–15 % for each 0.1 unit of pH change, up to pH value of 7.2. At pH 7.0–7.2, aerobic respiration of oysters was recorded at a minimum level of 4.6–4.8 µg O_2/(g dry tissue·h).

Keywords: mussel *Mytilus galloprovincialis*, oyster *Magallana gigas*, respiration, pH, acidification, Black Sea

Acknowledgments: The work was carried out within the framework of the state budget topic of IBSS RAS no. 121041400077-1.

For citation: Vialova, O.Yu., 2023. Metabolic Response of Cultivated Bivalve Mollusks to Acidification in the Black Sea. *Ecological Safety of Coastal and Shelf Zones of Sea*, (4), pp. 73–86.

Метаболический отклик культивируемых двустворчатых моллюсков на закисление Черного моря

О. Ю. Вялова

Федеральный исследовательский центр «Институт биологии южных морей имени А.О. Ковалевского РАН» (ФГБНУ «ФИЦ ИнБЮМ»), Севастополь, Россия

e-mail: vyalova07@gmail.com

Аннотация

В течение последних десятилетий наблюдается снижение pH в Черном море, которое потенциально является самым большим поглотителем CO_2 среди морей Атлантического океана. Сведения о закислении Черного моря и его влиянии на биосистему моря фрагментарны. На основании литературных и собственных экспериментальных данных проводится анализ влияния низких значений pH морской воды на энергетический метаболизм основных промысловых двустворчатых моллюсков – мидии *Mytilus galloprovincialis* и устрицы *Magallana gigas.* Данные виды показали способность адаптировать уровень энергетического метаболизма в широком диапазоне pH – от 7.0 до 8.1. При понижении pH на 0.1 ед. потребление кислорода мидиями снижалось в среднем на 10–20 % в диапазоне pH 7.5–8.2. При pH 7.2–7.5 интенсивность дыхания *M. galloprovincialis* не менялась и оставалась на уровне 9.15–9.38 мкг O_2/(г сух. тк.·ч), а затем падала до 6.8 мкг O_2/(г сух. тк.·ч) при pH 7.0. У *M. gigas* интенсивность потребления кислорода снижалась равномерно: в среднем на 10–15 % на каждые 0.1 ед. изменения pH до значения pH 7.2. При pH 7.0–7.2 аэробное дыхание устриц фиксировалось на минимальном уровне (4.6–4.8 мкг O_2/(г сух. тк.·ч)).

Ключевые слова: мидия *Mytilus galloprovincialis*, устрица *Magallana gigas*, дыхание, pH, закисление, Черное море, прибрежные экосистемы, двустворчатые моллюски, марикультура

Благодарности: работа выполнена в рамках госзадания ФИЦ ИнБЮМ по теме № 121041400077-1.

Для цитирования: *Вялова О. Ю.* Метаболический отклик культивируемых двустворчатых моллюсков на закисление Черного моря // Экологическая безопасность прибрежной и шельфовой зон моря. 2023. № 4. С. 73–86. EDN OVFSHX.

Introduction

Global changes in the world's ocean waters are altering almost all coastal ecosystems. The increase in carbon dioxide content in the marine environment and the resulting growth of its acidity are of reasonable concern. Ocean water acts as a major sink for atmospheric carbon, helping to offset the effects of global warming [1–3]. During the last decades, all seas of the world's ocean have been experiencing a decrease in pH, which is expected to fall to 7.1 by 2100 [2]. Obviously, different marine areas will not be affected to the same extent: it is determined by their geographical location and hydrological characteristics. In shelf seas, water acidification depends on the volume of river inflow, the degree of organic pollution, and the intensity of upwelling and production processes in the surface layers [4–6]. Of note, even with the reduction of greenhouse gas emissions

into the atmosphere, the seawater acidity will be increasing for a long time, since CO_2 is a long-lived atmospheric gas.

Reports by the Intergovernmental Panel on Climate Change argue that fresher and colder waters can absorb much more CO_2 from the atmosphere than more saline oceanic water masses can. The Black Sea is characterised by an average surface temperature of 17–19 °C (~14 °C in winter and ~25 °C in summer) and a salinity of 17–18 PSU. According to experts, the Black Sea is potentially the largest CO_2 sink among the nearest seas of the Atlantic Ocean [3, 6]. In the surface layers of the sea, this parameter is higher than typical oceanic values due to the high total alkalinity of the rivers flowing into the Black Sea [7]. The most significant decrease in pH values was recorded in the upper suboxic layer: on average by 0.15–0.20 per decade [4–6, 8]. According to the work [6], in the surface layer (0–30 m) in 1990–2014, the maximum and minimum mean annual pH values were ~ 8.7 and 7.4, respectively. Observational data in the coastal zones of the eastern part of the Black Sea showed that during the year the pH varied between 8.36 and 8.45 [5], while in the western part (Romanian coast) it ranged between 7.37 and 8.58. It is explained by more intensive production processes in the 0–10 m layer [3]. There are two seasons: the cold one (November to March) with minimum pH values and the warm one (April to October) with maximum values. These differences are related to general climatic patterns, river discharge, upwelling and seasonal variability of production processes in the Black Sea [6–8]. In addition, there are diurnal variations in pH in coastal areas, which can exceed unity [5, 9]. These changes often result from the fact that primary producers increase the pH of the surrounding seawater in the daytime during photosynthesis and decrease it at night during respiration [10, 11].

A number of widely cited meta-analyses and systematic reviews have been published, which concern the effects of ocean acidification on selected groups of hydrobionts [12–17]. The considered scenarios and predictions have revealed gaps in the study of physiological and behavioural responses of bivalves under conditions of decreasing pH values in the marine environment. This is due to the difficulty of determining the direct and/or indirect influence of the studied factor, and the contradictory results obtained by different authors. Marine organisms that use calcium carbonate ($CaCO_3$) to create shells or other body structures, so-called marine calcifiers, are directly threatened at all life stages – larval, juvenile and adult [12, 18–25]. A decrease in the amount of available carbonate ions can not only impede the formation of biogenic calcium structures in the body, but also make such structures vulnerable to dissolution under conditions of low pH values [24, 26, 27]. The authors note that the rate of pH change is extreme and already potentially dangerous for many calcifying marine species.

A decrease in seawater pH is detrimental to the physiology of bivalves, since it alters the extracellular acid-base balance [28–30] and metabolic activity [31].

Moreover, it leads to supression of respiration and excretion, decreased food intake [12, 32, 33], and impaired development of organisms occur [18, 27]. In some cases, a decrease in pH can lead to death [12]. Acidified marine environment results in deterioration of the mechanical properties of byssus filaments and in a decrease in their number [26, 34]. Embryonic and larval stages of mussels were found sensitive to the pH level. Due to acidification, the size of larvae decreases, their survival rate reduces, whereas the number of individuals with abnormalities and a longer developmental period increases [22].

At the same time, there is evidence of some positive effect of water acidification on shell growth [35]. Thus, a reduced pH value can mitigate the adverse impact of high temperature on biomineralisation and crystal ultrastructure of the genus Mytilus. Resistance of bivalves to environmental acidification has been described in such species from estuarine and upwelling areas as *M. chilensis* [22], *Argopecten purpuratus* [36, 37], *M. edulis* [22, 38, 39], *M. galloprovincialis* [39-41], *M. coruscus* [42], *Pinctada fucata* and *Perna viridis* [33]. Some studies indicate that food availability plays an important role in the resistance of mussels to acidification of the marine environment [20, 33].

Data on the Black Sea acidification and its impact on the marine biosystem are scarce. However, it is clear that many biota components may be affected by decreasing pH values, which in turn may cause ecological and economic problems in the region. Bivalves dominate the macrofauna of estuaries and bays. These organisms are an important element of the biotopes ecological structure and a commercial resource for fisheries and mariculture. Marine farms cultivating the two main commercial species, mussels *Mytilus galloprovincialis* and oysters *Magallana* (formerly *Crassostrea*) *gigas*, are located along the coastline of the Black Sea, including the Crimean Peninsula and Krasnodar Krai. Assessment of the effects of acidification on the state of commercially important species is a vital task of modern research.

Respiration intensity of molluscs is an important summarizing indicator of the level of metabolic processes in the organism. The volume of oxygen consumed by molluscs allows assessment of their physiological state and the extent of influence of various environmental factors on them [12, 31, 33]. The study investigates the level of energy metabolism of mussels *M. galloprovincialis* and oysters *M. gigas* under ongoing acidification of the Black Sea. The paper examines how a wide range of pH values (7.0-8.1), potentially possible in the Black Sea, can influence the adaptive capacity of these commercially important species.

Materials and methods

Specimens of mussels *Mytilus galloprovincialis* and oysters *Magallana gigas* were collected from a sea farm located in Laspi Bay (Black Sea, the South Coast of Crimea), placed into thermoboxes and delivered to the laboratory of Institute of Biology of Southern Seas (Sevastopol). Further, the molluscs were kept in flowing sea water at 20–21 °C, pH 8.2 and salinity 18.1 PSU for seven days. Molluscs were fed daily with *Isochrysis galbana*. The experiments were conducted

in 950 mL closed respirometers using filtered seawater. The duration of the experiments ranged from 2 to 2.5 h. The molluscs were pre-cleaned of epibionts, weighed and measured. One specimen was placed into each respirometer, and a peristaltic pump was used to continuously circulate filtered seawater in a closed cycle. The initial and final oxygen concentration was determined using a dissolved oxygen analyser MARK-404.

Seawater with different pH values was prepared using Tetra minus pH. This certified preparation is used in marine aquaristics to reduce pH and carbonate hardness and is safe for hydrobionts. By applying different dosages of the preparation, conditions were created with pH values ranging from 8.1 to 7.0, which is slightly wider than the expected pH range in the Black Sea. In each respirometer, the pH value was determined before and after the experiment using an Ohaus ST2100 laboratory pH-meter.

After completion of each of the experiments, the water in the respirometers with molluscs was replaced with new water with preset pH values. The temperature was 20–21 °C and salinity was 18.1 PSU. The experiments were carried out in four replicates. The total number of studied molluscs was 24.

The oxygen consumption RR, μg O_2/(g dry tissue·h), by molluscs was calculated by the formula

$$RR = (C_{beg.} - C_{end}) \cdot V/T/W_{dry\ tiss.},$$

where $C_{beg.}$ and C_{end} – O_2 content in respirometers with molluscs at the beginning and end of the experiment; V – volume of respirometer, mL; T – time, h; $W_{dry\ tiss.}$ – weight of dry tissues, g. The dry weight was obtained by drying soft tissues in thermostat at 98 °C to constant weight.

Statistical and graphical data were processed using Excel, one-way ANOVA.

Results

The main characteristics of the study objects (mussels *M. galloprovincialis* and oysters *M. gigas*) are presented in the table.

The study found that mussels normally had higher energy metabolism levels (18.23 ± 1.2 μg O_2/(g dry tiss.·h) than oysters (10.50 ± 1.1 μg O_2/(g dry tiss.·h)).

Size and weight characteristics of bivalves (mean ± SD)

Species	n, ind.	L, mm	W_{total}, g	W_{shell}, g	$W_{dry\ soft\ tiss.}$, g
Mussel	12	55.71 ± 4.82	19.96 ± 4.80	13.73 ± 4.22	0.224 ± 0.088
Oyster	12	64.88 ± 6.17	27.56 ± 8.88	10.19 ± 0.80	0.306 ± 0.217

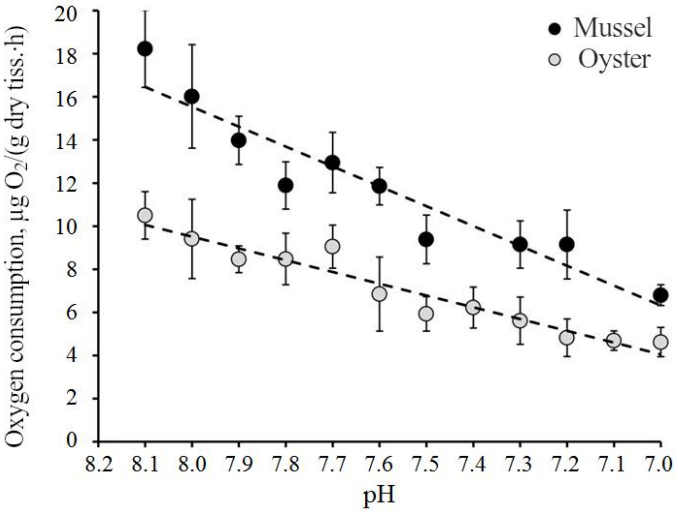

F i g. 1. Dependence of oxygen consumption by mussels *M. galloprovincialis* and oysters *M. gigas* on seawater pH, mean ± SD

A decrease in seawater pH led to a decrease in respiration in both mollusk species (Fig. 1). A linear negative dependence of oxygen consumption on pH values was found for mussels *M. galloprovincialis* ($R^2 = 0.90$) and oysters *M. gigas* ($R^2 = 0.93$).

The results showed that in the pH range of 7.5–8.2, when pH was lowered by 0.1 unit, the oxygen consumption by mussels decreased by 10–20% of the previous value. Further, at pH 7.2–7.5 the respiration of molluscs remained at 9.15–9.38 µg O_2/(g dry tissue·h), then a drop of this indicator to 6.8 µg O_2/(g dry tissue·h) was recorded at pH 7.0 (Fig. 2). In *M. gigas*, the observed decrease in oxygen consumption was more uniform, by 10–15% for each 0.1 pH unit, up to pH 7.2. Then this parameter did not change and was fixed at a minimum level (4.6–4.8 µg O_2/(g dry tissue·h)).

Thus, acidification of seawater led to a decrease in the respiration intensity in mussels *M. galloprovincialis* and oysters *M. gigas*. At pH 7.5–7.7, the most noticeable changes in the level of energy metabolism occurred in the studied molluscs (Fig. 2). After a uniform decrease in oxygen consumption in both species at pH 7.7, an unexpected increase in this indicator was recorded (by 8.9% in mussels and by 6.7% in oysters) followed by a sharp drop by 20–30% from the previous values (at pH 7.5–7.6). At the same time, the two species showed different physiological response: the mussels steadily maintained the level of aerobic metabolism when pH decreased from 7.4 to 7.1 (no changes in respiration rate), while the oysters demonstrated a uniform decrease of aerobic processes to minimum values.

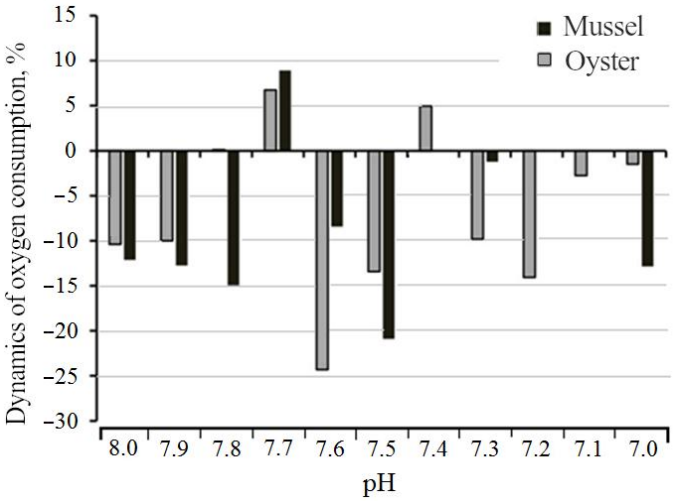

F i g. 2. Dynamics of oxygen consumption by mussels *M. galloprovincialis* and oysters *M. gigas* with a decrease in pH of seawater by 0.1 unit

Discussion

The ability of bivalves to compensate the level of energy metabolism in the setting of environmental changes is confirmed by a number of studies [31, 40, 43, 44]. This is due to the lifestyle of molluscs, which form dense settlements in the coastal area and are occasionally exposed to changing external factors such as temperature, salinity, and oxygen regime. In our study, the effect of low environmental pH values on the level of energy metabolism of bivalves cultured in the Black Sea was investigated for the first time.

On coastal farms, molluscs are grown in plastic cages and nets at depths of up to 10 m from the surface. Thus, mussels and oysters potentially fall within the areas of pH change caused by natural daily and seasonal dynamics of this indicator [5, 45] and by upwellings [6].

Studies of several species of mussels *M. edulis*, *M. galloprovincialis* and *M. trossulus* showed that the threshold of physiological tolerance is at pH ~7.8, which approximately corresponds to the lower values of the local natural background pH of marine waters [39, 40, 46]. The work [28] reports the results of keeping juvenile and adult *M. galloprovincialis* at pH ~7.3 (18 °C). Under such acidified conditions, the rate of oxygen consumption decreased significantly more in juvenile mussels: after 5 h of the experiment, oxygen consumption fell by 25%, after 10 h – by over 45% and after 20 h – by 60–65%. In adult molluscs, the maximum decrease in respiratory intensity was 35% of the control. Some authors believe that seawater pH < 7.5 is detrimental to shellfish, and pH values of ~7.3 may be fatal for them [28, 46].

The tolerance range of a species is known to be often closely related to the range of variability of environmental parameters. This allows us to conclude that the studied molluscs can be exposed to pH values > 7.6 in the natural environment, i. e. from 8.2 (normal) to 7.5–7.6 pH (acidification), and tolerate such changes well. Here are some examples of such studies on bivalves.

C. A. Vargas et al. [23, 25], based on their own and literature data, argue that organisms of the same species react differently to environmental acidification: the reaction was from negative to positive. For example, mussels *M. chilensis* from estuaries with high natural water CO_2 content showed greater tolerance to high pCO_2 levels than individuals from open areas. Molluscs *M. trossulus* retained the ability to repair damaged shells and shell mineralisation for 2.5 months at pH values ranging from 7.29 to 7.95 [47]. The data report *Bathymodiolus brevior* able to live in natural conditions at both pH 7.8 and pH 5.36 on the northwestern slope of the Eifuku submarine volcano of the Mariana Arc, whose hydrothermal environment contains liquid carbon dioxide and hydrogen sulfide [48]. Comparison of the two populations showed that the average daily growth rate and shell thickness of individuals from the volcano area were two times less than those of molluscs living in water at pH over 7.8.

Recent studies of natural populations of *M. galloprovincialis* from shallow lagoons and open coastal areas indicate that there is genetic diversity of adaptation to ocean acidification in molluscs [49]. An analysis of gene expression patterns revealed that differences in the pH fluctuations observed in coastal and lagoonal habitats potentially form patterns of plasticity and molecular-phenotypic differentiation between populations of the same species. The plasticity of expression in response to the effects of low pH was significantly higher in the coastal population, which lives in more stable conditions of the large masses of the Mediterranean Sea, as opposed to the conditions of shallow lagoons, which are characterised by abrupt fluctuations in environmental factors [49]. It is suggested that the tolerance of bivalves to pH changes may be fixed at the molecular genetic level.

The results of studies on the metabolic response of oysters to sea acidification are also controversial. For example, the work [50] reports a decrease in respiration rate of *C. virginica* exposed to high CO_2 partial pressure (0.8–1 kPa pCO_2) and low pH ($\leq$ 7) compared to controls (< 0.1 kPa pCO_2, pH = 8.2). In another study, high CO_2 for 30 days resulted in inhibition of food consumption and digestion processes, decreased adsorption efficiency in *C. gigas*, but at the same time it led to increased oxygen consumption and ammonium nitrogen excretion rate [51]. The results of a 55-day experiment on *C. gigas* are of interest, where at 15 °C the intensity of metabolic processes in the control (pH 7.9) and test (pH 7.09) groups of molluscs remained at the same stable level [29]. However, as the temperature increased to

20–25 °C, the situation changed: the level of metabolism increased considerably in the oysters under the acidified conditions. It is suggested that temperature is a more significant factor for oyster physiology than low pH values.

Under conditions of persistent and fluctuating acidification, Pacific oysters showed adaptability of such vital processes as calcification, respiration, nutrition and survival [52, 53]. Under low pH conditions (7.5–7.7), both male and female eastern oysters (*C. virginica*) showed accelerated reproductive development [54]. Observations of gametes during spawning, fertilisation, and embryo incubation showed a higher survival rate of the larvae (by 6–8% compared to the control).

In our study at pH 7.7, we recorded an increase in oxygen consumption by the molluscs of both species (by 8.9% in the mussels and 6.7% in the oysters). A similar response was observed in Black Sea mussels during DDT poisoning [55]. Thus, the effect of the toxicant initially inhibited respiration, then there was a short-term excitation (by the end of the first week of the experiment, the oxygen consumption in mussels was almost restored to the baseline), and after that the process was inhibited further. The authors explain this phenomenon by the fact that in order to restore the initial physiological state of the organism once the action of a negative factor (toxicant) started, the oxygen demand increases and oxidative processes intensify. However, the continuing gradual accumulation of DDT in the organs and tissues of molluscs eventually caused metabolic processes impairment in the latter, and the intensity of oxygen consumption by mussels began to decrease again. Analysing our results, we can assume that water acidification may have a similar effect on the level of metabolic processes in the organism of the studied molluscs.

In the course of evolution, molluscs have developed certain mechanisms of adaptation to unfavourable environmental factors, e. g. filtration stops, the valves close tightly and the rate of oxygen consumption decreases abruptly, respiration becomes anaerobic. The rate of energy processes in molluscs reduces to a minimum, and the animals enter a state of anaerobiosis. Adaptation of benthic organisms to unfavourable factors occurs at different levels: molecular, cellular, physiological, behavioural.

Conclusions

Recent studies show that the tolerance limit for most marine calcifying organisms is pH 7.5. Our results indicate that mussels *M. galloprovincialis* and oysters *M. gigas* inhabiting the Black Sea are adapted to the acidification of the marine environment and can maintain viability and energy metabolism level in a wide range of hydrogen ion concentration: from 7.0 to 8.1. During moderate stress, the organism can compensate for increased energy demand by higher energy intake and assimilation. However, under extreme impact of external factors, such physiological compensation for hydrobionts may be incomplete or impossible.

Thus, molluscs can enter a metabolic depression state to reduce energy expenditure and increase the survival time until the conditions return to optimal. This paper shows that at extremely low pH values, the energy homeostasis was disturbed, which led to a limitation of the aerobic capacity of the organism.

Along with the gradual global ocean acidification caused by high atmospheric CO_2 concentrations, the daily and seasonal dynamics of CO_2 and pH in seawater are expected to increase. Assessment of the effect which these systemic variables have on the physiological processes of hydrobionts on short time scales is at its onset. Our understanding of the effects of the ongoing acidification of the Black Sea on ecologically and economically important hydrobionts is still limited. In a laboratory setting, it is difficult to reproduce the environmental heterogeneity that occurs under natural conditions. Fluctuating decreases and increases in pH can mitigate some of the negative effects of acidification on shell organisms by providing them with periods of "respites" during which processes associated with calcification of structural elements are initiated. The vast majority of works study the effect of stable pH levels on different species of hydrobionts. At the same time, it becomes obvious that the ecological significance of such studies is limited. This can be explained by the fact that predicted ocean pH values will be different from those of today, and also by the fact that physiological adaptations of organisms and ultimately natural selection are stronger under extreme conditions.

REFERENCES

1. Bates, N.R., Astor, Y.M., Church, M.J., Currie, K., Dore, J.E., González-Dávila, M., Lorenzoni, L., Muller-Karger, F., Olafsson, J. [et al.], 2014. A Time-Series View of Changing Ocean Chemistry due to Ocean Uptake of Anthropogenic CO_2 and Ocean Acidification. *Oceanography*, 27(1), pp. 126–141. doi:10.5670/oceanog.2014.16
2. Masson-Delmotte, V., Zhai, P., Pirani, A., Connors, S.L., Pean, C., Chen, Y., Goldfarb, L., Gomis, M.I., Matthews, J.B.R. [et al.], eds., 2022. *Climate Change 2021. The Physical Science Basis. Contribution of Working Group I to the Sixth Assessment Report of the Intergovernmental Panel on Climate Change*. Cambridge: Cambridge University Press, 2391 p. doi:10.1017/9781009157896
3. Fowler, S.W., 2008. Ocean Acidification Issues in the Mediterranean and Black Seas: Present Status and Future Perspectives. In: F. Briand, ed., 2008. *Impacts of Acidification on Biological, Chemical and Physical Systems in the Mediterranean and Black Seas.* CIESM Workshop Monographs. No. 36. Monaco: CIESM, pp. 23–30.
4. Polonsky, A.B. and Grebneva, E.A., 2019. The Spatiotemporal Variability of pH in Waters of the Black Sea. *Doklady Earth Sciences*, 486(2), pp. 669–674. https://doi.org/10.1134/S1028334X19060072
5. Khoruzhii, D.S. and Konovalov, S.K., 2014. Diurnal and Inter-Diurnal Variations of Contents of Carbon Dioxide and Dissolved Inorganic Carbon in the Black Sea Coastal Waters. *Morskoy Gidrofizicheskiy Zhurnal*, (1), pp. 28–43 (in Russian).
6. Elge, M., 2021. Analysis of Black Sea Ocean Acidification. *International Journal of Environment and Geoinformatics*, 8(4), pp. 467–474. doi:10.30897/ijegeo.857893
7. Savenko, A.V. and Pokrovsky, O.S., 2022. Transformation of the Major and Trace Element Composition of Dissolved Matter Runoff in the Mouths of Medium and Small Rivers of Russia's Black Sea Coast. *Oceanology*, 62(3), pp. 324–345. doi:10.1134/s0001437022030110

8. Grebneva, E.A. and Polonsky, A.B., 2021. Decomposition of the Time Series of the pH Values of the Surface Water of the Deep Black Sea according to Archival Data of the Second Half of the XXth Century. *Monitoring Systems of Environment*, 44(2), pp. 29–38. doi:10.33075/2220-5861-2021-2-29-38 (in Russian).
9. Khoruzhii, D.S., 2016. Variability of Equilibrium Partial Pressure of Carbon Dioxide (pCO_2) and Concentration of Dissolved Inorganic Carbon (TCO_2) in the Black Sea Coastal Waters in 2010–2014. *Physical Oceanography*, (4), pp. 34–46. doi:10.22449/1573-160X-2016-4-34-46
10. Hurd, C.L., Cornwall, C.E., Currie, K., Hepburn, C.D., McGraw, C.M., Hunter, K.A. and Boyd, P.W., 2011. Metabolically-Induced pH Fluctuations by some Coastal Calcifiers Exceed Projected 22nd Century Ocean Acidification: a Mechanism for Differential Susceptibility? *Global Change Biology*, 17(10), pp. 3254–3262. doi:10.1111/j.1365-2486.2011.02473.x
11. Torres, O., Kwiatkowski, L., Sutton, A.J., Dorey, N. and Orr, J.C., 2021. Characterizing Mean and Extreme Diurnal Variability of Ocean CO_2 System Variables Across Marine Environments. *Geophysical Research Letters*, 48(5), pp. 1–12. doi:10.1029/2020GL090228
12. Gazeau, F., Parker, L.M., Comeau, S., Gattuso, J.-P., O'Connor, W.A., Martin, S., Pörtner, H.-O. and Ross, P.M., 2013. Impacts of Ocean Acidification on Marine Shelled Molluscs. *Marine Biology*, 160(8), pp. 2207–2245. doi:10.1007/s00227-013-2219-3
13. Kroeker, K.J., Kordas, R.L., Crim, R., Hendriks, I.E., Ramajo, L., Singh, G.S., Duarte, C.M. and Gattuso, J.-P., 2013. Impacts of Ocean Acidification on Marine Organisms: Quantifying Sensitivities and Interaction with Warming. *Global Change Biology*, 19(6), pp. 1884–1896. doi:10.1111/gcb.12179
14. Doney, S.C., Busch, D.S., Cooley, S.R. and Kroeker, K.J., 2020. The Impacts of Ocean Acidification on Marine Ecosystems and Reliant Human Communities. *Annual Review of Environment and Resources*, 45, pp. 83–112. doi:10.1146/annurev-environ-012320-083019
15. Kelaher, B.P., Mamo, L.T., Provost, E., Litchfield, S.G., Giles, A. and Butcherine, P., 2022. Influence of Ocean Warming and Acidification on Habitat-Forming Coralline Algae and their Associated Molluscan Assemblages. *Global Ecology and Conservation*, 35, e02081. doi:10.1016/j.gecco.2022.e02081
16. Leung, J.Y.S., Zhang, S. and Connell, S.D., 2022. Ocean Acidification Really a Threat to Marine Calcifiers? A Systematic Review and Meta-Analysis of 980+ Studies Spanning Two Decades. *Small*, 18(35), 2107407. doi:10.1002/smll.202107407
17. Townhill, B.L., Artioli, Y., Pinnegar, J.K. and Birchenough, S.N.R., 2022. Exposure of Commercially Exploited Shellfish to Changing pH Levels: How to Scale-Up Experimental Evidence to Regional Impacts. *ICES Journal of Marine Science*, 79(9), pp. 2362–2372. doi:10.1093/icesjms/fsac177
18. Ross, P.M., Parker, L., O'Connor, W.A. and Bailey, E.A., 2011. The Impact of Ocean Acidification on Reproduction, Early Development and Settlement of Marine Organism. *Water*, 3(4), pp. 1005–1030. doi:10.3390/w3041005
19. Bechmann, R.K., Taban, I.C., Westerlund, S., Godal, B.F., Arnberg, M., Vingen, S., Ingvarsdottir, A. and Baussant, T., 2011. Effects of Ocean Acidification on Early Life Stages of Shrimp (*Pandalus borealis*) and Mussel (*Mytilus edulis*). *Journal of Toxicology and Environmental Health*, 74(7–9), pp. 424–438, doi:10.1080/15287394.2011.550460
20. Thomsen, J., Casties, I., Pansch, C., Kortzinger, A. and Melzner, F., 2012. Food Availability Outweighs Ocean Acidification Effects in Juvenile *Mytilus edulis*: Laboratory and Field Experiments. *Global Change Biology*, 19(4), pp. 1017–1027. doi:10.1111/gcb.12109

21. Parker, L.M., Ross, P.M., O'Connor, W.A., Portner, H.O., Scanes, E. and Wright, J.M., 2013. Predicting the Response of Molluscs to the Impact of Ocean Acidification. *Biology*, 2(2), pp. 651–692. doi:10.3390/biology2020651
22. Duarte, C., Navarro, J.M., Acuna, K., Torres, R., Manriquez, P.H., Lardies, M.A., Vargas, C.A., Lagos, N.A. and Aguilera, V., 2014. Combined Effects of Temperature and Ocean Acidification on the Juvenile Individuals of the Mussel *Mytilius chilensis*. *Journal of Sea Research*, 85, pp. 308–314. doi:10.1016/j.seares.2013.06.002
23. Vargas, C.A., Lagos, N.A., Lardies, M.A., Duarte, C., Manriquez, P.H., Aguilera, V.M., Broitman, B., Widdicombe, S. and Dupont, S., 2017. Species-Specific Responses to Ocean Acidification Should Account for Local Adaptation and Adaptive Plasticity. *Nature Ecology and Evolution*, 1, 0084, pp. 1–7. doi:10.1038/s41559-017-0084
24. Wang, X., Shang, Y., Kong, H., Hu, M., Yang, J., Deng, Y. and Wang, Y., 2020. Combined Effects of Ocean Acidification and Hypoxia on the Early Development of the Thick Shell Mussel *Mytilus coruscus. Helgoland Marine Research*, 74(3), pp. 1–9. doi:10.1186/s10152-020-0535-9
25. Vargas, C.A., Cuevas, L.A., Broitman, B.R., San Martin, V.A., Lagos, N.A., Gaitan-Espitia, J.D. and Dupont, S., 2022. Upper Environmental pCO_2 Drives Sensitivity to Ocean Acidification in Marine Invertebrates. *Nature Climate Change*, 12, pp. 200–207. doi:10.1038/s41558-021-01269-2
26. Zhao, X., Guo, C., Zhumei, C., Wang, Y., Wang, X., Chai, X., Wu, H. and Liu, G., 2017. Ocean Acidification Decreases Mussel Byssal Attachment Strength and Induces Molecular Byssal Responses. *Marine Ecology Progress Series*, 565, pp. 67–77. doi:10.3354/meps11992
27. Fitzer, S.C., Vittert, L., Bowman, A., Kamenos, N.A., Phoenix, V.R. and Cusack, M., 2015. Ocean Acidification and Temperature Increase Impact Mussel Shell Shape and Thickness: Problematic for Protection? *Ecology and Evolution*, 5(21), pp. 4875–4884. doi:10.1002/ece3.1756
28. Michaelidis, B., Ouzounis, C., Paleras, A. and Portner, H.O., 2005. Effects of Long-Term Moderate Hypercapnia on Acid-Base Balance and Growth Rate in Marine Mussels *Mytilus galloprovincialis*. *Marine Ecology Progress Series*, 293, pp. 109–118. doi:10.3354/meps293109
29. Lannig, G., Eilers, S., Portner, H.O., Sokolova, I.M. and Bock, C., 2010. Impact of Ocean Acidification on Energy Metabolism of Oyster, *Crassostrea gigas* – Changes in Metabolic Pathways and Thermal Response. *Marine Drugs*, 8, pp. 2318–2339. doi:10.3390/md8082318
30. Lewis, C., Ellis, R.P., Vernon, E., Elliot, K., Newbatt, S. and Wilson, R.W., 2016. Ocean Acidification Increases Copper Toxicity Differentially in Two Key Marine Inverteb-rates with Distinct Acid-Base Responses. *Scientific Reports*, 6, 21554. doi:10.1038/srep21554
31. Thomsen, J. and Melzner, F., 2010. Moderate Seawater Acidification does not Elicit Long-Term Metabolic Depression in the Blue Mussel *Mytilus edulis*. *Marine Biology*, 157, pp. 2667–2676. doi:10.1007/s00227-010-1527-0
32. Fernández-Reiriz, J., Range, P., Alvarez-Saldago, X.A. and Labarta, U., 2011. Physiological Energetics of Juvenile Clams *Ruditapes decussatus* in a High CO_2 Coastal Ocean. *Marine Ecology Progress Series*, 433, pp. 97–105. doi:10.3354/meps09062
33. Liu, W. and He, M., 2012. Effects of Ocean Acidification on the Metabolic Rates of Three Species of Bivalve from Southern Coast of China. *Chinese Journal of Oceanology and Limnology*, 30(2), pp. 206–211. doi:10.1007/s00343-012-1067-1
34. Clements, J.C. and George, M.N., 2022. Ocean Acidification and Bivalve Byssus: Explaining Variable Responses Using Meta-Analysis. *Marine Ecology Progress Series*, 694, pp. 89–103. doi:10.3354/meps14101

35. Knights, A.M., Norton, M.J., Lemasson, A.J. and Stephen, N., 2020. Ocean Acidification Mitigates the Negative Effects of Increased Sea Temperatures on the Biomineralization and Crystalline Ultrastructure of Mytilus. *Frontiers in Marine Science*, 7, 567228. doi:10.3389/fmars.2020.567228

36. Lagos, N.A., Benítez, S., Duarte, C., Lardies, M.A., Broitman, B.R., Tapia, C., Tapia, P., Widdicombe, S. and Vargas, C.A., 2016. Effects of Temperature and Ocean Acidification on Shell Characteristics of Argopecten purpuratus: Implications for Scallop Aquaculture in an Upwelling-Influenced Area. *Aquaculture Environment Interactions*, 8, pp. 357−370. doi:10.3354/aei00183

37. Lardies, M.A., Benitez, S., Osores, S., Vargas, C.A., Duarte, C., Lohrmann, K.B. and Lagos, N.A., 2017. Physiological and Histopathological Impacts of Increased Carbon Dioxide and Temperature on the Scallops *Argopecten purpuratus* Cultured under Upwelling Influences in Northern Chile. *Aquaculture*, 479, pp. 455−466. doi:10.1016/j.aquaculture.2017.06.008

38. Clements, J.C., Hicks, C., Tremblay, R. and Comeau, L.A., 2018. Elevated Seawater Temperature, not pCO_2, Negatively Affects Post-Spawning Adult Mussels (*Mytilus edulis*) under Food Limitation. *Conservation Physiology*, 6(1), cox078. doi:10.1093/conphys/cox078

39. De Wit, P., Durland, E., Ventura, A. and Langdon, C.J., 2018. Gene Expression Correlated with Delay in Shell Formation in Larval Pacific Oysters (*Crassostrea gigas*) Exposed to Experimental Ocean Acidification Provides Insights into Shell Formation Mechanisms. *BMC Genomics*, 19(1), pp. 160−175. doi:10.1186/s12864-018-4519-y

40. Fernández-Reiriz, M.J., Range, P., Alvarez-Saldago, X.A., Espinosa, J. and Labarta, U., 2012. Tolerance of Juvenile *Mytilus galloprovincialis* to Experimental Seawater Acidification. *Marine Ecology Progress Series*, 454, pp. 65−74. doi:10.3354/meps09660

41. Gazeau, F., Alliouane, S., Bock, C., Bramanti, L., Lopez Correa, M., Gentile, M., Hirse, T., Portner, H.O. and Ziveri, P., 2014. Impact of Ocean Acidification and Warming on the Mediterranean Mussel (*Mytilus galloprovincialis*). *Frontiers in Marine Science*, 1, 62. doi:10.3389/fmars.2014.00062

42. Hu, M., Lin, D., Shang, Y., Hu, Y., Lu, W., Huang, X., Ning, K., Chen, Y. and Wang, Y., 2017. CO_2-Induced pH Reduction Increases Physiological Toxicity of Nano-TiO_2 in the Mussel *Mytilus coruscus. Scientific Reports*, 7, 40015. doi:10.1038/srep40015

43. Benitez, S., Lagos, N.A., Osores, S., Opitz, T., Duarte, C., Navarro, J.M. and Lardies, M.A., 2018. High pCO_2 Levels Affect Metabolic Rate, but not Feeding Behavior and Fitness, of Farmed Giant Mussel *Choromytilus chorus. Aquaculture Environment Interactions*, 10, pp. 267–278. doi:10.3354/aei00271

44. Duarte, C., Navarro, J.M., Quijon, P.A., Loncon, D., Torres, R., Manriquez, P.H., Lardies, M.A., Vargas, C.A. and Lagos, N.A., 2018. The Energetic Physiology of Juvenile Mussels, *Mytilus chilensis* (Hupe): The Prevalent Role of Salinity under Current and Predicted pCO_2 Scenarios. *Environmental Pollution*, 242, Part A, pp. 156–163. doi:10.1016/j.envpol.2018.06.053

45. Khoruzhii, D.S., 2018. Variability of the CO_2 Flux on the Water–Atmoshpere Interfaca 2 in the Black Sea Coastal Waters on Various Time Scales in 2010–2014. *Physical Oceanography*, 25(5), pp. 401–411. doi:10.22449/1573-160X-2018-5-401-411

46. Munari, M., Matozzo, V., Rieldi, V., Pastore, P., Badocco, D. and Marin, M.G., 2020. EAT BREATHE EXCRETE REPEAT: Physiological Responses of the Mussel *Mytilus galloprovincialis* to Diclofenac and Ocean Acidification. *Journal of Marine Science and Engineering*, 8(11), 907. doi:10.3390/jmse8110907

47. George, M.N., O'Donnel, M.J., Concodello, M. and Carrington, E., 2022. Mussels Repair Shell Damage Despite Limitations Imposed by Ocean Acidification. *Journal of Marine Science and Engineering*, 10(3), pp. 359. doi:10.3390/jmse10030359

48. Tunnicliffe, V., Davies, K.T.A., Butterfield, D.A., Embley, R.W., Rose, J.M. and Chadwick Jr., W.W., 2009. Survival of Mussels in Extremely Acidic Waters on a Submarine Volcano. *Nature Geoscience*, 2, pp. 344–348. https://doi.org/10.1038/ngeo500

49. Bitter, M.C., Kapsenberg, L., Silliman, K., Gattuso, J.-P. and Pfister, C.A., 2021. Magnitude and Predictability of pH Fluctuations Shape Plastic Responses to Ocean Acidification. *The American Naturalist*, 197(4), pp. 486–501. doi:10.1086/712930

50. Willson, L.L. and Burnett, L.E., 2000. Whole Animal and Gill Tissue Oxygen Uptake in the Eastern Oyster, *Crassostrea virginica*: Effect of Hypoxia, Hypercapnia, Air Exposure, and Infection with the Protozoan Parasite *Perkinsus marinus*. *Journal Experimental Marine Biology and Ecology*, 246, pp. 223–240. doi:10.1016/S0022-0981(99)00183-5

51. Jiang, W., Wang, X., Rastrick, S.P.S., Wang, J., Zhang, Y., Strand, Ø., Fang, J. and Jiang, Z., 2021. Effects of Elevated pCO_2 on the Physiological Energetics of Pacific Oyster, *Crassostrea gigas*. *ICES Journal of Marine Science*, 78(7), pp. 2579–2590. doi:10.1093/icesjms/fsab139

52. Bednaršek, N., Beck, M.W., Pelletier, G., Applebaum, S.L., Feely, R.A., Butler, R., Byrne, M., Peabody, B., Davis, J. and Štrus, J., 2022. Natural Analogues in pH Variability and Predictability Across the Coastal Pacific Estuaries: Extrapolation of the Increased Oyster Dissolution under Increased pH Amplitude and low Predictability Related to Ocean Acidification. *Environmental Science and Technology*, 56, pp. 9015−9028. doi:10.1021/acs.est.2c00010

53. Zuñiga-Soto, N., Pinto-Borguero, I., Quevedo, C. and Aguilera, F., 2023. Secretory and Transcriptomic Responses of Mantle Cells to Low pH in the Pacific Oyster (*Crassostrea gigas*). *Frontiers in Marine Science*, 10, 1156831. doi:10.3389/fmars.2023.1156831

54. Clements, J.C., Carver, C.E., Mallet, M.A., Comeau, L.A. and Mallet, A.L., 2021. CO_2-Induced Low pH in an Eastern Oyster (*Crassostrea virginica*) Hatchery Positively Affects Reproductive Development and Larval Survival but Negatively Affects Larval Shape and Size, with no Intergenerational Linkages. *ICES Journal of Marine Science*, 78(1), pp. 349–359. doi:10.1093/icesjms/fsaa089

55. Kozlova, G.V. and Gordienko, N.A., 2021. Infuence of Organochlorine Compounds on Respiratory Intensity and Glycogen Content in Mussels in the Kerch Strait. *Bulletin of the Kerch State Marine Technological University*, (4), pp. 46–58. doi:10.47404/2619-0605_2021_4_46 (in Russian).

Submitted 15.06.2023; accepted after review 5.07.2023;
revised 11.10.2023; published 20.12.2023

About the author:

Oksana Yu. Vialova, Senior Research Associate, A. O. Kovalevsky Institute of Biology of the Southern Seas of RAS (2 Nakhimova Ave, Sevastopol, 299011, Russian Federation), PhD (Biol.), **ORCID ID: 0000-0002-8304-0029, Scopus AuthorID: 6503936925**, **AuthorID: 979304**, *vyalova07@gmail.com*

The author has read and approved the final manuscript.

Original article

A Simulation Growth Model for the Cultured Oyster *Ostrea edulis* L.

T. A. Filippova *, E. F.Vasechkina

Marine Hydrophysical Institute of RAS, Sevastopol, Russia
** e-mail: filippovata@mhi-ras.ru*

Abstract

Cultivation of the flat oyster *Ostrea edulis* L., which has lost its commercial value due to reduction in abundance, is a relevant task. Simulation models of the flat oyster's growth can be used to improve oyster cultivation methods. The proposed simulation model of the *O. edulis* growth dynamics is based on the principles of dynamic energy balance. The model uses approximations of the oyster's physiological processes (filtration, respiration, excretion, growth, spawning) derived from published observational data. The paper determines functional dependencies of approximation parameters on the environmental conditions. The model was validated using *in situ* data on the linear and weight growth of the oyster *O. edulis* cultured in Donuzlav Bay for 30 months from April 2001 to October 2003. The model allowed us to obtain the dynamics of the energy balance components of the flat oyster at different life-cycle stages. The resulting quantitative distribution of growth energy between generative and somatic tissues of the oyster is confirmed by the qualitative description of the oyster's tissue growth based on *in situ* measurements. The developed model reproduces well the qualitative and quantitative characteristics of the flat oyster functioning processes. The model of the oyster's energy balance can be used as a block of a complex ecological model simulating the cultivation of mollusks on an oyster farm.

Keywords: flat oyster, *Ostrea edulis*, Donuzlav Bay, energy balance model, mariculture

Acknowledgments: The work was performed under state assignment on topic FNNN-2021-0005 "Complex interdisciplinary research of oceanologic processes, which determine functioning and evolution of the Black and Azov Sea coastal ecosystems".

For citation: Filippova, T.A. and Vasechkina, E.F., 2023. A Simulation Growth Model for the Cultured Oyster *Ostrea edulis* L. *Ecological Safety of Coastal and Shelf Zones of Sea*, (4), pp. 87–100.

Имитационная модель роста устрицы *Ostrea edulis* L. в условиях культивирования

Т. А. Филиппова *, Е. Ф. Васечкина

Морской гидрофизический институт РАН, Севастополь, Россия

* *e-mail: filippovata@mhi-ras.ru*

Аннотация

Культивирование плоской устрицы *Ostrea edulis* L., потерявшей свое промысловое значение вследствие сокращения численности, является актуальной задачей. Применение математических имитационных моделей может способствовать развитию технологии выращивания устриц в условиях морской фермы. Предложенная математическая модель динамики роста *O. edulis* построена на принципах динамического баланса энергии. В модели использованы математические аппроксимации физиологических процессов (фильтрация, дыхание, экскреция, рост, нерест), полученные на основе опубликованных данных наблюдений. Установлены функциональные зависимости параметров аппроксимаций от условий среды. Валидация модели выполнена по натурным данным о линейном и весовом росте устрицы *O. edulis*, выращиваемой в заливе Донузлав в течение 30 мес. с апреля 2001 по октябрь 2003 г. Использование модели позволило получить динамику составляющих энергетического баланса плоской устрицы, находящейся на разных стадиях жизненного цикла. Полученное количественное распределение энергии роста между генеративными и соматическими тканями устрицы подтверждается качественным описанием роста тканей устрицы по натурным измерениям. Разработанная модель хорошо воспроизводит качественные и количественные характеристики физиологических процессов плоской устрицы. Модель энергетического баланса устрицы может быть использована в качестве блока комплексной экологической модели, имитирующей культивирование моллюсков на устричной ферме.

Ключевые слова: плоская устрица, *Ostrea edulis*, залив Донузлав, модель энергетического баланса, аквакультура

Благодарности: работа выполнена в рамках государственного задания ФГБУН ФИЦ МГИ по теме: FNNN-2021-0005 «Комплексные междисциплинарные исследования океанологических процессов, определяющих функционирование и эволюцию экосистем прибрежных зон Черного и Азовского морей».

Для цитирования: *Филиппова Т. А., Васечкина Е. Ф.* Имитационная модель роста устрицы *Ostrea edulis* L. в условиях культивирования // Экологическая безопасность прибрежной и шельфовой зон моря. 2023. № 4. С. 87–100. EDN NZYAOP.

Introduction

The oyster *Ostrea edulis* is one of the most valuable species of the Black Sea coast mollusks. However, at present this species has lost its commercial value due to a shell fungal disease. In the second half of the last century, a catastrophic reduction in the habitat of the *Ostrea edulis* species took place in the Black Sea. It caused the work on artificial reproduction of the mollusks, which has been carried out since the 1980s. [1]. Thus, studies devoted to the quantitative description of physiological processes of this species are relevant and can be demanded when developing this mariculture.

In recent years, researchers have invested quite a lot of efforts to create mathematical models that make it possible to simulate the dynamics of oyster

growth depending on such environmental parameters as water temperature and feed suspension concentration. This paper is aimed at development of such a model for the oyster *O. edulis* cultured in Donuzlav Bay, a specific area of the Crimean coast. First, let us consider a number of the most interesting models close to our purpose, proposed by other authors [2–8].

In [2], a simulation model of population dynamics of the species *Magallana gigas* is given. The authors analyzed *in situ* data describing the growth of oysters, established functional dependencies of the growth rate on the size of the mollusk, then used the obtained dependencies as parameterizations in the population model. Due to the fact that filtration, respiration and excretion proceed differently in oysters of different stages of development, the researchers introduced separate mathematical functions to describe each stage of the oyster's life cycle and considered them separately from each other. The disadvantage of this approach is the difficulty in describing the continuous growth of individuals in a population.

In [3], a growth model of the Pacific oyster *M. gigas* cultivated in the Thau Lagoon, France, is presented. The control variables of the model are water temperature, concentration of organic matter and chlorophyll a, as well as salinity of waters. The model was verified based on the data concerning the linear and weight growth of two oyster populations grown in the lagoon in 2000–2001. The authors concluded that their model showed good field and simulation data convergence, but better results could be achieved using dynamic energy budget (DEB) models.

Thus, their later work [4] shows the model based on the DEB approach. The results of oyster growth modelling with an empirical model were compared with the results obtained using the DEB model. The latter makes it possible to achieve a better correspondence of the simulation results to the *in situ* data on the weight and linear growth of oysters [3].

In [5], the DEB model of the oyster *M. gigas* growth, which is quite universal for the Atlantic coast marine ecosystems, is presented. The authors applied a unified approach to six different ecosystems and used a nutrition coefficient that takes into account the peculiarities of the nutritional activity of oysters under various external conditions. The model reproduces well the periods of spawning and loss of biomass in the autumn-winter period. The disadvantage is the absence of an explicit dependence of the model variables on water temperature. The authors noted that the water temperature in all the considered areas was approximately the same in winter, and significant differences occurred in summer. Nevertheless, the model uses the same set of parameters for all locations, with the exception of the nutrition coefficient.

A similar model was developed for several Pacific coast marine ecosystems [6]. The oyster *M. gigas* growth DEB model showed good results when compared with measurement data of parameters that determined the growth and spawning processes. However, the authors concluded that three studied locations were characterized by similar external conditions. Therefore, in order to apply this model under conditions other than the specified ones, the model should be detailed by including a number of values that take into account different environmental conditions.

In [7], the DEB model is used to compare the life cycles of two oyster species: *O. edulis* and *M. gigas.* The DEB approach allowed the authors to determine the reaction of the two species to an increase in the average annual water temperature by 2 °C. *M. gigas* demonstrated sufficient resistance to environmental changes, while *O. edulis* changed its life cycle due to the suppression of spawning. Based on the results of the work, the authors were able to estimate the values of environmental parameters necessary to ensure the sustainable growth of the oysters *O. edulis*. The model was developed for regional conditions of the Limfjord, Denmark.

In [8], a mathematical model of the growth of the mussel *Mytilus galloprovincialis* was presented. The model was developed in accordance with the dynamic energy balance principles. The authors considered filtration, respiration, spawning and excretion of mussels in detail. The model was verified with *in situ* data obtained at a mussel farm in the Crimean coastal zone.

The given examples of successful application of DEB models determine our choice of constructing a simulation model of the oyster *O. edulis* based on the energy balance equation. The analysis of literature sources revealed that regional features played an important role in the construction of the model, since they significantly determine the specific type of parameterizations for the main physiological processes. In this regard, it seems relevant to develop a simulation model for the *O. edulis* cultivated in Donuzlav Bay. The model should describe the processes of assimilation of food, excretion, respiration, growth, reproduction. This paper aims at the development of such a model using the approaches described in [2–8] and its verification based on *in situ* observations.

Materials and methods

There are several marine farms in Donuzlav Bay where oysters and mussels are grown. Basically, all farms are concentrated in the central Donuzlav Bay. Many years of marine farming experience in this bay indicate the suitability of this water area for the cultivation of oysters and mussels [9]. With this in mind, the central Donuzlav Bay was selected for the test calculation as a possible location for oyster *O. edulis* mariculture.

Dynamic energy balance model. The main physiological processes that determine oyster growth are filtration, food consumption, respiration, excretion and spawning. The model below describes mathematically these processes for oysters that have already passed the larval stage and are fixed on a solid substrate. The model is built in accordance with the concept of dynamic energy balance. The quantitative characteristics of the processes are expressed in energy units: calories or joules. To switch from mass units to energy ones, the coefficients of caloric content of oyster tissues are used.

The energy balance is formed and then changes depending on physiological processes of the oyster, which, in their turn, depend on its weight, age, water temperature, salinity, period of year, availability of resources and individual characteristics. When using this approach in practice, in the mollusk life cycle

simulation model, it is necessary to describe mathematically all the physiological processes for a particular species as accurately as possible. This requires data from *in situ* observations and laboratory experiments. In this paper, we used approximations obtained from in situ data (Table) presented mainly in the thesis [1)] and the works of N.A. Sytnik [10, 11].

Morphometric relations. The wet weight of the oyster W (g) is represented as the sum of the shell W_{sh} (g) and soft tissues W_{soft} (g) weights. The wet and dry weight of the mollusk soft tissues is related by the ratio $W_d = 0.11 W_{soft}$ [12].

As the oyster grows, the height of the shell also increases. Based on the *in situ* data presented in work [1)], we proposed the following approximation of the dependence of the shell height on the wet weight of the mollusk:

$$\text{if } W_{soft} \le 0.35 \text{ г} \quad H = 154.67 W_{soft}^2 - 32.40 W_{soft} + 2.39,$$

$$\text{if } W_{soft} > 0.35 \text{ г} \quad H = -0.013 W_{soft}^2 - 1.88 W_{soft} + 17.70.$$

Food consumption. The oyster receives all the nutrients, i. e. the energy spent on maintaining the structure and growth, from seawater containing a feed suspension – phytoplankton and detritus. During the filtration process, the mollusk consumes the energy of diet I (cal/h), but assimilates only a part of it: $A = I - E_a$, where E_a – undigested part of the diet. The mollusk spends the assimilated energy on respiration R with the release of metabolites E_x, growth of soft tissues P_{som}, gonads P_{gen} and increase of the shell P_{sh}:

$$A = R + P + E_x;$$
$$P = P_{som} + P_{gen} + P_{sh},$$

where P – productive energy, cal/h; R – respiration cost, cal/h; E_x – excreted energy, cal/h. Thus, the distribution of energy costs of a flat oyster can be simplified in the form of the balance equation:

$$I = P + R + E_a + E_x. \quad (1)$$

Let us consider the components of balance (1) in more detail. The consumed energy (or diet) depends on the filtration rate F (L/h), concentration of feed suspension in water C (mg/L) and caloric content of the suspension K_c (cal/mg): $I = F \cdot K_C \cdot C$. The amount of assimilated energy depends on the efficiency of digestion, traditionally described with the assimilation coefficient: $A = A_e \cdot F \cdot K_C \cdot C$. Then, the total energy release can be considered as follows: $E = F \cdot K_C \cdot C\,(1 - A_e) + E_x$.

Productive energy. When growing, the oyster increases the mass of the shell and of soft tissues. Let us assume that the weight of the shell can increase or remain unchanged, while the mass of soft tissues can both increase and decrease depending on the periods of life (the spawning state or nutrient deficiency can lead

---

[1)] Sytnik, N.A., 2015. [*Functional Ecology of the flat oyster (Ostrea edulis L., 1758, Ostereidae, Bivalvia) of the Black Sea.* Extended Abstract of Doctoral Dissertation]. Sevastopol, 23 p. (in Russian).

to weight loss). The change in body weight of the oyster depends on the amount of energy spent by the body when growing:

$$K_d \frac{dW_d}{dt} = P_{som} + P_{gen},$$

where K_d = 5307 cal/(g DW) – caloric content of the dry weight of oyster soft tissues; W_d – dry weight of the soft tissues, g. According to [10], the energy costs for the shell growth P_{sh} amount on average to 12% of the total productive energy available to a mollusk, based on energy balance equation (1). Taking into account these observations, we assumed that $P_{som} + P_{gen} = 0.88P$ in the model

Spawning. The growth of oysters is closely related to the spawning process. To start spawning, a number of conditions must be met. As a rule, oysters spawn at a shell height of more than 35 mm and a mass of generative tissues of more than 0.015 g dry weight. The researchers note that in different regions, the beginning of *O. edulis* oyster spawning can occur at different water temperature. Thus, in Galicia (Spain), oysters spawn at a temperature of 12–13 °C, in the Northern Adriatic (Italy) – at a temperature of 13–17 °C, in the Norwegian fjords – at a temperature of 25 °C [1, 13, 14]. For the Black Sea, *in situ* data on the intensity of spawning processes show that the temperature range of spawning is 17–25 °C [1, 10]. This range of water temperature was adopted in the model. The distribution of energy spent on the growth of somatic and generative tissues can be estimated using the empirical energy costs ratio P_{gen}/P_{som}. According to [15], this ratio increases linearly with the mollusk size, and for the oyster *O. edulis* it can be expressed by the following equation:

$$\frac{P_{gen}}{P_{som}} = 0.013 \ W_d + 0.09. \qquad (2)$$

The model assumes the condition according to which positive productive energy is distributed between P_{som} and P_{gen} in accordance with equation (2), and P_{gen} is assumed to be zero with negative one (nutrient deficiency).

Filtration. The European oyster filtration intensity depends on the age and size of the mollusk, water temperature, concentration of feed suspension and its caloric content, and the time of day. With an increase in water temperature from 7 to 23 °C, the intensity of mollusks filtration increases, and with a further increase in water temperature, it decreases. At a temperature of 7 °C and below, the vital activity of the mollusk is suppressed [11]. The filtration rate, like some other vital functions of a mollusk, can be approximated by a power function of dry body weight – an allometric dependence. Also, taking into account the dependence of the filtration rate on water temperature, we write the following:

$$F_T = a_f(T) W_d^{b_f(T)},$$

if $T < 23$ °C $\quad a_f(T) = 0.1161T - 0.2678$,

if $T \geq 23$ °C $\quad a_f(T) = -0.1T + 4.67$,

$$b_f(T) = 10^{-4} T^2 + 0.0046\ T + 0.38.$$

where T – water temperature, °C; $a_f(T)$ and $b_f(T)$ – empirical coefficients obtained from *in situ* data (Table).

Coefficients of allometric dependencies of the form aW_d^b for the main physiological processes (based on the works of N. A. Sytnik and R. Mann)

Process	Temperature, °C	Coefficient		Work
		a	*b*	
Filtration	7	0.54	0.443	[11]
	10	0.88	0.435	
	13	1.20	0.583	
	16	1.69	0.512	
	20	2.05	0.602	
	23	2.37	0.487	
	27	1.97	0.606	
Respiration	6	0.112	0.617	Work [1)]
	11	0.291	0.773	
	13	0.320	0.813	
	18	0.491	0.688	
	19	0.475	0.721	
	23	0.725	0.737	
Excretion	12	10.92	0.601	[16]
	15	13.88	0.501	
	18	12.71	0.796	
	21	11.73	0.874	

Note: The estimates were derived from *in situ* data.

Observations show that the filtration rate depends on the concentration of feed suspension in the water. There is a kind of optimal concentration, above and below which the filtration rate decreases. To record these features, it is necessary to introduce a modulating function varying from 0 to 1 [8]. The filtration rate *in situ* data given in [11], were approximated by the following function (Fig. 1):

$$F_C = 0.4 + 0.65\,C\exp(-0.18\,C^{2.3}).$$

Thus, the filtration rate is determined as $F = F_T F_C$, and the diet (consumption) – as $I = K_C F_T F_C C$.

According to [11], oysters filter water only during a certain part of the day. The minimum filtration time is 6 hours for small oysters. With the growth of an individual, it increases to 18 hours. To record the duration of filtration, an empirical function was introduced into the model, which made it possible to calculate the number of filtration hours: $h = 6 + 14t/(t + 50)$, where t – time since the oyster was attached to the substrate.

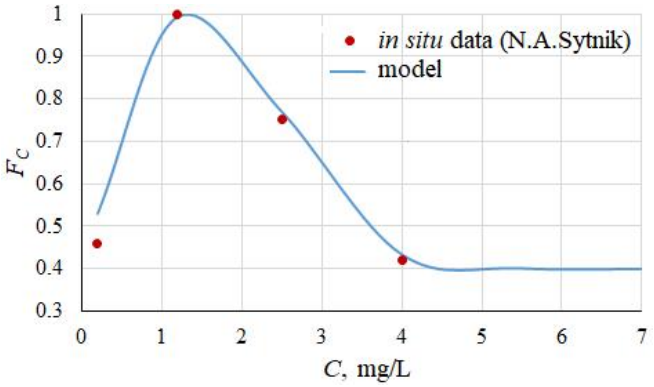

F i g. 1. Dependence of the normalized to maximum filtration rate on the feed suspension concentration in water

Respiration. Bivalves spend part of the assimilated energy on metabolic processes, namely, respiration. The intensity of respiration is determined by water temperature and size of the oyster. Based on the *in situ* data presented in Table, the following approximation was obtained:

$$R_{\mathrm{O}} = a_r(T) W_d^{b_r(T)}$$
$$a_r(T) = 0.0357T - 0.1161,$$
$$b_r(T) = 0.0042T + 0.642,$$

where R_{O} – oxygen consumption rate, mL O_2/h. The oxycaloric coefficient K_{ox} = 4.74 cal/mL O_2 (the ratio of the amount of energy in calories released during the oxidation of matter to the mass of oxygen consumed by the hydrobiont) was used for the conversion into energy units. Therefore, the respiration costs are $R = R_{\mathrm{O}} K_{ox}$.

Excretion. The energy assimilated by the oyster is also spent on excretion of metabolites from the body. The main excreted substance is ammonium. The rate of excretion depends on the water temperature and size of the mollusk, which can be expressed by an allometric equation. The maximum excretion rate of the oyster *O. edulis* is observed at a temperature of about 15 °C. Above and below this value, the rate decreases slightly [16]. Table shows the coefficients of the allometric excretion equation obtained under laboratory conditions at different water temperatures. Based on these values, the approximation was performed and an allometric excretion equation was derived, which is a function of two variables (water temperature and dry weight of the oyster):

$$A_m = a_{ex}(T) W_d^{b_{ex}(T)},$$
при $T < 15$ °C $\quad a_{ex}(T) = 0.9867\,T - 0.92,$
при $T \geq 15$ °C $\quad a_{ex}(T) = -0.3583\,T + 19.22,$
$$b_{ex}(T) = 0.0371\,T + 0.0803,$$

where A_m – excretion rate, μg NH_4/h. Taking into account the caloric content of oyster tissues and the percentage of nitrogen in the dry weight of soft tissues of the mollusk (7 % according to data from [16]), the excretion energy costs E_x (cal/h) can be calculated using the following formula:

$$E_x = 0.0758\,A_m,$$

where E_x – energy costs for excretion, cal/h.

Energy balance components. A graphical description of the energy balance variations depending on water temperature and marine suspension concentration is of interest. Fig. 2 shows the model dependencies of the oyster energy balance components presented in absolute and specific terms. Fig. 2, *a*, *c*, *e* shows the distribution of assimilated energy among growth, excretion and respiration processes depending on temperature in oysters of various sizes. The larger the mollusk is, the more energy it is able to assimilate. The maximum values of assimilated energy are fixed at an ambient temperature of 22–24 °C, which takes place due to the maximum filtration rate in this temperature range (the most comfortable conditions for this species).

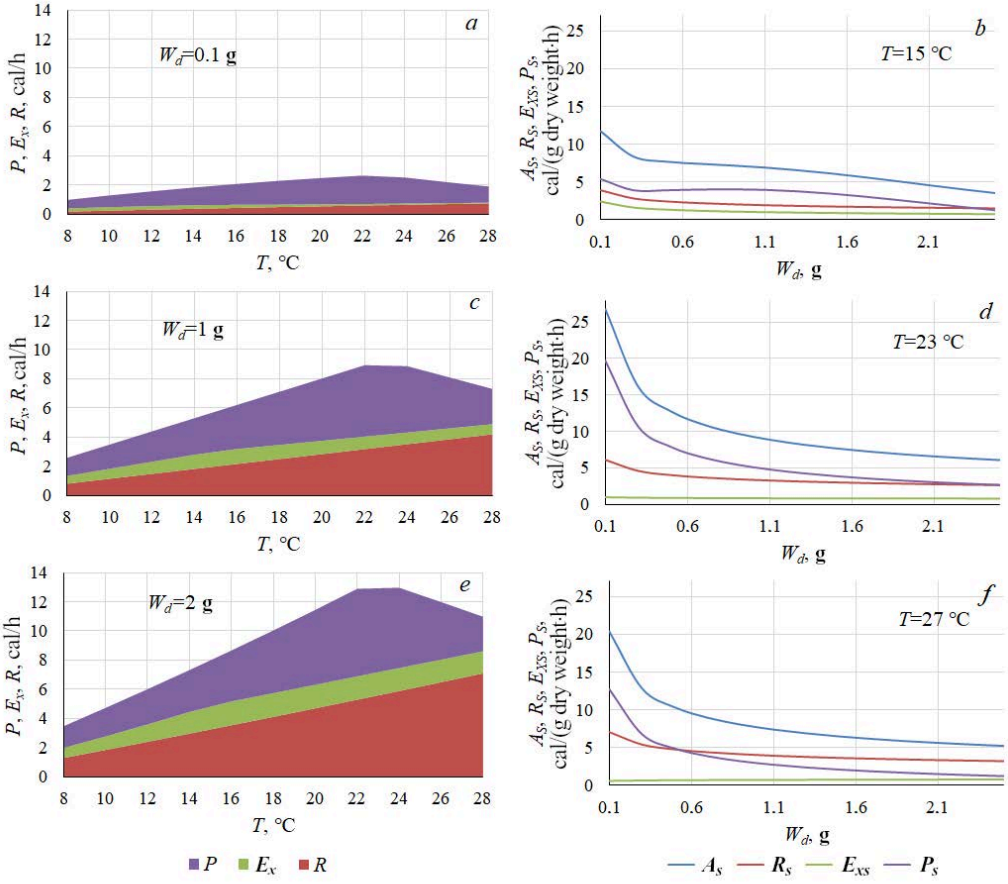

F i g. 2. Dependence of the energy balance components on water temperature T (*a*, *c*, *e*) and oyster dry weight W_d (*b*, *d*, *f*). P – productive energy; E_x – excretion energy; R – respiration costs; A – assimilated energy. The S indices denote specific quantities

In small oysters, more than half of the assimilated energy is spent on growth, while in larger mollusks, the growth and respiration energy costs are almost equal. At the same time, the size of the oyster has almost no effect on the amount of excreted energy, which accounts for 10–15% of the assimilated energy.

Fig. 2, *b*, *d*, *f* shows specific (normalized for dry weight) components of the energy balance depending on the dry weight of soft tissues of the oyster for different temperatures. Some special features of the energy balance variations of oysters should be noted. At temperatures of 22–24 °C, assimilation and production take on maximum values. The growth energy costs are determined by the difference between assimilation and metabolic costs (respiration and excretion). In small-sized mollusks, productive energy exceed excretion and respiration, and less energy is spent on growth with increasing body weight. With the growth of a mollusk, the specific values of assimilated energy, growth energy and respiration decrease, while the excreted energy remains the same. In too warm water (27 °C), the respiration costs of oysters exceed the productive energy.

Fig. 3 shows the dynamics of changes in productive energy due to the combined action of two variables (feed suspension concentration and temperature) for oysters of two sizes: W_{soft} = 4.5 g, H = 26 mm and W_{soft} = 27 g, H = 59 mm. For oysters of both sizes, it is possible to identify areas of lack of growth due to nutrient deficiency at low feed suspension concentrations in sufficiently warm water. The growth of oysters begins at a feed suspension concentration above 1 mg/L and a temperature greater than 8 °C. Maximum growth rates are observed at a maximum feed suspension concentration and a temperature of 23 °C.

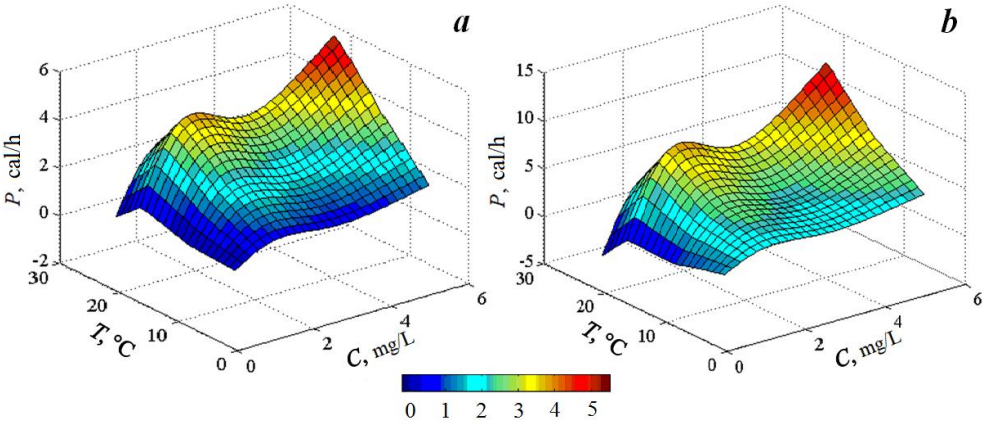

F i g. 3. Dependence of the productive energy on water temperature and feed suspension concentration for oysters with a shell height of 26 mm (*a*) and 59 mm (*b*)

Discussion of results

Model validation. The study [1)] presents *in situ* data on the linear and weight growth of oysters *O. edulis* cultured in Donuzlav Bay for 30 months from April 2001 to October 2003. The intervals between successive measurements of the average weight and height of oysters vary from 1 to 2 months. The model was validated by comparing the simulation results with these data. The model integration step was one day. The time of the model experiment was 30 months. The experiment began on 19 April 2001 and ended on 29 October 2003. The series of control variables for the model (water temperature and suspension concentration) were also taken from work [1)] (Fig. 4). They corresponded to the average characteristics of the central Donuzlav Bay during the study of the mollusks growth .

Fig. 5 shows modelling results compared with *in situ* data. Linear and weight growth indicators demonstrate good convergence with *in situ* data. However, there are some differences. The model graph of oyster weight dynamics shows some peculiarities corresponding to the beginning of spawning periods. Such features are not recorded in the *in situ* data due to their large discreteness, which makes it impossible to record such rapid changes in the physiological state of oysters. During 30 months of model integration, oyster spawning was recorded three times: in June 2002, April and July 2003. Thus, the oysters spawned 15, 25 and 28 months after their attachment to a solid substrate.

The simulation results allow detailed studying the dynamics of the energy balance components of cultivated oysters. Fig. 6 shows how much energy the oyster assimilates daily and how this energy is distributed among the processes of growth, respiration and excretion during 30 months of cultivation. Assimilated energy maxima correspond to feed suspension concentration maxima, which are usually followed by spawning periods. Productive energy is positive for a long time, and a mollusk grows. However, as a result of spawning, mass of a mollusk decreases, the assimilated energy is not enough to cover the costs of respiration and excretion, and growth is inhibited.

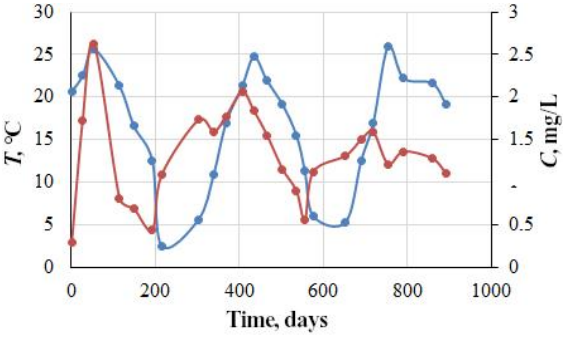

F i g. 4. Environmental parameters of the central Donuzlav Bay which affect the oyster cultivation. The red curve is water temperature; the blue curve is feed suspension concentration

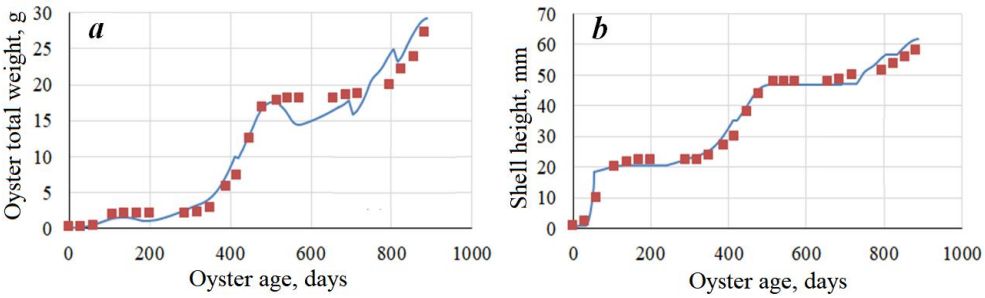

F i g. 5. Simulation results (curve) compared with *in situ* data (squares) on the oyster growth at a farm in Donuzlav, 2001–2003: *a* – total fresh weight; *b* – linear size

Two periods of mollusk growth inhibition, which are not related to spawning, are recorded during the cultivation. They are determined by a sharp decrease in the feed suspension concentration (negative values P in Fig. 6). Similar conclusions were drawn from *in situ* experiments given in study [1)] and [17].

The distribution of growth energy between generative and somatic tissues is of interest. In the first year of cultivation, P_{gen}/P_{som} increases from 10 to 16%, the mollusk develops to an adult state, increasing mainly somatic tissues. In the second year, P_{gen}/P_{som} increases from 16 to 33%, the oyster is already quite large, most of the productive energy is spent on the growth of generative tissues needed to ensure reproduction. During the third year of observations, the energy costs for growth of generative tissues increase to 47 %. These modelling results confirm the qualitative conclusions on the flat oyster growth made in study [1)] and [17].

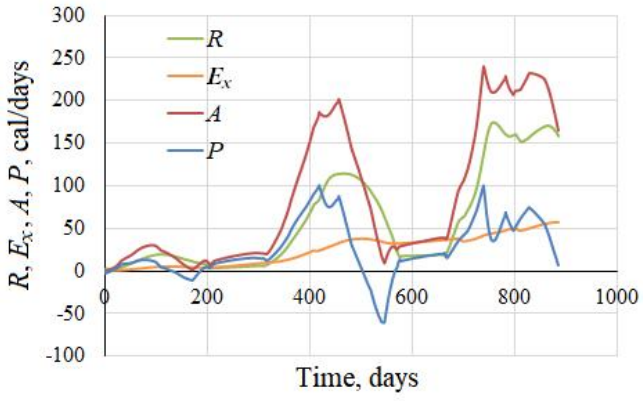

F i g. 6. Dynamics of the energy-balance components distribution during 30 months of cultivation

Conclusion

The study presents the simulation model of flat oyster growth. The model makes it possible to calculate the energy of respiration, filtration, excretion, reproduction processes. The paper examines the processes of functioning of the oyster *O. edulis* in detail and identifies factors (temperature, feed suspension concentration, age of an individual) that affect these processes and their relationship. Approximations of such vital functions of the oyster as respiration, filtration, excretion, spawning are proposed.

The model was validated using *in situ* data obtained during the study of the oyster *O. edulis* cultured in Donuzlav Bay in 2001–2003. The simulation results show good qualitative and quantitative correspondence to the *in situ* data on linear and weight growth, distribution of energy costs, ratio of the energy spent on growth of generative tissues to the energy of structural growth. The model can be used as a block of a complex ecological model simulating the cultivation of mollusks on an oyster farm.

References

1. Krakatitsa, T.F., 1976. [*Biology of the Black Sea Oyster Ostrea edulis L. Concerning its Reproduction*]. Kiev: Naukova Dumka, 80 p. (in Russian).
2. Kobayashi, M., Hofmann, E.E., Powell, E.N., Klink, J.M. and Kusaka, K., 1997. A Population Dynamics Model for the Japanese Oyster, *Magallana gigas. Aquaculture*, 149, pp. 285–321. doi:10.1016/S0044-8486(96)01456-1
3. Gangnery, A., Chabirand, J.-M., Lagarde, F., Le Gall, P., Oheix, J., Bacher, C. and Buestel, D., 2003. Growth Model of the Pacific oyster, *Magallana gigas*, Cultured in Thau Lagoon (Méditerranée, France). *Aquaculture*, 215(1–4), pp. 267–290. doi:10.1016/S0044-8486(02)00351-4
4. Bacher, C. and Gangnery, A., 2006. Use of Dynamic Energy Budget and Individual Based Models to Simulate the Dynamics of Cultivated Oyster Populations. *Journal of Sea Research*, 56, pp. 140–155. doi:10.1016/j.seares.2006.03.004
5. Alunno-Bruscia, M. Bourlès, Y., Maurer, D., Robert, S., Mazurié, J., Gangnery, A., Goulletquer, P. and Pouvreau, S., 2011. A Single Bio-Energetics Growth and Reproduction Model for the oyster *Magallana gigas* in Six Atlantic Ecosystems. *Journal of Sea Research*, 66(4), pp. 340–348. doi:10.1016/j.seares.2011.07.008
6. Pouvreau, S., Bourles, Y., Lefebvre, S., Gangnery, A. and Alunno-Bruscia, M., 2006. Application of a Dynamic Energy Budget Model to the Pacific Oyster, *Magallana gigas*, Reared under Various Environmental Conditions. *Journal of Sea Research*, 56(2), pp. 156–167. doi:10.1016/j.seares.2006.03.007
7. Stechele, B., Maar, M., Wijsman, J., Van der Zande, D., Degraer, S., Bossier, P. and Nevejan, N., 2022. Comparing Life History Traits and Tolerance to Changing Environments of Two Oyster Species (*Ostrea edulis* and *Magallana gigas*) through Dynamic Energy Budget Theory. *Conservation Physiology*, 10(1), coac034. doi:10.1093/conphys/coac034
8. Vasechkina, E.F. and Kazankova, I.I., 2014. Mathematical Modelling of the Growth and Development of the Mussel *Mytilus galloprovicialis* on Artificial Substrates. *Oceanology*, 54(6), pp. 763–770. doi:10.1134/S0001437014060113
9. Vyalova, O.Yu., 2019. Growth and Terms of Obtaining Marketable Triploid Oystersin Donuzlav Liman (Black Sea, Crimea). *Marine Biological Journal*, 4(1), pp. 24–32. doi:10.21072/mbj.2019.04.1.03

10. Sytnik, N.A. and Polyakova, T.V., 2018. [Characteristics of Allometric Growth of the Flat Oyster (*Ostrea edulis*, Linnaeus (1758)) in Ontogenesis]. In: G. A. Motul, ed., 2018. *Water Bioresources and Aquaculture of the South of Russia: Proceedings of the All-Russian Scientific and Practical Conference on the Occasion of the 20th Anniversary (Krasnodar, 17–19 May, 2018)].* Krasnodar: Kubanskiy gosudarstvennyy universitet, pp. 138–142 (in Russian).
11. Sitnik, N.A., 2010. About Some Ecological Laws of a Filter Feeding of Oyster (Ostrea edulis L.). *Scientific Notes of Taurida V. Vernadsky National University. Series: Biology, Chemistry*, 23(3), pp. 143–153 (in Russian).
12. Mo, C. and Neilson, B., 1994. Standardization of Oyster Soft Tissue Dry Weight Measurements. *Water Research*, 28(1), pp. 243–246. doi:10.1016/0043-1354(94)90140-6
13. His, E., Beiras, R. and Seaman, M.N.L., 1999. The Assessment of Marine Pollution – Bioassays with Bivalve Embryos and Larvae. *Advances in Marine Biology*, 37, pp. 1–178. doi:10.1016/s0065-2881(08)60428-9
14. Maathuis, M.A.M., Coolen, J.W.P., van der Have, T. and Kamermans, P., 2020. Factors Determining the Timing of Swarming of European Flat Oyster (*Ostrea edulis* L.) Larvae in the Dutch Delta Area: Implications for Flat Oyster Restoration. *Journal of Sea Research*, 156, 101828. doi:10.1016/j.seares.2019.101828
15. Sytnik, N.A., 2011. Growth and Production of Oyster (Ostrea edulis L.) in the Donuzlav Liman in the Black Sea. In: MHI, 2011. *Ekologicheskaya Bezopasnost' Pribrezhnoy i Shel'fovoy Zon i Kompleksnoe Ispol'zovanie Resursov Shel'fa* [Ecological Safety of Coastal and Shelf Zones and Comprehensive Use of Shelf Resources]. Sevastopol: MHI. Iss. 25, vol. 1, pp. 429–434 (in Russian).
16. Mann, R., 1979. Some Biochemical and Physiological Aspects of Growth and Gametogenesis in *Magallana gigas* and *Ostrea edulis* Grown at Sustained Elevated Temperatures. *Journal of the Marine Biological Association of the United Kingdom*, 59(1), pp. 95–110. doi:10.1017/S0025315400046208
17. Kholodov, V.I., Pirkova, A.V. and Ladigina, L.V., 2010. Cultivation of Mussels and Oysters in Black Sea. Sevastopol, 424 p. (in Russian).

Submitted 3.07.2023.; accepted after review 29.07.2023;
revised 11.10.2023; published 20.12.2023

About the authors:

Tatiana A. Filippova, Junior Research Associate, Marine Hydrophysical Institute of RAS (2 Kapitanskaya St., Sevastopol, 299011, Russian Federation), **ORCID ID: 0000-0001-5762-5894**, **Scopus Author ID: 56190548500**, **ResearcherID: AAO-5512-2020**, *filippovata@mhi-ras.ru*

Elena F. Vasechkina, Deputy Director for Research, Methodology and Education, Marine Hydrophysical Institute of RAS (2 Kapitanskaya St., Sevastopol, 299011, Russian Federation), DrSci (Geogr.), **ORCID ID: 0000-0001-7007-9496, Scopus Author ID: 6507481336, ResearcherID: P-2178-2017**, *vasechkina.elena@gmail.com*

Contribution of the authors:

Tatiana A. Filippova – computational model development, performance of simulation experiments, data analysis, article text writing

Elena F. Vasechkina – conceptual model, parametrisation selection, modelling results analysis, text editing

All the authors have read and approved the final manuscript.

Original article

Self-Purification Capacity of Sevastopol Bay Ecosystems in Relation to Inorganic Forms of Nitrogen and Phosphorus from 2012 to 2020

I. V. Mezentseva [1], E. E. Sovga [2]*, T. V. Khmara [2]

[1] *Sevastopol Branch of the N. N. Zubov State Oceanographic Institute, Sevastopol, Russia*
[2] *Marine Hydrophysical Institute of RAS, Sevastopol, Russia*
* *e-mail: science-mhi@mail.ru*

Abstract

The paper uses the 2012–2020 joint oceanographic database of MHI RAS and SB FSBI SOI to estimate the self-purification capacity of Sevastopol Bay ecosystems in relation to biogenic nitrogen and phosphorus. The assimilation capacity and its specific value were calculated using the balance method. The paper estimates the average and maximum concentrations of inorganic phosphorus (PO_4) and nitrogen (NO_2, NO_3, NH_4), as well as the average and maximum rates and time of removal of these nutrients from the bay ecosystems. The paper shows changes in the percentage of forms of inorganic nitrogen (NO_2, NO_3, NH_4) in the water area of all parts of Sevastopol Bay for two periods (1998–2012 and 2012–2020). These changes had a greater impact on the content of the reduced form of ammonium nitrogen which has increased in all ecosystems of the bay in recent years. Changes in the self-purification capacity of the bay ecosystems were manifested as a spread of data on the assimilation capacity of the study ecosystems in relation to nutrients. At the same time, the lowest self-purification capacity was observed for the ecosystem of the eastern part of the bay. The paper assesses possible causes of the observed situation, which are associated with changes in the wind regime over the bay water area in the last decade and the resulting formation of the system of surface currents. The surface currents in the bay under prevailing easterly winds were calculated using the computational modeling method. The paper shows that an increase in the frequency of such winds contributes to increased ventilation of the waters of Yuzhnaya Bay and a more intense input of pollutants in the westerly direction. The paper analyzes the reasons for deterioration in the self-purification ability of the eastern part of the bay in the last decade in relation to all inorganic forms of nitrogen and phosphates. It was shown that changes in the self-purification ability of ecosystems throughout the Sevastopol Bay waters were associated with an increase in the recreational load on the bay coast.

Keywords: Sevastopol Bay, biogenic nitrogen, biogenic phosphorus, ecosystem, self-purification ability, assimilation capacity, surface currents

Acknowledgements: The study was performed under state assignment of MHI RAS on topic no. 0827-2020-0004 “Coastal research”.

For citation: Mezentseva, I.V., Sovga, E.E. and Khmara, T.V., 2023. Self-Purification Capacity of Sevastopol Bay Ecosystems in Relation to Inorganic Forms of Nitrogen and Phosphorus from 2012 to 2020. *Ecological Safety of Coastal and Shelf Zones of Sea*, (4), pp. 101–115.

Самоочистительная способность экосистем Севастопольской бухты в отношении неорганических форм азота и фосфора в период с 2012 по 2020 год

И. В. Мезенцева [1], Е. Е. Совга [2]*, Т. В. Хмара [2]

[1] *Севастопольское отделение Государственного океанографического института им. Н. Н. Зубова, Севастополь, Россия*
[2] *Морской гидрофизический институт РАН, Севастополь, Россия*
* *e-mail: science-mhi@mail.ru*

Аннотация

На основе сводной базы океанографических данных МГИ РАН и СО ФГБУ ГОИН за 2012–2020 гг. выполнены оценки самоочистительной способности экосистем Севастопольской бухты в отношении биогенных элементов – азота и фосфора, рассчитанные балансовым методом по величине ассимиляционной емкости и ее удельной величине. Оценены средние и максимальные концентрации неорганических форм фосфора (PO_4) и азота (NO_2, NO_3, NH_4) за указанный период, а также значения средней и максимальной скорости и времени удаления этих биогенных элементов из экосистем бухты. Показаны изменения в процентном соотношении форм неорганического азота (NO_2, NO_3, NH_4) в акватории всех частей Севастопольской бухты за два периода (1998–2012 гг. и 2012–2020 гг.). Эти изменения в большей степени отразились на содержании восстановленной формы азота аммония, которое за последние годы увеличилось в экосистемах всей бухты. Изменения самоочистительной способности экосистем бухты проявились в разбросе данных об ассимиляционной емкости исследуемых экосистем в отношении биогенных элементов. При этом наиболее низкая самоочистительная способность наблюдается в экосистеме восточной части бухты. Оценены возможные причины наблюдаемой ситуации, которые связаны с изменениями ветрового режима над акваторией бухты в последнее десятилетие и формирующейся под его влиянием системой поверхностных течений. Методом математического моделирования рассчитаны поверхностные течения в бухте при преобладающих ветрах восточных направлений. Показано, что увеличение периодичности действия таких ветров способствует усилению вентиляции вод Южной бухты и более интенсивному поступлению загрязняющих веществ в западном направлении. Проанализированы причины ухудшения самоочистительной способности восточной части бухты в отношении всех неорганических форм азота и фосфатов в последнее десятилетие. Показано, что изменения самоочистительной способности экосистем всей акватории Севастопольской бухты связаны с ростом рекреационной нагрузки на побережье бухты.

Ключевые слова: Севастопольская бухта, биогенные элементы, биогенный азот, биогенный фосфор, экосистема, самоочищение, самоочистительная способность, ассимиляционная емкость, поверхностные течения

Благодарности: работа выполнена в рамках государственного задания ФГБУН МГИ по теме № 0827-2020-0004 «Прибрежные исследования».

Для цитирования: *Мезенцева И. В., Совга Е. Е., Хмара Т. В.* Самоочистительная способность экосистем Севастопольской бухты в отношении неорганических форм азота и фосфора в период с 2012 по 2020 год // Экологическая безопасность прибрежной и шельфовой зон моря. 2023. № 4. С. 101–115. EDN MQUMMV.

Introduction

Sevastopol Bay is one of the city-forming factors of Sevastopol, and it serves as an indicator of the ecological health of the region. The bay is a semi-enclosed estuarine-type water area with a length of about 7 km, a maximum width of up to 1 km, and a mirror area of over 7 km^2. Water exchange in the bay is hindered, besides, it is constantly under active anthropogenic impact. Systematic studies of water quality in Sevastopol Bay began in 1975 after the introduction of the programme of the National Environmental Monitoring and Control Service [1]. The results of hydrological and hydrochemical studies of Sevastopol Bay [1)] have been repeatedly reviewed in the literature (e.g., [2, 3]). These works show that depending on the localisation of pollution sources, bottom shape and hydrometeorological conditions, both relatively clean zones and those with a persistent high-pollution level (e.g., Yuzhnaya Bay) are formed in Sevastopol Bay. According to the pollution level, the bay water area was divided into four areas [3] (Fig. 1).

Ecological well-being of shallow-water marine ecosystems, irrespective of environmental protection measures, is determined primarily by their self-purification capacity, the intensity of which depends on a number of mutually causal factors. The capacity of shallow water area ecosystems for self-purification can be assessed by calculating their assimilation capacity (AC) in relation to a priority pollutant or a complex of pollutants.

Sevastopol Bay is a water body with complex geographical and hydrological-hydrochemical characteristics. This implies the presence of fresh water sources and zones of their mixing with sea waters, as well as heterogeneity of the anthropogenic load. Therefore, the water area should be zoned and the self-purification capacity (AC of the ecosystem) should be calculated for each zoned area.

F i g. 1. Zoning of Sevastopol Bay according to the anthropogenic influence level: *W* – western area, *E* – eastern area, *C* – central area and *S* – southern area (from work [3])

[1)] Konovalov, S.K., Romanov, A.S., Moiseenko, O.G., Vnukov, Yu.L., Chumakova, N.I. and Ovsyany, E.I., 2010. [*Atlas of Oceanographic Characteristics of Sevastopol Bay*]. Sevastopol: ECOSI-Gidrofizika, 320 p. (in Russian).

The article analyses the self-purification capacity of the eastern, central, western parts of the bay and Yuzhnaya Bay, as well as the water area of the entire Sevastopol Bay. Several works [4–7] consider the self-purification capacity of the Sevastopol Bay ecosystem in relation to all forms of inorganic nitrogen and inorganic phosphorus. They study the ecosystem of the entire bay or its separate parts (western, central, eastern ones and Yuzhnaya Bay) using calculated data on the hydrodynamics of the bay waters. Thus, [4] compared the ecosystem self-purification capacity for the western part of the bay bordering the open sea in relation to all forms of inorganic nitrogen and that for the southern, most polluted part of the bay. The work [5] estimates the self-purification capacity of ecosystems of the whole Sevastopol Bay in relation to reduced forms of nitrogen (nitrites and ammonium).

In [6], the self-purification capacity of the bay ecosystems in relation to all inorganic forms of nitrogen is compared, and trophic state indices for the studied ecosystems are given. The work [7] studies the self-purification capacity for the ecosystems of Yuzhnaya Bay and the eastern part of Sevastopol Bay (which is under the influence of the Chernaya River runoff during flooding and low water periods) in relation to phosphates under changes in the hydrodynamic regime of the bay. The works [4–7] share the fact that the self-purification capacity of the Sevastopol Bay ecosystems was calculated based on the oceanographic database of MHI RAS for 1998–2012.

Seasonal water dynamics in some parts of Sevastopol Bay was calculated using the hydrothermodynamic module of the numerical three-dimensional nonstationary model MECCA (Model for Estuarine and Coastal Circulation Assessment) [8]. The results obtained for the eastern part of the bay and Yuzhnaya Bay are presented in [7], and those for the central part of the bay are given in [5].

The study aims to calculate the self-purification capacity of the ecosystems for all parts of Sevastopol Bay in relation to inorganic nitrogen and phosphorus using the database of MHI RAS and SB FSBI SOI for 2012–2020, taking into account changes in the hydrometeorological situation in the last decade.

Study methods and materials

The authors used the joint database of archival materials of MHI RAS and SB FGBU SOI for 2012–2020, including 8277 determinations of phosphate, nitrite, nitrate and ammonium content. To assess the AC of the selected areas of Sevastopol Bay, 5567 concentration values of the above indicators were selected (Table 1).

The AC of ecosystems of the selected areas of Sevastopol Bay was calculated using the balance method [9]. When using this method, to calculate the integral time of pollutants staying in the studied ecosystem is the most complicated part. This time is largely determined by physical and chemical properties of a particular pollutant, hydrodynamic parameters of the water area and a complex of processes (physical, chemical, microbiological) responsible for the destruction of pollutants or their removal from the studied water area.

T a b l e 1. Concentration of inorganic phosphorus and nitrogen compounds in different parts of Sevastopol Bay (according to database of MHI RAS and Sevastopol Branch of SOI) in 2012–2020

Compounds	Mean content for the period, μM/L	Concentration range, μM/L	Standard deviation	Number of determinations
Phosphates	0.10	0–3.65	0.082	1520
Nitrites	0.24	0–7.67	0.711	1354
Nitrates	5.70	0–67.28	1.765	1355
Ammonium	1.40	0–40.66	1.021	1338

The final formulae for estimating the mean value $\overline{A}_{mi}$ and standard deviation $\sqrt{D[A_{mi}]}$ of the AC of a marine ecosystem (m) in relation to the i-th pollutant are as follows:

$$\mathrm{AE}_{mi} = \overline{A}_{mi} \pm \sqrt{D[A_{mi}]},$$

$$\overline{A}_{mi} = \frac{Q_m \cdot C_{\mathrm{thr}i}}{C_{\max i}} \cdot \overline{v}_i, \quad D[A_{mi}] = \left(\frac{Q_m \cdot C_{\mathrm{thr}i}}{C_{\max i}} \right)^2 \cdot D[v_i],$$

where Q_m – water volume in the calculation area; $C_{\mathrm{thr}i}$ – threshold concentration of a pollutant; $C_{\max i}$ – maximum concentration of a pollutant in the ecosystem; v_i – rate of pollutant removal from the ecosystem, the mean value $\overline{v_i}$ and dispersion $D[v_i]$ of which are determined by the original algorithm [10].

Results and discussion

Comparison of relatively new data for 2012–2022 with the materials of previously published studies (1998–2012) showed a significant change in the content of biogenic forms of nitrogen and phosphorus in the waters of the selected areas of Sevastopol Bay. Table 2 presents the mean and maximum values of the concentration of inorganic phosphorus and nitrogen compounds in different parts of the bay in 2012–2020.

Thus, over the study period 2012–2020, the mean **phosphate** content either remained unchanged (the eastern part of the bay) or decreased by 0.02–0.06 μM/L (in all other water areas). Maximum concentration values increased significantly in the eastern part (2.6 times) and decreased slightly in the rest of the bay.

T a b l e 2. Content (μM/L) of inorganic phosphorus and nitrogen compounds in different parts of Sevastopol Bay in 2012–2020

Area	(PO_4^{3-}) / Phosphates		(NO_2^-) / Nitrites		(NO_3^-) / Nitrates		(NH_4^+) / Ammonium	
	Mean	Max	Mean	Max	Mean	Max	Mean	Max
Yuzhnaya Bay	0.10	0.95	0.23	2.54	14.79	286.40	1.59	16.02
Eastern part	0.15	3.65	0.30	7.06	3.71	67.28	2.25	40.66
Central part	0.07	0.66	0.19	5.18	2.08	14.67	1.05	9.94
Western part	0.07	0.77	0.23	7.67	2.22	8.29	0.72	9.09

The **nitrite** content increased in all parts of the bay: the maximum concentration in the eastern part was 7.06 μM/L, in the western part – 7.67 μM/L.

A 1.1-fold and 1.6-fold decrease in the mean and maximum **nitrate** content (to 2.22 and 8.29 μM/L, respectively) was observed in the waters of the cleaner western part of Sevastopol Bay. In the other selected water areas, an increase in concentration was observed. In the central part, the maximum value was 14.7 μM/L, in the eastern part – 67.3 μM/L, and in Yuzhnaya Bay – 286.4 μM/L.

In the ecosystem waters of all parts of Sevastopol Bay, the average **ammonium** content increased by 0.15–1.20 μM/L, while the maximum content decreased by 1.5 times in the central part of the bay and changed slightly in the western part (decreased to 9.09 μM/L). At the same time, the maximum values of this indicator doubled in Yuzhnaya Bay (up to 16.02 μM/L) and increased eightfold in the eastern part (up to 40.66 μM/L).

Fig. 2 shows that in the last decade the percentage ratio of different forms of inorganic nitrogen has changed in all parts of Sevastopol Bay. This mostly concerns the content of the reduced form of nitrogen – ammonium. In recent years, an increase in its content has been observed in all water areas of the bay, with the largest increase (from 23 to 36%) in the western part of the bay. Apparently, the presence of Khrustalny Beach in this part of the bay and the growth of recreational load on the water area have an impact. At the same time, the nitrate content decreases (Fig. 2). In the western part of the bay their content decreased from 72 to 59%. The smallest changes in the content of inorganic forms of nitrogen are observed in the water area of Yuzhnaya Bay.

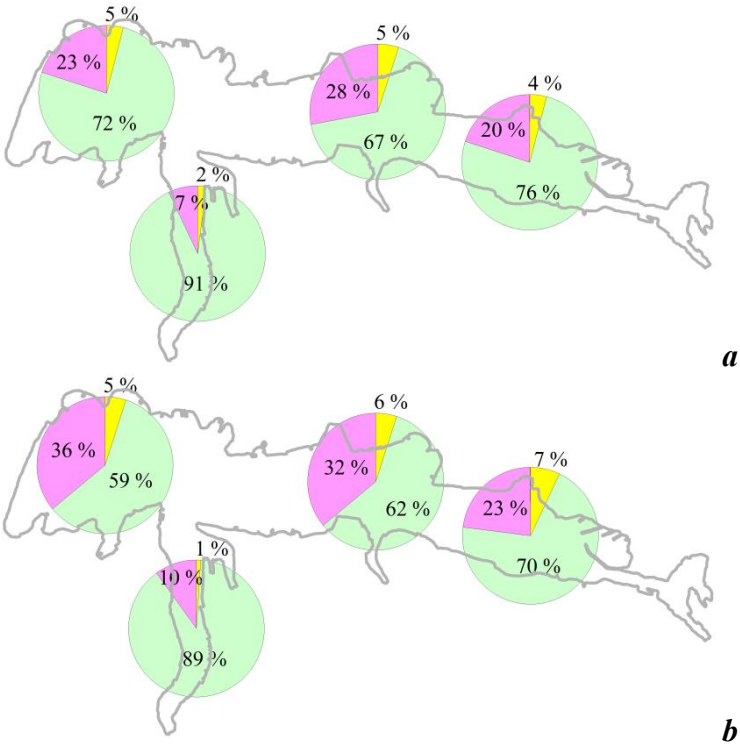

F i g. 2. Distribution of content shares for mineral forms of nitrogen in the Sevastopol Bay in 1998–2012 (*a*) [6] and 2012–2020 (*b*). Yellow colour – NO_2; green – NO_3; pink – NH_4

A comparative analysis of the removal rate and time for inorganic forms of nitrogen and phosphorus in the Sevastopol Bay ecosystem in 2012–2020 and in the previous period 1998–2012 showed different trends of changes in these parameters in the water areas of the selected areas. Thus, the time of **phosphate** removal from the ecosystems of all parts of the bay has decreased in recent years, but still remains maximum in the eastern part of Sevastopol Bay (Table 3). Obviously, the decrease in the time of phosphate presence is due to an increase in the average elimination rate everywhere except in Yuzhnaya Bay, where this rate decreased from 0.007 to 0.005 μM/(L·day). The maximum estimated phosphate removal rate (0.039 μM/(L·day)) was recorded in the central part of the bay, while in the other areas, the removal rate did not exceed 0.023–0.024 μM/(L·day).

In the eastern and central parts of Sevastopol Bay, an increase in the average nitrite removal rate by 2.3–2.5 times was observed. The maximum values of the indicator were determined for the eastern and western parts of the bay (0.085 and 0.097 μM/(L·day), respectively). In the central part, the removal rate decreased from 0.126 μM/(L·day) in 1998–2012 to 0.062 μM/(L·day) in 2012–2020. Nitrite removal time decreased for all parts of the bay except the western part, for which there was an increase in the time nitrite was in the ecosystem with a relatively stable elimination rate.

T a b l e 3. Rate v_i (μM/(L·day)) and time t_r (day) of removal of inorganic phosphorus and nitrogen from different parts of Sevastopol Bay in 2012–2020

Area	(PO_4^{3-}) / Phosphates		(NO_2^-) / Nitrites		(NO_3^-) / Nitrates		(NH_4^+) / Ammonium	
	v_i	t_r	v_i	t_r	v_i	t_r	v_i	t_r
Yuzhnaya Bay	0.005	18–22	0.006	33–37	0.536	22–28	0.033	49–53
Eastern part	0.005	30–38	0.010	25–29	0.051	63–72	0.029	76–81
Central part	0.008	9–15	0.007	24–27	0.048	40–43	0.031	34–42
Western part	0.006	13–22	0.013	15–18	0.037	58–61	0.036	20–29

A clear pattern is observed for **nitrates**: even a small increase in their removal rate from Yuzhnaya Bay and the central part of Sevastopol Bay reduces the elimination time. On the contrary, when the removal rate of nitrates from the water area of the eastern and western parts of the bay significantly decreases (by 2.7 and 7.5 times, respectively), their elimination time considerably increases (by 2.3 and 7.4 times, respectively). The maximum removal rate (2.098 μM/(L·day)), as in the previous period, was observed in Yuzhnaya Bay, while in the other areas it did not exceed 0.396 μM/(L·day).

During the study period in all parts of the Sevastopol Bay water area, as shown above, the **ammonium** content increased. Its average removal rate decreased threefold in the Yuzhnaya Bay water area and 5.8 times in the western, cleanest part of Sevastopol Bay. The maximum removal rate in all selected areas did not exceed 0.181 μM/(L·day) compared to the maximum of 0.940 μM/(L·day) observed in the previous calculation period (1998–2012, western part of the bay [5]). The drop in the rate of ammonium removal caused an increase in the time required for self-purification of the ecosystems. Thus, the staying time of ammonium in the waters of Yuzhnaya Bay and in the eastern part of Sevastopol Bay increased by 2.8 and 2.3 times, respectively. As for the water area of the western part of the bay, the estimated time increased more than eight times.

Of particular interest is the information on specifying the ability of ecosystems of all parts of Sevastopol Bay to self-purification according to the AC value for the last decade (Table 4), in particular by its specific, i. e. calculated per fixed unit of volume (in our case per 1 litre), value ($AC_{spec.}$), which allows levelling the differences in the volume of different parts of the Sevastopol Bay water area.

T a b l e 4. Characteristics of capacity of the study water areas of Sevastopol Bay to self-purification $AC_{spec.}$ (μM/(L·day)) and AC of water area (t/year) in 2012–2020

Area	(PO_4^{3-}) / Phosphates		(NO_2^-) / Nitrites		(NO_3^-) / Nitrates		(NH_4^+) / Ammonium	
	AC_{spec}	AC	AC_{spec}	AC	AC_{spec}	AC	AC_{spec}	AC
Yuzhnaya Bay	0.0076	0.89	0.0046	0.24	1.524	79.86	0.389	20.39
Eastern part	0.0017	0.25	0.0029	0.19	0.565	37.37	0.142	9.41
Central part	0.0111	2.89	0.0026	0.30	2.315	269.75	0.519	60.43
Western part	0.0070	2.69	0.0034	0.58	3.003	519.04	0.571	98.69

In the period under consideration 2012–2020, in relation to **phosphates**, the minimum $AC_{spec.}$ value was observed in the eastern part of the bay – 0.0017 μM/(L·day). According to the calculated AC of this water area, up to 0.25 tonnes of phosphorus per year can enter the ecosystem without damage to the latter. In the previous calculation period 1998–2012, this value was 0.64 tonnes of phosphorus per year, i. e. the permissible level threshold decreased by 2.6 times [7]. For the Yuzhnaya Bay ecosystem, the value was 0.0076 μM/day or 0.89 t/year, indicating a slight decrease in the permissible level threshold (0.93 t for 1998–2012 [7]). The western part of the bay is also characterised by a similar value of $AC_{spec.}$ The increased self-purification capacity of the central part is offset by the difference between the volumes of its water area and that of the western part, so the AC values of these parts are close (2.89 and 2.69 tonnes of phosphate per year, respectively). For comparison, in 1998–2012, the difference was more significant – 1.17 and 2.00 tonnes of phosphate per year [7], indicating an improvement in the current situation.

In relation to **nitrites**, it is important to note a significant decrease in the self-purification capacity of the western part of Sevastopol Bay. Thus, in comparison with the previous calculation period (1998–2012), the $AC_{spec.}$ decreased 14.3 times, which resulted in a 12.6-fold decrease in the AC of this water area (7.38 and 0.58 tonnes of nitrite per year, respectively). The ecosystem of the central and eastern parts of the bay also showed a decrease in AC, but it was not so sharp – up to 0.30 and 0.19 tonnes of nitrite per year, respectively, against 0.48 and 0.39 tonnes of nitrite per year in the previous period [6]. In the southern part of the bay, no changes were observed in the two periods: $AC_{spec.}$ was 0.005 μM/(L·day), AC of the water area was 0.24–0.25 t/year.

The $AC_{spec.}$ value in relation to **nitrates** in the ecosystem of the eastern part of the bay did not change significantly in comparison if compared with the previous calculation period. In the last decade, the ecosystem of this area has been characterised by the weakest self-purification capacity. The self-purification capacity of the Yuzhnaya Bay ecosystem more than doubled, reaching the nitrates removal limit of 79.86 t/year. The AC of the central part of Sevastopol Bay changed even more, reaching a value of almost 270 tonnes of nitrates per year, $AC_{spec.}$ increased from 0.614 to 2.315 μM/(L·day) compared to the previous calculation period. As in the case of nitrites, the western part of the bay bordering the open sea has experienced a decrease in self-purification capacity, with 519 tonnes of nitrates per year over the last decade, compared to 882 tonnes per year for 1998–2012. [6].

With respect to **ammonium**, the minimum $AC_{spec.}$ value was observed in the ecosystem of the eastern part of the bay – 0.142 μM/(L·day), which corresponds to an AC of 9.41 tonnes of ammonium per year. High values of $AC_{spec.}$ are observed for the ecosystems of the western and central parts of the bay – 0.571 and 0.519 μM/(L·day), respectively, which corresponds to an AC of the water area of 98.69 and 60.43 t/year. For comparison, based on the data from 1998–2012, these values were 6.90 tonnes of ammonium per year for Yuzhnaya Bay, 8.36 t for the eastern part of the bay, 9.33 t for the central part of the bay, and 93.40 t for the western part of the bay [5]. Thus, for the water areas of the eastern and western parts of the bay, the changes in self-purification capacity in relation to ammonium are insignificant. However, despite a significant increase in ammonium concentration in the central part of the bay, the self-purifying capacity of its ecosystem has improved. Apparently, the relevant hydrometeorological conditions and hydrodynamics of waters in the bay may have played a significant role. A slightly less significant improvement of the self-purification capacity took place in Yuzhnaya Bay, where the $AC_{spec.}$ increased from 0.132 to 0.389 μM/(L·day).

Thus, there is a large spread of data on the AC of the ecosystem in relation to both a particular nutrient and each separate part of the water area of Sevastopol Bay. The distribution of nutrient concentrations between different parts of Sevastopol Bay is somewhat inconsistent with the changes in the AC value. This is due to the complexity of AC, which is determined by processes of different nature.

The information presented in Table 4 allows us to assess the current situation for each specific water area with respect to all nutrients by the value of their specific assimilation capacity.

Thus, the obtained results made it possible to assess the general state of Sevastopol Bay ecosystems by the AC value:

Yuzhnaya Bay. For phosphates – slight decrease in $AC_{spec.}$; for nitrates and ammonium – increase in $AC_{spec.}$, and for nitrites – no change. In general, the situation has improved.

Central part of the bay. For phosphates – significant increase in $AC_{spec.}$; for nitrates and ammonium – significant increase; for nitrites – decrease. In general, the situation has significantly improved.

Eastern part of the bay. For phosphates – decrease in $AC_{spec.}$; for nitrates – insignificant decrease; for ammonium – insignificant increase; for nitrites – significant decrease. In general, the situation has deteriorated.

Western part of the bay. For phosphates – increase in $AC_{spec.}$; for nitrates – significant decrease; for ammonium and nitrites – decrease. In general, the situation, as in the eastern part, has recently deteriorated.

To provide the reasons for this situation, it is necessary to consider the changes in the hydrometeorological situation for the last decade.

Due to the zonally elongated orientation of the bay surrounded by high shores, the prevailing wind directions are easterly (23.1%) and southerly (19.6%) [11]. The changes in wind recurrence by direction for two periods (1998–2012 [11] and 2012–2020 [2)] are presented in Fig. 3.

Fig. 3, *b* shows that in the modern period, the duration of easterly winds increased to 35%, and the share of southerly winds significantly decreased compared to the previous decade (Fig. 3, *a*). As is known from the data of [7], it is the southerly winds that complicate the water exchange in Yuzhnaya Bay with the water area of the entire Sevastopol Bay. To establish the reasons for the differences in the $AC_{spec.}$ values in the ecosystems of different parts of the bay, let us consider the features of their hydrodynamic situation calculated using the hydrothermodynamic module of the numerical three-dimensional non-stationary model MECCA [8] at prevailing winds of eastern directions (Fig. 3, *b*). The results of the currents calculation obtained for the water area of Sevastopol Bay are presented in Fig. 4.

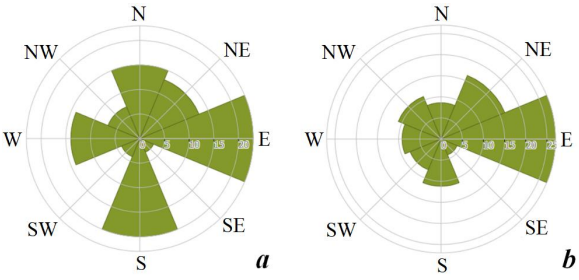

F i g. 3. Wind rose for the Sevastopol water area in 1998–2012 (*a*) and 2012–2020 (*b*)

Fig. 4 shows that the increase in the easterly wind recurrence observed in the last decade contributes to increased ventilation of the Yuzhnaya Bay waters and their transfer to the western part of the bay. Yuzhnaya Bay is characterised by a hindered water exchange with the adjacent water area. The waters of the bay receive record volumes of residential and storm water runoff, moreover, there are berths in its water area.

When northerly and northeasterly winds prevail over the bay water area, a surface drift current directed along the bay axis to the west is formed. This favours more intensive water inflow into Yuzhnaya Bay both in the surface and bottom layers. The northerly and northwesterly winds cause a surge effect and the corresponding compensatory rise of water from the bottom horizons to the surface of the middle part of Yuzhnaya Bay [7].

[2)] Raspisanie Pogody, Ltd. [Weather Archive Sevastopol]. 2023. [online] Available at: https://rp5.ru/Архив_погоды_в_Севастополе [Accessed: 10 December 2023] (in Russian).

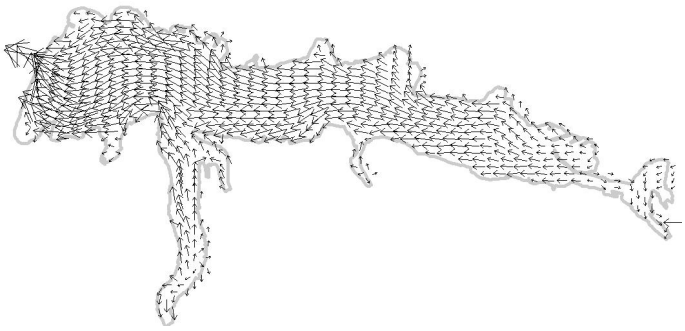

F i g. 4. Map of surface currents in Sevastopol Bay under an easterly wind of 5–10 cm/s

Let us focus on the peculiarities of the dynamic regime in the central part of the bay as a possible reason for the increase in the self-purification capacity of its ecosystem in the last decade. Due to the location of the central part of the bay, the currents here are determined mainly by the wind. Under the influence of the easterly wind, a direct flow of the west direction is formed in the surface water layer, which also persists under the northerly and southerly winds and contributes to the transfer of pollutants to the western part of the bay (Fig. 4).

According to the work [5], in the central part of Sevastopol Bay there are two counter flows – one from east to west from the Chernaya River and the other from the open part of the sea. This contributes to the formation of a buffer zone in the central part of the bay, in which multidirectional flows carrying pollutants are "closed". This is explained by the orientation and morphometric characteristics of the bay, as well as by the inflow of river water from the east, which creates a slope of the water surface and causes runoff currents.

The eastern part of Sevastopol Bay receives water from the Chernaya River, the major runoff (up to 80%) of which occurs in winter and spring. During the high-water period with weak winds, the runoff currents caused by the inflow of the Chernaya River waters become predominant. The deterioration of the self-purification capacity of this part of the bay in the last decade is associated with an increase in the flux of biogenic nitrogen and phosphorus with the runoff of the Chernaya River. This flux is especially intensified during the formation of winter and spring floods, when distributed surface flood waters spread up to the Neftyanaya Gavan area. Flood waters contain elevated levels of silicium, nitrates, ammonium and phosphorus, which enter the river and bay waters from residential waste-water in the lower reaches of the river, as well as from sewage discharges from settlements and enterprises located in the water protection zone. More detailed information on the influence of the regimes of a particular winter and spring flood and summer low water of the Chernaya River in 2015 on the self-purification capacity of the eastern part of the bay is presented in the work [12].

For this part of the Sevastopol Bay water area, the peculiarities of the bottom structure are also significant. Longer removal of phosphates in the eastern part of Sevastopol Bay (Table 3), observed by us in the last decade, may indicate their accumulation in bottom soils and increase the risk of secondary pollution of the water area. Thus, the work [13] provides data, obtained in the expedition of MHI RAS, on an artificial deepening of the bottom (depths of 19–20 m) in the area of the floating dock located near the southern shore of the eastern part of Sevastopol Bay are given. This deepening of the bottom in the eastern part of the bay resulted in reductive conditions under which, due to hypoxia, phosphorus accumulated in bottom sediments can re-enter the bottom water layer [7]. This also favours the oxidation of organic matter at the expense of nitrates with the formation of ammonium and nitrites.

Recently, some decrease in the self-purification capacity of the ecosystem of the western part of the bay has been observed, especially in relation to inorganic forms of nitrogen (Table 4). This is associated both with the hydrodynamic regime (Fig. 4), according to which the transport of pollutants, including nutrients, is carried out in the western direction, and with the growth in the number of sources of nutrient inputs as a result of increased recreational load on the bay coast.

Conclusions

Based on the consolidated database of archival materials of MHI RAS and SB FGBU SOI for 2012–2020, the authors used the balance method to calculate the value of assimilation capacity AC of the Sevastopol Bay ecosystems in relation to biogenic forms of nitrogen and phosphorus as well as its specific component $AC_{spec.}$, which allows calculating the differences in the volume of the studied parts of the bay.

Mean and maximum concentrations of inorganic forms of phosphorus (PO_4) and nitrogen (NO_2, NO_3, NH_4) for the specified period were estimated, values of mean and maximum rates of removal of the mentioned nutrients from the bay ecosystems were obtained, and the time of their removal from the bay ecosystems was calculated.

The paper presents the results of comparison of changes in the percentage of inorganic nitrogen forms (NO_2, NO_3, NH_4) in the water area of all parts of Sevastopol Bay for two periods (1998–2012 and 2012–2020). These changes mostly influenced the content of the reduced form of ammonium nitrogen. In recent years, its content has been increasing in all water areas of the bay, with the greatest increase observed in the western part of the bay – from 23 to 36%. The mean and maximum concentration of nitrites (NO_2) in the ecosystems of all parts of the bay is only increasing. The maximum concentration value was observed in the eastern and western parts of the bay (7.07 and 7.67 μM/L, respectively).

It is shown that over the last decade certain changes in the self-purification capacity of the bay ecosystems have occurred, which manifested themselves in a large variation of data on the value of assimilation capacity of the studied ecosystems with respect to both a specific nutrient and the ecosystem of each separate part of the bay water area. For all studied water areas of Sevastopol Bay, in some cases, improvement of self-purification capacity was observed, whereas in some cases, deterioration was noted.

Thus, the self-purification capacity of the Yuzhnaya Bay ecosystem improved in relation to nitrates and ammonium and deteriorated in relation to phosphates.

For the central part of the bay, an increase in the self-purification capacity for phosphates, nitrates and ammonium and a decrease only for nitrites was noted. In general, the situation has significantly improved.

For the ecosystem of the eastern part of the bay, which is under the influence of the Chernaya River runoff, a decrease in the self-purification capacity in relation to phosphates and all forms of nitrogen has been observed in the last decade. Therefore, the ecosystem condition has deteriorated, too.

For the ecosystem of the western part of the bay, a decrease in the self-purification capacity for all inorganic forms of nitrogen and a slight increase in that for phosphates were observed. In general, as in the eastern part of the bay, the ecosystem condition has deteriorated.

It is shown that the data on the state of Sevastopol Bay ecosystems, obtained in this work, can be associated with changes in the wind regime over the water area in the last decade and the system of surface currents formed under its influence in the water area of the bay. In addition, the current state of the bay ecosystems is associated with an increase in the number of sources of nutrients as a result of the growth of recreational load on the bay coast.

References

1. Simonov, A.I. and Ryabinin, A.I., eds., 1996. [*Hydrometeorology and Hydrochemistry of Seas. Vol. 4. The Black Sea. Iss. 3. Modern State of the Black Sea Waters Pollution*]. Sevastopol: ECOSI-Gidrofizika, 230 p. (in Russian).
2. Lopukhin, A.S., Ovsyany, E.I., Romanov, A.S., Kovardakov, S.A., Sysoeva, I.V., Braynzeva, Yu.V., Rylkova, O.A., Gavrilova, N.A., Gubanov, V.V. [et al.], 2007. Seasonal Peculiarities of Hydrologic-Hydrochemical Structure of Sevastopol Bay Water, Microplankton and Distribution of its Biochemical Components (the Black Sea, Observations of 2004–2005). In: MHI, 2007. *Ekologicheskaya Bezopasnost' Pribrezhnoy i Shel'fovoy Zon i Kompleksnoe Ispol'zovanie Resursov Shel'fa* [Ecological Safety of Coastal and Shelf Zones and Comprehensive Use of Shelf Resources]. Sevastopol: ECOSI-Gidrofizika. Iss. 15, pp. 74–109 (in Russian).
3. Ivanov, V.A., Ovsyany, E.I., Repetin, L.N., Romanov, A.S. and Ignatyeva, O.G., 2006. *Hydrological and Hydrochemical Regime of the Sebastopol Bay and its Changing under Influence of Climatic and Anthropogenic Factors*. Sevastopol: MHI NAS of Ukraine, 90 p. (in Russian).
4. Sovga, E.E., Mezentseva, I.V. and Kotelyanets, E.A., 2017. Assimilation Capacity of the Marine Shallow Water Ecosystems with Various Anthropogenic Impacts as the Estimation Method of Its Self-Purification Ability. *Problems of Ecological Monitoring and Ecosystem Modelling*, 28(4), pp. 38-51. doi:10.21513/0207-2564-2017-4-38-51 (in Russian).
5. Sovga, E.E., Mezentseva, I.V. and Khmara, T.V., 2021. Natural-Climatic and Anthropogenic Factors Determining the Self-Purification Capacity of Shallow-Water Marine Ecosystems in Relation to Reduced Nitrogen Forms. *Ecological Safety of Coastal and Shelf Zones of Sea*, (3), pp. 23–36. doi:10.22449/2413-5577-2021-3-23-36 (in Russian).
6. Sovga, E.E., Mezentseva, I.V. and Slepchuk, K.A., 2020. Comparison of Assimilative Capacity and Trophic Index for Various Parts of the Sevastopol Bay Water Area. *Ecological Safety of Coastal and Shelf Zones of Sea*, (3), pp. 63–76. doi:10.22449/2413-5577-2020-3-63-76 (in Russian).

7. Sovga, E.E., Mezentseva, I.V. and Khmara, T.V., 2022. Simulation of Seasonal Hydrodynamic Regime in the Sevastopol Bay and of Assessment of the Self-Purification Capacity of its Ecosystem. *Fundamental and Applied Hydrophysics*, 15(2), pp. 110–123. doi:10.59887/fpg/92ge-ahz6-n2pt (in Russian).
8. Ivanov, V.A. and Tuchkovenko, Yu.S., 2008. *Applied Mathematical Water-Quality Modeling of Shelf Marine Ecosystems*. Sevastopol: ECOSI-Gidrofizika, 311 p. (in Russian).
9. Izrael, Yu.A. and Tsyban, A.V., 1989. [*Anthropogenic Ecology of the Ocean*]. Moscow: Gidrometeoizdat, 529 p. (in Russian).
10. Sovga, E., Mezentseva, I. and Verzhevskaia, L., 2015. Assimilation Capacity of the Ecosystem of Sevastopol Bay. In: E. Ozhan, 2015. *Proceedings of the Twelfth International Conference on the Mediterranean Coastal Environment MEDCOAST' 2015, 6–10 October 2015. Varna, Bulagaria*. Varna. Vol. 1, pp. 317–326.
11. Repetin, L.N., Belokopytov, V.N. and Lipchenko, M.M., 2003. Wind and Wave Perturbations in the Southwest Crimean Coast. In: MHI, 2003. *Ekologicheskaya Bezopasnost' Pribrezhnoy i Shel'fovoy Zon i Kompleksnoe Ispol'zovanie Resursov Shel'fa* [Ecological Safety of Coastal and Shelf Zones and Comprehensive Use of Shelf Resources]. Sevastopol: ECOSI-Gidrofizika. Iss. 9, pp. 13–28 (in Russian).
12. Sovga, E.E. and Khmara, T.V., 2020. Influence of the Chernaya River Runoff during High and Low Water on the Ecological State of the Apex of the Sevastopol Bay Water Area. *Physical Oceanography*, 27(1), pp. 28–36. doi:10.22449/1573-160X-2020-1-28-36
13. Kondratev, S.I. and Vidnichuk, A.V., 2020. Local Seasonal Hypoxia and Hydrogen Sulphide Formation in the Bottom Waters of the Sevastopol Bay in 2009–2019. *Ecological Safety of Coastal and Shelf Zones of Sea*, (2), pp. 107–121. doi:10.22449/2413-5577-2020-2-107-121 (in Russian).

Submitted 21.08.2023; accepted after review 15.09.2023;
revised 11.10.2023 ; published 20.12.2023

About the authors:

Irina V. Mezentseva, Senior Research Associate, Sevastopol Branch of the N. N. Zubov State Oceanographic Institute (61 Sovetskaya St., Sevastopol, 299011, Russian Federation), PhD (Geogr.), **ORCID ID: 0000-0001-9771-0380**, *mez-irina@mail.ru*

Elena E. Sovga, Leading Research Associate, Marine Hydrophysical Institute of RAS (2 Kapitanskaya St., Sevastopol, 299011, Russian Federation), DrSci (Geogr.), **ORCID ID: 0000-0002-0670-4573**, **ResearcherID: A-9774-2018**, *esovga@mhi-ras.ru*

Tatiyana V. Khmara, Research Associate, Marine Hydrophysical Institute of RAS (2 Kapitanskaya St., Sevastopol, 299011, Russian Federation), **Scopus Author ID: 6506060413**, **ResearcherID: C-2358-2016**, *xmara@mhi-ras.ru*

Contribution of the authors:

Irina V. Mezentseva – calculation of the assimilation capacity for ecosystems of parts of Sevastopol Bay, analysis of calculation results

Elena E. Sovga – study task statement, analysis of methods for calculating the assimilation capacity, comparison of assimilation capacity values for ecosystems of different parts of Sevastopol Bay, formation of the article

Tatiyana V. Khmara – calculations, discussion of the study results, data presentation in the text, data analysis, manuscript revision

All the authors have read and approved the final manuscript.

Original article

Organochlorine Xenobiotics in the Salgir River Ecosystem: Content, Distribution, Ecological Risk

L. V. Malakhova [1, 2] *, E. P. Karpova [1, 2], R. E. Belogurova [1, 2], V. V. Gubanov [2], G. A. Prokopov [1, 3], I. I. Chesnokova [1, 2], S. V. Kurshakov [1, 2], S. V. Statkevich [1, 2], D. G. Shavriev [2], S. V. Ovechko [1]

[1] *Research Center for Freshwater and Brackish Water Hydrobiology, Kherson, Russia*

[2] *A.O. Kovalevsky Institute of Biology of the Southern Seas of RAS, Sevastopol, Russia*

[3] *V. I. Vernadsky Crimean Federal University, Simferopol, Russia*

* *e-mail:malakh2003@list.ru*

Abstract

The content and distribution of organochlorine pesticides of the DDT group and polychlorinated biphenyls (PCBs) in water, amphipods, fish and sediments of the Salgir River, as well as in bottom sediments of the Biyuk-Karasu River, were determined. Samples were collected in May and July 2023. An analysis of organochlorine xenobiotics was performed using a GC Chromatec-Crystal 5000 (Russia), equipped with an electron capture microdetector. The ∑DDT concentration in water ranged from 0.53 in the area of the village of Dobroye up to 14.91 ng/L in the village of Molochnoye, whereas ∑6PCB changed from 0.50 to 37.87 ng/L, respectively. The lowest ∑DDT content (9.06 ng/g) in sediments was detected in the village of Dobroye, the highest one was registered in the village of Molochnoye (71.69 ng/g). The minimum ∑6PCB concentration (3.41 ng/g) was determined in the area of the village of Beloglinka, the maximum one was in the village of Molochnoye (61.88 ng/g). The pollutants distribution in water and bottom sediments indicates the presence of local DDTs and PCBs sources along the river between the villages of Beloglinka and Molochnoye. The lowest pollutants concentrations in hydrobionts were determined in muscles of schneider caught near the village of Dobroye. The highest ones were registered in the spined loaches caught near the village of Novogrigoryevka and in the bleak caught near the village of Molochnoye. In these fish, the maximum permissible concentration ∑DDT (300 ng/g wet weight) was exceeded. The obtained results were compared with water and sediments pollution in other Crimean, European and Asian rivers. An environmental risk assessment showed that pollution levels are not of concern in the area above Simferopol. In other sampling sites, high environmental risk was noted. The results showed that the environmental risk of PCBs pollution near the village of Molochnoye was higher than that of DDTs pollution.

Keywords: DDT, PCBs, water, bottom sediments, hydrobionts, environmental risk, Salgir River

Acknowledgments: This work was supported by the state contracts with the RC FBH "Study of peculiarities structure and dynamics of freshwater ecosystems of the Northern Black Sea coast" (no. 123101900019-5) and partially within the state contracts of IBSS of RAS "Molismological and biogeochemical foundations of homeostasis of marine ecosystems" (no. 121031500515-8), "Regularities of formation and anthropogenic transformation of biodiversity and bioresources of the Azov-Black Sea basin and other areas of the World Ocean" (no. 121030100028-0) and "Fundamental studies of population biology of marine animals, their morphological and genetic diversity" (no. 121040500247-0).

For citation: Malakhova, L.V., Karpova, E.P., Belogurova, R.E., Gubanov, V.V., Prokopov, G.A., Chesnokova, I.I., Kurshakov, S.V., Statkevich, S.V., Shavriev, D.G. and Ovechko, S.V., 2023. Organochlorine Xenobiotics in the Salgir River Ecosystem: Content, Distribution, Ecological Risk. *Ecological Safety of Coastal and Shelf Zones of Sea*, (4), pp. 116–133.

Хлорорганические ксенобиотики в экосистеме реки Салгир: содержание, распределение, экологический риск

Л. В. Малахова [1, 2]*, Е. П. Карпова [1, 2], Р. Е. Белогурова [1, 2], В. В. Губанов [2], Г. А. Прокопов [1, 3], И. И. Чеснокова [1, 2], С. В. Куршаков [1, 2], С. В. Статкевич [1, 2], Д. Г. Шавриев [2], С. В. Овечко [1]

[1] *ФГБНУ «Научно-исследовательский центр пресноводной и солоноватоводной гидробиологии», Херсон, Россия*

[2] *ФИЦ «Институт биологии южных морей имени А. О. Ковалевского РАН», Севастополь, Россия*

[3] *ФГАОУ ВО Крымский федеральный университет имени В. И. Вернадского, Симферополь, Россия*

* *e-mail:malakh2003@list.ru*

Аннотация

Определено содержание и распределение хлорорганических пестицидов группы ДДТ и полихлорированных бифенилов (ПХБ) в воде, амфиподах, рыбах и донных осадках р. Салгир, а также в донных отложениях ее притока Биюк-Карасу, отобранных в мае и июле 2023 г. Анализ хлорорганических ксенобиотиков проводили на газовом хроматографе «Хроматэк-Кристалл 5000», оснащенном микродетектором электронного захвата. Концентрация ∑ДДТ в воде изменялась в широком диапазоне: от 0.53 в районе с. Доброго до 14.91 нг/л в с. Молочном, ∑6ПХБ – от 0.50 до 37.87 нг/л соответственно. Наименьшее содержание ∑ДДТ (9.06 нг/г) в донных отложениях обнаружено в с. Добром, наибольшее – в с. Молочном (71.69 нг/г). Минимальная концентрация ∑6ПХБ (3.41 нг/г) определена в районе с. Белоглинка, максимальная – в с. Молочном (61.88 нг/г). Распределение загрязнителей в воде и донных отложениях свидетельствует о том, что по течению реки между селами Белоглинка и Молочным расположены локальные источники поступления ДДТ и ПХБ. В пробах гидробионтов наиболее низкие концентрации ДДТ и ПХБ определены в мышцах быстрянок у с. Доброго. Максимальное содержание загрязнителей обнаружено в тканях щиповок у с. Новогригорьевка и уклеи у с. Молочного, у которых было отмечено превышение ПДК ∑ДДТ, составляющей 300 нг/г сырой массы. Полученные результаты были сопоставлены с загрязнением воды и донных отложений в других реках Крыма,

Европы и Азии. Оценка экологического риска показала, что уровень загрязнения Салгира выше Симферополя не вызывает беспокойства. На остальных территориях отмечен высокий экологический риск. Результаты показали, что экологический риск, связанный с загрязнением ПХБ в районе с. Молочного был выше, чем связанный с загрязнением ДДТ.

Ключевые слова: ДДТ, ПХБ, вода, донные отложения, гидробионты, экологический риск, река Салгир

Благодарности: работа выполнена по теме ФГБНУ «НИЦ ПСГ» 123101900019-5 «Изучение особенностей структуры и динамики пресноводных экосистем Северного Причерноморья» и частично в рамках тем ФИЦ ИнБЮМ 121031500515-8 «Молисмологические и биогеохимические основы гомеостаза морских экосистем», 121030100028-0 «Закономерности формирования и антропогенная трансформация биоразнообразия и биоресурсов Азово-Черноморского бассейна и других районов Мирового океана» и 121040500247-0 «Фундаментальные исследования популяционной биологии морских животных, их морфологического и генетического разнообразия».

Для цитирования: Хлорорганические ксенобиотики в экосистеме реки Салгир: содержание, распределение, экологический риск / Л. В. Малахова [и др.] // Экологическая безопасность прибрежной и шельфовой зон моря. 2023. № 4. С. 116–133. EDN LZDHFW.

Introduction

Organochlorine pesticides of the dichlorodiphenyltrichloroethane (DDT) group and polychlorobiphenyls (PCBs) are among the most common and dangerous persistent organochlorine compounds (OCs) synthesized by humans. In this regard, the content, distribution and influence of OCs on environmental components became the subject of study all over the world in the 1970s. It was determined that OCs have a toxic effect on aerobic organisms, leading to various pathologies of the reproductive, nervous, immune and endocrine systems [1–4].

In May 2001, the United Nations Environment Programme adopted the Stockholm Convention on Persistent Organic Pollutants, which prohibits the production and use of twelve hazardous chemicals, including DDT and PCBs [1)]. However, OCs are still found in significant concentrations in the environment [5], including freshwater and marine coastal waters of the Crimea [6, 7].

The largest Crimean river system is the Salgir River with its side streams. The study of pollution in the Crimean rivers is carried out by the Crimean Department of Hydrometeorology and Environmental Monitoring, which conducts observations including analysis of water quality in accordance with sanitary and hygienic standards. In general, according to reports from government agencies, the water of the Salgir River is characterized as "dirty" [2)], and according to the indicators of biological and chemical oxygen consumption, the water of the Salgir River in the area of the village of Dvurechye was characterized as

---

[1)] UNEP, 2023. *History of the Negotiations of the Stockholm Convention; Nations Environment Programme.* Available at: https://chm.pops.int/TheConvention/Overview/History/Overview/tabid/3549/Default.aspx [Accessed: 19 November 2023].

[2)] Council of Ministers of the Republic of Crimea, 2023. [*Report on State and Protection of Environment of Republic of Crimea*]. Simferopol: OOO Print, 448 p. (in Russian).

"very polluted" [3] in 2020. However, data on the content of persistent organic pollutants DDT and PCBs in the Salgir River ecosystem are not provided either in reports or in any other open sources.

The paper aims to study the current pollution of the Salgir and Biyuk-Karasu Rivers ecosystem with DDT and PCBs. To achieve this purpose, the following tasks were solved: determination of the OCs concentration in the water and soils of the Salgir River and the soils of the Biyuk-Karasu River; assessment of the OCs accumulation in hydrobionts; determination of the components of the Salgir middle course ecosystem that accumulate OCs as much as possible; assessment of the environmental risk from the OCs effects.

Materials and methods

To achieve this goal, in May and July 2023, samples of water, sediments, crustaceans and fish fauna were taken in four districts of Salgir above (in the area of the village of Dobroye – Stations *1* and *2*) and below the city of Simferopol (the village of Beloglinka – Stations *3* and *4*), near the village of Molochnoye (Station *5*), near the village of Novogrigoryevka (Station *6*). In three districts of the Biyuk-Karasu River near Belaya Skala (Station *7*), the villages of Zybiny (Station *8*) and Uvarovka (Station *9*), samples of bottom sediments only were taken.

Water samples were taken in glass jars with a volume of 6 liters. The OCs in the water were determined with the help of gas chromatography in accordance with the environmental requirements PND F 14.1:2:3:4.204-04 (2014). Sediments (0–5 cm layer) were also taken directly into glass containers. In a stationary laboratory, the soils were thoroughly homogenized and dried in air. The natural humidity as a percentage of the wet weight was calculated from the difference between the wet and dry weight. The OCs in sediments were determined in accordance with the standard procedure GOST R 53217-2008 (ISO 10382:2002).

The fish were selected with a dragnet, gill and hand nets with a mesh from 3 to 18 mm. The fish were identified using determinants [4]. Bottom invertebrates were collected manually with tweezers from rocks and also with a hydrobiological scraper and sieve. The collected material was not fixed, but cooled for further processing. The determination of the material was carried out using profile determinants [5].

The OCs content was determined in the tissues of amphipods (Amphipoda) *Dikerogammarus villosus* (Sowinsky, 1894), in the gonads, muscles and internal organs of the following male and female fish (Teleostei): schneiders *Alburnoides maculatus* (Kessler, 1859), chubs *Squalius cephalus* (Linnaeus, 1758), juvenile bleaks *Alburnus alburnus* (Linnaeus, 1758) and zopes *Ballerus ballerus* (Linnaeus, 1758). The whole bodies of juvenile specimens of round gobies *Neogobius melanostomus* (Pallas, 1814) and spined loaches *Cobitis taenia* (Linnaeus, 1758) were analyzed.

---

[3] Trofimchuk, M.M., ed., 2021. [*Quality of Surface Waters of the Russian Federation. Information on the Most Polluted Water Bodies of the Russian Federation (Annex to Year-Book for 2020)*]. Rostov-on-Don, 160 p. (in Russian).

[4] Movchan, Yu.V. and Smirnov, A.I., 1981. [*Fauna of Ukraine, Vol. 8. Fishes, Issue 2 Cyprinidae, Part 2*]. Kiev: Naukova Dumka, 360 p. (in Ukranian).

[5] Tsalolikhin, S.Ya., ed., 1995. [*Keys to Freshwater Invertebrates of Russia and Adjacent Lands. Vol. 2.*] St. Petersburg, 629 p. (in Russian).

In the samples of hydrobionts, the OCs concentrations were determined in accordance with the method MVI.MN 2352-2005, and the content of total lipids was determined gravimetrically [8]. The sum of total extracted lipids is expressed in fractions (%) per wet weight.

Qualitative and quantitative analysis of OCs was carried out with the help of the gas chromatographic method in the Shared Use REC "Spectrometry and Chromatography" of IBSS of RAS using a CG Chromatec-Crystal 5000 (Russia), equipped with an electron capture microdetector. The content of p,p'-DDT, its metabolites p,p'-DDE and p,p'-DDD, as well as six congeners of polychlorinated biphenyls (according to IUPAC: 28, 52, 101, 138, 153 and 180), were determined. Quantitative determination of the OCs was performed by absolute calibration within the linear range of the detector. The detection limit for the OCs varied from 0.05 to 0.1 ng/L in water samples, from 0.01 to 0.05 ng/g in sediments and hydrobionts. The OCs concentration in sediments is calculated for the dry weight of samples, in hydrobionts – for the wet weight.

According to the OCs data in water, sediments and hydrobionts of the Salgir, the accumulation factor (AF) in sediments and bioaccumulation factor in hydrobionts (BAF) were calculated using the following formula: AF(BAF) = Cs(h),g/Cw·1000, where Cs,h – concentration of OCs in sediments or in tissues of hydrobionts (ng/g); Cw – concentration of OCs in water (ng/L).

T a b l e 1. Organochlorine compound (OC) toxicity data for fish and crustacea in freshwater ecosystems

OC	EC50, mg/L [6)]	
	Fish	Crustacea
p,p'-DDE	0.0960	0.0535
p,p'-DDD	0.1100	0.0090
p,p'-DDT	0.0800	0.0090
PCB 28	0.1600	0.1600
PCB 52	0.0030	0.0030
PCB 101	0.0100	0.0100
PCB 138	0.0026	0.0010
PCB 153	0.0013	0.0013
PCB 180	0.0250	0.0010

To assess the environmental risk from the effects of OCs on the Salgir hydrobionts, the internationally accepted risk coefficient RQ was used, which was calculated using equation [9]: $RQ = MEC/PNEC$, where MEC – measured concentration of OCs in hydrobionts; $PNEC$ – concentration of OCs, below which no harmful effects on organisms will occur with prolonged or short–term exposure. $PNEC$ is usually calculated by dividing toxicological dose descriptors ($LC50$ or $EC50$) by assessment factor [9]:

[6)] EPA. *ECOTOX Knowledgebase*. 2023. [online] Available at: https://cfpub.epa.gov/ecotox/search.cfm [Accessed: 19 November 2023].

PNEC = (*LC*50 or *EC*50)/*Assessment Factor*. Most commonly used mortality indicator *LC50* and *AF* = 1000 factor were taken for calculating *PNEC* during the study. Toxicological parameters *EC*50 were taken from the open *ECOTOX* database [6] (Table 1).

An RQ value greater than one means high environmental risk, in the range from 0.1 to 1 – average environmental risk, from 0.01 to 0.1 – low environmental risk, and below 0.01 – insignificant environmental risk [9].

Results

At Stations *1–4*, the DDT and PCBs concentration in the water was low in May and July. On average, the sum of the concentration of DDT and its metabolites (ΣDDT) was 1.30, the sum of the concentration of PCB congeners (Σ6PCB) was 1.85 ng/L (see Fig. 1, *a*). The composition and the same content of DDT and metabolites at these stations indicate a single source of pesticide intake in the Simferopol Region. Among PCB congeners at Stations *1–4*, only PCBs 138 and 153 were found in all samples. The low content of Σ6PCBs indicates the absence of significant sources of PCBs in the areas of these stations.

Downstream of the Salgir, at Stations *5* and *6*, a significant increase in the OCs concentration was observed (Fig. 1, *a*). The highest ΣDDT content was determined at Station *5* in the area of the village of Molochnoye (Table 2). At this site, the content of the initial DDT was 72% of the total concentration of DDT and metabolites, which means its recent entry into the river area. Downstream,

T a b l e 2. Concentrations (ng/L) of DDT, its metabolites, and indicator PCB congeners in the Salgir River water in May and July 2023

Station no.	Sampling date	p,p'-DDE	p,p'-DDD	p,p'-DDT	PCB 28	PCB 52	PCB 101	PCB 153	PCB 138	PCB 180
1	23.05	0.23	0.27	BDL	0.12	1.64	0.20	0.41	0.29	BDL
2	06.07	1.02	0.20	1.04	N/D	N/D	N/D	0.09	0.41	N/D
3	23.05	0.83	0.47	0.22	0.41	2.36	N/D	0.32	0.48	N/D
4	06.07	0.35	0.24	0.30	0.13	N/D	N/D	0.28	0.14	N/D
5	18.07	5.36	5.21	27.29	1.30	2.81	6.24	1.59	2.98	N/D
6	18.07	2.02	1.15	N/D	1.29	2.54	7.46	1.04	1.32	N/D

Note: BDL – below detection limit; N/D – not detected.

at Station 6, the initial DDT pesticide was not detected in the water, and the sum of the concentrations of its metabolites DDE and DDD turned out to be an order of magnitude lower than at Station *5*, but three times higher on average than in the Simferopol Region.

The content of Σ6PCB at Stations *5* and *6* turned out to be almost the same and amounted to 14.91 and 13.65 ng/L (Fig. 1, *a*), respectively. In the areas of Stations *5* and *6*, the sum of the concentrations of OCs in water exceeded on average 11 times their total content at Stations *1–4*.

No DDT and PCBs should be recorded in the water of fishery reservoirs, and the approximate permissible level (APL) is 10 ng/L [7]. In the Salgir water above and below Simferopol, both in May and in July, the OCs APL was not exceeded. At Station *5*, an excess of the ∑DDT APL was detected by 4 times, and that of the ∑6PCB APL by 1.5 times. At Station *6*, the ∑DDT APL was exceeded 1.3 times.

The results of geochemical analysis showed that at different sampling points, the sediments of the Salgir and the Biyuk-Karasu differed in natural moisture (NM) and, as a result, in granulometric composition. The sediments of the Salgir River were represented by multigrained sands with varying degrees of siltation. Thus, at Stations *1* and *3*, it was silted coarse odorless sand with an NM content of 33 and 38%, respectively, at Station *5* – sandy silt (NM – 40%) with putrid odor, at Station *6* – pelitic silt (NM – 54%). In the area of Station *7*, the soils of the Biyuk-Karasu River contained 95% of coarse cobbled gravel (from 0.5 to 3 cm) and 5% of aleuritic silt (NM – 19%) with putrid odor, at Station *8* – yellow-gray silt with 27% of NM with inclusions of gravelly fractions, at Station *9* – black silt with algae residues and with 55% of NM.

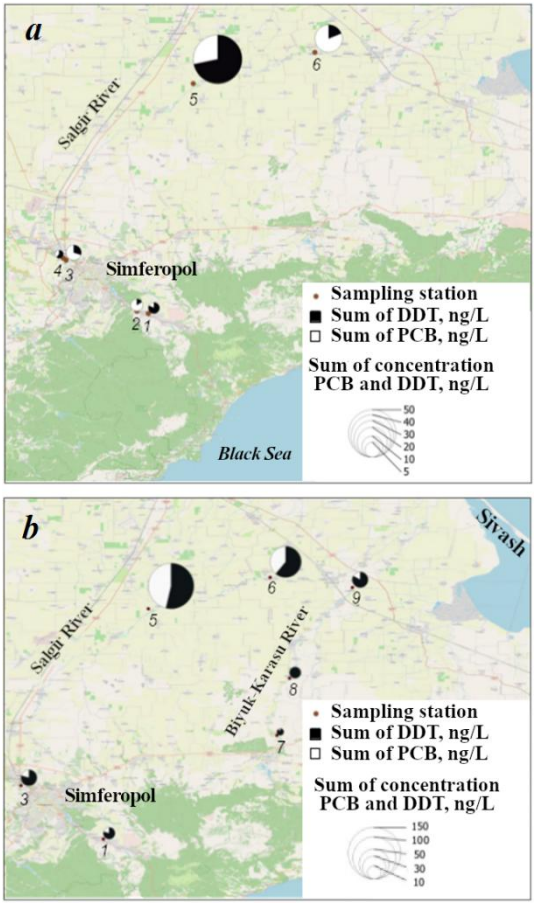

F i g. 1. ∑DDT and ∑6PCB concentrations in the Salgir River water (*a*) and sediments of the Salgir River (Stations *1–6*) and the Biyuk-Karasu River (Stations *7–9*) (*b*)

[7] *On the Approval of Water Quality Standards for Water Bodies of Commercial Fishing Importance, Including Standards for Maximum Permissible Concentrations of Harmful Substances in the Waters of Water Bodies of Commercial Fishing Importance*: Order of the Ministry of Agriculture of Russia dated December 13, 2016, No. 552 (in Russian).

The amount of OCs concentration in sediments varied in a wide range from 3.03 to 133.57 ng/g (Fig. 1, *b*). The lowest concentrations of ΣDDT and Σ6PCB were 2.73 and 0.30 ng/g at Station *7*, the maximum was 71.69 and 61.88 ng/g at Station *5*, respectively.

In the Russian Federation, there are only regional permissible levels (PLs) of the OCs content in sediments [8], where a safe level of 2.5 ng/g is set for ΣDDT. With the ΣDDT concentrations from 2.5 to 10 ng/g, precipitation is considered slightly polluted, at higher concentrations – polluted. The regional ΣDDT PLs coincide with the norms accepted in international practice in the Dutch Sheets [9], where there is also ΣPCB PL, which is less than 20 ng/g of wet weight. According to the above standards, sediments in terms of the level of PCB contamination in the area of Stations *7–9* can be classified as clean, at Stations *1* and *4* – slightly polluted, at Stations *5* and *6* – polluted, according to the level of ΣDDT pollution at Stations *1*, *7* and *9* – slightly polluted, at Stations *4–6*, *8* – polluted.

Fig. 2 shows the results of the determination of lipids and OCs in samples of hydrobionts. The content of total lipids varied from 1.3% in the muscles of female chub to 29.8% in the internal organs of bleak (Fig. 2, *a*). The concentration of OCs in fish tissue samples varied in a wide range: for ΣDDT – from 0.94 to 1153, for Σ6PCB – from "not detected" to 739 ng/g. The lowest concentration of OCs was determined in the muscles of male and female schneider at Station *1*, the highest – in the internal organs of bleak at Station *5* (Fig. 2, *b*). The DDT metabolites, DDE and DDD, were found in all samples of hydrobionts, and in 80 % of samples – the initial DDT. At Station *1*, PCBs were not detected in the muscles of male schneider, as well as in the muscles and gonads of female schneider. At more polluted Stations *5* and *6*, the concentration of ΣDDT in the bodies of juvenile individuals of bleak, goby and spined loach exceeded the content of Σ6PCB by 1.5 times on average.

A comparison of the OCs concentration with the MPC, which in freshwater fish for ΣDDT is 300, for ΣPCB – 2000 (in the liver – 5000) ng/g of wet weight, showed that the MPC of OCs was not achieved in muscles, which are a food product. It is obvious that there is no health risk for people when eating fish caught in the studied areas.

In such benthophages as spined loach and round goby, the ΣDDT and Σ6PCB concentration exceeded on average 4 and 7 times the concentration in potential food items – amphipods (Fig. 2, *b*). This can indicate the process of biomagnification – an increase in the level of OCs content in living organisms of the river trophic chain.

---

[8] LenmorNIIproekt, 1996. [*Standards and Assessment Criteria of Bottom Sediment Pollution in Water Bodies of St.Petersburg, Regional Standard*]. St. Petersburg: LenmorNIIproekt, 20 p. (in Russian).

[9] AMAP, 2004. PTS Limits and Levels of Concern in the Environment, Food and Human Tissues. In: AMAP, 2004. *Persistent Toxic Substances, Food Security and Indigenous Peoples of the Russian North*. Final Report. Oslo, 2004. Ch. 3, pp. 29–32. Available at: https://www.amap.no/documents/download/1069/inline [Accessed: 6 December 2023].

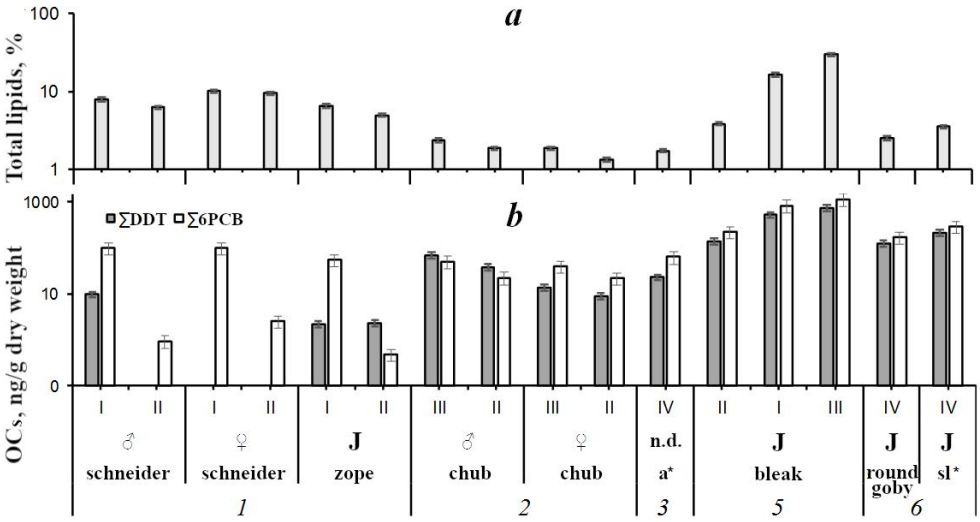

F i g. 2. Total lipids (*a*) and OCs concentrations (*b*) in Salgir hydrobionts: I – gonads; II – muscles; III – internal organs; IV – whole body; n.d. – not determined; J – juveniles, a* – amphipods, sl* – spined loach. Digits indicate station numbers

Discussion

Reasons for uneven distribution of OCs in the abiotic components of the Salgir ecosystem

The unequal contamination of the abiotic components of the Salgir ecosystem with the OCs indicates that between Stations *4* and *5*, there are sources of OCs intake, which influenced a significant increase in the concentration of pollutants at Stations *5* and *6*. At this stage of study, it is impossible to determine the exact source of OCs in this area. Potentially, pollutants can come with wastewater from municipal facilities [1]. It is known that in the Crimea, treated and untreated wastewater is discharged in the Salgir River, the Black Sea and Lake Sivash [2)]. DDT can appear in residential wastewater from pharmaceuticals. Despite the fact that DDT has been prohibited by the Russian government for several decades, pharmacy chains still offer DDT as an insecticide, as well as insecticidal soap containing DDT, in the 21st century [10]. Drainage waters of more than 80 water consuming enterprises, which take the Salgir water for irrigation of agricultural lands, can also be a source of OCs pollution [10)].

[10)] Rodyushkina, N.N., 2017. [*Information on Providing Water Bodies for Use on the Basis of Water Use Agreements and Decisions on Providing Water Bodies for Use in the Republic of Crimea as of 11 October 2017*] (in Russian).

In the late 1990s, 6.04 kg/ha of pesticides, including DDT, were applied to 1 hectare of farmland to control pests [11)]. The appearance of DDT in the river water can indicate its possible flushing from the drainage area, where warehouses of obsolete pesticides are located. On the territory of the Crimea, 866.9 tons of prohibited and unidentified pesticides are accumulated at 28 solid waste landfills, and the number of unofficial landfills of obsolete pesticides has never been recorded [11]. Filtrates containing dangerous chemical compounds and products of their metabolism enter aquifers from such landfills [1]. In addition, stock-raising facilities (including poultry farms) are the sources of OCs intake to the environment [1]. In the Krasnogvardeyskoye District, at least 11 large stock-raising farms are located in the Salgir drainage area [10)]. Thus, high local contamination of water and sediments at Stations *5* and *6* can be a consequence of the integral influence of the above-mentioned potential sources. It can be assumed that the main sources of DDT at Stations *5* and *6* were warehouses of obsolete pesticides stored in improper conditions, and the sources of PCBs were atmospheric transport precipitation and residual amounts from previous years of active use of OCs in industry and agriculture. The low concentration of OCs in the water at other stations, which is comparable to the pollution of the Crimean open marine areas [12], can be a consequence of so-called background pollution. Such a background is created by atmospheric transport from southern latitudes, where DDT is still allowed to be used to control insect vectors of malaria, typhus, tick-borne encephalitis, etc. [13, 14].

To identify the factors influencing the accumulation of OCs in sediments, correlation analysis was performed. Close ratio was found between the concentration of DDT, its metabolites and hexachlorobiphenyls 138 and 153 in sediments and their content in water (Fig. 3). For tri-CB 28, such ratio was absent (R^2_{PCB28} = –0.09), and for tetra- and penta-CB 52 (R^2_{PCB52}= 0.38) and 101 (R^2_{PCB101} = 0.40), it was weak. Thus, the concentration of DDT and highly chlorinated PCB congeners in the Salgir soils is closely related to water pollution.

The granulometric composition of sediments can be another factor influencing the accumulation of OCs by them. Indirectly, the granulometric composition can be judged by the NM: the higher the NM, the higher the content of silty fractions. The coefficients of determination (R^2) between the NM and the concentration of ΣDDT and Σ6PCB in the sediments of rivers were 0.36 and 0.25, respectively, which indicates a low correlation between fine fractions and the OCs content. Consequently, the content of pollutants in water was a more significant factor affecting the accumulation of OCs in soils.

[11)] Goskomgidromet, 1988. [*Yearbook of the Content of Residual Amounts of Pesticides in the Natural Objects of Certain Regions of the Soviet Union. Book II*]. Obninsk: Goskomgidromet, 132 p. (in Russian).

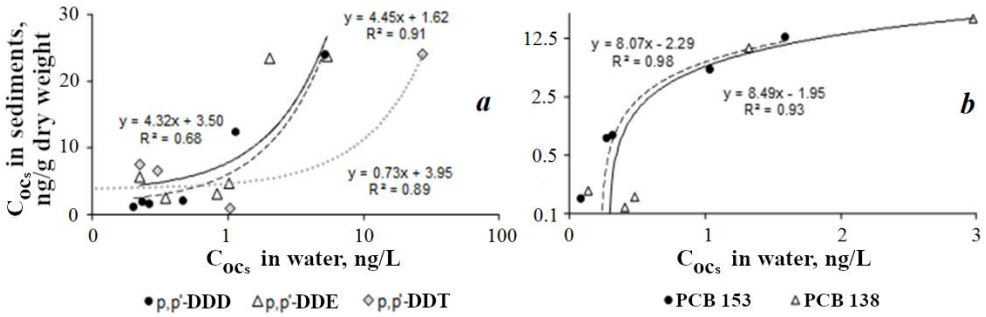

F i g. 3. Ratios of the DDT and its metabolites (*a*) and PCBs 153 and 138 (*b*) concentrations in the Salgir River sediments at st.*1–6* by the respective values in water

Comparison of the OCs concentration in water and sediments with other rivers

A comparison of the contamination of water and river soils showed that the concentration of ΣPCBs was higher in the Salgir than in the studied Crimean rivers – Chernaya and Uchan-Su [6, 12], as well as Biyuk-Karasu (Table 3), and was comparable to the data obtained in the Czech Republic [15]. At the same time, in such European rivers as the Sele, the Volturno, the Bahlui, the Someșul Mic [16, 17] and the Moscow [18], as well as in the rivers of India [19, 20], this indicator was lower. The content of ΣDDT in the sediments of the Salgir middle course turned out to be one of the highest among the compared areas. The pesticide concentration was three times higher only in the Indian Yamuna River (Table 3).

Mechanisms of removal of OCs from the Salgir waters

The intensive accumulation of OCs from the water by both sediments and biotic components of the Salgir ecosystem is evidenced by the calculated accumulation factor (AF) and bioaccumulation factor (BAF) of OCs (Fig. 4). In different areas of the Salgir, the ΣDDT AF in sediments varied from $2 \cdot 10^3$ at Station *5* to $1 \cdot 10^4$ at Station *6*. The AF of Σ6PCB in sediments was lower and ranged from $9 \cdot 10^2$ at Station *3* to $4 \cdot 10^3$ at Station *5*.

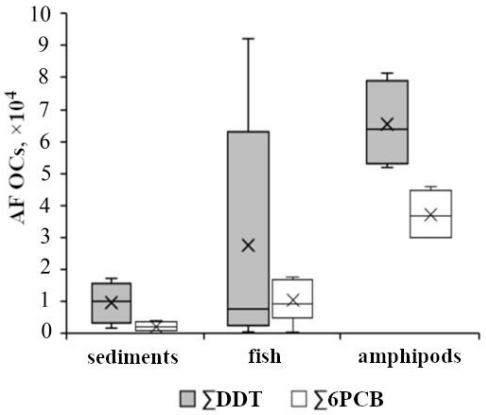

F i g. 4. Accumulation factor (AF) of OCs in sediments and bioaccumulation factor (BAF) of OCs in fish and amphipods of the Salgir River. Horizontal lines show median, crosses are the mean, boxes are interquartile ranges (25 and 75%), whiskers are ranges of AF and BAF values

T a b l e 3. OCs concentration in water and bottom sediments of freshwater ecosystems

Area	Date	Object	Ranges (mean) of ∑DDT	Ranges (mean) of ∑PCB	Work
Bahlui River, Romania	2002	Bottom sediments	(37) ng/g	24–158 (59) ng/g	[16]
Nove Mlyny Reservoir, South Moravia, Czech Republic	2007	Water	N/Dtm	(17.78) ng/L *[1]	[15]
		Bottom sediments	N/Dtm	2.09–38.11 (9.02) ng/g dry weight *[2]	
Yamuna River, India	January 2012	Water	0.1–354 (83±26) ng/L	2–779 (99±38) ng/L	[19]
	June 2018	Bottom sediments	0.41–18 ng/g dry weight	553–20 983 ng/g dry weight	[20]
Moscow River	2014	Water	N/Dtm	BDL – 180.7 ng/L *[3]	[18]
Someșul Mic River, Romania	May 2017	Bottom sediments	1.00–39.24 ng/g dry weight	2.74–252.72 ng/g dry weight	[21]
Volturno River, South Italy	April – July 2017, April – July 2018	Water	N/Dtm	22.3–24.5 ng/L *[2]	[17]
		Bottom sediments	N/Dtm	(64.4) ng/g dryweight	

Continued Table 3

Area	Date	Object	Ranges (mean) of ∑DDT	Ranges (mean) of ∑PCB	Work
Sele River, South Italy	April–February 2020, April – February 2017	Water	ND – 1.96 ng/L *3	20.8–39.3 ng/L *3	[5]
		Bottom sediments	0.10–6.12 ng/g dry weight	(79.3) ng/g dry weight	
Chernaya River mouth, south-eastern Crimea	2020–2021	Water	(0.57) ng/L	(3.45) ng/L	[12]
		Bottom sediments	7.3–13.6 (10.0) ng/g dry weight	3.9–27.4 (13.98) ng/g dry weight	[6]
Uchan-Su River (Yalta)	2020–2021	Water	(0.32) ng/L	(1.09) ng/L	[12]
Salgir River	May – July 2023	Water	0.53–37.87 (7.71) ng/L	0.50–14.91 (5.99) ng/L	TW
		Bottom sediments	9.06–71.69 (32.91) ng/g dry weight	3.11–61.88 (23.80) ng/g dry weight	
Biyuk-Karasu River	July 2023	Bottom sediments	2.73–13.08 (8.02) ng/g dry weight	BDL – 2.70 (1.00) ng/g dry weight	TW

Note: N/Dtm– the values were not determined; ND – not detected; BDL – below detection limit, TW – this work.
*1 Sum of concentrations of six PCB indicator congeners.
*2 Sum of the dissolved and weighed forms.
*3 Sum of concentrations of 28, 42, 45, and 49 PCB congeners.

Another mechanism of the aquatic environment purification is the extraction of hydrophobic OCs from water by hydrobionts [22]. According to our data, at a low concentration in the water, ΣDDT BAF and Σ6PCB BAF in the muscles of the Salgir fish at Station *1* were $9 \cdot 10^2$ and $8 \cdot 10^2$, respectively. At Station *6*, where the concentration of OCs was two orders of magnitude higher, BAF was higher than at Station *1*, and reached a maximum of $9 \cdot 10^4$ for ΣDDT and $1.5 \cdot 10^4$ for Σ6PCB (Fig. 4). The highest BAF were determined in crustaceans: the components at Station *3* averaged $7 \cdot 10^4$ for ΣDDT and $4 \cdot 10^4$ for Σ6PCB.

Assessment of the environmental risk from the effects of OCs on hydrobionts

Depending on the research area, the values of the environmental risk coefficients RQ of individual OCs varied in a wide range from 0.00001 to 25.8 in hydrobionts (Table 4). In general, the RQ of highly chlorinated PCB congeners turned out to be higher than the RQ of DDT group compounds and low-chlorinated PCBs. At Station *1*, RQ did not exceed the high risk threshold for all types.

T a b l e 4. Environmental risk coefficient *RQ* for fish and crustaceans in the Salgir River ecosystem

OC	Schneider and zope (St. *1*)	Chub (St. *2*)	Amphipods (St. *3*)	Bleak (St. *5*)	Goby (St. *6*)	Spined loach (St. *6*)
p,p'-DDE	0.0018	0.21	0.066	**1.94**	**1.0**	**1.9**
p,p'-DDD	0.0002	0.012	**1.1**	0.38	0.45	0.81
p,p'-DDT	0.0036	0.0014	**1.9**	0.38	0.17	0.29
PCB 28	0.0003	0.012	0.00001	0.038	0.025	0.045
PCB 52	0.27	**2.2**	**1.4**	**1.68**	**1.1**	**2.2**
PCB 101	0.012	**4.9**	0.47	**5.4**	**4.0**	**8.4**
PCB 138	0.61	**4.5**	**6.1**	**20.8**	**21.7**	**31.9**
PCB 153	0.19	**1.5**	**5.8**	**16.8**	**16.8**	**25.8**
PCB 180	0.003	0.0053	0.063	0.13	0.18	0.29

Note: RQ values of high environmental risk are given in bold.

Thus, it indicated average environmental risk for PCBs 52, 138 and 153 and no risk for DDT group compounds. At Stations *5* and *6*, the DDE RQ exceeded the high risk threshold for fish, and at Station *3*, RQ exceeded such a threshold for crustaceans concerning DDD and DDT content. The highest RQ coefficient was determined for hexachlorobiphenyls 138 and 153 for fish at Stations *2*, *5* and *6* and amphipods at Station *3*.

The results obtained at Stations *5* and *6* suggest that, despite the higher level of DDT pollution, PCB pollution poses a higher environmental risk for these areas of the Salgir ecosystem.

Conclusion

It is difficult to overestimate the economic importance of the Salgir River. The quality of life of people living on the banks of the river and the work of enterprises that are supplied with the Salgir water, depend on the condition of its water. The conducted studies of the levels of pollution of the components of the Salgir and Biyuk-Karasu ecosystems with such organochlorine xenobiotics as DDT and PCBs made it possible to identify the areas of environmental danger for biological objects and, possibly, for people near the villages of Molochnoye and Novogrigoryevka. The results of the study showed that the contamination of the OCs components of the Salgir middle course ecosystem was a serious environmental problem. Therefore, the task is to identify the OCs sources and prevent their intake to the river.

References

1. Galiulin, R.V., Galiulina, R.A., Khorobrykh, R.R. and Bashkin, V.N., 2019. Risk of Modern Contamination of River Waters by Pesticide DDT and HCH. *Issues of Risk Analysis*, 16(5), pp. 62–69. doi:10.32686/1812-5220-2019-16-5-62-69 (in Russian).
2. Fedorov, L.A. and Yablokov, A.V., 1999. *Pesticides – The Chemical Weapon That Kills Life (the USSRs Tragic Experience)*. Moscow: Nauka, 462 p. (in Russian).
3. Peivasteh-Roudsari, L., Barzegar-Bafrouei, R., Sharifi, K.A., Azimisalim, S., Karami, M., Abedinzadeh, S., Asadinezhad, S., Tajdar-Oranj, B., Mahdavi, V. [et al.], 2023. Origin, Dietary Exposure, and Toxicity of Endocrine-Disrupting Food Chemical Contaminants: A Comprehensive Review. *Heliyon*, 9(7), e18140. doi:10.1016/j.heliyon.2023.e18140
4. Vasseghian, Y., Hosseinzadeh, S., Khataee, A. and Dragoi, E-N., 2021. The Concentration of Persistent Organic Pollutants in Water Resources: A Global Systematic Review, Meta-Analysis and Probabilistic Risk Assessment. *Science of the Total Environment*, 796, 149000. doi:10.1016/j.scitotenv.2021.149000
5. De Rosa, E., Montuori, P., Triassi, M., Masucci, A. and Nardone, A., 2022. Occurrence and Distribution of Persistent Organic Pollutants (POPs) from Sele River, Southern Italy: Analysis of Polychlorinated Biphenyls and Organochlorine Pesticides in a Water–Sediment System. *Toxics*, 10(11), 662. doi:10.3390/toxics10110662
6. Malakhova, L.V., Lobko, V.V., Malakhova, T.V. and Murashova, A.I., 2022. Comparative Assessement of Organochlorine Pollution of Bottom Sediments in Different Types of Water Bodies in the Sevastopol Region (Crimea). *Chemistry for Sustainable Development*, 30(2), pp. 169–181. doi:10.15372/CSD2022371
7. Malakhova, L., Giragosov, V., Khanaychenko, A., Malakhova, T., Egorov, V. and Smirnov, D., 2014. Partitioning and Level of Organochlorine Compounds in the Tissues

of the Black Sea Turbot at the South-Western Shelf of Crimea. *Turkish Journal of Fisheries and Aquatic Sciences*, 14(5), pp. 993–1000. doi:10.4194/1303-2712-v14_4_19

8. Babkina, E.I. and Bobovnikova, Ts.I., 1978. [On Quantitative Extraction of Organochlorine Pesticides and Polychlorinated Biphenyls from Organs and Tissues of Fish]. *Gidrobiologichesky Zhurnal*, 14(3), pp. 103–105 (in Russian).
9. Lin, X., Xu, J., Keller, A.A., He, L., Gu, Y., Zheng, W., Sun, D., Lu, Z., Huang, J. [et al.], 2022. Occurrence and Risk Assessment of Emerging Contaminants in a Water Reclamation and Ecological Reuse Project. *Science of The Total Environment*, 744, 140977. doi:10.1016/j.scitotenv.2020.140977
10. Yaglova, N.V. and Yaglov, V.V., 2012. Endocrine Disruptors are a Novel Direction of Endocrinologic Scientific Investigation. *Annals of the Russian Academy of Medical Sciences*, 67(3), pp. 56–61. doi:10.15690/vramn.v67i3.186
11. Dubrovin, I.R. and Dubrovin, E.R., 2017. To a Question about Ecological Safety of the Autonomous Republic of Crimea. *Technico-Tehnologicheskie Problemy Servisa*, (4), pp. 24–28 (in Russian).
12. Malakhova, L.V. and Lobko, V.V., 2022. Assessment of Pollution of the Yalta Bay Ecosystem Components with Organochlorine Xenobiotics. *Ecological Safety of Coastal and Shelf Zones of Sea*, (3), pp. 104–116. doi:10.22449/2413-5577-2022-3-104-116
13. Mandavilli, A., 2006. Health Agency Backs Use of DDT Against Malaria. *Nature*, 443, pp. 250–251. doi:10.1038/443250b
14. Ranson, H., N'Guessan, R., Lines, J., Moiroux, N., Nkuni, Z. and Corbel, V., 2011. Pyrethroid Resistance in African Anopheline Mosquitoes: What are the Implications for Malaria Control? *Trends in Parasitology*, 27(2), pp. 91–98. doi:10.1016/j.pt.2010.08.004
15. Zelníčková, L., Svobodová, Z., Maršálek, P. and Dobšíková, R., 2015. Persistent Organic Pollutants in Muscle of Fish Collected from the Nové Mlýny Reservoir in Southern Moravia, Czech Republic. *Environmental Monitoring and Assessment*, 187(7), 448. doi:10.1007/s10661-015-4460-3
16. Dragan, D., Cucu-Man, S., Dirtu, A.C., Mocanu, R., Van Vaeck, L. and Covaci, A., 2006. Occurrence of Organochlorine Pesticides and Polychlorinated Biphenyls in Soils and Sediments from Eastern Romania. *International Journal of Environmental Analytical Chemistry*, 86, pp. 833–842. doi:10.1080/03067310600665571
17. Montuori, P., De Rosa, E., Sarnacchiaro, P., Di Duca, F., Provvisiero, D.P., Nardone, A. and Triassi, M., 2020. Polychlorinated Biphenyls and Organochlorine Pesticides in Water and Sediment from Volturno River, Southern Italy: Occurrence, Distribution and Risk Assessment. *Environmental Sciences Europe*, 32, pp. 1–22. doi:10.1186/s12302-020-00408-4
18. Eremina, N., Paschke, A., Mazlova, E.A. and Schüürmann, G., 2016. Distribution of Polychlorinated Biphenyls, Phthalic Acid Esters, Polycyclic Aromatic Hydrocarbons and Organochlorine Substances in the Moscow River, Russia. *Environmental Pollution*, 210, pp. 409–418. doi:10.1016/j.envpol.2015.11.034
19. Kumar, B., Singh, S.K., Mishra, M., Kumar, S. and Sharma, C.S., 2012. Assessment of Polychlorinated Biphenyls and Organochlorine Pesticides in Water Samples from the Yamuna River. *Journal of Xenobiotics*, 2(1), e6. doi:10.4081/xeno.2012.e6
20. Kumar, B., Verma, V.K., Mishra, M., Piyush, Kakkar, V, Tiwari, A., Kumar, S., Yadav, V.P. and Gargava, P., 2021. Assessment of Persistent Organic Pollutants in Soil and Sediments from an Urbanized Flood Plain Area. *Environmental Geochemistry and Health*, 43(9), pp. 3375–3392. doi:10.1007/s10653-021-00839-9
21. Barhoumi, B., Beldean-Galea, M.S., Al-Rawabdeh, A.M., Roba, C., Martonos, I.M., Bălc, R., Kahlaoui, M., Touil, S., Tedetti, M. [et al.], 2019. Occurrence, Distribution

and Ecological risk of Trace Metals and Organic Pollutants in Surface Sediments from a Southeastern European River (Someşu Mic River, Romania). *Science of the Total Environment*, 660, pp. 660–676. doi:10.1016/j.scitotenv.2018.12.428

22. Polikarpov, G.G. and Egorov, V.N., 1986. *Marine Dynamic Radiochemoecology*. Moscow: Energoatomizdat, 174 p. (in Russian).

Submitted 21.06.2023; accepted after review 15.08.2023;
revised 11.10.2023; published 20.12.2023

About the authors:

Ludmila V. Malakhova, Senior Research Associate, Research Center for Freshwater and Saltwater Hydrobiology (87 Marii Fortus St, Kherson, 273003, Russian Federation), Leading Research Associate, A. O. Kovalevsky Institute of Biology of the Southern Seas of RAS (2 Nakhimova Ave, Sevastopol, 299011, Russian Federation), PhD (Biol.), **ORCID ID: 0000-0001-8810-7264, Scopus Author ID: 35604200900, ResearcherID: E-9401-2016,** *malakh2003@list.ru*

Evgeniia P. Karpova, Senior Research Associate, Research Center for Freshwater and Saltwater Hydrobiology (87 Marii Fortus St, Kherson, 273003, Russian Federation), Senior Researcher, A. O. Kovalevsky Institute of Biology of the Southern Seas of RAS. (2 Nakhimova Ave, Sevastopol, 299011, Russian Federation), PhD (Biol.), **ORCID ID: 0000-0001-9590-9302, Scopus Author ID: 26639409000, ResearcherID: T-5944-2019,** *karpova_jey@mail.ru*

Raisa E. Belogurova, Research Associate, Research Center for Freshwater and Saltwater Hydrobiology (87 Marii Fortus St, Kherson, 273003, Russian Federation), Research Associate, A. O. Kovalevsky Institute of Biology of the Southern Seas of RAS (2 Nakhimova Ave, Sevastopol, 299011, Russian Federation), PhD (Biol.), **ORCID ID: 0000-0002-3101-7708, Scopus Author ID: 57221541105, ResearcherID: P-9056-2016**, *prishchepa.raisa@yandex.ru*

Vladimir V. Gubanov, Leading Engineer, A. O. Kovalevsky Institute of Biology of the Southern Seas of RAS (2 Nakhimova Ave, Sevastopol, 299011, Russian Federation), **ORCID ID: 0000-0002-0077-2129,** *gubanov76@mail.ru*

Gregoryi A. Prokopov, Research Associate, Research Center for Freshwater and Saltwater Hydrobiology (87 Marii Fortus St, Kherson, 273003, Russian Federation), Senior Lecturer, V. I. Vernadsky Crimean Federal University (4 Vernadskogo Ave, Simferopol, 295007, Russian Federation), **ORCID ID 0000000-0077-2129, Scopus Author ID: 22958408500, ResearcherID: JFB-3418-2023**, *prokopov@cfuv.ru*

Irina I. Chesnokova, Senior Research Associate, Research Center for Freshwater and Saltwater Hydrobiology (87 Marii Fortus St, Kherson, 273003, Russian Federation), Senior Research Associate, A. O. Kovalevsky Institute of Biology of the Southern Seas of RAS (2 Nakhimova Ave, Sevastopol, 299011, Russian Federation), PhD (Biology), **ORCID ID: 0000-0002-7883-0755, Scopus Author ID: 57194774884, ResearcherID: X-2173-2019**, *mirenri@bk.ru*

Sergey V. Kurshakov, Research Associate, Research Center for Freshwater and Saltwater Hydrobiology (87 Marii Fortus St, Kherson, 273003, Russian Federation), Research Associate, A. O. Kovalevsky Institute of Biology of the Southern Seas of RAS (2 Nakhimova Ave, Sevastopol, 299011, Russian Federation), **ORCID ID: 0000-0001-8129-5944, Scopus Author ID: 57200942626, ResearcherID: T-9557-2019**, *kurshackov@yandex.ru*

Svetlana V. Statkevich, Senior Research Associate, Research Center for Freshwater and Saltwater Hydrobiology (87 Marii Fortus St, Kherson, 273003, Russian Federation), Senior

Research Associate, A. O. Kovalevsky Institute of Biology of the Southern Seas of RAS (2 Nakhimova Ave, Sevastopol, 299011, Russian Federation), PhD (Biol.), **ORCID ID: 0000-0003-4108-459X, Scopus Author ID: 57190605963, ResearcherID: T-5972-2019**

Dmitry G. Shavriev, Leading Engineer, A. O. Kovalevsky Institute of Biology of the Southern Seas of RAS (2 Nakhimova Ave, Sevastopol, 299011, Russian Federation), *shavrievd@gmail.com*

Sergey V. Ovechko, Director, Research Center for Freshwater and Saltwater Hydrobiology (87 Marii Fortus St, Kherson, 273003, Russian Federation), **ORCID ID: 0009-0007-1050- 9918, ResearcherID: JFJ-7762-2023**, *hgbs1@yandex.ru*

Contribution of the authors:

Ludmila V. Malakhova – statement of the problem, preparation of water samples, sediments and hydrobionts for gas chromatographic analysis, determination of organochlorine pollutants, analysis and discussion of the obtained results, writing and design of the article

Evgeniia P. Karpova – management of expeditionary work in May 2023, participation in expeditionary sampling of components of the Salgir River ecosystem, determination of the species composition of ichthyofauna, discussion of results, editing of the article

Raisa E. Belogurova – management of expeditionary work and July 2023, sampling of ecosystem components of Salgir River and Biyuk-Karasu River, determination of the species composition of ichthyofauna, preparation and preparation of samples for analysis, discussion of results, editing of the article

Vladimir V. Gubanov – participation in expeditionary sampling of components of the Salgir River ecosystem and biological analysis of samples

Gregoryi A. Prokopov – planning and sampling of abiotic components and benthos in Salgir River and Biyuk-Karasu River, determination of the species composition of benthic organisms, discussion of the results, graphical presentation of the analysis results, editing the article

Irina I. Chesnokova – participation in expeditionary sampling of components of the Salgir River ecosystem, determination of the species composition of ichthyofauna, preparation and preparation of samples for analysis, discussion of results, editing of the article

Sergey V. Kurshakov – participation in expeditionary sampling of components of the Salgir River ecosystem and biological analysis of samples

Svetlana V. Statkevich – participation in expeditionary sampling of components of the Salgir River ecosystem and biological analysis of samples

Dmitry G. Shavriev – participation in expeditionary sampling of components of the Salgir River ecosystem and biological analysis of samples

Sergey V. Ovechko – statement of the problem, work planning, analysis of results, discussion and final editing of the article

All the authors have read and approved the final version of the manuscript.

Original article

Efficacy of Ballast Water Treatment Systems Installed Onboard Ships Entering the Seaport of Novorossiysk, the Black Sea

O. N. Yasakova [1]*, O. T. Zuykov [2], Y. B. Okolodkov [3]

[1] *Southern Scientific Center, Russian Academy of Sciences, Rostov-on-Don, Russia*

[2] *The Federal State Budgetary Institution "Administration of Seaports of the Black Sea", Novorossiysk, Russia*

[3] *Laboratorio de Botánica Marina y Planctología, Instituto de Ciencias Marinas y Pesquerías, Universidad Veracruzana, Veracruz, Mexico*

* *e-mail: yasak71@mail.ru*

Abstract

The paper aims to assess the quality of ballast water purification of phyto- and microzooplankton using various ballast-water treatment systems. The analysis of treatment systems performance was based on the results of the study of phyto- and microzooplankton taxonomic composition and abundance in 19 samples of ballast water treatment after their treatment in the ships' systems. The samples were taken onboard 12 oil tankers and 7 bulk carriers originating from the ports representing the Mediterranean basin, tropical West Africa and the NW Indian Ocean. The vessels entered the seaport of Novorossiysk for cargo loading from October 2022 to March 2023. In 90% of all cases of the systems use, the ballast water purification of unicellular organisms met the Regulation D-2 Ballast Water Performance Standard of the International Convention for the Control and Management of Ships' Ballast Water and Sediments. The ballast of 10% of the vessels (from Turkish ports in the Marmara and Aegean Seas) equipped with DESMI CompactClean CC-500 (treatment by filtration + UV) and Pureballast 3.2 1500 EX (treatment by UV system) did not meet the cleaning quality standard: 1.19×10^6 and 1.21×10^4 cells/L, respectively, were detected after treatment. The ballast waters of vessels from the Gulf of Suez and Mauritania represented a moderate risk in terms of cell abundance (7.16×10^3 and 2.03×10^3 cells/L, respectively). In total, 20 microalgal species were found: diatoms (13), dinoflagellates (6), a silicoflagellate (1), several algal taxa not identified to species, as well as ciliates. *Proboscia alata* and *Prorocentrum micans* were the most frequent. No planktonic algae classified as invasive to the Black Sea were found.

Keywords: ballast water, marine ballast, seaport of Novorossiysk, ballast water systems, taxonomic composition, phytoplankton, Black Sea, anthropogenic pollution, biological invasion, invasive species

Acknowledgments: The authors are grateful to the Captain of the Port of Novorossiysk S. A. Uryupin for the opportunity to examine ballast waters, to the inspectors of the Federal State Budgetary Institution "Administration of Seaports of the Black Sea" O. V. Sinayskiy,

A. B. Krylovskiy and A. A. Rassokhin for sampling, as well as to N. A. Okolodkova (Mexico City, Mexico) for preparing the map, plate of micrographs and graphical abstract, S. N. Olenin (Marine Research Institute, Klaipeda University, Klaipeda, Lithuania) for help with the literature, Nina Lundholm (Department of Biology, University of Copenhagen, Copenhagen, Denmark) for consulting us about the diatom genus *Pseudo-nitzschia* and M. M. Gowing (Seattle, WA, USA) for improving the English style. The manuscript was prepared within the framework of the federal state task of the Southern Scientific Center, Russian Academy of Sciences, No. 122011900153-9.

For citation: Yasakova, O.N., Zuykov, O.T. and Okolodkov, Y.B., 2023. Efficacy of Ballast Water Treatment Systems Installed Onboard Ships Entering the Seaport of Novorossiysk, the Black Sea. *Ecological Safety of Coastal and Shelf Zones of Sea*, (4), pp. 134–154.

Эффективность применения систем обработки балластных вод на судах, заходящих в морской порт Новороссийск, Черное море

О. Н. Ясакова [1]*, О. Т. Зуйков [2], Ю. Б. Околодков [3]

[1] *Южный Научный Центр РАН, Ростов-на-Дону, Россия*

[2] *Федеральное государственное бюджетное учреждение «Администрация морских портов Черного моря», Новороссийск, Россия*

[3] *Laboratorio de Botánica Marina y Planctología, Instituto de Ciencias Marinas y Pesquerías, Universidad Veracruzana, Veracruz, México*

* *e-mail: yasak71@mail.ru*

Аннотация

Цель работы – оценить качество очистки судового балласта от фито- и микрозоопланктона с помощью различных систем обработки балластных вод. В основу анализа эффективности систем очистки легли результаты исследования таксономического состава и численности фито- и микрозоопланктона в 19 пробах балластных вод после их обработки в судовых системах. Отбор проб морского балласта был осуществлен на борту 12 нефтяных танкеров и семи сухогрузов, прибывших из портов стран Средиземноморского бассейна, Тропической Западной Африки и северо-западной части Индийского океана и заходивших под погрузку в морской порт Новороссийск в октябре 2022 г. – марте 2023 г. Исследования показали, что в 90 % всех случаев использования установок результат очистки балластных вод от одноклеточных организмов удовлетворял стандарту *D*-2 Международной конвенции о контроле судовых балластных вод и осадков и управления ими. Балласт 10 % исследованных судов (из портов Турции в Мраморном и Эгейских морях), оснащенных системами *DESMI CompactClean CC*-500 (способ очистки: фильтрация + обработка ультрафиолетом) и *Pureballast* 3.2 1500 *EX* (способ очистки: обработка ультрафиолетом), не соответствовал стандарту качества очистки. После обработки численность одноклеточных водорослей в балласте составляла $1.19 \cdot 10^6$ и $1.21 \cdot 10^4$ кл./л соответственно. Балластные воды судов из Суэцкого залива и Мавритании представляли собой умеренную угрозу/опасность для окружающей среды: численность микроводорослей составляла $7.16 \cdot 10^3$ и $2.03 \cdot 10^3$ кл./л соответственно. Всего обнаружено 20 видов микроводорослей: 13 диатомовых, 6 динофлагеллят, 1 силикофлагеллят и несколько не идентифицированных до вида таксонов водорослей, а также инфузории. Наиболее часто встречались *Proboscia alata* и *Prorocentrum micans*. Видов планктонных водорослей, классифицируемых как вселенцы в Черное море, в балласте обнаружено не было.

Ключевые слова: балластные воды, морской балласт, порт Новороссийск, системы обработки балласта, таксономический состав, фитопланктон, Черное море, антропогенное загрязнение, биологические инвазии, виды-вселенцы

Благодарности: авторы выражают благодарность за предоставленную возможность провести исследования балластных вод капитану морского порта Новороссийск С. А. Урюпину и за осуществление отбора проб судового балласта инспекторам ФГБУ «АМП Черного моря» О. В. Синайскому, А. Б. Крыловскому и А. А. Рассохину, а также Н. А. Околодковой (Мехико, Мексика) за подготовку карты, таблицы микрофотографий и графической аннотации, С. Н. Оленину (Институт морских исследований при Клайпедском университете, Клайпеда, Литва) за помощь с литературой, Nina Lundholm (Department of Biology, University of Copenhagen, Copenhagen, Denmark) за консультацию по роду диатомовых *Pseudo-nitzschia* и M. M. Gowing (Seattle, WA, USA) за помощь в редактировании английского текста. Публикация подготовлена в рамках государственного задания ЮНЦ РАН № 122011900153-9.

Для цитирования: *Ясакова О. Н., Зуйков О. Т., Околодков Ю. Б.* Эффективность применения систем обработки балластных вод на судах, заходящих в морской порт Новороссийск, Черное море // Экологическая безопасность прибрежной и шельфовой зон моря. 2023. № 4. С. 134–154. EDN OERTEH.

Introduction

Biological pollution is one of the most important problems of anthropogenic influences on the ecosystems of the World Ocean. Every day, on a planetary scale, vessels carry from 3000 to 4000 species of organisms [1, 2]. The involuntary and uncontrolled transfer of microalgae and their cysts in ships' ballast water began in the 1870s. Due to the rapid development of metallurgy, wooden vessel hulls were replaced by metal ones, and instead of stones, gravel or sand, sea water began to be used as ballast [3].

The current composition of the Black Sea flora and fauna was formed under the influence of the fresh waters of the Sea of Azov and large European rivers on the one hand and the Mediterranean waters on the other. Therefore, it is of a mixed nature and includes both freshwater and marine species.

Natural migration of species from the Mediterranean Basin through the Bosphorus and Dardanelles straits to the Black Sea and their distribution in the sea under the influence of currents have always existed since the formation of the Bosphorus Strait (presumably, 8–10 thousand years ago [4]) and still exist today.

Despite the fact that the salinity does not exceed 18 in the surface layer, the sea has low "biological immunity" against invasive species due to a significant proportion of relict and endemic species [1)]. Over the last half century, more than 200 species of flora and fauna new to this region, arriving from other areas of

[1)] Zaitsev, Y.P., 2006. *An Introduction on the Black Sea Ecology*. Odessa: Even, 224 p. (in Russian).

the World Ocean, have been found in the Black Sea, while about 150 Mediterranean species have successfully adapted to new conditions [5, 6]. By the beginning of the 20th century, more than 40 invasive species had become common inhabitants of the Black Sea and the Sea of Azov [7]. It is predicted that the rate of invasion of new species into the Black Sea will increase (up to two species per year). This is generally caused by the increase in shipping intensity and disruption of ecosystem stability due to eutrophication [8, 9].

Not every invasion of an alien organism results in tangible environmental and economic consequences, but some cases have been recorded. Thus, the invasion of the North American ctenophore *Mnemiopsis leidyi* A. Agassiz (Ctenophora: Tentaculata: Bolinopsidae) into the Black Sea in the early 1980s led to a decrease in the numbers of the European anchovy *Engraulis encrasicolus* (L.) (Clupeiformes: Engraulidae) and other commercial fish species. Consequently, economic losses amounted to US$240 million per year [2)].

Most phytoplankton cells do not survive in dark ballast tanks. However, resting stages of planktonic diatom and dinoflagellate species were found to be viable even after being transported in sediments at the bottom of ballast tanks for six months at 4 °C [10]. A microalgal study of 343 vessels entering 18 Australian ports found that 65% of the vessels carried significant amounts of sediments in their tanks [11]. Dinoflagellates account for the vast majority of toxic species compared to other marine microalgae, and almost all toxic dinoflagellate species are capable of photosynthesis.

In 2004, to reduce the environmental, epidemiological and other stresses on the aquatic environment caused by untreated ballast water discharge, the International Maritime Organization (IMO) adopted the International Convention for the Control and Management of Ships' Ballast Water and Sediments [3)]. The Convention includes five standard ballast water treatment procedures. The first, most reliable method of preventing the introduction of unwanted invasive species is the complete exclusion of ballast water discharge in the port water area. The remaining four methods involve treating ballast water to minimize the risk of discharge of unwanted organisms. From practical experience, they are all far from perfect [4)] [8, 12–15]. The second method includes the reduction of the marine organism

---

[2)] Zaitsev, Y. and Öztürk, B., 2001. *Exotic Species in the Aegean, Marmara, Black, Azov and Caspian Seas*. Istanbul: Turkish Marine Research Foundation, 267 p.

[3)] IMO, 2004. *2004 International Convention for the Control and Management of Ships' Ballast Water and Sediments*. London: International Maritime Organization, 28 p.

[4)] Kudyukin, A.A., 2003. [Ballast Water Treatment in Shipboard Conditions: World Experience, Technological Approaches. Expert Evaluation of Proposals of National Manufacturers. First Results, Conclusions]. In: Global Ballast Water Management Program, 2003. [*The 4th Scientific-Practical Seminar on the Problem of Ship Ballast Water Management (for Specialists of Scientific Institutions Related to the Problem of Shipping, Marine Biology, Ecology and Environmental Protection), Odessa, Ukraine, 26–27 August 2003: Workshop Report*]. Odessa, pp. 19–23 (in Russian).

concentrations in the ballast water loaded by the vessel, by limiting the amount of water, selecting receiving sites, etc. The third method is coastal ballast treatment. The fourth and most widely used method is ballast change in open sea or ocean water (regulation D-1). The fifth, most effective, method involves ballast water treatment onboard the vessel (regulation D-2). This is a ballast water quality standard that requires vessels to install a ballast water treatment system (BWTS) onboard. BWTSs must discharge into the marine environment fewer than 10 viable organisms ≥ 50 μm in length per cubic metre and fewer than 10 viable organisms 10–50 μm in length per milliliter. By 2010, about 60 BWTSs were known, and new ones appear every year [15].

IMO developed several technological methods for this process, which can be divided into four groups [5)] [16]: 1) physical (heating, ultrasonic and ultraviolet treatment, silver ionization, etc.); 2) mechanical (filtration); 3) chemical (ozonation, deoxygenation, chlorination, use of bioreagents, etc.); 4) biological (adding predatory or parasitic organisms to ballast water to destroy unwanted invasive species).

The results of the study of various ballast water treatment methods revealed almost no sufficiently effective and economical ones [17].

To minimize damage from biological pollution, IMO required all merchant vessels to comply with regulation D-1 (full ballast water exchange or three sequential pumpings of ballast water) in the area of the recipient water body. However, the Convention stipulates that vessels built in 2017 and later must comply with regulation D-2. According to the binding regulations for the seaport of Novorossiysk, discharge of ballast is allowed subject to compliance with regulations D-1 and D-2.

In 2008, IMO developed and published Guidelines for approval of ballast water management systems (MEPC 2008). These Guidelines define the minimum BWTS technical specifications and technical documentation requirements. Furthermore, they define a manner of testing and targeted results of analysis of ballast water samples. Special attention is paid to the size and concentration of living organisms, including some types of bacteria [6)].

Long-term (2004–2019) monitoring studies of the marine environment conducted in the water areas of the large Russian commercial ports and resort cities, as well as in the open areas of the northeastern Black Sea, showed that in recent decades new invasive species continued to appear there despite the application of regulations D-1 and D-2 [5, 18–20]. It should be noted that some caused significant economic damage, as was the case with the emergence of the ctenophore *Mnemiopsis leidyi.*

[5)] Tamelander, J., Riddering, L., Haag, F. and Matheickal, J., 2010. *Guidelines for Development of a National Ballast Water Management Strategy*. London; Gland: GEF-UNDP-IMO GloBallast, 43 p.

[6)] MEPC, 2008. *Resolution MEPC.174(58). Guidelines for Approval of Ballast Water Management Systems (G8)*. 28 p. MEPC 58/23, Annex 4.

The literature covers the results of studies of phyto- and zooplankton in ballast water for the regulation D-1 efficacy evaluation. At the same time, there are fewer publications on the results of applying regulation D-2 in practice, and they mainly concern microbiological studies [23]. No information was published on the efficacy of long-term practical use of ballast water treatment systems for minimizing the concentration of plant and animal planktonic organisms in them. The aim of this paper is to assess the quality of ballast water treatment of phyto- and microzooplankton of the BWTSs on the vessels that entered the seaport of Novorossiysk in 2022–2023.

Materials and methods

Nineteen ballast water samples that underwent the treatment procedures of BWTSs were taken by inspectors of the Federal State Budgetary Institution "Administration of Seaports of the Black Sea" using a ship's cylindrical metal 1 liter sampler through ballast holes onboard 19 vessels (12 oil tankers and 7 bulk carriers) that entered the seaport of Novorossiysk for cargo loading from October 2022 to March 2023 (Table 1). The vessels loaded ballast in the ports of the following countries (Fig. 1): Romania (the Black Sea, 1 vessel), Turkey (8 vessels), Greece (1 vessel), Italy (1) and Tunisia (1) (the Mediterranean countries), Mauritania (1) (tropical West Africa), Egypt (5 vessels) (the Gulf of Suez, the Red Sea, the Indian Ocean) and Iran (1 vessel) (the Persian Gulf, the Indian Ocean). Marine ballast samples were fixed with neutral formaldehyde to a final concentration of 1–2% [7)] and concentrated in a land-based laboratory by sedimentation in cylinders with a diameter of 5.3 cm and a height of 36 cm for 2–3 weeks. Cell counts of phytoplankton were carried out using a MIKMED-2 microscope (LOMO, St. Petersburg, Russia), applying the bright-field technique in transmitted light using the 10×/0.30 and 40×/0.65 achromatic objectives produced by LOMO (St. Petersburg, Russia) in a 0.05 mL Nageotte counting chamber. To count rare and large species of phytoplankton and microzooplankton, an aliquot of the concentrate (1/2–1/10) and the entire sample were examined in a 1 mL Sedgwick–Rafter chamber. The minimum size of the cells taken into account was 3–5 μm. Phytoplankton abundance was calculated in accordance with the following formula:

$$N = \frac{V_2 \; n}{V_1 \; V_3},$$

where V_1 – filtered water volume, mL; V_2 – concentrate volume, mL; V_3 – counting chamber volume, mL; n – number of cells in the counting chamber. The taxonomic affiliation of organisms was determined according to generally

---

[7)] Makarevich, P.R. and Druzhkov, N.V., 1989. [*Guidelines for the Analysis of Quantitative and Functional Characteristics of Marine Biocenoses of the Northern Seas. Part 1. Phytoplankton. Zooplankton. Suspended Organic Matter*]. Apatity: KNTs RAN, MMBI, 50 p. (in Russian).

T a b l e 1. Characteristics of the surveyed vessels entering the seaport of Novorossiysk for loading in 2022-2023, the ballast water systems and the phyto- and zooplankton abundance after the ballast water treatment

Vessel number	Sampling date	Port of ballast water loading	Vessel name and type, flag	Type of BWTS	Ballast volume, m^3	BWTS treatment method	Total abundance of organisms, cells/L
1	19.10.2022	Suez, Egypt	BEKS FENIX, oil product carrier, Marshall Islands	HMT-1500-EX	17 152	Electrocatalysis	N/D
2	22.10.2022	Iskenderun, Turkey	MV POSEIDONS, bulk carrier, Liberia	HMT-800	12 714	Electrocatalysis	N/D
3	23.10.2022	Agioi Theodoroi, Greece	MT PHOENIX AN, oil tanker, Malta	Hiballast BWMS-HUB-1000-EX	14 025	Electrochlorination + Neutralization	N/D
4	28.10.2022	Damietta, Egypt	MV CLEAR SKY, bulk carrier, Panama	BalClor BC-1000	17 359	Electrolysis + Filtration	21
5	31.10.2022	Tuzla, Turkey	GEORGY MASLOV, crude oil tanker, Liberia	NK-03-Blue Ballast II Plus	37 998	Ozone Injection + Neutralization	4

Continued Table 1

Vessel number	Sampling date	Port of ballast water loading	Vessel name and type, flag	Type of BWTS	Ballast volume, m^3	BWTS treatment method	Total abundance of organisms, cells/L
6	31.10.2022	Suez, Egypt	CALIPSO, bulk carrier, Liberia	BalClor BC-2000	19 994	Electrolysis + Filtration	N/D
7	31.10.2022	Constanta, Romania	ELANDA OSPREY, oil tanker, Liberia	HiBallast TM System HIB-2000-EX	44 764	Electrolysis + Filtration	16
8	12.11.2022	Tutunciflik, Turkey	MARINER A, oil-chemical Tanker, Malta	HiBallast NF System	16 651	Electrolysis + Filtration	8
9	09.12.2022	Ain Sokhna, Egypt	IKARA, crude oil tanker, Panama	Ecochlor Series 200	46 801	Chlorine system + Filtration	N/D
10	11.12.2022	Искендерун, Турция / Iskenderun, Turkey	VIVA ECLIPSE, bulk carrier, Panama	Erma First FIT 800	13 973	Electrolysis+ Filtration	27
11	14.12.2022	La Skhirra, Tunisia	HISTRIA PERLA, oil-chemical tanker, Malta	Pure Ballast 3:2	16 773	Filter + UV treatment	6

Continued Table 1

Vessel number	Sampling date	Port of ballast water loading	Vessel name and type, flag	Type of BWTS	Ballast volume, m^3	BWTS treatment method	Total abundance of organisms, cells/L
12	16.12.2022	Porto Monfal-cone, Italy	YASAR KEMAL, bulk carrier, Panama	Blue Ocean Shield BOS 300	11 390	Filter + UV treatment	6
13	15.01.2023	Nouadhibou, Mauritania	SEA HELIOS, oil tanker, Malta	Gloen-1200 Patrol	18 840	Filter + UV treatment	2034
14	26.02.2022	Tuzla, Turkey	NISSOS PAROS, oil tanker, Greece	Ex-Els-3000B 1:1	36 204	Electrolysis + electrochlorination	368
15	28.02.2023	Suez, Egypt	EUROSTRENGTH, oil tanker, Liberia	Erma First BWTS FIT-3000	34 400	Electrolysis + Filtration	7163
16	03.03.2023	Izmir, Turkey	SEA PEARL J, bulk carrier, Barbados	DESMI Compact Clean CC-500	11 332	Filtration + UV treatment	1 190 862

End of Table 1

Vessel number	Sampling date	Port of ballast water loading	Vessel name and type, flag	Type of BWTS	Ballast volume, m^3	BWTS treatment method	Total abundance of organisms, cells/L
17	14.03.2023	Tuzla, Turkey	MRC BELIZ, oil chemical tanker, Malta	Pureballast 3.2 1500 EX	23 202	UV System	12 057
18	27.03.2023	Port of BANDAR IMAM KHOMEINI (BIK), Iran	MV LEGENDI, балкер, Либерия / MV LEGENDI, bulk carrier, Liberia	Electro-Cleen System ECS-1350B	18 397	Electrolysis + Neutralization	9
19	31.03.2023	Aliaga, Turkey	TAHITI, oil carrier, Malta	Ecochlor Inc./Et-5000-4.0 Series 200	45 153	Chlorine system + Filtration	N/D

Note: Information obtained from the Ballast Water Reporting Form (Resolution A.868(20).
N/D – not determined.

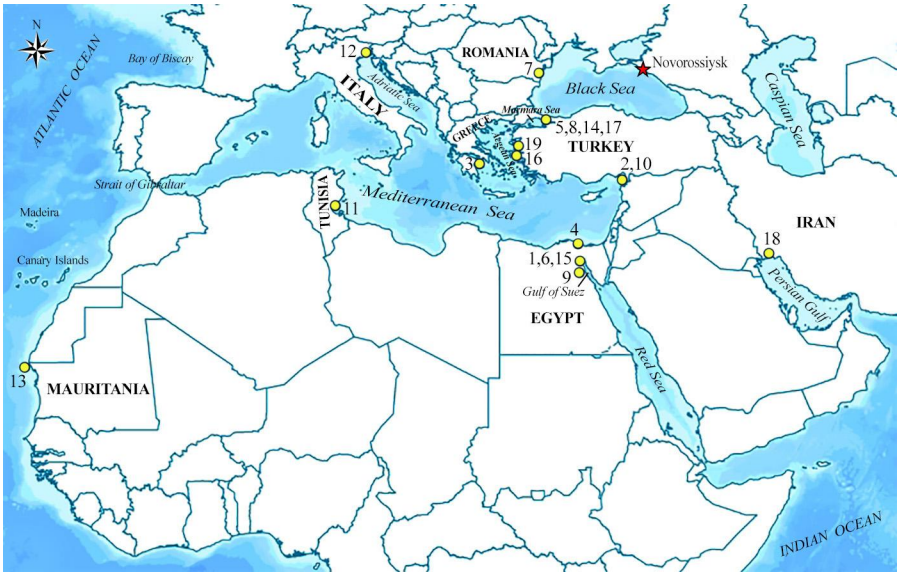

F i g. 1. The routes of the ballast water transport in 2022–2023 onboard the surveyed ships from the ports of origin (yellow circles) to the port of destination (Novorossiysk, Russia, the Black Sea; marked with a red star). The examined vessels are indicated on the map by Arabic numerals at the location of their ports of origin (see Table 1)

accepted guidelines [8), 9)]. Intact algae cells with brightly colored chloroplasts were considered viable. Whole animal organisms that were accidentally included in the samples without visible destruction were also taken into account.

Results

Twenty species of planktonic algae belonging to four major taxonomic categories were found in the samples of the surveyed ships' ballast: Bacillariophyceae (diatoms), Dinoflagellata (dinoflagellates), Dictyochophyceae (silicoflagellates) and Euglenophyceae (euglenids) (Table 2, Fig. 2). Diatoms (13 species) and dinoflagellates (6 species) had the highest species richness. Silicoflagellates were represented by one species, *Dictyocha speculum*; in addition, the euglenid *Euglena* sp. was found in the ballast of some vessels. The total number of viable algae in each sample of the surveyed ballast varied from 0 to 1.19×10^6 cells/L.

---

8) Dodge J. D. *Marine Dinoflagellates of the British Isles.* London : Her Majesty's Stationary Office, 1982. 303 p.

9) Tomas, C., 1997. *Identifying Marine Phytoplankton.* San Diego: Academic Press, Inc., 821 p.

T a b l e 2. Taxonomic composition of unicellular planktonic organisms in the ballast water of the surveyed ships

Taxa	Number of the vessel (Table 1), in the ballast of which live cells of phyto- and microzooplankton were found
PHYTOPLANKTON	
BACILLARIOPHYCEAE	
Chaetoceros affinis Lauder (Fig. 2, *a*)	16
Chaetoceros danicus Cleve (Fig. 2, *b*)	16
Coscinodiscus sp. * (Fig. 2, *c*)	15, 16
Dactyliosolen fragilissimus (Bergon) Hasle	4
Ditylum brightwellii (T. West) Grunow *(Fig. 2, *d*)	14, 17
Melosira moniliformis (O.F. Müller) C. Agardh	17
Nitzschia tenuirostris Manguin	13, 15,
Proboscia alata (Brightw.) Sundström * (Fig. 2, *e*)	10, 14, 15, 16, 17
Pseudo-nitzschia delicatissima (Cleve) Heiden complex sp. (рис. 2, *f*)	7, 15, 16, 17
Pseudo-nitzschia seriata (Cleve) H. Perag. complex sp.	14, 15, 16, 17
Pseudo-nitzschia sp.	14
Pseudosolenia calcar-avis (Schultze) B.G. Sundström *	13, 14, 16, 17
Skeletonema costatum (Grev.) Cleve (Fig. 2, *g*)	15, 16, 17
Sundstroemia setigera (Brightw.) Medlin in Medlin et al. (=*Rhizosolenia setigera* Brightw.) ** (Fig. 2, *h*)	12, 17
Thalassionema nitzschioides (Grunow) Mereschk. (Fig. 2, *i*)	5, 14, 15, 16
Thalassiosira sp. (Fig. 2, *j*)	4, 7, 17
DINOFLAGELLATA	
Alexandrium sp.	14
Ensiculifera carinata Matsuoka, Kobayashi et Gains	16
Gonyaulax sp.	16
Prorocentrum compressum (J.W. Bailey) T.H. Abé ex J.D. Dodge (Fig. 2, *l*)	13
Prorocentrum micans Ehrenb. (Fig. 2, *m*)	10, 11, 13, 14, 16
Prorocentrum scutellum Schröd. (Fig. 2, *n*)	11, 14, 15, 17
Prorocentrum sp.	14
Protoperidinium sp. *	16
Scrippsiella acuminata (Ehrenb.) Kretschmann (Fig. 2, *o*)	16
Tripos furca (Ehrenb.) F. Gómez, 2013 * (Fig. 2, *k*)	16

Continued Table 2

Taxa	Number of the vessel (Table 1), in the ballast of which live cells of phyto- and microzooplankton were found
DICTYOCHOPHYCEAE	
Dictyocha speculum Ehrenb.	16
EUGLENOPHYCEAE	
Euglena sp.	8
MICROZOOPLANKTON	
PROTOZOA	
Amphorellopsis acuta (Schmidt, 1902)	10
Ciliophora gen. sp. (? *Euplotes* sp.)	13, 15, 18
Ciliophora gen. sp. (? *Vorticella* sp.) (Fig. 2, *p*)	18

* The species with cells of > 50 μm long.

** Species not characteristic of the northeastern Black Sea.

The total number of living microzooplankton organisms (ciliates) ranged from 0 to 6.20×10^3 cells/L.

No living organisms were found in the ballast water of six vessels (1–3, 6, 9 and 19) out of 19 (32% of all cases) (100% ballast treatment). These vessels used the HMT-1500-EX, HMT-800, HiBallast BWMS-HUB-1000-EX, BalClor BC-2000, Ecochlor Series 200 or Ecochlor Inc./Et -5000-4.0 Series 200 BWTSs. The following treatment methods are used in these systems: electrocatalysis, electrolysis + filtration, chlorination + filtration, electrochlorination + neutralization.

DESMI CompactClean CC-500 (treatment method: filtration + UV) and Pureballast 3.2 1500 EX (treatment method: UV) systems used on vessels 16 and 17 (10% of all cases) failed to treat marine ballast. The number of unicellular algae (1.21×10^4 and 1.19×10^6 cells/L) in their ballast exceeded the permissible concentrations of living organisms from 10 μm to 50 μm long (< 1.00×10^4 cells/L) established by regulation D-2. In the case of vessel 17 (ballast water loading region: the Marmara Sea, the port of Tuzla, Turkey), this excess was insignificant – by 1.2 times, but the number of phytoplankton cells in the ballast water of vessel 16 (ballast water loading region: the Aegean Sea, the port of Izmir, Turkey) exceeded the maximum permissible concentration of regulation D-2 by 119 times. The unsatisfactory degree of ballast water treatment on these vessels could be associated with improper operation or ineffective ballast systems operation.

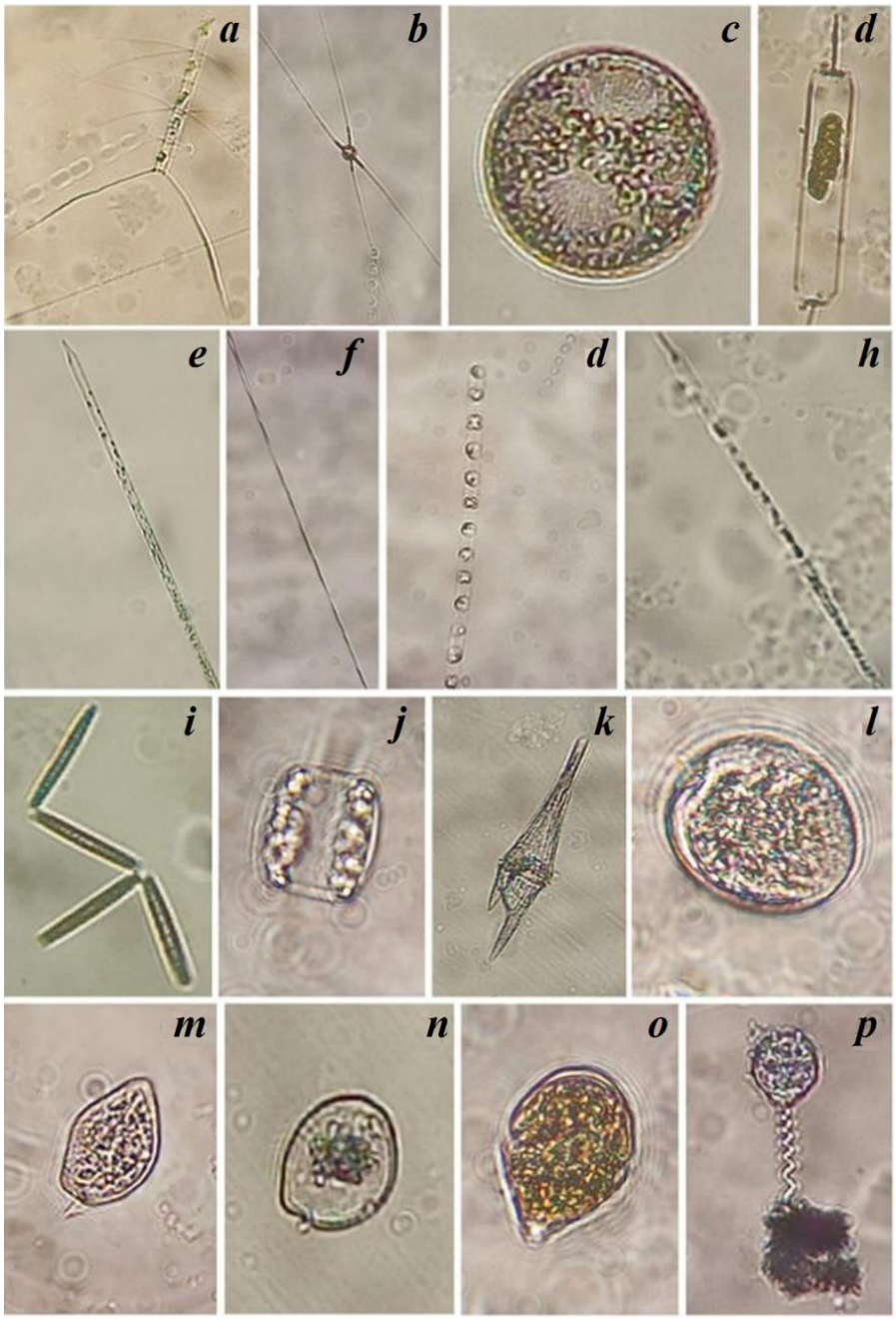

F i g. 2. Phyto- and zooplankton found in the ballast water of the surveyed vessels (light microscope): *a – Chaetoceros affinis*; *b – Chaetoceros danicus*; *c – Coscinodiscus* sp.; *d – Ditylum brightwellii*; *e – Proboscia alata*; *f – Pseudo-nitzschia* sp.; *g – Skeletonema costatum*; *h – Sundstroemia setigera*; *i – Thalassionema nitzschioides*; *j – Thalassiosira* sp.; *k – Tripos furca*; *l – Prorocentrum compressum*; *m – Prorocentrum micans*; *n – Prorocentrum scutellum*; *o – Scrippsiella acuminata*; *p – Ciliophora* gen. sp. (?*Vorticella* sp.)

Onboard the other eleven vessels (No. 4, 5, 7, 8, 10–15, and 18 – 58% of cases) the following BWTS systems of classes NK-03-Blue-Ballast II Plus, HiBallast TM System HIB-2000-EX, HiBallast NF System, Erma First FIT-800, Pure Ballast 3:2, Blue Ocean Shield BOS 300, Gloen-1200 Patrol, Ex-Els-3000B 1:1, Erma First BWTS FIT-3000 or Electro-Cleen System ECS-1350B were used. Their procedures were based on the following treatment methods: electrolysis + neutralization, electrolysis + filtration, electrolysis + electrochlorination, UV treatment + filtration, ozonation + neutralization. These systems coped with the ballast water disposal: the content of live phytoplankton cells in ballast water ranged from 4 to 963 cells/L, microzooplankton (ciliates – Ciliophora) did not exceed 6.20×10^3 cells/L, which met regulation D-2: the discharge of less than 10 viable organisms that are from 10 μm to 50 μm long, per milliliter, that is, no more than 1.00×10^4 cells/L. It should be noted that the concentration of large-celled (more than 50 μm in length) phytoplankton species (mainly the diatoms *Proboscia alata, Pseudosolenia calcar-avis* and *Ditylum brightwellii*) found in the ballast of vessels No. 10, 12–17 (37% of cases) ranged from 2 to 312 cells/L (i.e. from 2 to 3.1×10^5 cells/m^3) and exceeded the requirements of regulation D-2: discharge of fewer than 10 viable organisms ≥ 50 μm in length, per cubic metre. Since the width of the cells of these algal types did not exceed 30 μm, the ballast of the vessels in which they were found can be considered conditionally clean.

Discussion

In the published literature containing the results of the analysis of ballast water and sediment samples, most of the studies were carried out on bulk carriers [24]. Our study is based on phytoplankton samples collected from the ballast tanks of 12 oil tankers and 7 bulk carriers.

All species of unicellular [10] algae found in ballast water were previously found in the Black Sea [25]. However, the diatom *Sundstroemia setigera*, which lives in the southern Black Sea, is not characteristic of the northeastern part [11]. Although this species is not toxic, it can be classified as potentially harmful. With its long and stiff setae located at both ends of the cell, it can injure the gill apparatus of anchovies (anchovies *Engraulis encrasicolus*) and small herring fish species: sprat *Sprattus sprattus* (L.) (Clupeiformes: Clupeidae) and kilka – *Clupeonella cultriventris* (von Nordmann) (Clupeiformes: Ehiravidae). Similarly, the diatoms [12] *Chaetoceros convolutus* Castracane and *C. concavicornis* L.A. Mangin injure the gill apparatus of other fish species [26–29].

Unspecified taxa from two *Pseudo-nitzschia* complexes (Table 1) arguably pose the greatest threat to ecosystems and human health. They can cause amnesic

---

[10] UP-GRADE BS-SCENE project, 2010. *Phytoplankton Check List.* Seventh Framework Programme. Work Package 9. Deliverable D 9-1-3 Annex A. Grant agreement No. 226592. 66 p.

[11] Boicenco, L., 2014. *Black Sea Phytoplankton Checklist.*

[12] Hasle G. R., Fryxell G. A. Taxonomy of Diatoms. In: IOC, 1995. *Manual on Harmful Marine Microalgae. IOC Manual and Guides No. 33*. Paris: UNESCO, pp. 339–364.

shellfish poisoning. In addition, some potentially toxic organisms are capable of producing domoic acid. *P. delicatissima* and *P. prolongatoides* (Hasle) Hasle from the *Pseudo-nitzschia delicatissima* complex, *P. inflatula* (Hasle) Hasle from the *P. pseudodelicatissima* complex and *P. seriata,* and *P. pungens* from the *Pseudo-nitzschia seriata* complex were found in the Black Sea [10]. Of these taxa, *P. delicatissima, P. pseudodelicatissima, P. pungens* and *P. seriata* are potentially toxic.

Species of the genus *Alexandrium* Halim produce neurotoxins and toxins that cause paralytic shellfish poisoning. In some cases, they cause fish death [30].

Ciliates, apparently, should be considered one of the most common zooflagellates transported with ballast waters [2]. For example, during a microscopic examination of marine ballast brought from Japan to the State of Washington (the Pacific coast of the USA), living ciliates 5–30 μm long were found in half of the tank sediment samples. The euglenid *Eutreptiella* sp. was also cultivated from sediments [31]. In general, protozoa are the dominant component of ballast water biota [32].

Thus, our research showed that in not all cases of using different BWTS types onboard vessels that discharged ballast in the seaport of Novorossiysk was 100% elimination of living organisms from ballast water achieved. The use of a number of ballast systems in 32% of the surveyed vessels showed excellent results (100% ballast treatment). Treatment results that met regulation D-2 were observed in 58% of vessels: their BWTSs did not completely cope with the ballast water disposal, but did significantly reduce the number of viable organisms in the ballast. In 10% of all studied cases, the result of ballast water treatment was unsatisfactory (a high number of living organisms remained in ballast water).

The Black Sea is a part of the Mediterranean Basin, and it has been intensively exchanging waters with the Mediterranean Sea over the past 8–10 thousand years. Therefore, the taxonomic compositions of the marine flora and fauna of these two water bodies have significant similarities [4]. The process of mediterranization of the Black Sea has accelerated significantly over the past half century. The mediterranization of fauna means the acquisition of a Mediterranean appearance by the fauna of the Black Sea and the Sea of Azov as a result of constant penetration of the Mediterranean animal species into these seas. In the biogeographical context, the term was introduced by I. I. Puzanov in 1960 [13]. Over the period from 1960 to 2010, more than 100 new records of plants and animals of the Mediterranean origin were reported in the northern and western Black Sea. Forty-three species had successfully adapted to new conditions [5].

Whereas the majority of the surveyed vessels (12 out of 19) loaded ballast water exclusively in the Mediterranean Basin (Fig. 1), a relatively low-risk scenario can be assumed. However, the significant proportion of vessels arriving

---

[13] Puzanov, I.I., 1960. [*Over Untraversed Crimea*]. Moscow: Geografgiz, 286 p. (in Russian).

from the ports of the Gulf of Suez (the Red Sea), the coast of tropical West Africa and the Persian Gulf (the Indian Ocean) should be taken into account. It is expected that the likelihood of harmful effects from living organisms of Mediterranean origin penetrating the Black Sea will be less than from species coming from other regions of the World Ocean. Hence, elevated concentrations of phytoplankton transported in ballast water to the seaport of Novorossiysk from the Gulf of Suez (7.16×10^3 cells/L; vessel 15) and Mauritania (2.03×10^3 cells/L; vessel 13) can pose a moderate risk. However, without more detailed studies of the species composition and cell viability, it is still impossible to assess the real risk.

In general, it is assumed that among cargo ships, it is bulk carriers from the countries exporting raw materials (timber, grain, sugar, coal, iron ore) that pose the greatest risk because this category of vessels spends 50% of the time at sea with ballast water, and after delivery of cargo it needs full ballast water exchange [31]. Previously, a detailed study was carried out on phytoplankton collected using a 10-liter water bottle from the ballast waters of 9 vessels in the State of North Carolina (the Atlantic coast of the USA), followed by filtration through a set of sieves (333, 62 and 33 μm) and cultivation. As a result of this study, 342 species of microalgae (mainly blue-greens, dinoflagellates, diatoms and greens) were found in marine ballast [33]. This number greatly exceeds the number of species found by other authors, suggesting that ships carry thousands of phytoplankton species across the planet at any given time. Thus, most published results of studies of ballast water phytoplankton do not provide a true picture of the risk associated with the penetration of invasive microalgae into new regions. Moreover, we should remember the role of intraregional maritime transport in the distribution of invasive species [34].

Green and blue-green algae were also common biota components in ships' ballast water in the European Region [2], although they were not found in our samples. This fact is probably associated with the complete or almost complete absence of large rivers in the areas where the marine ballast was taken. It should be noted that these two taxonomic groups are most characteristic of freshwater bodies.

We believe that continued monitoring of the biological diversity of ballast water to assess the efficacy of using various types of BWTSs for the ballast water disposal is one of the priority areas in the field of applied scientific research of the Russian Academy of Sciences and Ministry of Transport of the Russian Federation. However, without knowledge of local biodiversity, which is an area of fundamental research, it is impossible to separate invasive species from native inhabitants.

Conclusions

Biological pollution is one of the most important problems of anthropogenic influences on the ecosystems of the World Ocean. To reduce environmental, epidemiological and other stresses on the aquatic environment caused by untreated ballast water discharge, the International Maritime Organization has required all merchant vessels to follow regulation D-1 in the area of the recipient water body

since 2004, and since 2017, all new vessels must comply with regulation D-2, which requires vessels to have a ballast water treatment system (BWTS) onboard. According to the binding regulations for the seaport of Novorossiysk, it is allowed to discharge ballast that complies with regulations D-1 and D-2. For the first time concerning Russian waters, this paper presents the results of a study of the quality of ballast water treatment from unicellular planktonic organisms using BWTSs on vessels that entered the seaport of Novorossiysk.

Ballast water studies were carried out on 19 vessels (12 oil tankers and 7 bulk carriers) that entered the seaport of Novorossiysk for cargo loading from October 2022 to March 2023. The vessels loaded ballast in the ports of the following countries: Romania (the Black Sea, 1 vessel), Turkey (8 vessels), Greece (1 vessel), Italy (1) and Tunisia (1) (the Mediterranean countries), Mauritania (1) (tropical West Africa), Egypt (5 vessels) (the Gulf of Suez, the Red Sea, the Indian Ocean) and Iran (1 vessel) (the Persian Gulf, the Indian Ocean). In our opinion, the greatest risk of introducing harmful organisms into the Black Sea ecosystem with ballast water is represented by the vessels arriving from more distant ports with the warmest waters, i. e. from the Red Sea, the coast of tropical West Africa and the Indian Ocean.

Twenty species of planktonic algae were found in the samples of the surveyed ships' ballast. Diatoms (13 species) and dinoflagellates (6 species) had the highest species richness. Moreover, ciliates *Amphorellopsis acuta*, *Euplotes* sp. and *Vorticella* sp. were found. All species of unicellular organisms found in the ballast water are common in the Black Sea. Potentially dangerous representatives of diatoms and dinoflagellates were also found among them. The total number of viable algae in each sample of the surveyed ballast varied from 0 to 1.19×10^6 cells/L. The total number of living microzooplankton organisms (ciliates) ranged from 0 to 6.20×10^3 cells/L.

No living organisms were found in the ballast water of six vessels (32% of all cases) (100% ballast treatment). These vessels used the HMT-1500-EX, HMT-800, HiBallast BWMS-HUB-1000-EX, BalClor BC-2000, Ecochlor Series 200, Ecochlor Inc./Et-5000-4.0 Series 200BWTSs. The following treatment methods are used in these systems: electrocatalysis, electrolysis + filtration, chlorination + filtration, electrochlorination + neutralization.

DESMI CompactClean CC-500 (treatment method: filtration + UV) and Pureballast 3.2 1500 EX (treatment method: UV treatment) systems used on two vessels (10% of all cases) arriving from the Marmara (the port of Tuzla, Turkey) and the Aegean Sea (the port of Izmir, Turkey) failed to treat marine ballast. The number of unicellular algae (1.21×10^4 and 1.19×10^6 cells/L) in their ballast exceeded the permissible concentrations of living organisms established by regulation D-2.

The systems of 11 out of 19 ships coped with the ballast water disposal: the content of live phyto- and microzooplankton cells in their ballast water met regulation D-2. These were BWTS systems of classes NK-03-Blue-Ballast II Plus, HiBallast TM System HIB-2000-EX, HiBallast NF System, Erma First FIT-800, Pure Ballast 3:2, Blue Ocean Shield BOS 300, Gloen-1200 Patrol, Ex-Els-3000B 1:1,

Erma First BWTS FIT-3000, Electro-Cleen System ECS-1350B. These systems use the following treatment methods: electrolysis + neutralization, electrolysis + filtration, electrolysis + electrochlorination, UV treatment + filtration, ozonation + neutralization.

Thus, the studies have shown that the use of different BWTS types onboard vessels does not always provide 100% clearance of living organisms from ballast water. Therefore, continued research and biological control of ballast water to assess the efficacy of using various types of BWTSs for ballast disposal, as well as monitoring of local biodiversity, are key tasks for minimizing possible biological pollution of the Black Sea.

REFERENCES

1. Carlton, J.T., 1999. The Scale and Ecological Consequences of Biological Invasions in the World's Oceans. In: O. T. Sandlund, P. J. Schei and A. Viken, eds., 1999. *Invasive Species and Biodiversity Management.* Dordrecht: Kluwer Academic Publishers, pp. 195–212. doi:10.1007/978-94-011-4523-7_13
2. Gollasch, S., Macdonald, E., Belson, S., Botnen, H., Christensen, J.T., Hamer, J.P., Houvenaghel, G., Jelmert, A., Lucas, I. [et al.], 2002. Life in Ballast Tanks. In: E. Leppäkoski, S. Gollasch and S. Olenin, eds., 2002. *Invasive Aquatic Species in Europe. Distribution, Impacts and Management.* Dordrecht: Kluwer Academic Publishers, 2002. P. 217–231. doi:10.1007/978-94-015-9956-6_23
3. Carlton, J.T., 1985. Transoceanic and Interoceanic Dispersal of Coastal Marine Organisms: the Biology of Ballast Water. *Oceanography and Marine Biology: an Annual Review*, 23, pp. 313–371.
4. Sorokin, Y.I., 1982. [*Black Sea: Nature, Resources*]. Moscow: Nauka, 217 p. (in Russian).
5. Shiganova, T.A., Musaeva, E.I., Lukasheva, T.A., Stupnikova, A.N., Zasko, D.N., Anokhina, L.L., Sivkovich, A.E., Gagarin, V.I. and Bulgakova, Yu.V., 2012. Increasing of Mediterranean Non-Native Species Findings in the Black Sea. *Rossiysky Zhurnal Biologicheskikh Invaziy*, 3, pp. 61–99 (in Russian).
6. Shalovenkov, N.N., 2020. Tendencies of Invasion of Alien Zoobenthic Species into the Black Sea. *Rossiysky Zhurnal Biologicheskikh Invaziy*, 1, pp. 72–80 (in Russian).
7. Gomoiu, M.-T., Alexandrov, B., Shadrin, N. and Zaitsev, Y., 2002. The Black Sea – a Recipient, Donor and Transit Area for Alien Species. In: E. Leppäkoski, S. Gollasch, S. Olenin, eds., 2002. *Invasive Aquatic Species in Europe. Distribution, Impacts and Management*. Dordrecht: Kluwer Academic Publishers, pp. 341–350. doi:10.1007/978-94-015-9956-6_23
8. Zviagitsev, A.Yu. and Guk, Yu.G., 2006. Estimation of Ecological Risks Arising from Bioinvasion in Marine Coastal Ecosystems of Primorye Region (with Sea Fouling and Ballast Waters as an Example). *Izvestiya TINRO*, 145, pp. 3–38 (in Russian).
9. Gomoiu, M.T., 2001. Impacts of Naval Transport Development on Marine Ecosystems and Invasive Species. *Journal of Environmental Protection and Ecology*, 2(2), pp. 475–481.
10. Hallegraeff, G.M., Bolch, C.J., Bryan, J. and Koerbin, B., 1990. Microalgal Spores in Ship's Ballast Water: a Danger to Aquaculture. In: E. Granéli, B. Sundström, L. Edler and D. M. Anderson, eds., 1990. *Toxic Marine Phytoplankton*. New York, Amsterdam, London: Elsevier Science Publishing Co., pp. 475–480.
11. Hallegraeff, G.M. and Bolch, C.J., 1992. Transport of Dinoflagellate Cysts in Ship's Ballast Water: Implications for Plankton Biogeography and Aquaculture. *Journal of Plankton Research*, 14(8), pp. 1067–1084. doi:10.1093/plankt/14.8.1067
12. Kozlov, D.N., 2013. [On Ballast Water Purification from Biological Contaminants on Fishing Fleet Vessels]. *Problemy Razvitiya Korabelnogo Vooruzheniya i Sudovogo Radioelektronnogo Oborudovaniya*, (2), pp. 112–123 (in Russian).

13. Bolch, C.J. and Hallegraeff, G.M., 1993. Chemical and Physical Options to Kill Toxic Dinoflagellate Cysts in Ships' Ballast Water. *Journal of Marine Environmental Engineering*, 1, pp. 23–29.
14. Rigby, G. and Hallegraeff, G., 1996. Ballast Water Controls to Minimise the Translocation and Establishment of Toxic Marine Phytoplankton – What Progress Have We Made and Where are We Going? In: T. Yasumoto, Y. Oshima and Y. Fukuyo, eds., 1996. *Harmful and Toxic Algal Blooms : Proceedings of the Seventh International Conference on Toxic Phytoplankton, Sendai, Japan, 12–16 July 1995.* Intergovernmental Oceanographic Commission of UNESCO, 1996. P. 169–176.
15. Satir, T., 2014. Ballast Water Treatment Systems: Design, Regulations, and Selection under the Choice Varying Priorities. *Environmental Science and Pollution Research*, 21, pp. 10686–10695. doi:10.1007/s11356-014-3087-1
16. Sutherland, T.F., Levings, C.D., Elliott, C.C. and Hesse, W.W., 2001. Effect of a Ballast Water Treatment System on Survivorship of Natural Populations of Marine Plankton. *Marine Ecology Progress Series*, 210, pp. 139–148. doi:10.3354/meps210139
17. Hallegraeff, G.M., 1998. Transport of Toxic Dinoflagellates via Ships' Ballast Water: Bioeconomic Risk Assessment and Efficacy of Possible Ballast Management Strategies. *Marine Ecology Progress Series*, 168, pp. 297–309. doi:10.3354/meps168297
18. Boltacheva, N.A., Lisitskaya, E.V. and Podzorova, D.V., 2020. Distribution of Alien Polychaetes in Biotopes of the Northern Part of the Black Sea. *Rossiysky Zhurnal Biologicheskikh Invaziy*, 4, pp. 15–33 (in Russian).
19. Yasakova, O.N., 2020. The Status of Plankton Algocenosis of the Black Sea Northeastern Shelf in the Period 2015–2019. *Nauka Yuga Rossii = Science in the South Russia*, 16(4), pp. 39–50 (in Russian).
20. Yasakova, O.N., 2011. New Species of Phytoplankton in the Northeastern Part of the Black Sea. *Russian Journal of Biological Invasions*, 2(1), pp. 65–69. doi:10.1134/S2075111711010103
21. Matishov, G.G. and Selifonova, J.P., 2006. Experience of Commercial Vessels' Water Ballast Control in the Port of Novorossiysk. *Vestnik SSC RAS*, 2(3), pp. 58–62. doi:10.23885/1813-4289-2006-2-3-58-62
22. Zvyagintsev, A.Yu. and Selifonova, J.P., 2008. Study of Ballast Waters of Commercial Ships in the Sea Ports of Russia. *Rossiysky Zhurnal Biologicheskikh Invaziy*, 2, pp. 22–33 (in Russian).
23. Vodyanitskaya, S.Yu., Sergienko, O.V., Ivanova, N.G., Balachnova, V.V., Arkhangelskaya, I.V., Rengach, M.V., Nepomnyashchaya, N.B. and Volovikova, S.V., 2020. About the Results of Monitoring Researches of Ballast Waters and Data of Identification of the Vibrioes Strains Selected During the Ships Researches in Russian Seaports in 2018. *Journal of Microbiology, Epidemiology and Immunobiology*, 97(1), pp. 55–61. doi:10.36233/0372-9311-2020-97-1-55-61
24. Williams, R.J., Griffiths, F.B., Van der Wal, E.J. and Kelly, J., 1988. Cargo Vessel Ballast Water as a Vector for the Transport of Non-Indigenous Marine Species. *Estuarine, Coastal and Shelf Science*, 26(4), pp. 409–420. doi:10.1016/0272-7714(88)90021-2
25. Krakhmalnyi, A.F., Okolodkov, Y.B., Bryantseva, Y.V., Sergeeva, A.V., Velikova, V.N., Dereziuk, N.V., Terenko, G.V., Kostenko, A.G. and Krakhmalnyi, M.A., 2018. Revision of the Dinoflagellate Species Composition of the Black Sea. *Algology*, 28(4), pp. 428–448. doi:10.15407/alg28.04.428
26. Bell, G.R., 1961. Penetration of Spines from a Marine Diatom into the Gill Tissue of Lingcod (*Ophiodon elongatus*). *Nature*, 192, pp. 279–280. doi:10.1038/192279b0
27. Albright, L.J., Yang, C.Z. and Johnson, S., 1993. Sub-Lethal Concentrations of the Harmful Diatoms, *Chaetoceros concavicornis* and *C. convolutus*, Increase Mortality Rates of Penned Pacific Salmon. *Aquaculture*, 117(3–4), pp. 215–225. doi:10.1016/0044-8486(93)90321-O

28. Yang, S.Z. and Albright, L.J., 1992. Effects of the Harmful Diatom *Chaetoceros concavicornis* on Respiration of Rainbow Trout *Oncorhynchus mykiss*. *Diseases of Aquatic Organisms*, 14, pp. 105–114.
29. Dickman, M. and Zhang, F., 1999. Mid-Ocean Exchange of Container Vessel Ballast Water. 2: Effects of Vessel Type in the Transport of Diatoms and Dinoflagellates from Manzanillo, Mexico, to Hong Kong, China. *Marine Ecology Progress Series*, 176, pp. 253–262. doi:10.3354/meps176253
30. Yasakova, O.N., 2013. The Seasonal Dynamics of Potentially Toxic and Harmful Phytoplankton Species in Novorossiysk Bay (Black Sea). *Russian Journal of Marine Biology*, 39(2), pp. 107–115. doi:10.1134/S1063074013020090
31. Kelly, J.M., 1993. Ballast Water and Sediments as Mechanisms for Unwanted Species Introductions into Washington State. *Journal of Shellfish Research*, 12(2), pp. 405–410.
32. Hülsmann, N. and Galil, B.S., 2002. Protists– a Dominant Component of the Ballast-Transported Biota. In: E. Leppäkoski, S. Gollasch and S. Olenin, eds., 2002. *Invasive Aquatic Species in Europe. Distribution, Impacts and Management*. Dordrecht: Kluwer Academic Publishers, pp. 20–26. doi:10.1007/978-94-015-9956-6
33. McCarthey, H.P. and Crowder, L.B., 2000. An Overlooked Scale of Global Transport: Phytoplankton Richness in Ships' Ballast Water. *Biological Invasions*, 2, pp. 321–322. doi:10.1023/A:1011418432256
34. Wasson, K., Zabin, C.J., Bedinger, L., Diaz, M.C. and Pearse, J.S., 2001. Biological Invasions of Estuaries Without International Shipping: The Importance of Intraregional Transport. *Biological Conservation*, 102, pp. 143–153. doi:10.1016/S0006-3207(01)00098-2

Submitted 16.06.2023; accepted after review 13.07.2023;
revised 11.10.2023; published 20.12.2023

About the authors:

Olga N. Yasakova, Senior Research Associate, Southern Scientific Center, Russian Academy of Sciences (41 Chekhov Str., Rostov-on-Don, 344006, Russian Federation), PhD (Biol.), **ORCID ID 0000-0002-0728-6836**, *yasak71@mail.ru*

Oleg T. Zuykov, Deputy Head of the Federal State Budgetary Institution "Administration of Seaports of the Black Sea" (2 Khvorostyanskiy Str., Novorossiysk, 353925, Russian Federation), PhD (Tech.), **ORCID ID: 0009-0002-5130-2570**, *oleg@ampnovo.ru*

Yuri B. Okolodkov, Researcher, Laboratorio de Botánica Marina y Planctología, Instituto de Ciencias Marinas y Pesquerías, Universidad Veracruzana (Mar Mediterráneo 314, Fracc. Costa Verde, Boca del Río, Veracruz, 94294, Mexico), DSc (Biol.), **ORCID ID: 0000-0003-3421-3429**, *yuriokolodkov@yahoo.com*

Contribution of the authors:

Olga N. Yasakova – conducting research, processing samples of marine ballast, description of the results of the study, qualitative and quantitative analysis of the results and their interpretation

Oleg T. Zuykov – development of the concept, formulation and statement of the research problem, conducting a critical analysis of materials related to the technical side of the study of ballast water

Yuri B. Okolodkov – analysis of the results and their interpretation, preparation of graphic materials, editing of the manuscript

All the authors have read and approved the final version of the manuscript.